RECOMBINANT CELLS AND CHIMERAPLASTY AS TOOLS TO STUDY ATHEROPROTECTIVE EFFECTS OF APOLIPOPROTEIN E

By

Zahra Mohri

A thesis submitted in partial fulfillment of the requirements for the degree of

Doctor of Philosophy

Royal Free Hospital
School of Medicine
University College London

2004

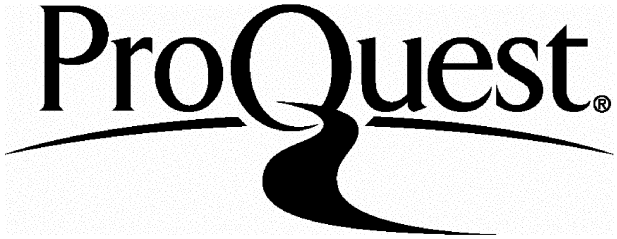

Abstract

RECOMBINANT CELLS AND CHIMERAPLASTY AS TOOLS TO STUDY ATHEROPROTECTIVE EFFECTS OF APOLIPOPROTEIN E

Zahra Mohri, Department of Medicine, Royal Free & University College Medical School, London NW3 2PF

Apolipoprotein (apo) E is secreted by liver and macrophages and is atheroprotective, in part by contributing to plasma cholesterol homeostasis. Three common isoforms arise from single nucleotide polymorphisms (SNPs): the rarest variant, apoE2, differs from wild-type apoE3 by an R158C substitution, and causes recessive Type III hyperlipidaemia, while apoE4 (C112R) produces a dominant hyperlipidaemia. One aim of this thesis was to determine whether lipidated apoE3 particles, newly-secreted by recombinant Chinese hamster ovary (CHO), were biologically active, using CHO cells engineered to secrete antiatherogenic apoAI as positive controls. An ELISA was established to quantify levels of secreted apoE, while apoAI was measured by immunoblotting and scanning densitometry. Although secreted apoAI was about 55 % better at activating the cholesterol esterifying enzyme, LCAT (lecithin-cholesterol acyltransferase), than apoE after 0.5 ($P<0.05$) or 1 h ($P<0.001$) of incubation, both particles were equally effective at promoting cholesterol efflux. These data suggest that these atheroprotective actions may be normal physiological roles for apoE.

The second aim was to test the hypothesis that: **'synthetic RNA-DNA oligonucleotides (chimeraplasts) can convert the *APOE3* gene to mutant *APOE2* and *APOE4* in human hepatoblastoma (HepG2) and human monocyte-macrophage (THP-1) cells'**. Such new cell lines, secreting dysfunctional apoE2 or apoE4, would allow the atheroprotective properties of the three main human apoE isoforms to be compared in future studies. Initially, CHOE3 and human embryonic kidney (HEK-293; ε3/ε3) cells, which are both readily transfected, were targeted with apoE3-to-apoE2 chimeraplast complexed with polyethylenimine (PEI); the expected conversions were detected. Dose-dependent conversions using apoE3-to-apoE2 or apoE3-to-apoE4 chimeraplast were also seen in HepG2 cells, as judged by direct sequencing and PCR-RFLP, whereas THP-1 cells proved refractory and the conversion was limited. Trials with end-protected all-DNA molecules proved unsuccessful. Increasing efficiency was subsequently investigated: by using different PEIs (linear *vs.* branched, and tagging with melittin, galactose or mannose); by centrifugation to enhance cell-complex contact; and by nuclear microinjection. Linear PEI (L-PEI) alone worked best with the apoE3-to-apoE2 chimeraplast, while galactose-4-PEI mixed with L-PEI (1:1) gave good conversion with the apoE3-to-apoE4 reagent. Unexpectedly, the conversion appeared unstable in both THP-1 and HepG2 cells after freeze-thawing and/ or repeated passaging. Attempts to understand this problem were then hampered by difficulties in synthesizing active chimeraplasts. In conclusion, although an emerging technology with enormous potential, chimeraplast-directed gene mutation/ repair remains problematical and factors such as chimeraplast quality and design, gene target and cell type all require detailed study in future investigations.

TABLE OF CONTENTS

LIST OF FIGURES

Number *Page*

CHAPTER 1

CHAPTER 2

CHAPTER 3

CHAPTER 4

CHAPTER 5

LIST OF TABLES

DEDICATION

I wish to dedicate this thesis to my loving and caring husband, Nasim, and to my parents, Ashraf & Ahmad Mohri, and Zahida & Ishfaq Ahmad (who have cared for me like their own daughter) for their love, support and encouragement through the years, and for being the most loving grandparents in the world.

ACKNOWLEDGEMENTS

I would like to express my gratitude to Prof. Jim Owen for his guidance, encouragement and support over the course of my PhD. I am also extremely grateful to him and my colleagues and friends, Dr. A. Tagalakis, Mr. N. Ahmad, Mr. S. Thilakawardhana, and Dr. A. Manzano, for their critical reviewing and proof reading of this manuscript. I would like to also thank Mr. T. Athanasopoulos, and Dr. I. Graham for proof reading parts of this project.

I wish to thank Dr. Anna Manzano who gave me constant guidance, as well as friendship that is lasting a life time. Thanks must also go to Dr. Anita Stannard for assisting me with ELISA assays. Furthermore, I thank all my friends at the Royal Free especially Drs' Jane Mulcahy, Aris Tagalakis, Galia Sperber, Anna Manzano, Stuart Beattie, Bhim Odedra and Ms. Sarah Choudhary, and Mr. Shani Thilakawardhana, for bringing joy and fun to our times in the laboratory. The financial support of the 'British Heart Foundation' is also gratefully acknowledged.

Last but not least, I wish to thank my dear husband, Mr. Nasim Mazahar Ahmad, for his words of wisdom and constant support and encouragement. Without you and our ray of sunshine, little Hana, I would have not completed this book. Thank you for always being there.

Zahra Mohri, April 2004

ABBREVIATIONS

α..... anti-

ABC-A1.....ATP-binding cassette transporter, class A1

AP.....alkaline phosphatase

apoAI.....apolipoprotein AI

apoAI-M.....apolipoprotein AI-Milano

apoE.....apolipoproteinE

apoE-R2.....apoE receptor 2

APS.....ammonium persulphate

ARH.....autosomal recessive hypercholesterolemia

ARP.....arginine-rich protein

ASGPR.....asialoglycoprotein receptor

β-GAL.....β-D-galactosidase

BCA..... bicinchoninic acid

bisacrylamide..... N,N'-methylenebisacrylamide

BMT.....bone-marrow transplantation

B-PEI.....branched polyehylenimine

BSA.....bovine serum albumin

CE.....cholesteryl-ester

CERP.....cholesterol-efflux regulatory protein

CETP..... cholesteryl-ester-transfer protein

CHO.....Chinese hamster ovary

CIP.....calf intestinal alkaline phosphatase

CMV.....cytomegalo virus

CNS.....central nervous system

CSF.....cerebrospinal fluid

CTL.....cytotoxic-T-lymphocyte

CV.....coefficient of variation

DEPC.....diethylpyrocarbonate

D-loop.....displacement loop

DMD.....Duchenne muscular dystophy

DMSO.....dimethylsulphoxide

dNTPs..... deoxynucleotide triphosphates

dpm..... disintegrations per minute

DTT..... dithiothreitol

ECACC.....European collection of animal cell culture

ECL.....enhanced chemiluminescence

EDTA.....ethylenediaminetetra-acetate

EGF.....epidermal growth factor

EL.....endothelial lipase

ELISA.....enzyme-linked immunosorbent assay

FBS..... fetal bovine serum

FC..... free cholesterol

FDB.....familial defective apolipoprotein B

FED.....fish-eye disease

FH.....familial hypercholesterolemia

FHD.....familial HDL deficiency

FLD.....familial lecithin cholesterol acyltransferase deficiency

GFP..... green fluorescent protein

HDL.....high density lipoprotein

HDL-C..... high density lipoprotein cholesterol

HL.....hepatic lipase

HRP.....horseradish peroxidase

HSPG.....heparin sulphate proteoglycan

HSV.....herpes simplex virus

HSV-1.....herpes simplex virus, type-1

IDL.....intermediate density lipoprotein

IEF.....isoelectric focusing

Ig..... immunoglobulin

LB.....Luria-Bertani

LCAT.....lecithin cholesterol acyltransferase

LDL.....low density lipoprotein

LDL-C..... low density lipoprotein cholesterol

LDL-R..... low density lipoprotein receptor

Lp(a)..... lipoprotein (a)

L-PEI.....linear polyethylenimine

LPL..... lipoprotein lipase

LRF.....low density lipoprotein receptor family

LRP.....low density lipoprotein receptor-related protein

LSC.....liquid scintillation counting

LTR.....long terminal repeat

mAb..... monoclonal antibody

MCP-1..... monocyte chemotactic protein-1

MTX.....methotrexate

MWCO..... molecular weight cut-off

NDGGE.....non-denaturing gradient gel electrophoresis

NFκB.....nuclear factor kappaB

OPD.....ortho-phenylene diamine

OTC.....ornithine transcarbamylase

PBS..... phosphate-buffered saline

PBS-T..... phosphate-buffered saline-tween

PCR.....polymerase chain reaction

PEI.....polyethylenimine

PLG.....poly(D,L-lactide-co-glycolide)

PLTP.....phospholipid transfer protein

PMA..... phorbol 12-myristate 13-acetate

PNS.....peripheral nervous system

PTB.....phosphotyrosine binding domain protein

RAF.....receptor-associated protein

RCT.....reverse cholesterol transport

RDO.....RNA-DNA oligonucleotide

RFLP.....restriction fragment length polymorphism

RIA.....radioimmunoassay

RNAi.....RNA-mediated gene interference

RSV.....Rous Sarcoma virus

SCID.....severe combined immunodeficiency disease

(SCID)-XI.....severe combined immunodeficiency disease, type XI

SDS.....sodium dodecyl sulphate

SDS-PAGE..... sodium dodecyl sulphate-polyacrylamide gel electrophoresis

SFHR.....short fragment homologous recombination

S-HRP.....streptavidin horseradish peroxidase

SNP.....single nucleotide polymorphism

SR-BI..... scavenger receptor class B, type I

SSO.....single-stranded oligonucleotide

SV40.....simian virus 40

TBE.....tris-borate ethylenediaminetetra-acetate

TEMED..... N, N, N, N'-tetramethylethylenediamine

TFO.....triple helix-forming oligonucleotide

TLC..... thin layer chromatography

TMB.....tetra-methylbenzidine

UV.....ultraviolate

VCAM-1.....vascular cell adhesion molecule-1

VLDL..... very low density lipoprotein

VLDL-R.....very low density lipoprotein receptor

WHHL.....Watanable heritable hyperlipidaemic

Chapter 1

1. INTRODUCTION

1.1 Atherosclerosis

The aetiology of atherosclerotic cardiovascular disease (CVD), the leading cause of death worldwide, is multifactorial and complex. Gene-gene and gene-environment interactions contribute to the clinical manifestation of the disease. There are different forms of CVD including coronary heart disease, stroke, cardiomyopathy, congenital heart defects, rheumatic heart disease, and congestive heart failure. Women are at lower risk of developing CVD compared to men before the age of 60, but their risk increases after the protective effects of estrogen is lost. The primary factors implicated in CVD risk are cigarette smoking, hypertension, sedentary lifestyle, diabetes mellitus, decreased high density lipoprotein (HDL) cholesterol, and elevated total low density lipoprotein (LDL) cholesterol (Grundy SM *et al*, 1999). These risk factors are associated with other arterial disorders (such as thrombotic stroke), although their degree of impact varies by disease.

Atherosclerosis is a multi-step process involving the interaction of different pathways including lipoprotein metabolism, inflammation, and coagulation (Hokanson JE *et al*, 1996; Meade TW *et al*, 1986). The initial stage of atherosclerosis involves the recruitment of monocytes and T-lymphocytes to the artery wall. This process can be triggered by various stimuli including oxidized lipids, inflammatory agents, cytokines, and shear stress, affecting the overlying endothelial cells. Repetitive stimulation of the vascular endothelium allows lipoproteins to penetrate and lipids to accumulate in the sub-endothelial space. This is followed by leukocyte entry into the artery wall, which involves upregulating the expression of a number of chemotactic factors and adhesion molecules, including the vascular cell adhesion molecule-1 (VCAM-1) and the intracellular cell adhesion molecule-1 (ICAM-1), by cytokines (Ross R, 1999).

The first step of adhesion, the 'rolling' of leukocytes along the endothelial surface, is mediated by P- and E-selectins that bind to carbohydrate ligands on leukocytes (Collins RG *et al*, 2000). Integrin VLA-4 facilitates the firm adhesion of monocytes and T-cells to endothelium via interaction with VCAM-1 on endothelium and CS-1 splice variant of fibronectin. Monocyte integrins do not bind their ligands unless activated. This activation involves conformational changes of integrins in response to chemokines such as monocyte

chemotactic protein-1 (MCP-1). Studies in mice deficient in MCP-1 or its receptor CCR2, demonstrated the importance of MCP-1/CCR2 interaction in monocyte recruitment and initiation of atherosclerosis (Boring L *et al*, 1998).

Once monocytes are bound firmly to the endothelial adhesion molecules via their complementary ligands, they infiltrate into the subendothelial space where they differentiate into macrophages and take up oxidized LDL particles. Cholesterol loaded macrophages in the arterial intima are characteristic feature of early atherosclerotic lesions. The initial free (unesterified) cholesterol (FC) loading of macrophages is not toxic because the cells increase their biosynthesis of phosphatidylcholine to maintain a constant FC:phospholipid ratio in their membraneslevels (Tabas I, 2000). In addition, excess FC is also esterified and the accumulation of this cholesteryl ester in macrophage cytoplasm gives them an appearance referred to as foam cells. However, with prolonged loading of cholesterol, the FC:phospholipid ratio becomes elevated and as a result macrophages die.

Extensive oxidation of LDL is essential for its uptake by macrophages and foam cell formation. Oxidation is triggered by a number of enzymes including myeloperoxidase and sphingomyelinase in addition to reactive oxygen species generated by macrophages and endothelial cells. Metal ions also contribute to LDL oxidation. Macrophage scavenger receptors including SR-A and CD-36, the LDL receptor-related protein (LRP), and the very low density lipoprotein receptor (VLDL-R) contribute to the progression of atherogenesis by mediating the uptake of lipids and triglyceride-depleted remnant particles (Febbraio M *et al*, 2000). In addition, LDL uptake takes place via the internalization of proteoglycan-bound lipoprotein lipase-LDL (LPL-LDL) complexes (Rumsey SC *et al*, 1992). Both the heparin- and the lipid-binding domains of LPL are believed to act as a bridge between the lipoprotein particles and the matrix proteoglycans. Lipids not only accumulate within macrophages, but also they deposite in the extracellular spaces (Ball RY *et al*, 1995).

Foam cells secret their own growth factors and cytokines and invade smooth muscle cells. The lipid content of foam cells is released into the core of atherosclerotic lesion after their death. The lesion grows towards the adventitia prior to expanding inwards and encroaching on the lumen. Interaction of CD40 with its ligand CD40L (CD154) is important in

development of advanced lesions (Schonbeck U *et al*, 2000). This interaction results in the production of inflammatory cytokines, matrix-degrading proteases, and adhesion molecules.

Advanced atherosclerotic plaques comprise a fibrous cap consisting of smooth muscle cells and extracellular matrix surrounding a necrotic core. As the cap calcifies and becomes unstable, the plaque can rupture and release the thrombogenic debris from its necrotic core into the blood stream leading to actue cardiovascular disorders such as myocardial infarction and stroke (Lusis AJ, 2000). Calcification involves secretion of a matrix scaffold (by pericyte-like cells) that is regulated by oxysterols and cytokines. The thrombogenicity of the necrotic core depends on the production of tissue factor by endothelial cells and macrophages, which is enhanced by oxidized LDL, infection, or ligation of CD40 on endothelial cells to CD40L on inflammatory cells (Schonbeck U *et al*, 2000).

Several genetic loci that influence plasma lipid levels and thus affect CVD risk have been an area of great interest. Apolipoprotein (apo) E, apolipoprotein (apo) B-100, LDL-R, lipoprotein (a), lipoprotein lipase, HDL, and cholesteryl ester transfer protein (CETP) are examples of such genetic factors. ApoE is one of the most comprehensively studied genes (*Section* 1.3) from a list of many potential candidates implicated in CVD (Wilson PW *et al*, 1999). This polymorphic glycoprotein is the focus of this thesis and is discussed in *Sections* 1.3 and 1.6.2.

1.2 Lipoproteins and Apolipoproteins

1.2.1 LIPOPROTEINS

Lipoproteins are spherical bodies of lipids and proteins held together by non-covalent bonds. Each type of lipoprotein has a characteristic mass, chemical composition, density, and physiological role. Throughout the body, lipoproteins are mainly involved in the transport of lipids including triglycerides, phospholipids and cholesterol that are sparingly soluble in the aqueous environment. Irrespective of size and density, these lipoprotein particles consist of a nonpolar lipid core composed of triglycerides and CEs, and an external layer of phospholipids and apolipoproteins (Havel RJ *et al*, 1995). The main protein parts of these particles, apolipoproteins, have a role in metabolism of lipoproteins. The lipid moieties with

hydrated mass of 0.8 to 0.9 g/ml provide a unique density range for lipoproteins that is lighter than other plasma proteins (~1.3 g/ml). Separation of lipoproteins was achieved by the development of ultracentrifugal flotation. They were then classified into five groups: chylomicrons, intermediate density lipoproteins (IDL), VLDL, LDL, and HDL. Another group of lipoproteins, Lp (a), is present in plasma and is isolated by ultracentrifugation as a minor class (Lusis AJ, 2000). Lp (a) is a LDL-like particle containing cholesterol, phospholipid, triglycerides, and apoB-100, which is linked to a large protein called apo (a) via a single disulfide bond. Increased plasma concentrations of Lp (a) are related to an increased risk of atherosclerosis, though the exact physiological function of this protein remains unknown.

1.2.1.1 Chylomicrons

Chylomicrons are synthesized in the small intestine for transporting dietary triglycerides and cholesterol from the site of absorption by the intestinal epithelium to different cells in the body. Despite the low protein content of chylomicrons, they still contain apoA, apoB, and apoC. ApoB-48 synthesized in the intestinal mucosal cells is present in human chylomicrons. LPL located on the endothelial surface of the capillaries, hydrolyses the triglyceride part of these lipoproteins generating chylomicron remnants. These remnants are cleared from the liver and plasma in a process involving apoE (*Section* 1.3.6.1). Accumulation of chylomicron remnants have been observed in patients with type III hyperlipoproteinaemia and animals on high fat and cholesterol diets. An excess of these cholesterol-enriched remnants in plasma is believed to be linked with the development of accelerated atherosclerosis (Mahley RW *et al*, 1998).

1.2.1.2 VLDL & IDL

VLDLs are synthesized in the liver and are involved in lipid transport as discussed in *Section* 1.3.6.1. VLDL particles contain the higher molecular weight of apoB (apoB-100), all the apoC subgroups, apoD, and apoE. Following lipolysis of the VLDL triglycerides in plasma and liver via LPL, IDL and LDL are formed. VLDL remnants refer to smaller VLDL particles and IDL, which are believed to be atherogenic (Mahley RW, 1985; Mahley RW *et al*, 1998). After clearance of the majority of the VLDL remnant via apoE, the remainder is converted to LDL that contains only apoB-100. Thus, LDL is the end product of VLDL catabolism.

1.2.2 LDL

In humans most of the circulating cholesterol (70%) is carried by LDL, unlike rodents where HDL is the major cholesterol carrier. A single molecule of apoB-100 constitutes >95% of the protein content of LDL, while only traces of apoA, apoC, and apoE are present. LDL is the end product of VLDL catabolism. Most of plasma LDL is removed after binding to hepatic LDL receptor (LDL-R) via apoB-100. Subsets of patients with familial hypercholesterolaemia (FH) have very high plasma LDL-cholesterol and, consequently, cholesterol deposition in tissues leading to xanthomas and coronary atherosclerosis. This disease is caused by mutations in the *LDL-R* gene and its prevalence in most populations is about 1/500. Homozygous FH patients are classified into two groups: a) patients with <2% of normal LDL-R activity (receptor-negative), b) patients with 2-25% of normal LDL-R activity (receptor-defective). Plasma levels of LDL-cholesterol are much lower in FH heterozygotes and much more dependent on environmental factors and other genetic factors than are those in FH homozygotes.

Another disorder, known as familial defective apoB (FDB) that is phenotypically indistinguishable from FH, is caused by mutations in apoB-100 (Rabes JP *et al*, 2000). Like FH, FDB is characterized by elevated plasma LDL-cholesterol, tendon xanthomas, and premature atherosclerosis. Khachadurian and co-workers described an unusual family with clinical features of homozygous FH, yet an almost normal function for LDL-R in their cultured fibroblasts (Khachadurian AK *et al*, 1973). This disorder was named autosomal recessive hypercholesterolaemia (ARH) and is caused by a mutation in the *ARH* gene, which encodes an adapter phosphotyrosine binding (PTB) domain protein (Garcia CK *et al*, 2001).

1.2.3 HDL

HDL is an heterogeneous macromolecule incorporating a range of different apolipoproteins including apoAI (70%), apoAII (20%), apoCI, apoCII, apoCIII, apoD, and apoE. In plasma, HDL has various sizes, densities, shapes and electrophoretic mobilities depending on its composition of lipid and protein.

1.2.3.1 HDL Metabolism

Nascent HDL particles (<10 nm in diameter) containing apoAI, apoAIV, and apoE, are secreted from the liver and small intestine or as a by-product of chylomicron and VLDL

catabolism. Their size varies depending on their lipid and protein composition, however, their phospholipids bilayer thickness is conserved (Hamilton RL *et al*, 1976). These discoidal particles can acquire cholesterol from peripheral tissues either through scavenger receptor class B, type I (SR-BI) or via a pathway mediated by ATP-binding cassette transporter, class A1 (ABC-A1) (Bodzioch M *et al*, 1999; Rust S *et al*, 1999). Spherical and mature CEs containing HDL particles are formed after the action of lecithin cholesterol acyltransferase (LCAT), the plasma cholesterol esterifying enzyme. Spherical HDL particles may contain two or four apoAI molecules. Approximately 11 different HDL sub-classes have been identified the major five of which, in order of increasing density and decreasing size, are as follows: HDL_{2b}, HDL_{2a}, HDL_{3a}, HDL_{3b}, and HDL_{3c} (Blanche PJ *et al*, 1981). The majority of HDL sub-classes are protein-rich and exhibit α-mobility when subjected to agarose gel electrophoresis (Fielding CJ *et al*, 1995). The rest of HDL sub-classes are lipid-poor or lipid-free with pre-β or γ-mobilities.

HDL delivers cholesterol to different cells via pathways involving LDL-R family and/or HDL receptors. Catabolism of the mature HDL occurs through different routes namely, the selective HDL-cholesterol uptake pathway, the CETP-mediated pathway, and the hepatic lipase (HL)-mediated pathway. In the selective HDL-cholesterol pathway, cholesterol is taken up directly by the cells without internalization of HDL or degradation of HDL apolipoproteins (Glass C *et al*, 1983). The CETP-mediated pathway involves transfer of HDL-cholesterol by CETP to triglyceride-rich lipoproteins such as VLDL, which are further metabolized via lipoprotein receptor-mediated endocytosis (Tall AR, 1995). The majority of mammals possess this pathway, while it is absent in most rodents. Catabolism of HDL via different cell surface molecules such as heparin sulphate proteoglycan (HSPG) and HL is the third route of HDL-cholesterol delivery (Ji ZS *et al*, 1997). Following cholesterol delivery to cells and other apolipoproteins, apoAI dissociates from cholesterol-poor HDL and is believed to be absorbed and degraded by the proximal endothelial cells of the kidney through cubilin-mediated endocytic pathway (Hammad SM *et al*, 1999). Cubilin (vitamin B12 receptor) is a cell surface associated protein that lacks a transmembrane domain, hence, ligand uptake is thought to involve a co-receptor that is able to undergo coated pit-mediated endocytosis (Kozyraki R *et al*, 1999).

1.2.3.2 Reverse Cholesterol Transport (RCT)

Intracellular cholesterol homeostasis is a complex mechanism depending on the balance between cholesterol synthesis, influx, degradation, efflux and transfer from the peripheral tissues back to the liver. Approximately 1 g cholesterol/day is synthesized and degraded in the human body.

Cholesterol flux in general is divided into three steps: cholesterol efflux, influx, and net flux. Cholesterol efflux is defined as the movement of FC from the cell to an extracellular acceptor (Johnson WJ *et al*, 1991). The movement of cholesterol from an extracellular source back to the cell is referred to as influx, which includes both FC and CE. Net flux refers to changes in cholesterol content of the cell. Hence, net efflux occurs if cellular cholesterol content decreases while, net influx refers to an increase of cellular cholesterol levels (Johnson WJ *et al*, 1991).

The concept of RCT, which was first formulated in 1968 (Glomset JA, 1968), refers to a process whereby excess cholesterol in peripheral tissues is transported via HDL or sub-classes of HDL back to the liver and sterol metabolizing organs (Rothblat GH *et al*, 1999). This transport can occur via a direct or an indirect route (*Figure* 1.1). The direct route involves the uptake of unesterified cellular cholesterol by HDL, its esterification by LCAT followed by the direct uptake of HDL-CE by the liver. The indirect pathway, however, involves transport of CE from HDL to VLDL, LDL, and IDL mediated by CETP. CE eventually reaches the liver via the LDL-R. Furthermore, two important proteins, ABC-A1 and SR-BI, influence cholesterol movement between cells and extracellular acceptors (Bodzioch M *et al*, 1999). ABC-A1 interacts with nascent HDL and mediates efflux of cholesterol and phospholipids to HDL, while SR-BI interacts with mature HDL and influences the uptake of CE molecules by the liver. The rate of cholesterol efflux varies between different cell types and is under the influence of acceptor molecules. Ineffective cholesterol efflux in macrophages leads to the deposition of foam cells in the arterial wall and hence progressing atherosclerosis.

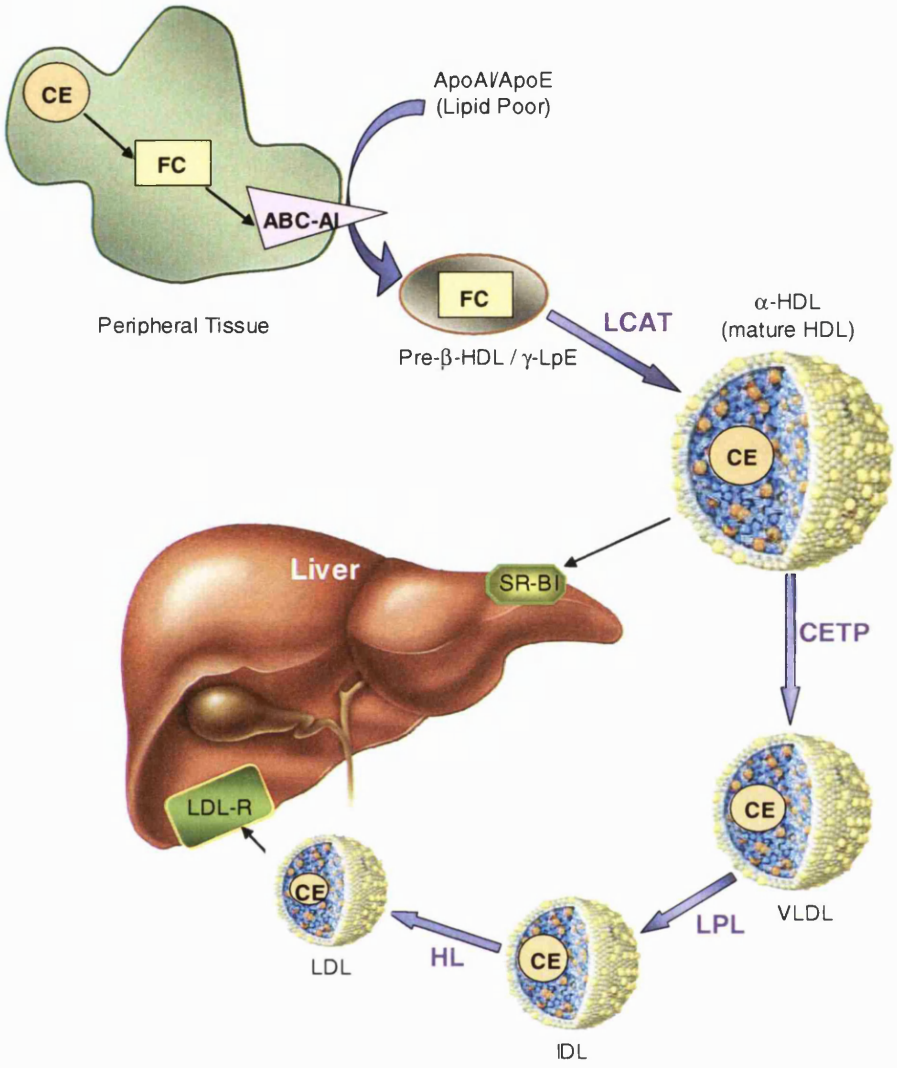

Figure 1.1 Schematic representation of reverse cholesterol transport (RCT) pathway. *RCT refers to the collection of cholesterol from peripheral cells, including those of the arterial wall, for delivery to the liver. Free cholesterol obtained from de novo synthesis or from cholesterol ester pools is sequestered in the cell surface by lipid poor apoAI or apoE. This process involves addition of phospholipid and cholesterol to the lipid-poor lipoproteins facilitated by ABC-A1. The resulting pre-β HDL or γ-LpE contains only apoAI or apoE. The cholesterol is esterified by LCAT forming mature HDL particles. Cholesterol esters in mature HDL are transferred to the liver directly via SR-BI without the concomitant uptake and degradation of the HDL. Alternatively, CE is routed back to the liver via an indirect route following transfer to the apoB-containing lipoproteins (VLDL/IDL/LDL) by CETP. The CETP-mediated pathway involves other enzymes (LPL, HL) and allows CE clearance by the liver through the LDL-R.*

1.2.3.3 Proteins That Influence HDL Lipid Content

There are a number of different proteins and enzymes involved in HDL metabolism and RCT. These include SR-BI, ABC-A1, LCAT (*Section* 1.4.3.2), phospholipid transfer protein (PLTP), CETP, and lipases, all of which are discussed briefly in this section.

SR-BI

SR-BI is a member of the CD36 protein superfamily that binds to HDL, LDL, and VLDL (Hauser H *et al*, 1998). It is an 83 kDa glycoprotein that is mainly expressed in liver and steroidogenic tissues (Hauser H *et al*, 1998). SR-BI expression in steroidogenic tissues is under the control of trophic hormones that influence uptake of HDL-cholesterol and synthesis of steroid hormones. In addition to facilitating the hepatic uptake of HDL-cholesterol (final step of RCT) SR-BI is also believed to be involved in the first part of RCT (ie efflux of cholesterol). Overexpression of hepatic SR-BI in mice results in reduction of HDL-cholesterol levels (Wang N *et al*, 1998), while mice with 50% of normal hepatic SR-BI expression, exhibit increased plasma HDL-cholesterol levels (Rigotti A *et al*, 1997). Consequently, levels of HDL-cholesterol are inversely correlated with the amount of expressed SR-BI. The paradox of SR-BI as a gene therapy candidate requires further investigation as its overexpression is believed to be atheroprotective despite lowering HDL-cholesterol. Polymophisms in SR-BI are thought not to be related to plasma HDL-cholesterol in humans (Acton S *et al*, 1999).

ABC-A1

ABC-A1 belongs to the ATP-binding cassette family of transmembrane transporters, the members of which hydrolyze ATP to carry diverse ligands such as ions, amino acids, phospholipids, vitamins, sterols, various drugs and sugars across membranes. About 49 members in humans have been identified so far with structural similarities. ABC-A1 itself was originally cloned by Chimini and co-workers (Luciani MF *et al*, 1994) and consists of two ATP-binding cassettes, two membrane spanning domains each with six transmembrane polypeptides, two large extracellular loops, and an amino-terminal section. This protein consists of 2201 amino acids with a molecular weight of 220 kDa. It is important in HDL metabolism by converting lipid-poor apoAI into nascent HDL particles. In the absence of ABC-A1, lipid-poor apoAI is rapidly cleared from plasma via kidney (cubilin-mediated pathway, *Section* 1.2.3.1) without acquiring any cellular lipids.

The combined effort of several groups led to the discovery of Tangier disease, a recessive disorder caused by mutations in the *ABC-A1* gene, resulting in defective removal of cellular cholesterol and phospholipids by lipid-poor apoAI (Brook-Wilson A *et al*, 1999; Bodzioch M *et al*, 1999; Rust S *et al*, 1999). *ABC-A1* mutations were reported in five families suffering from an autosomal dominant disorder known as familial HDL deficiency (FHD) (Rust S *et al*, 1999). As a result of an inability of apoAI to sequester cellular cholesterol and phospholipid to generate discoidal pre-β-HDL, the apoAI protein is rapidly catabolized by the kidney. Therefore, Tangier disease is characterized with extremely low levels of apoAI and HDL, and excess CE accumulation in cells (Owen JS, 1999). Heterozygous mutations of *ABC-A1* can lead to the development of familial hypoalphalipoproteinaemia that is characterized by low HDL-cholesterol and CE accumulation in tissues (Brooks-Wilson A *et al*, 1999). Patients with heterozygous mutations of *ABC-A1*, as well as ABC-A1 knock-out mice, have half the normal concentrations of HDL (Marcil M *et al*, 1999; McNeish J *et al*, 2000). ApoAI synthesis, secretion and gene sequence is reported to be normal in Tangier disease (Makrides SC *et al*, 1988).

PLTP and CETP

PLTP and CETP are plasma lipid transfer proteins that belong to the lipid transfer/polysaccharide binding protein (LBP) gene family (Yamashita S *et al*, 2001). In humans, PLTP has ~20% sequence homology to CETP. PLTP transfers phospholipids from lipoproteins and possibly cellular plasma membranes to HDL, whereas CETP is involved in the transfer of CE from HDL to apoB-containing lipoproteins in exchange for triglycerides (Lagrost L *et al*, 1998). The CE is ultimately taken up by peripheral cells or is routed towards the liver.

Lipases

Three triglyceride lipases: LPL, HL, and EL (endothelial lipase), belonging to the same family are involved in HDL metabolism (Bensadoun A *et al*, 1996). LPL is synthesized in adipose tissue and hydrolyses triglycerides in the triglyceride-rich lipoproteins, chylomicrons, and VLDL (Goldberg IJ *et al*, 1996). After hydrolysis of triglyceride-rich lipoproteins, their excess surface apolipoproteins and phospholipids are acquired by HDL. HL is synthesized in hepatocytes and hydrolyses triglycerides, and possibly phospholipids,

in HDL_2 leading to the formation of smaller HDL_3 particles (Rye KA *et al*, 1999). EL was cloned from a human monocyte macrophage cell line (THP-1) after treatment with oxidized LDL (Jaye M *et al*, 1999). It shares 45% and 40% homology with LPL and HL respectively. EL is believed to play a role in HDL metabolism by hydrolyzing HDL phospholipids though more studies are required to confirm this (Jaye M *et al*, 1999).

1.2.4 APOLIPOPROTEINS

Human apolipoproteins are designated by five different letters including apoAs (apoAI, apoAII, apoAIV, and newly discovered apoAV), apoBs (apoB-48, and apoB-100), apoCs (apoCI, apoCII, and apoCIII), apoD and apoE. Other apolipoproteins such as apoH (Takada D *et al*, 2003), apoJ/clusterin (Trougakos IP *et al*, 2002), apoL (Page NM *et al*, 2001), and apoM (Richter S *et al*, 2003) are reported in the literature. The coding regions of the apolipoprotein gene family consist of tandem repeats of 11 codons suggesting that they have evolved by duplication of a primordial gene (Luo CC *et al*, 1986). The helical content of apolipoproteins is high based on data from circular dichroism spectroscopy. All apolipoproteins contain internal sequence repeats that are believed to form amphipathic α-helices (Luo CC *et al*, 1986). These α-helices act as protein detergents to stabilize the structure and size of lipoproteins (Luo CC *et al*, 1986). Generally, apolipoproteins are involved in lipid metabolism including acting as co-factors for enzymatic reactions, being ligands for lipoprotein receptors, and maintaining structural integrity of lipoproteins.

1.3 Apolipoprotein (Apo) E

1.3.1 APOE DISCOVERY AND TISSUE DISTRIBUTION

ApoE is a significant plasma lipid carrying protein present in all lipoprotein particles with the exception of LDL. It was originally discovered in the early 1970s as an "arginine-rich protein" (ARP) (Shore VG *et al*, 1973), prior to the designation of "apoE", which was universally adopted in the late 1970s (Utermann G, 1975).

ApoE is synthesized and secreted by many tissues, with the major site being liver (Blue ML *et al*, 1983). In humans and rats, the brain is considered to be the second important site of apoE synthesis. Astrocytes are the predominant site of brain apoE synthesis (Boyles JK *et*

al, 1985). Macrophages are significant producers of extrahepatic apoE (Basu SK *et al*, 1981) (*Section* 1.3.6.2). Furthermore, apoE is localized in keratinocytes assisting lipid uptake and redistribution in the epidermis (Barra RM *et al*, 1994). ApoE synthesis has also been demonstrated in human kidney, adrenal glands, and ovaries (Blue ML *et al*, 1983).

1.3.2 APOE STRUCTURE

ApoE has a 22 kDa amino terminal domain joined by a hinge to a 10 kDa carboxy terminal domain as observed after digestion by thrombin (Aggerbeck LP *et al*, 1988). Extensive analysis of the secondary structure of apoE revealed the functional properties of each of the named domains. The NH_2 terminal contains the receptor-binding and heparin proteoglycan-binding regions, while the COOH terminal forms amphipathic α-helices and is proven to mediate binding of apoE to the surface of lipoproteins (Weisgraber KH, 1990). All apolipoproteins have lipid-binding capacity as a result of having amphipathic α-helices.

There are three α-helical regions in the carboxy terminal, namely helix 1 (residues 203-223), helix 2 (residues 225-266), and helix 3 (residues 268-289). In the absence of lipids, apoE self-associates as a tetramer over a range of concentrations (Aggerbeck LP *et al*, 1988). C-terminal truncation studies by Westerlund *et al* demonstrated the importance of helix 3 in tetramer formation as well as for lipoprotein association (Westerlund JA *et al*, 1993). The amino terminal domain of apoE is similar to other globular proteins and remains monomeric in solution (Aggerberck LP, 1988). The tertiary structures of the amino terminal domain of apoE isoforms have been determined by X-ray crystallography (Dong LM *et al*, 1996). This domain contains the following four antiparallel helices: helix 1 (residues 44-53), helix 2 (residues 54-81), helix 3 (residues 87-122), and helix 4 (residues 130-164). The four helix bundle undergoes a conformational change exposing a hydrophobic phase that allows interaction with lipids (Weisgraber KH, 1994b). Acidic and basic residues in this region are mainly involved in salt-bridges that increase the stability of this bundle (Weisgraber KH, 1994b).

The receptor-binding site (residues 136-150) is situated in helix 4, which is enriched in basic amino acids (Arg_{136}, His_{140}, Arg_{142}, Lys_{143}, Arg_{145}, Lys_{146}, Arg_{147}, and Arg_{150}). The importance of these residues for receptor binding has been demonstrated by chemical

modification (Mahley RW *et al*, 1977). ApoE possesses two heparin binding sites, one (residues 142-147) coincides with the receptor binding region. The second heparin binding region is located between amino acids 202-243 as indicated from experiments with synthetic peptides (Cardin AD *et al*, 1986).

1.3.3 APOE BIOSYNTHESIS AND GENE REGULATION

Direct amino acid sequencing of apoE purified from human VLDL was the initial step in determining the primary structure of this protein (Rall SC *et al*, 1992). This was later confirmed by nucleic acid sequencing of rat apoE full-length cDNA (McLean JW *et al*, 1983). Discovery of the primary structure of apoE provided many insights into its function. The human *APOE* gene (3.7 kb) contains four exons separated by three introns and is located on chromosome 19q13.2 (Das HK *et al*, 1985). ApoE is synthesized as a 317 amino-acid prepeptide. An 18-residue signal peptide is cleaved co-translationally during protein translocation through the endoplasmic reticulum membrane yielding the 34 kDa apoE glycoprotein consisting of 299 amino acids (Das HK *et al*, 1985). The LDL receptor, apoCII, apoCI, and apoCI pseudogene have also been mapped to chromosome 19 (Francke U *et al*, 1984; Humphries SE *et al*, 1984). However, only apoCI and apoCI pseudogene are linked to *APOE*.

The TATAATT promoter sequence is located approximately 30 base pairs upstream from the transcriptional initiation site of *APOE*. Two enhancers from human apoE flanking sequence, termed multienhancer 1 (ME1) and multienhancer 2 (ME2), have been shown to direct macrophage- and adipose-specific expression of apoE in transgenic mice (Shih SJ *et al*, 2000). Later apoE transcription by macrophages and adipose tissue was reported to be under the control of liver X receptor (LXR)/retinoid X receptor (RXR) hetrodimers through their interaction with conserved LXR response element present in both ME1 and ME2 (Laffitte BA *et al*, 2001). Recently, Liang *et al* provided evidence that LXR/RXR hetrodimers also regulate apoE tissue expression in astrocytes (Liang Y *et al*, 2004).

1.3.4 APOE POLYMORPHISM

Single nucleotide polymorphisms (SNPs) of the apoE gene were first reported about 20 years ago (Rees A *et al*, 1983), and have been extensively studied. Polymorphism of *APOE* was first described by Utermann *et al* (Uttermann G *et al*, 1979). Later, direct sequencing of

the cDNA and isoelectric focusing (IEF) of the protein confirmed the existence of three common alleles (ε2, ε3, and ε4) producing three major apoE isoforms; apoE2, apoE3, and apoE4 (Zannis VI *et al*, 1981). This genetically determined polymorphism leads to the presence of six different phenotypes in human subjects: three homozygous phenotypes (apoE2/2, apoE3/3, and apoE4/4) and three heterozygous phenotypes (apoE2/3, apoE2/4, and apoE3/4). As shown in Table 1.1, apoE4 is the most cationic isoform differing from apoE2 and apoE3 by two charge units and one charge unit, respectively. Furthermore, at least 30 rare apoE variants have been described (de Knijff P *et al*, 1994).

ApoE isoform	Residue 112	Residue 158	Relative IEF charge
ApoE2/E2	Cys	Cys	0
ApoE3/E3	Cys	Arg	+1
ApoE4/E4	Arg	Arg	+2

Table 1.1 Arginine-cysteine interchanges of the three homozygous apoE phenotypes: apoE2/E2, apoE3/E3, and apoE4/E4. *ApoE3/3 contains cysteine (Cys) at position 112 and arginine (Arg) at position 156, while apoE4/4 has Arg at both positions and apoE2/2 has Cys at both positions (the only Cys residues in apoE). These isoforms differ in isoelectric point by one charge unit, apoE4 being the most basic and apoE2 the most acidic isoform.*

The polymorphism in the *APOE* gene affects the level of its product; apoE2 is associated with higher concentrations of apoE and apoE4 with lower concentrations (Siest G *et al*, 1995). The ε3 allele is the most frequent (~72%) in the general population based on studies of *APOE* allele distribution in a variety of populations (Corbo RM *et al*, 1999). The allelic frequencies of ε2 and ε4 were estimated at 0.11 and 0.17 respectively (Corbo RM *et al*, 1999). ApoE2 has only 1% of the normal affinity for binding to the LDL receptor. Patients with homozygous apoE2 are predisposed to type III hyperlipidaemia (Mahley RW *et al*, 1989). In addition, the ε2 allele has the potential to provide protection from the development of coronary atherosclerosis (Weisgraber KH, 1994b). Many studies have demonstrated an association between apoE4 and late-onset familial and sporadic forms of Alzheimer's disease while apoE2 might be protective against this neurological disorder (Corder EH *et al*, 1998; Weisgraber KH *et al*, 1994a). Furthermore, apoE4 is linked to dominant hyperlipidaemia even though this isoform displays normal receptor binding ability

(Siest G *et al*, 1995). In humans, this isoform is also associated with CHD risk in females but not in males (Wilson PW *et al*, 1994). In addition, individuals with the apoE4 isoform are more prone to restenosis while those with apoE3 isoform are thought to be protected (Tada H, 2001). Finally, different apoE alleles determine the outcome of several viral and bacterial infections as discussed in *Section* 1.3.6.3.

Non-genetically determined polymorphism of apoE arose from results showing degrees of post-translational sialylation of the mature protein (Zannis VI *et al*, 1981). About 10-20% of plasma apoE is accounted for by these sialylated isoforms, which arise from unique O-linked glycosylation of threonine at position 194 of apoE (Wernette-Hammond ME *et al*, 1989). This glycosylation has no effect on the production and secretion of apoE into the circulation and about 90% of the protein in plasma is desialylated.

1.3.5 APOE RECEPTORS

LDL-R was the first discovered apoE receptor (Brown MS *et al*, 1986). Although initially shown to mediate the uptake of LDL via apoB-100, it can also bind apoE-containing lipoproteins. LDL-R is present in many cell types and expressed in different tissues including liver. It has the following five domains: an amino terminal domain, a unit of five tandom YWTD repeats (~50 residues) followed by a cluster of three epidermal growth factor (EGF) precursor repeats, an O-linked sugar domain enriched in clusters of serine and threonine, a short transmembrane domain of ~20 amino acids, and a cytoplasmic domain containing a tetra-amino acid NPxY (asparagine-proline-x-tyrosine) consensus sequence that is involved in receptor internalization via coated pits (Yamamoto T *et al*, 1996). The amino terminal domain is the ligand-binding region having seven type A repeats consisting of ~40 residues, each having six cysteine residues that are disulphide bonded in the following pattern: one to three, two to five, and four to six. Ligand-binding is abolished by the reduction of these disulphide bridges (Brown MS *et al*, 1997).

Additional stabilization of the ligand-binding region is achieved by formation of complexes between each of the type A repeats and Ca^{2+} ions (Fass D *et al*, 1997). The EGF precursor region consists of type B repeats (containing six cysteine residues each) and tetrapeptide YWTD (tyrosine-tryptophan-threonine-aspartate). It is responsible for the acid-dependent dissociation of ligands from the LDL-R (Davis CG *et al*, 1987). In 1998, Herz *et al*

discovered that the LDL-R belongs to a group of receptors with similar structural domains known as the LDL receptor family (LRF) (Herz J *et al*, 1988). Members of LRF include the prototypic LDL-R itself, LRP, VLDL receptor (VLDL-R or LR8), apoE receptor 2 (apoE-R2), and gp330/megalin (Kim DH *et al*, 1996; Chatelet F *et al*, 1986). Members of the LRF differ in size and tissue distribution, but they all recognize apoE. The role of these receptors in remnant metabolism and lipoprotein interaction with cells has been studied extensively. Furthermore, they are implicated in signaling mechanisms critical for a number of cellular processes (Hoang BH *et al*, 2004).

1.3.6 PHYSIOLOGICAL FUNCTIONS OF APOE

1.3.6.1 ApoE and Lipid Metabolism

ApoE is found in chylomicrons and their remnants, in VLDL, and in HDL, and plays an important role in distribution of lipids between different tissues. It is involved in the metabolism of dietary (chylomicrons) and endogenous (VLDL) triglycerides and cholesterol, which it delivers to extrahepatic cells (via VLDL and its remnants) or directly to the liver (via chylomicron remnants). In the liver, cholesterol is eliminated via the bile, and fatty acids are resecreted as triglycerides within VLDL. In addition to this "endocrine-like" function, apoE also possesses a "paracrine-like" function, which includes lipid distribution within a tissue (Mahley RW *et al*, 1999).

The delivery of lipids via apoE is achieved through two receptor pathways, the LDL-R pathway, and the HSPG/LRP pathway (*Figure* 1.2) (Mahley RW *et al*, 1999). ApoE exhibits 25-fold higher affinity than apoB-100 for the LDL-R (Innerarity TL, 1987). Cholesterol-enriched remnant lipoproteins are cleared from plasma by the liver via the LDL-R or LRP facilitated by apoE (Rohlmann A *et al*, 1998). VLDL contains apoE and undergoes a lipolytic cascade producing VLDL remnants and IDL both of which contain apoB-100 and apoE. IDL and VLDL remnants are cleared by the liver as a result of interaction of apoE with the LDL-R and the HSPG/LRP pathway. However, in healthy humans almost all the IDL is converted to LDL through the action of HL. Mature LDL is also degraded primarily by the liver via the LDL-R, but through apoB-100 (*Figure* 1.2).

From studies of patients with FH (having defective or absent LDL-R), it was deduced that LDL and remnant metabolism occur through different pathways. This led to the discovery

of the HSPG/LRP pathway. This multi-step pathway is for hepatic metabolism of remnant lipoproteins. Initially, the sequestration occurs whereby lipoproteins are captured in the space of Disse and bound to HSPG with the aid of apoE and HL. In a process known as secretion capture, large amounts of lipid-free apoE are secreted by hepatocytes in the space of Disse, facilitating remnant clearance (Ji ZS *et al*, 1994). This is followed by lipolytic processing that involves HL and LPL (Ji ZS *et al*, 1994; Mulder M *et al*, 1993). Finally, lipoproteins are taken up for internalization via one of the three following routes: 1) transfer from HSPG to LRP, 2) transfer after forming a tertiary complex by binding to HSPG and LRP, 3) transfer via HSPG alone (Ji ZS *et al*, 1994). Reduction of lipoprotein lipolysis has been demonstrated as a result of apoE accumulation on the surface of these macromolecules (Huang Y *et al*, 1998). In addition, an increase in apoE concentration in plasma causes elevation of VLDL synthesis and secretion (Huang Y *et al*, 1999).

Several reports indicate recycling of apoE after the internalization of the lipoprotein particle (Schwiegelshohn B *et al*, 1995; Fazio S *et al*, 1999). This physiological phenomenon is not dependent on the existence of endogenous apoE or the LDL-R. Linton *et al* analyzed liver sections of mice deficient in LDL-R and apoE and hypothesized events leading to apoE recycling (Linton MF *et al*, 1998). Based on their data, after lipoprotein entry into the endosome, a drop in pH separates apoE from the lipoprotein while the receptor is still attached to apoE. Following dissociation from the receptor, apoE is recycled and is involved in important physiological functions such as cholesterol efflux or capture of new remnant lipoproteins.

Chylomicron- and VLDL-derived apoE was shown to recycle back to the plasma membrane following receptor-mediated endocytosis of these lipoproteins into the liver. The recycled apoE was then associated with HDL (Heeren J *et al*, 2001). It was later reported that HDL_3 acts as an extracellular acceptor for the recycled apoE and that this recycling is accomponied by mobilization of cellular cholesterol (ie cholesterol efflux) from human hepatoma cells and fibroblasts (Heeren J *et al*, 2003).

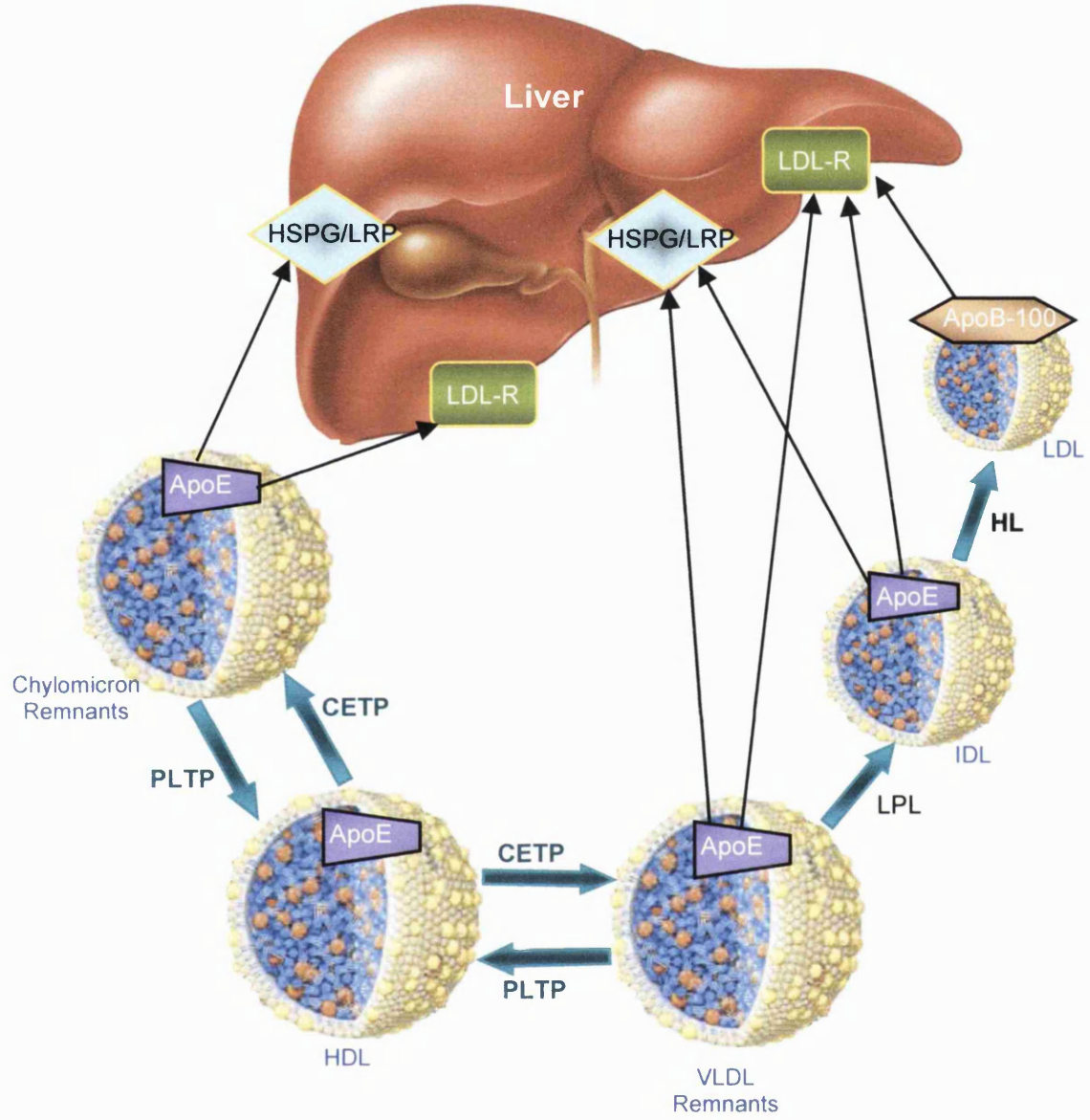

Figure 1.2 Role of apoE in lipoprotein metabolism. *ApoE acquired from HDL becomes a protein constituent of chylomicron remnants and VLDL remnants. This is under the influence of CETP that mediates the transfer of CE from HDL to the remnant lipoproteins. Another enzyme, PLTP, is involved in the transport of phospholipids in the opposite direction. ApoE mediates hepatic clearance of chylomicron remnants via LDL-R and/or HSPG-LRP pathway. VLDL undergoes a lipolytic cascade producing VLDL remnants, IDL, and LDL. VLDL remnants and IDL contain apoE and apoB-100, but are taken up by the liver as a result of apoE interaction with LDL-R or HSPG-LRP pathway. However, in healthy individuals, almost all of the IDL is converted to LDL that has apoB-100 as its main protein. LDL uptake by the hepatocytes is achieved via apoB-100 and through the LDL-R pathway.*

1.3.6.2 Macrophage-Secreted ApoE

Although the majority of apoE in plasma is produced by hepatocytes, significant amounts are secreted by macrophages including those present in atherosclerotic plaques (O'Brien KD *et al*, 1994). Macrophages secrete apoE in association with sphingomyelin as a component of spherical-shaped lipoproteins that are similar in size to HDL but solely contain apoE. The lipoprotein is 12-16 nm in diameter and is referred to as γ-LpE due to exhibiting γ-mobility upon electrophoresis (Huang Y *et al*, 1994). Expression of macrophage apoE is modulated by cholesterol and cytokines at transcriptional level (Duan H *et al*, 1995).

γ-LpE is atheroprotective in part due to apoE-mediated efflux of cholesterol from macrophages (Mazzone T *et al*, 1994). Macrophage-specific expression of apoE in transgenic mice has been demonstrated to protect against atherosclerotic lesion development even in the presence of atherogenic circulating lipoproteins (Bellosta S *et al*, 1995). In addition, expression of γ-LpE in apoE (-/-) mice by apoE transgene macrophages, restored the cholesterol efflux capacity of apoE-deficient plasma (Zhu Y *et al*, 1998). Thus, apoE whether secreted from hepatocytes or derived from macrophages is anti-atherogenic as will be discussed more in *Section* 1.6.2.

1.3.6.3 Other Functions of ApoE

ApoE-containing lipoproteins and LDL can inhibit or stimulate antigen- and mitogen-induced T lymphocyte activation and proliferation (Cardin AD *et al*, 1988). Binding of low concentrations of apoE-containing lipoproteins and LDL to LDL-R improves responsiveness of lymphocytes to mitogens causing lymphocyte proliferation (Cuthbert JA *et al*, 1984). Hui *et al* showed that apoE-containing lipoproteins are about three times more effective than apoB-containing lipoproteins in the inhibition of lymphocyte proliferation (Hui DY *et al*, 1980a). In addition, apoE that is defective in LDL-R binding, as well as lipid-free apoE, suppress proliferation of lymphocytes (Cuthbert JA *et al*, 1984). The transferrin receptor and HSPG have been proposed as immunoregulatory receptors for apoE. They function in concert to bind apoE and initiate inhibition of lymphocyte proliferation (Hui DY *et al*, 1980b).

Another function of apoE that adds to its anti-atherogenecity repertoire is stimulating endothelial cells to produce heparin sulphate (Paka L *et al*, 1999). This molecule has anti-atherogenic activities by preventing association of monocytes with the matrix and inhibiting smooth muscle cell proliferation. In addition, Riddell and colleagues reported another atheroprotective function for apoE due to inhibition of platelet aggregation (Riddell DR *et al*, 1997). This is due to the release of nitric oxide (NO), a free radical anti-atherogenic gas, by platelets. Furthermore, macrophage-derived apoE is anti-inflammatory at the lesion site by stimulating endothelial cells to release NO and suppress VCAM-1 (vascular cell adhesion molecule-1) expression (Stannard AK *et al*, 2001).

It is possible that apoE plays a role in reducing susceptibility to bacterial infections as shown in studies with *Listeria monocytogenes* (Roselaar SE *et al*, 1998) and *Klebsiella pneumoniae* (de Bont N *et al*, 1999). In addition, the ε2 allele may be a risk factor for early infection by the malaria protozoon as was shown by studies in infants infected with the parasite (Wozniak MA *et al*, 2003).

A significant association has been found between possession of the ε4 allele and severity of liver damage caused by hepatitis C virus (HCV) (Wozniak MA *et al*, 2002). As outlined in *Section* 1.3.6.1, apoE binds to a number of cell surface receptors including LDL-R and HSPG. HCV and human immunodeficiency virus (HIV) also bind to similar sites of these receptors (Dobson CB *et al*, 1999). As a consequence, each virus might compete with apoE for entry into cells. For example, there may be a competition between HCV and apoE isoforms in binding to HSPG for entry into cultured hepatocytes with apoE4 competing more efficiently than the other isoforms (Mamotte CD *et al*, 1999). This could explain the protective effects of apoE4 against HCV-mediated damage of liver cells. This mechanism might also apply to the findings of Wozniak *et al* with regard to influence of apoE in determining the outcome of infection with malaria since this parasite also uses a member of the LRF as well as HSPG for invading hepatocytes (Marshall P *et al*, 2000). Since the affinities of the apoE isoforms for receptors on HepG2 cells differ (apoE4 higher affinity than the other two isoforms), the extent of the parasite entry into cultured cells can be determined by the apoE isoform of the host (Mamotte CD *et al*, 1999).

ApoE is also linked to neurodegenerative disorders such as Alzheimer's disease. ApoE2 is protective against neurological disorders while apoE4 is associated with such defects (Weisgraber KH *et al*, 1996; Slooter AJC *et al*, 1997). HIV-infected subjects carrying the ε4 allele have excess dementia and peripheral neuropathy (Corder EH *et al*, 1998). ApoE3 and apoE2 isoforms modulate neurite extension (Nathan BP *et al*, 1994). Conversely, apoE4 is believed to have an inhibitory effect on neurite outgrowth (Nathan BP *et al*, 1995). Elevated levels of apoE might be associated with the pathology of schizophrenia as reported by Dean and co-workers (Dean B *et al*, 2003). Harrington *et al* demonstrated changed frequencies of differing *APOE* alleles in schizophrenia (Harrington CR *et al*, 1995). However, other researchers failed to show such a correlation (Durany N *et al*, 2000; Hong CJ *et al*, 2000).

1.4 Apolipoprotein (Apo) AI

1.4.1 APOAI TISSUE DISTRIBUTION AND GENE REGULATION

ApoAI is the major protein component of circulating HDL particles comprising ~70% of the total protein. It is a multifunctional and exchangeable protein found in fish, birds and mammals (Narayanaswami V *et al*, 2000). Human apoAI is synthesized in liver and small intestine as pre-pro-apoAI that undergoes proteolytic processing to cleave the 18 amino acid signal peptide co-translationally. As a result the 249 amino acid pro-apoAI is formed, which is further processed to the mature form of 243 residues (Brewer HB *et al*, 1978).

Brewer and colleagues were the first group to determine the sequence of apoAI (Brewer HB *et al*, 1978) prior to cloning and characterization of its cDNA (Breslow JL *et al*, 1982) and genomic DNA (Karathanasis SK *et al*, 1983). The gene encoding apoAI belongs to a cluster of genes encoding other apolipoproteins (apoCIII, apoAIV, and apoAV) that is located on chromosome 11q23-q24.

1.4.2 APOAI STRUCTURE

Structural studies of apoAI are mainly performed on homogeneous populations of discoidal HDL particles obtained by detergent dialysis or reaction of apoAI with phospholipid vesicles as summarized by Jonas *et al* (Jonas A, 1986). A vast range of biophysical

techniques such as polarized attenuated total internal reflection (PATIR) infrared spectroscopy in addition to recombinant proteins expressing proteins with specific deletions or mutations of specified amino acid residues have been used to better understand apoAI structure-function relationships. It has been demonstrated that particular regions of apoAI are involved in each of its physiological functions. ApoAI consists of an N-terminal domain (residues 1-98) separated by a central hinge region from a C-terminal domain (residues 187-243). The N-terminal domain is highly conserved between mammals while the C-terminal domain has conservative substitutions between species (Collet X *et al*, 1997). Helix 44-65 from the N-terminal domain, and 210-241 from the C-terminal domain are important in lipid binding. Additionally, in the central domain, helix 100-121 is involved to a lesser extent in lipid association and maturation of HDL. In its secondary structure, apoAI consists of a series of 11- and 22-mer repeats of amphipathic α-helices (McLachlan AD, 1977).

The "bicycle tyre" model was originally suggested by Segrest and co-workers for the orientation of amphipathic α-helices of apoAI on discoidal HDL particles (Segrest JP *et al*, 1974). In this model, apoAI has a disc-shaped structure with the helices forming a strip around the disk with tangential orientation. Further structural studies of apoAI led to the proposal of two other models namely, the "belt model" and the "picket-fence" model. In the belt model, the helices are perpendicular to the lipid acyl chains, while in the picket-fence model, the helices are parallel to the phospholipid bilayer surface (Tall AR *et al*, 1977). Further investigation is required to determine the orientation of apoAI in lipid complexes under native conditions.

1.4.3 PHYSIOLOGICAL FUNCTIONS OF APOAI

1.4.3.1 ApoAI and RCT

It is well accepted that ApoAI is the main activator of cholesterol efflux from peripheral cells, the first step of RCT (*Section* 1.2.3.3). ApoAI is the preferential acceptor of cellular cholesterol and the major co-factor of LCAT (*Section* 1.4.3.2) (Rothblat GH *et al*, 1992).

It is believed that the C-terminal domain of apoAI is involved in cholesterol efflux mediated by passive aqueous phase diffusion (Frank PG *et al*, 1998). Studies in naturally occurring mutants of apoAI indicated that those mutants that can associate with phospholipid have the

ability to promote cellular cholesterol efflux (Burgess JW *et al*, 1999). Some mutations lead to the dimerization of apoAI via covalent cysteine bridges and hence influence the accessibility of the C-terminal domain for lipid binding. ApoAI-milano (apoAI-M), a naturally occurring apoAI mutant (Cys173Arg), dimer has an increased ability for cholesterol efflux from macrophages and Fu5AH rat hepatoma cells compared to wild-type apoAI (Calabresi L *et al*, 1999). Investigations into the importance of the N-terminal domain in cholesterol efflux requires further attention. Direct interaction between apoAI and ABC-A1 leads to the formation of phospholipid-apoAI complexes that are essential for ABC-A1 facilitated cholesterol efflux (Wang N *et al*, 2001).

1.4.3.2 LCAT and its Activation via ApoAI

Human LCAT is a glycoprotein with a relative molecular mass of ~65 kDa. Loop sections, β-sheets and α-helical segments comprise its secondary structure. This enzyme is mainly hepatic in origin, but is found at a very low concentration in the cerebrospinal fluid (CSF) and in the brain. Its function in the brain is as yet unknown, however in plasma it is the key enzyme in maintaining cholesterol homeostasis mainly by esterification of FC present in circulating lipoproteins (Jonas A, 1998). LCAT catalyses the transacylation of the sn-2 fatty acid of lecithin to the 3-β-hydroxyl group of cholesterol, generating lysolecithin and CE. In addition to this acyltransferase activity, LCAT also has a phospholipase A_2 activity since it can hydrolyse the sn-2 fatty acid from phosphatidylcholine.

The major substrate of the acyltransferase activity of LCAT is HDL that contains apoAI, the preferred co-factor of LCAT. The activity of LCAT at the surface of HDL and LDL is referred to as α and β activity respectively. The former requires the presence of apoAI or apoAIV, which are absent in β activity (Jonas A, 1998). In addition to its role in altering the plasma concentration of HDL and apoB-containing lipoproteins, LCAT is essential for maturation of HDL particles, facilitating RCT, and assisting in clearance of the surface coat of triglyceride-rich lipoproteins following lipolysis. LCAT aids HDL in protection of LDL particles from oxidation by hydrolysing phosphatidylcholines formed from oxidation of lipids (Subramanian VS *et al*, 1999).

Human *LCAT* gene and cDNA were cloned and sequenced by McLean and colleagues (McLean J *et al*, 1986). This gene is located on chromosome 16q encoding a protein with 416 amino acid residues. Several mutations in the human LCAT gene have been identified of which the most severe ones are associated with the development of familial LCAT deficiency (FLD) and fish-eye disease (FED) (Kuivenhoven JA *et al*, 1997). FLD is characterized by the complete absence of plasma LCAT activity, while in FED only the α-activity of this enzyme is eliminated. In both groups of patients, apoAI and apoAII synthesis is normal, however plasma concentration of these apolipoproteins is reduced due to the loss of maturation of nascent HDL particles as a result of LCAT deficiency (Rader DJ *et al*, 1994).

LCAT can directly bind lipids and hydrolyse small soluble substrates, but optimum reaction requires activation by one of the exchangeable apolipoproteins, of which apoAI is the most potent as it activates LCAT 80% more than other apolipoproteins (Steinmetz A *et al*, 1985). Both enzymatic activities of LCAT, acyltransferase and phospholipase A_2, are under the influence of apoAI (Sparks DL *et al*, 1998). The lipid and apolipoprotein composition of HDL can modulate the charge and conformation of apoAI and thus influence its effect on LCAT (Sparks DL *et al*, 1998). Several studies have shown the importance of the central domain of apoAI (residues 144-186) in the activation of LCAT (Dhoest A *et al*, 1997). Though the underlying mechanism is still unclear, it is believed that the positive charges in the central region of apoAI interact with the negative charges present on residues 152-169 of LCAT (Sparks DL *et al*, 1998). However, the C-terminal domain of apoAI was suggested as not being essential for the activation of this plasma esterifying enzyme (Han H *et al*, 1999). Affinity for phospholipids is also required for efficient LCAT activation, and this is attributed to the last helix (220-241) of the C-terminal domain. The N-terminal domain (residues 1-43) of apoAI might indirectly influence activation of LCAT as a result of its interaction with the central domain that stabilizes the protein when in a lipid-free state. Point mutations of specific residues in the N-terminal domain might shed light on its exact involvement in various physiological roles of apoAI.

1.4.3.3 Other Functions of ApoAI

In addition to its major responsibility in the anti-atherogenic properties of HDL, apoAI displays other properties that may be involved in HDL protection against vascular disease. ApoAI inhibits LDL oxidation and thus protects endothelial cells from the cytotoxic effects of oxidized LDL (Suc I *et al*, 1997). Miyazaki *et al* reported involvement of apoAI in preventing cholesterol accumulation in macrophages by modified LDL (Miyazaki A *et al*, 1994). ApoAI has been demonstrated as a stabilizing factor for prostacyclin and for stimulating the release of this compound in smooth muscle cells (Vinals M *et al*, 1997).

1.5 Gene Therapy

1.5.1 UNDERLYING CONCEPT

Gene therapy is a broad term encompassing any approach to treating or preventing disease by introducing an exogenous gene, gene segments or oligonucleotides into an affected individual. The recent completion of the human genome project and advances in functional genomics has provided tremendous insight into discovering novel therapeutic interventions. Gene therapy is regarded by many to potentially revolutionize medicine in the next decade with its major aim of eradicating the cause of a disease ahead of the onset of its symptoms. A committee appointed by the National Institute of Health (USA) recommended that gene therapy trials should be focused on more basic preclinical studies instead of premature clinical trials (Wadman M, 1995). Experiments from 1996 onwards have mainly focused on improvement of: a) specificity and efficiency of gene transfer; b) duration of expression; c) immunogenicity; and d) ease of manufacturing. Each gene transfer system available has inherent advantages and disadvantages, and will be discussed in *Sections* 1.5.3-1.5.6.

Gene therapy strategies can be classified into three distinct approaches: gene augmentation, modulation of gene expression, and gene repair. Gene augmentation involves the introduction of a new therapeutic gene or a correct copy of a mutant gene into the cells of an affected individual, usually under the control of an heterologous promoter. It can be applied to the treatment of cancers and genetic disorders, and in transplantations (Dhabhars FS, 2003). However, the genetic defect should generally be a loss-of-function mutation as the

mutant gene remains unmodified after the treatment. Exceptions to this rule arise when the therapeutic gene has either a cytotoxic or an epistatic effect on the host.

Modulation of gene expression is mainly applied to disorders where there is no genetic defect, but an abnormal expression of normal genes or allelic variations of normal genes that can become pathogenic (reviewed in Jarad G *et al*, 2003). This can be applied to multigenic disorders such as hypertension and viral infections, including HIV-1 (human immunodeficiency virus type-1) (Lee NS *et al*, 2002) and hepatitis (Morrissey DV *et al*, 2002). The majority of studies investigating the modulation of gene expression are based on using antisense or ribozymes which are small RNA molecules interfering with gene expression in a number of ways such as blocking mRNA maturation, and degrading mRNA. Additionally, RNA-mediated gene interference (RNAi) has recently opened up an exciting avenue in gene expression modulation. RNAi utilizes an endogenous cellular pathway that inhibits mRNA translation or degrading mRNA (Hannon GJ, 2002).

Gene repair involves the repair of a mutant endogenous gene, at either the DNA or RNA level. It can be achieved by delivering only a portion of a gene to cells. In addition, repair agents may be biologicals or synthetic pharmaceuticals. Antisense oligomers, ribozymes, and RNA-DNA oligonucleotides (RDOs) are a few examples of practical methods available to repair of a mutant gene. Gene repair is further discussed in *Sections* 1.5.5 and 1.5.6.

1.5.2 SOMATIC GENE TRANSFER

Gene therapy has the potential to be applied to both somatic and germ line cells even though all the reported clinical studies have been directed towards somatic cells. Germ line gene therapy has been the subject of numerous ethical debates (Wadman M, 1998). Currently it is prohibited in human subjects in most countries. Somatic cells can be subject to *in vivo* or *ex vivo* gene transfer. In the former approach, the genetic material is directly administered to patients by means of gene transfer vehicles. It is beneficial for tissues where cells cannot be cultured in sufficient quantities or re-implantation of cultured cells are difficult. *In vivo* gene targeting is economically beneficial as it is not patient-specific. In the *ex vivo* approach, genetic material is inserted into the patient's cells grown *in vitro* often prior to the expansion of the transfected cells and their introduction back into the patient (Van Tendeloo VF *et al* 2001). Autologous cells are used in order to avoid rejection by the host's immune

system. Even though the *ex vivo* approach may be an effective gene therapy strategy, it has the disadvantage of being patient specific. This creates an inherently costly approach, which also requires extensive cell manipulation and quality control.

1.5.3 VIRAL GENE TRANSFER SYSTEMS

One of the main challenges facing today's genetic engineers is the development of efficient and safe carriers (vectors) for transferring the therapeutic gene into a cell. Viral and non-viral vectors are two types of transfer techniques commonly used in gene therapy. Viral vectors generally offer efficient routes for gene transfer when compared to non-viral systems (Mountain A, 2000). However, there are many potential adverse repercussions associated with the use of viral vectors including one or more of the following: a) random integration into the host chromosome with possible activation of proto-oncogenes leading to tumor formation, b) clearance of viral vectors delivered systemically due to complement activation, c) generation of an immune response to the *in vivo* delivered viral vector in addition to a humoral immune response to some viral vectors as a result of previous exposure to the naturally occurring virus, d) possible generation of replication competent virus through recombination of the viral vector with DNA sequences in the host chromosome, e) size limitation of the virally packaged therapeutic genes, f) high cost for producing large quantities of viral stock for clinical use, and g) the inability to administer certain viral vectors more than once (Fox JL, 1999).

1.5.3.1 Retroviruses

Oncoretroviruses (mammalian and avian C-type retroviruses), lentiviruses (*Section* 1.5.3.2), and spumaviruses are all lipid-enveloped particles belonging to the retroviral family. Their genome comprises two long terminal repeat (LTR) sequences framing the *gag*, *pol*, and *env* genes encoding the structural proteins, nucleic acid polymerases/integrases, and surface glycoproteins, respectively. The majority of first generation retroviruses are less immunogenic than adenoviruses (*Section* 1.5.3.3) due to lack of expression of residual viral genes. Retroviruses, with the exception of the lentivirus sub-class, are ineffective in transfecting non-proliferating or poorly-proliferating cells such as macrophages since productive transduction by retroviral vector is strictly dependent on mitosis of target cells (Miller DG *et al*, 1990); nuclear membrane disruption is required for viral access of the chromatin (Roe T *et al*, 1993). Another drawback of retroviruses is their small insert-size

limit, typically of ~8 kb. Encouraging clinical results of gene therapy have been obtained with retroviruses largely due to their capability of prolonged expression, but have been associated with a number of serious adverse events (*Section* 1.5.7).

1.5.3.2 Lentiviruses

Like retroviruses, this group of transfer systems can take up to 8 kb of exogenous DNA. However, they have a more complex genome; encoding a number of additional regulatory genes (including *tat* and *rev*), in addition to the *gag*, *pol*, and *env* genes. Unlike retroviruses, they rely on the nuclear import facilities of the target cell for active transport of exogenous DNA through the nuclear pore and thus they can infect dividing as well as quiescent cells (Bukrinsky MI *et al*, 1999; Schroers R *et al*, 2000). Lentivriruses are less prone to transcriptional silencing (Mountain A, 2000). Replication-deficient vectors were originally derived from HIV-1 to transduce lymphocytes. This group of gene transfer systems, even when used in the replication-deficient form is dangerous due to the risk of producing replication-competent viruses. Efforts are underway to produce novel packaging systems that could reduce this risk i.e. improve vector biosafety (Wu X *et al*, 2000). Replication-deficient vectors have also been derived from non-human lentiviruses such as equine, feline, bovine, and simian since these will not be infectious to humans (Mitrophanous K *et al*, 1999). Lentiviral gene transfer into the central nervous system (CNS) of animal models of Parkinson's disease (Kordower JH *et al*, 2000) and metachromatic leukodystrophy (Consiglio A *et al*, 2001) have been reported to be long-term. Nevertheless, limits and potentials of *in vivo* gene delivery with these vectors are still subject to investigation (Park F *et al*, 2000).

1.5.3.3 Adenoviruses

Adenoviruses are capable of infecting both dividing and quiescent cells with high efficiency *in vivo* and *ex vivo* (Mountain A, 2000). Their importance as gene transfer vehicles became apparent after undergoing clinical trials for the treatment of cystic fibrosis (Alton E *et al*, 2000). It was further demonstrated that adenoviral vectors were capable of gene transfer into a variety of tissues (Benihoud K *et al*, 1999). Transgene expression is high but transient, as the vector is unable to integrate and is replication deficient for safety reasons. Adenoviral vectors are, therefore, adequate for some acute diseases, including direct killing of cells, but are less suitable for long-term correction of chronic disease. They have been

applied in preclinical animal studies to transduce liver, heart, brain, skeletal muscle, and tumors (Bramson JL *et al*, 1995). Recent clinical trials with adenoviral vectors include treatment of peripheral vascular and coronary artery disease (Rosengart TK *et al*, 1999), and cancer treatment (Aghi M *et al*, 2000). From approximately 50 different human adenoviral (Ad) serotypes, current vectors are derived from Ad2 and Ad5 serotypes. About 55% of adults have pre-existing anti-adenoviral antibodies (Chirmule N *et al*, 1999) though it is not clear whether this can reduce the efficacy of vector administration. The early (E) genes, E1, E2, and E4 are required for viral genome replication. First generation vectors have their E1 and E3 regions deleted. They deliver the transgene (size limit of 7.5 kb) alongside many viral genes; expression of these genes leads to cytotoxic-T-lymphocyte (CTL) responses directed to transfected cells. Second generation vectors containing deletions of E1, E3, E2 and/or E4 genes have been developed with reported decreased toxicity in animal studies (Christ M *et al*, 2000). However, after administration of an E1/E4 deleted adenoviral vector into the hepatic artery of a young male patient suffering from ornithine transcarbamylase (OTC) deficiency, the first case of fatality from gene therapy was reported (Somia N *et al*, 2000). Helper-dependent or gutted adenoviral vectors (also known as third generation, fully-deleted and pseudo-adenovirus or PAV) with virtually all viral genes deleted can accommodate inserts up to 30 kb alongside the advantage of increased persistence of transgene expression (Schiedner G *et al*, 1998). These vectors, however, present a number of difficulties in terms of construction and manufacture (Mountain A, 2000).

1.5.3.4 Adeno-Associated Viruses

Adeno-associated virus (AAV), a human parvovirus, was initially discovered as a contaminant in an adenovirus preparation. AAV transfects by integration of the transgene into the chromosome of a target cell or through episomal transgene expression (Miao CH *et al*, 1998), for which it requires the presence of a helper virus such as adenovirus or HSV. The exact mechanism of the integration is not well defined, but wild-type AAV in the presence of *rep* integrates specifically into a single site on human chromosome 19. The viral genome consists of *rep* (for genome replication) and *cap* (encoding structural proteins) genes. AAV vectors lack the viral coding sequence. Thus, they are not associated with toxicity or inflammatory responses, although the generation of neutralizing antibodies could potentially prevent re-administration. The vector can be delivered to different organs *in vivo* including liver, lung, and CNS (Monahan PE *et al*, 2000), and sustained transgene

expression (up to two years) has been demonstrated after *in vivo* administration in humans (Wagner JA *et al*, 1998), primates (Conrad CK *et al*, 1996), mice, and dogs (Linden RM *et al*, 1999). After using AAV for expression of human clotting factor IX in haemophilia B patients, clinical trials using AAV for treatment of cystic fibrosis, and muscular dystrophy are underway (Kay MA *et al*, 2000). Recent reports by High and co-workers have shown improved efficacy and safety of AAV-mediated gene transfer for haemophilia B (High KA, 2003).

1.5.3.5 Hybrid Vectors

Efforts are under way for combining properties of more than one virus in order to improve beneficial effects of viral therapy. One example is a combination of double-stranded AAV genomes in adenoviral caspids as described by Lieber *et al* (Lieber A *et al*, 1999). Another approach involved placing an AAV vector into gutless adenoviruses and using this hybrid vector for site-specific integration avoiding insertional mutagenesis (Recchia A *et al*, 1999). Furthermore, an adenoviral vector containing the retroviral genome could integrate in the absence of retroviral integrase activity (Zheng C *et al*, 2000). Roberts *et al* have used an adeno-retroviral hybrid vector that combines the high efficiency of infection of adenoviruses with the retroviral ability to integrate its genome into transduced muscle cells (Roberts ML *et al*, 2002). Further characterization of hybrid vectors is required before their value to human *ex vivo* and *in vivo* gene therapy can be fully realized.

1.5.3.6 Other Viral Vectors

A number of other viral transfer systems other than the viral vectors discussed previously are available that might contribute towards our understanding of gene therapy. These include hepatitis viruses, negative strand RNA viruses such as influenza and ebola, Epstein-Barr virus, α-viruses, and vectors based on simian virus 40 (SV40) (Palese P *et al*, 1996; Chaisomchit S *et al*, 1997; Wahlfors JJ *et al*, 2000). Poxviruses such as Vaccinia and HSV have the advantage of increased genome capacity. Vaccinia Ankara has been reported to transfer genes expressing tumor-specific antibodies to macrophage cell lines *in vitro* (Paul S *et al*, 2000). HSV-1 vector is the most extensively engineered herpesvirus and has been successful in transferring transgenes to macrophages (Paludan SR *et al*, 2001). Significant attributes of HSV include its ability to harbour at least 30 kb transgene, to be grown to high

titre in complementing cell lines, having a broad host range and efficient infectivity. Animal studies have shown successful treatments of cancer, specific brain diseases, and peripheral nervous system (PNS) disease with HSV vectors (Burton EA *et al*, 2001; Martino G *et al*, 2000).

1.5.4 NON-VIRAL GENE TRANSFER SYSTEMS

One of the advantages of non-viral vectors is that the time-consuming process of designing viral constructs is avoided and large numbers of various non-viral structures can be tested rapidly. Many non-viral vectors are being tested for transgene delivery since they are safer than their viral counterparts. However, they suffer from low efficiency and lack of specificity.

1.5.4.1 Naked DNA

Transgene expression following direct injection of naked DNA has been reported to last several months in skeletal muscle of mice, but only a few days in skin (Wolff JA *et al*, 1992; Hengge UR *et al*, 1995). The major limitation of plasmid DNA is poor transfection efficiencies in comparison to viral vectors, with some of the earlier reports of direct gene transfer only transfecting 1% of muscle fibers (Acsadi G *et al*, 1991). In order to improve transfection efficiency in most tissues, novel techniques such as ultrasound or packaging DNA with soluble degradable polymers are being developed (Taniyama Y *et al*, 2002; Ferber D, 2001). In addition, there have been numerous studies employing intramuscular injection of naked DNA followed by electroporation (Vicat JM *et al*, 2000; Mir LM *et al*, 1999; Mathiesen I, 1999).

It is known that certain sequences in bacterial DNA stimulate the immune system, mainly due to the presence of unmethylated CpG sequences in bacteria (Krieg AM *et al*, 2001). This immunogenecity is of great importance in vaccine applications. Indeed, vaccination is a promising application of naked DNA as reported in a Phase I clinical study whereby malaria-naïve volunteers were intramuscularly vaccinated with a plasmid DNA encoding a malaria protein (from *Plasmodium falciparum*). The majority of subjects demonstrated a CTL response directed towards epitopes of the parasite (Wang R *et al*, 1998). Injection of the myocardium to generate therapeutic effects is another example of naked DNA application in gene therapy (Ferber D *et al*, 2001).

1.5.4.2 Cationic Lipids and Cationic Polymers

Cationic polymers (polycations) were used as transfer systems long before cationic lipids (lipoplexes) (Ehrlich M *et al*, 1976). However, progress with polycations (*e.g.* poly-L-lysine and protamine sulphate) was marginal until the introduction of polyethylenimine (PEI) as a transfer reagent (Boussif O *et al*, 1995). Polycations provide several advantages over lipoplexes in gene therapy: a) formation of polycations is simpler without the need for adjuvants, which are required for efficient transfection with some lipoplexes (Hui SW *et al*, 1996); b) chemical modification of polycations is more feasible in order to improve transfection efficiency and achieve specific cell targeting; and c) lipoplexes have interaction between lipid molecules in addition to that with DNA itself. This limits the ability to control their macroscopic characteristics such as size, shape, and interaction with cell membranes and DNA.

Liposomes are microscopic bubbles of lipids surrounding an aqueous interior. Based on the charge of the head group, they can be divided into non-ionic, cationic, anionic, and zwitterionic liposomes. Cationic liposomes can interact with negatively charged DNA forming liposome-DNA complexes also referred to as lipoplexes. In this form, complex endocytosis through the cell membrane takes place and there will be some degree of protection for the DNA from DNases. In addition, lipoplexes can deliver a number of nucleic acids (RNA, oligonucleotides, antisense molecules), proteins with low isoelectric point, and also encapsulate and deliver viruses (Yotnda P *et al*, 2002). They lack immunogenity and can transfer exogenous nucleic acid to non-proliferating cells. They have been used for *ex vivo* and *in vivo* gene therapy in treatment of cystic fibrosis and cancer (Alton EW *et al*, 1998; Xing X *et al*, 1998). Their main disadvantages include inactivation in blood, formulation instability, relatively low transfection efficiency, and poor targeting.

Polycations have been used to condense DNA by electrostatic interactions in order to enhance cellular uptake and provide some protection to the nucleic acid. Numerous natural and synthetic polycations have been employed in gene delivery studies. Among naturally occurring ones are peptides such as chitsoan and histones (Borchard G, 2001; Esser D *et al*, 2000). The synthetic polycations include poly-L-lysine and PEI (Boussif O *et al*, 1995). Like most non-viral approaches, polycations have the advantage of robust manufacturing. They are also suitable for enhancing specificity and efficiency of transfection by attaching

intracellular trafficking enhancers and targeting ligands to the DNA condensing peptide. Among polycations to date, PEI (*Section* 2.5.2) is considered an advanced delivery system providing significant levels of transfection in the lung of mice after tail-vein injection, as well as improved targeted transfection efficiency (Goula D *et al*, 1998). One of the hurdles in gene targeting by polycations is the delivery of intact DNA to the nucleus. DNA-polycation complexes have to attach to the target cell surface, be internalized, escape from endosomal degradation in their path towards the nucleus, and finally disassemble to allow the DNA to be accessed by the transcription apparatus.

1.5.4.3 Physical Techniques of Gene Transfer via Non-Viral Vectors

In vivo and *ex vivo* non-viral gene transfer systems can be achieved with various physical techniques including encapsulation, electroporation, needle-free injection, and microinjection (*Section* 2.5.3).

Encapsulation

In this technique the therapeutic cells or DNAs/plasmids are encapsulated into a liposome formulation such as poly (D, L-lactide-co-glycolide) or PLG (Stern M *et al*, 2003). The cells or DNAs/plasmids can then be released slowly into the target tissue. However, the efficiency is extremely low, limiting the use of this approach for large-scale production and clinical use. Additionally, cell membrane penetration is limited for most of the developed liposomes.

Electroporation

Electroporation involves passing a brief electrical pulse through a suspension of cells and exogenous DNA. The electric pulse is believed to induce areas of transient membrane breakdown allowing entry of DNA into the nucleus whilst directly bypassing endosomal degradation. This technique proved fatal to the majority of cells, up to about 60% in some cell lines within 72 h (Kusumawati A *et al*, 1999). However, Gollins and co-workers have reported high efficiency of plasmid DNA transfer into muscle cells by the application of an electric field (Gollins H *et al*, 2003).

Needle-free injection

Gene delivery by injection without needles is possible via two methods: jet gun (intrajet) and gene gun. In the former approach, liquid under high pressure is used for DNA delivery into interstitial spaces. The gene gun method is based on delivery of DNA coated on gold particles, directly into the cytoplasm via high-pressure helium steam. Gene gun delivery of DNA into the skin gives a moderate transfection efficiency and is a promising alternative to naked DNA injection into muscle for genetic vaccination (Mathei C *et al*, 1997).

1.5.5 TARGETED GENE REPAIR VIA NON-VIRAL VECTORS

There are several advantages of targeted gene repair over gene augmentation. Firstly, large quantities of the therapeutic molecule can be prepared at a relatively low cost using simple non-viral vector systems. Secondly, gene integrity and cell-specific expression are maintained. In addition, the need for designing an expression system or using integrating viral vector systems is eliminated, making targeted gene repair an attractive strategy. Gene repair is expected to have a permanent effect, and is believed to occur by homologous recombination and/or to work by activation of the cell's endogenous mismatch repair apparatus. A number of targeted gene therapy approaches (e.g. triple helix-forming oligonucleotides) are discussed below. Two other approaches, gene repair via RNA-DNA oligonucleotides or RDOs (known as chimeraplasty) and single-stranded oligonucleotides (SSOs), were the focus of experiments performed in *Chapter* 5 and will be discussed in *Section* 1.5.6.

1.5.5.1 Homologous Recombination

Homologous recombination increases genetic diversity as a result of sharing parts of DNA between strands with some level of homology. Over the past 15 years, this technique has been used extensively to investigate gene function, and it has been the basis of generating knock-out and knock-in animals from embryonic stem cells with specific mutations for study of human diseases (Thomas KR *et al*, 1986). *In situ* gene replacement (substituting a mutated gene with a normal one) is based on homologous recombination. This could be an ideal gene therapy approach, but the low efficiency (10^{-4}-10^{-6}) of homologous recombination in differentiated mammalian cells makes it impractical for gene therapy applications (Lai LW *et al*, 1999). Some researchers believe that the principal barrier to facile gene targeting in mammalian cells is not the low frequency of homologous recombination, but rather the

high frequency of random integration (non-homologous) that affects one cell in every 10^2 or 10^4 treated cells (Vasquez KM *et al*, 2001). Despite these drawbacks, the pioneering work of homologous recombination is the basis of the recent new strategies of targeted gene repair that are discussed in the following sections.

1.5.5.2 Small Fragment Homologous Recombination (SFHR)

SFHR utilizes the observation that short DNA fragments in the order of hundreds of bases correct small mutations (point mutations or mutations in a number of bases) by homologous exchange between the incoming DNA fragments and genomic or episomal endogenous sequences (Goncz KK *et al*, 2002). The DNA fragments can interact with the target sequence as single-stranded DNA (sense or anti-sense) or double-stranded DNA. However, the mechanism that underlies this requires further investigation (Goncz KK *et al*, 2002). This technique has been applied both *in vitro* and *in vivo*. In a series of studies, the *CFTR* (cystic fibrosis transmembrane conductance regulator) gene for cystic fibrosis, the *dys* (dystrophin) gene for Duchenne muscular dystrophy, and the *HBB* (human β-globin) gene for sickle cell anaemia have been targets of SFHR-mediated modification (Sangiuolo F *et al*, 2002; Goncz KK *et al*, 2002).

1.5.5.3 Triple Helix-Forming Oligonucleotides (TFOs)

TFOs bind as a third strand to the major groove of a double-stranded target sequence by Hoogsteen or reverse-Hoogsteen hydrogen bonds (non-Watson-Crick base pairing) forming a triple helix in a sequence-specific manner on polypurine:polypyrimidine tracts that are abundant in mammalian genomes (Schroth GP *et al*, 1995). To date, most work conducted with TFOs has been focused on defining the kinetics of TFO-gene interaction (Bernal-Mendez E *et al*, 2002). Unconjugated TFO and TFO conjugated to psoralen (a DNA intercalating and cross-linking agent) are able to induce site-directed mutagenesis in mammalian cells and yeast (Barre FX *et al*, 2000; Wang G *et al*, 1996). These and other studies also demonstrated that triplex formation by itself, or with psoralen, can trigger DNA repair and stimulate recombination by gene conversion rather than cross-over recombination. This led to applying TFOs for targeted gene correction using a bifunctional oligomer comprised of a 40-mer donor domain and a 30-mer TFO domain that proved to correct a point mutation in *supF* reporter gene within a SV40 (simian virus 40) vector in

COS-7 cells (fibroblasts), with correction frequencies of 0.1-0.5% (Chan PP *et al*, 1999). The capacity of TFOs to bind as third strands, and to provoke gene correction potentially in areas with more than one base mutation, would appear challenging and promising in the field of gene therapy.

1.5.6 RNA-DNA OLIGONUCLEOTIDES (RDOs or CHIMERAPLASTS) AND SINGLE-STRANDED OLIGONUCLEOTIDES (SSOs)

Site-specific gene repair has many advantages over gene augmentation techniques (*Section* 1.5.5). Each of the previously described gene repair techniques has its advantages and limitations. The advantages and disadvantages of gene targeting by chimeraplasts (RDOs) and SSOs that were employed in *Chapter* 5 of this thesis will be discussed in this section.

1.5.6.1 Structure of Chimeraplasts or RDOs

RDOs are self-complementary duplex structures including DNA and RNA sequences. A standard RDO molecule is 68 nucleotides in length with two strands, a chimeric strand and an all-DNA strand (*Figure* 1.3). The two ends of the duplex are composed of polythymidine hairpin loops that avoid destruction by helicases and exonucleases. Additional resistance of the secondary structure is achieved via a five base pair GC clamp at the 3' end. The 5' and 3' ends of the molecule are not joined, but juxtaposed and sequestered to permit greater flexibility allowing the molecule to unwind in order for interaction with its homologous target as well as possible recombinase proteins (Kren BT *et al*, 1999b). The chimeric strand consists of a pentameric central DNA region flanked by ten modified RNA residues (2'-O-methylated RNA) on either side. The methylation of RNA residues increases the half-life of RDO inside the cell by assisting in resistance to RNaseH enzymatic activity (Kotani H *et al*, 1996, Kren BT *et al*, 1999a). In addition, it increases the strength of hybridization to target sequence since the Tm of a hybrid between DNA and 2'-O-methyl RNA is higher than that of either DNA-RNA or DNA-DNA (Gamper HB *et al*, 2000b). The all-DNA strand comprises DNA residues that are complementary to the target sequence with the exception of one mismatch site that lies in the middle with its complementary base located at the centre of the pentameric DNA block in the chimeric strand. The central base in the middle of the pentameric DNA region corresponds to the base in the target that will be mutated. Once bound to its target sequence, the RDO acts as a template for nucleotide exchange in a process governed by the DNA pairing and repairing machinery of the cell (*Section* 1.5.6.2).

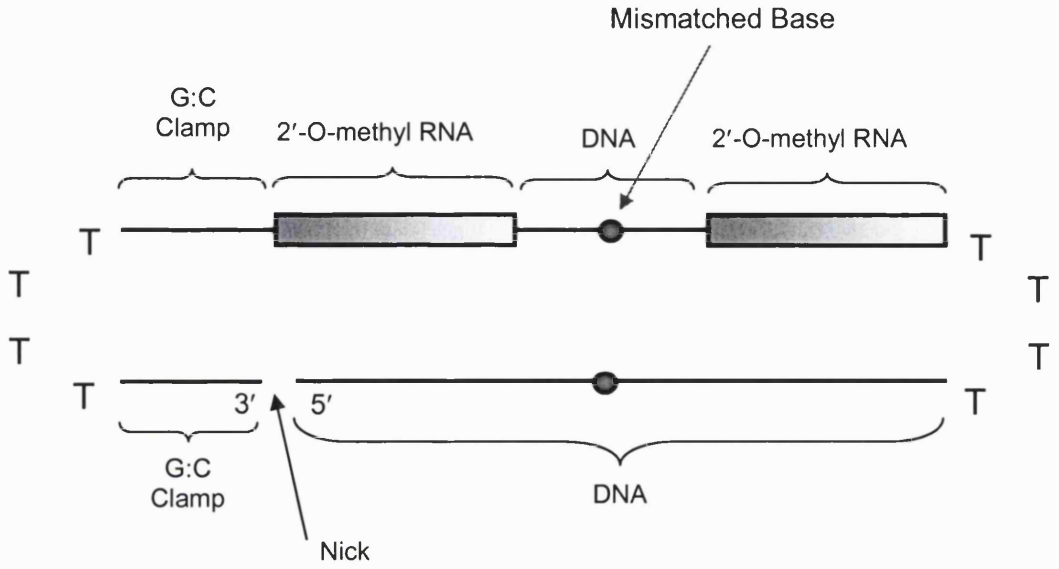

Figure 1.3 Structure of a typical RDO molecule. *An RDO molecule consists of a chimeric strand (top strand) that contains a pentameric DNA region (with the mismatched base in the centre) flanked by 10-base stretches of 2'-O-methylated RNA residues. The strand complementary to this has only DNA bases (the all-DNA strand). T loops at both ends and a G:C clamp provide greater stability to the molecule. The strand nick facilitates topological interwinding with the target DNA.*

1.5.6.2 Mechanism of Action of Chimeraplasts

The exact underlying mechanism of gene repair by RDO remains unclear, but biomedical and genetic studies in yeast have demonstrated a two step process involving DNA pairing and DNA repairing (Gamper HB *et al*, 2000a, Rice MC *et al*, 2001a). Thus, RDO's mode of action is not limited by low frequency of homologous recombination. In the first phase, the bacterial pairing protein RecA (RAD 51/52 in humans, and RECA/2 in yeast) (Shinohara A *et al*, 1993) allows the oligonucleotide to hybridize to its complementary target sequence with the exception of the pre-designed mismatched base in the RDO structure. This leads to the formation of a displacement loop (D-loop) between the RDO molecule and its target. The formation of such a heteroduplex structure has been observed in other recombinational processes catalyzed by RecA (Jayasena VK *et al*, 1993). The D-loop is stable following the dissociation of RecA (Jayasena VK *et al*, 1993). The endogenous mismatch-repair system then recognizes the unusual four-stranded structure of this complement-stabilized D-loop and catalyses nucleotide exchange in the second phase (Gamper HB *et al*, 2000b). Repair proceeds via excision of the mismatched-base and possibly about 100 bases in the vicinity of

the D-loop followed by DNA replication. It remains unclear as to which proteins (DNA polymerases, ligases, and other) are involved in the replication process, however cell-free extract studies have demonstrated the involvement of MSH2 and MSH3 proteins (Cole-Strauss A *et al*, 1999). Similar studies in yeast have also indicated the possibility of chimeraplasty dependence on RAD51/54 (Liu L *et al*, 2002a). Thorpe and co-workers observed significant correction of an episomal target in HT1080 cells overexpressing Rad51, but not in other investigated cell lines (Thorpe PH *et al*, 2002).

1.5.6.3 Chimeraplasty Trials in Mammalian Systems

In 1987, Inoue and co-workers applied single-stranded chimeric RNA-DNA oligonucleotides in antisense gene therapy (Inoue H *et al*, 1987). Experiments for elucidating the role of RNA in homologous recombination led to the design of double-stranded RNA-DNA oligonucleotides for targeted gene repair or correction (Kotani H *et al*, 1996). Chimeraplasty-directed gene repair was initially demonstrated in a landmark study wherein episomal correction of a mutated alkaline phosphatase gene in CHO (Chinese hamster ovary) cells was demonstrated (Yoon K *et al*, 1996). The same group successfully demonstrated correction of a chromosomal target (β globin gene) in lymphoblastoid cells; the first report of this technique in a genomic context (Cole-Strauss A *et al*, 1996). The broad potential and applicability of chimeraplasty in various cultured mammalian cells, animals (*Section* 1.5.6.4), plant cells (*Section* 1.5.6.5), cell-free systems, and yeast (*Section* 1.5.6.5) has been confirmed in a consistent body of publications from numerous groups worldwide.

Genomic nucleotide exchange in the alkaline phosphatase gene was achieved in cultured human HuH7 cells by Kren and co-workers (Kren BT *et al*, 1997). They reported a correction efficiency in excess of 40% prior to targeting *Factor IX* gene in primary hepatocytes (*Section* 1.5.6.4) (Kren BT *et al*, 1998). Chimeraplasty was also used by Lai and colleagues for correction of a mutation in the carbonic anhydrase gene in kidney cells (Lai LW *et al*, 1998). Mutations in epithelial cells including HeLa cells were also repaired (Santana E *et al*, 1998). Repair of a mutation responsible for albinism in a strain of mice was also reported. The albino cells regained the ability to make tyrosinase and produce melanin that led to restored pigmentation in cultured epithelial cells (Alexeeve V *et al*,

1998). Two years later, the same group published a similar success *in vivo* in a mouse model (*Section* 1.5.6.4) (Alexeeve V *et al*, 2000). In both studies the phenotypic and genotypic changes were observed for several months, indicating the permanence and stability of gene conversion. To rule out the possibility of random integration of RDOs, researchers sequenced several hundred bases surrounding the target site and observed no alteration (Cole-Strauss A *et al*, 1996; Xiang Y *et al*, 1997).

Recent examples of *in vivo* and *in vitro* gene alteration by RDOs include, *in vivo* correction of pro-atherogenic apoE2 to wild-type apoE3 in mice (Tagalakis AD *et al*, 2001), *in vitro* repair of a point mutation in β-thalasaemia (Li ZH *et al*, 2001), and *in vitro* and *in vivo* correction of *mdx* (dystrophin) gene in muscle cells (Bertoni C *et al*, 2002). The potential of chimeraplasty-mediated gene targeting is enormous based on reports of gene correction in various tissues including liver, muscle and skin. However, the correction efficiencies vary dramatically from as low as 0.1% in a mammalian cell-free extract system (Cole-Strauss A *et al*, 1999) to as much as ~60% in human lymphocytes (Tagalakis AD *et al*, 2001). Concerns and limitations of chimeraplasty are discussed in *Chapter* 6 (*Section* 6.2).

1.5.6.4 Animal Models of Chimeraplasty

The dawn of gene repair as a novel therapeutic approach for the treatment of human inherited disease was signalled by several reports of successful correction of point mutations in animal models of chimeraplasty. Liver is a potential target for chimeraplasty-mediated gene repair as most of its inherited disorders arise from point mutations. Furthermore, RDOs can be delivered to hepatocytes via the asialoglycoprotein receptor (ASGPR) by tail-vein injection. The first demonstration of successful gene targeting was reported by Kren and coworkers for correcting a mutation in *Factor IX* gene in liver of live rats (Kren BT *et al*, 1998). Lactosylated-PEI was used for efficient delivery of RDO to the liver via tail-vein injection. A single dose of the oligonucleotide resulted in 11% correction of the mutated allele. Greater than 40% of the gene was converted after administration of two doses of the RDO molecule. Moreover, the decrease in factor IX clotting activity was stable for two years in quiescent and regenerated liver after 70% partial hepatocectomy.

A similar liver-specific approach was applied to repair a single base deletion of the *UGT1A1* gene in the gunn-rat model of the human disease Crigler-Najjar syndrome, type I (Kren BT *et al*, 1999a). This mutation causes hyperbilirubinaemia as a result of a premature stop codon that renders the enzyme UGT1A1 inactive. Hepatocyte targeting was achieved with the RDO encapsulated in liposomes or complexed with lactosylated-PEI. Greater than 20% of the *UGT1A1* gene pool in the liver was corrected and the following parameters remained stable throughout the 2 year study period: protein expression, enzymatic activity, bilirubin glucuronidation, and reduced serum bilirubin. Specific targeting of rat hepatocytes via the ASGPR was also demonstrated by Bandyopadhyay and colleagues (Bandyopadhyay P *et al*, 1998; Bandyopadhyay P *et al*, 1999).

ApoE2 is associated with type III hyperlipoproteinaemia and premature atherosclerosis as discussed in *Section* 1.3.4. Tagalakis *et al* demonstrated correction of a point mutation converting pathogenic apoE2 to the wild-type isoform (apoE3) not only in CHO cell lines expressing human apoE2, but also in liver of a hyperlipidaemic apoE knock-out mouse that was also transgenic for the human *APOE2* gene (Tagalakis AD *et al*, 2001). About 25% of mouse hepatocytes were converted after intraperitoneal injection of the RDO. This was clearly an example of application of chimeraplasty-mediated gene targeting for treatment of cardiovascular disease.

Skin was another *in vivo* target of RDO molecules with reports of gene correction in melanocytes that was extended from tissue culture to live albino mice (BALB/c) (Alexeev V *et al*, 2000). A mutation in the tyrosinase gene was corrected and pigmentation of hairs in a localized area was observed after topical application and intradermal injection of chimeric RDO molecules. The color change brought about by chimeraplasty was maintained over a period of three months.

Another example of *in vivo* chimeraplasty-mediated gene repair was for dystrophin point mutations that lead to the human disorder of Duchenne muscular dystrophy (DMD) even though not all types of DMD are from single base mutations. A single nucleotide mutation in the dystrophin gene of mdx mouse model was targeted with a 78-mer chimeraplast. As a result, dystrophin gene expression was observed and remained stable for a few months (Rando TA *et al*, 2000). Direct muscular injection was also performed in a canine model of

DMD, the golden retriever muscular dystrophy (GRMD) dog (Bartlett RJ *et al*, 2000). In this case, a point mutation in a splice site, which leads to a frameshift due to exon exclusion, was corrected leading to persistent dystrophin expression for months after the initial injection in the dogs.

1.5.6.5 Chimeraplasty Trials in Yeast and Plants

The ability of synthetic DNA oligonucleotides to alter point mutations in yeast was demonstrated by Sherman's group (Moerschell RP *et al*, 1988; Yamamoto T *et al*, 1992). Later experiments were designed by several researchers to analyze mechanisms of RDO action (*Section* 1.5.6.2) in yeast (*S. cerevisiae*) extracts, *in vivo* and *in vitro* (Liu L *et al*, 2001, Rice MC *et al*, 2001a).

There are several reports of successful chimeraplast-mediated gene correction in plant cells. Beetham *et al* created a mutation in the acetolactate synthase gene in tobacco plants *in vivo* providing herbicide resistance (Beetham PR *et al*, 1999). Similar studies based on generating a mutation in acetohydroxy acid synthase generated herbicide-resistant maize (Zhu T *et al*, 1999; Zhu T *et al*, 2000). Analysis of progeny after site-specific nucleotide exchange by RDO indicated genetic inheritance via Mendelian segregation (Zhu T *et al*, 1999). These studies also demonstrated an unspecific nucleotide conversion, which was later on confirmed in experiments using tobacco cell-free extracts (Rice MC *et al*, 2000). This may suggest a plant-specific repair system, which is distinct from the high-fidelity mechanism that is observed in mammalian cells.

1.5.6.6 Single-Stranded Oligonucleotides (SSOs)

The use of SSOs in gene therapy goes back to almost two decades, when a 40-mer oligonucleotide repaired a plasmid containing a mutant copy of the neomycin phosphotransferase gene (Campbell CR *et al*, 1989). Synthetic RDOs (*Section* 1.5.6.1), as their name suggests consist of two strands, an all-DNA strand and a chimeric (both RNA and DNA) strand. Experiments designed to elucidate the function of each strand and the mechanism of targeted repair by RDOs initiated the idea of using single-stranded oligonucleotides for targeted gene correction (Gamper HB *et al*, 2000a). It was reported that SSOs with RNA and DNA in their structure were devoid of efficient gene conversion. In addition, DNA SSOs showed about 20% lower gene correction as compared to chimeric

RDOs. The low rate of repair was suggested to arise from rapid degradation or partial degradation of the synthetic molecules. Consequently, modified SSOs (referred to as SSO throughout this thesis) were designed with terminal 2'-O-methyl uracil or terminal phosphorothioate linkages for exonuclease protection. SSOs with modified ends were shown to be four times more active than original SSO molecules without any modifications (Gamper HB *et al*, 2000a). Studies in mammalian cells and yeast suggested a strand bias towards the non-transcribed strand (Igoucheva O *et al*, 2001; Liu L *et al*, 2002b). Moreover, 25-61 nucleotides was the determined optimal length of SSO molecules (Igoucheva O *et al*, 2001). Regardless of their length, SSOs are perfectly homologous to the target sequence with the exception of a central mismatched base (*Figure* 1.4). Upon binding to the target region, a D-loop is formed around the area of the mismatched base, attracting the endogenous repair machinery that catalyses base exchange at the target site (Brackman EE *et al*, 2002). Like chimeraplasty, the precise mechanism of SSO action remains unclear, though it is believed to be less complex due to nucleotide conversion by SSO being independent of mismatch proteins MSH2 and MSH3 (*Section* 1.5.6.2). The elucidation of the repair process was based on studies in *Saccharomyces cerevisiae* (Rice MC *et al*, 2001a; Liu L *et al*, 2001). Compared to RDO molecules, SSOs have a simplified structure and can be produced in a cost-effective way. With more research into understanding the exact mechanism of action and identification of suitable targets, SSOs have the potential to be a powerful method for site-specific correction of mutated genes in hereditary disorders.

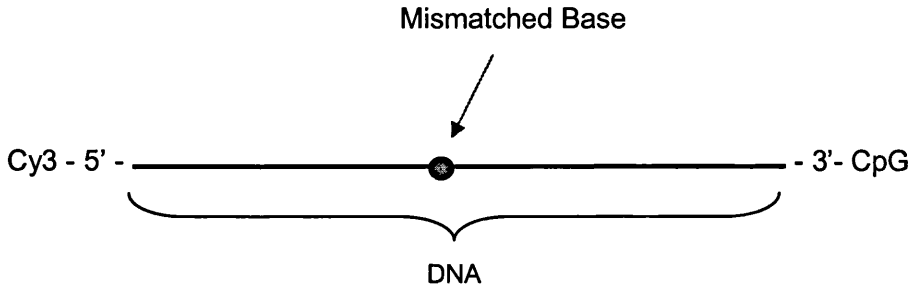

Figure 1.4 Structure of a typical SSO molecule. *SSOs consist of DNA nucleotides that are homologous to the target DNA with the exception of a central mismatched base. Cy3 is a dye in the 5' end of the molecule protecting it from endonuclease degradation. This dye fluoresces red under an inverted fluorescent microscope. Inverted 3'CpG nucleotides refer to a cytosine followed by a guanosine nucleoside that are linked in a 3'-3' manner to the hydroxyl group of the 3' end nucleotide. They also protect the SSO from endonuclease degradation.*

1.5.7 CLINICAL TRIALS

More than a decade ago, the era of clinical gene transfer began with the introduction of an antibiotic drug-resistance gene into tumor-infiltrating lymphocytes of patients with melanoma. *In vivo* expression of the transgene was demonstrated for more than two months (Rosenberg SA *et al*, 1990). Worldwide more than 400 clinical trials are currently underway, for treatment of cancer, HIV, arthritis, cardiovascular disease, and neurodegenerative disease. With over 5000 patients enrolled in clinical studies, gene therapy represents one of the fastest growing areas in therapeutic research (www. wiley.co.uk/genetherapy/clinical/). The majority of reported trials are based on gene transfer via retroviral vectors (Roth JA *et al*, 1997).

The first breakthrough of gene therapy was reported by Alain Fischer's group for treatment of severe combined immunodeficiency disease (SCID), which has different fatal forms. The first trial was performed in 1990 by a retroviral-mediated transfer of adenosine deaminase (ADA) into the T cells of a four-year-old girl with SCID caused by ADA (reported by Blaese RM *et al*, 1995). The girl remains in stable condition more than ten years after her treatment (Anderson WF, 2000). Later, the same group reported successful treatment of two infants (8- and 11-months-old) with another form of this fatal disorder known as SCID-X1. Retroviral vectors were used for *ex vivo* treatment of lymphoid progenitor cells from the patients (Cavazzana-Calvo M *et al*, 2000). It is possible to treat SCID with bone-marrow transplantation. However, finding a perfectly matched donor has reduced the chances of survival for individuals with this life-threatening disorder. Another retroviral-mediated *ex vivo* trial by Fischer's group for curing 9 children with SCID was reported (Hacein-Bey-Abina S *et al*, 2002). Unfortunately, the two youngest patients developed leukaemia-like symptoms both arising from *LMO2* (the gene responsible for causing leukaemia) activation due to retroviral integration in the proximity of this gene's promoter (Hacein-Bey-Abina S *et al*, 2003).

Haemophilia (A and B) is another promising candidate for clinical trials as the deficient protein does not have to be provided from its normal cellular source. To date three different phase I studies for haemophilia A and two for haemophilia B have been carried out with a total of 40 subjects under trial (High KA, 2003). One example of clinical trials for treatment of inherited disorders is that of five patients (aged between 7 and 41 years) with familial

homozygotic hypercholesterolaemia (FHH), a monogenic disorder that results from mutations in the *LDL-R*. Three patients showed a reduction in their LDL level up to four months following *ex vivo* gene therapy with the aid of retroviral vectors carrying the *LDL-R* gene (Grossman M *et al*, 1994). Dzou reports an up to date list of clinical trials in atherosclerotic CVD with a prediction that by 2005 a number of phase III studies will be under way, with the products of some being in regular clinical use by year 2010 (Dzau VJ, 2003).

1.6 Gene Therapy for Atherosclerosis

1.6.1 MOUSE MODELS OF ATHEROSCLEROSIS

Atherosclerosis is a multifactorial disease with progressive cellular changes before the manifestation of acute cardiovascular disease (*Section* 1.1). Several studies in pig, monkey and rabbit models led to some understanding of the initial events in development of this complex disorder (Gerrity RG 1981; Faggiotto A *et al*, 1984; Rosenfeld ME *et al*, 1987). A better understanding of the events that lead to the development of atherosclerosis has been achieved with the availability of genetically modified animal models of the disease. In recent years there has been a great interest in mouse models due to several advantages: a) the small size of mice is an advantage for studying the efficacy of new drugs that are initially only manufactured in small quantities; b) ability to perform experiments with large numbers of mice (due to their small size) and hence develop statistically valid and reliable data; c) extensive genetic information available about different strains of mice; and d) availability of a range of targeted knock-out mice in order to produce suitable models that permit defining pathways for the atherogenic process. The main differences between mice and humans in terms of lipoprotein metabolism and susceptibility to atherosclerosis are as follows: a) the major carrier of esterified cholesterol is HDL in mice and LDL in humans, b) mice liver produces both apoB-100 and apoB-48 whereas human liver produces only apoB-100, c) HL is membrane-bound in humans and soluble in mice, d) CETP activity is absent in mice, and e) long-term administration of high-fat and high-cholesterol diet is necessary due to their resistance to atherosclerosis (Knowles JW *et al*, 2000).

1.6.1.1 ApoE Mouse Models

ApoE is an important modulator of lipoprotein interactions with a range of receptors including the LDL-R (*Section* 1.3.5). ApoE in mice is believed to be apoE4-like. In addition to the three major apoE isoforms (*Section* 1.3.4), there are a number of other mutants that influence the biological functions of apoE in humans. Transgenic mice that express two of these mutants, apoE3-Leiden and apoE2 (Arg112, Cys142), develop an abnormal form of VLDL that is a characteristic of type III hyperlipidaemia (Groot PH *et al*, 1996; Paigen B *et al*, 1987). ApoE knock-in animals are also available based on replacing a normal gene with a mutant form providing tissue specific expression of the variant gene at the same position of the normal gene in the genome. Mice expressing human apoE2 develop a plasma lipoprotein profile characteristic of type III hyperlipidaemia in humans (Sullivan PM *et al*, 1998). They also develop spontaneous atherosclerotic lesions that are rich in foam cells. Another type of genetic modification is the deletion of a specific allele in mice also referred to as knock-out. Generating mice with deficient apoE gene i.e. apoE knock-out mice or apoE (-/-) led to appearance of hyperlipidaemic and atherosclerotic phenotypes even on a normal diet (van Ree JH *et al*, 1994). The extent of the atherosclerosis is believed to be dependent on the strain of apoE (-/-) mice produced (Shi W *et al*, 2000a).

As a result of their well-defined genetics, inbred strains of mice have provided insight into atherogenic mechanisms such as inflammation and acquired immunity (Schreyer SA *et al*, 1996; Fyfe AI *et al*, 1994). For apoE, three inbred strains are available namely C57BL/6, BALB/c and C3H, in the order of decrease of their susceptibility to atherosclerosis induced by a diet rich in saturated fat, cholesterol, and cholate, often referred to as the Paigen diet (Paigen B *et al*, 1985).

1.6.1.2 Other Mouse Models of Atherosclerosis

Increased plasma concentration of apoB is linked to development of cardiovascular disease and this protein is involved in metabolism of VLDL and LDL. Transgenic mice expressing human apoB had normal levels of plasma apoB and no phenotype of vascular disease (Linton MF *et al*, 1993). However, placing them on a high fat and cholesterol diet resulted in formation of lesions with macrophage foam cell morphology (Purcell-Huynh DA *et al*, 1995). LDL-R knock-out mice or LDL-R (-/-) showed only modest hypercholesterolaemia

when on a normal diet, in contrast to humans with LDL-R deficiency being highly hypercholesterolaemic (Ishibashi S *et al*, 1994). By crossing apoB transgenic and LDL-R (-/-) mice, more atherosclerotic lesions were formed compared to the individual strains maintained on a normal diet (Sanan DA *et al*, 1998).

1.6.2 APOE AND GENE THERAPY FOR ATHEROSCLEROSIS

Complications of atherosclerotic CVD are believed to be reduced by lowering LDL-cholesterol levels in plasma, through changing life style and diet, as well as through drug therapy such as use of statins, niacin and fibrates (Smith J *et al*, 1995). However, despite the availability of these options, a large number of patients are unable to reduce their LDL-cholesterol back to normal and hence there is requirement for novel gene therapy techniques. Some examples of using apoE (*Sections* 1.6.2.1-1.6.2.3) and apoAI (*Section* 1.6.3) in preclinical gene therapy trials for atheroprotection will be discussed.

1.6.2.1 Bone-Marrow Transplantation (BMT)

Currently, BMT into apoE-deficient mice serves as a genetic approach for understanding the role of macrophage-derived apoE in atherosclerosis and lipoprotein metabolism. Transplantation of bone-marrow from apoE (-/-) mice into wild-type mice resulted in transplanted mice becoming more prone to atherosclerosis (Fazio S *et al*, 1997). However, lipid levels remained normal as the treated mice still had normal hepatic apoE expression. The opposite experiment was also carried out by other groups. The effect of BMT of wild-type mice into apoE (-/-) mice (6-12-weeks-old) were tested by three different groups (Linton MF *et al*, 1995; Boisvert WA *et al*, 1995; Van Eck M *et al*, 1997). As a result of apoE production (10% of normal circulating levels of apoE) from the transplanted macrophages, normalization of plasma cholesterol and triglyceride levels was observed for two months. Furthermore, these studies demonstrated prevention of atherosclerosis in the arterial wall. Consequently, macrophage-derived apoE was functional and possibly involved in the protection of the arterial wall.

As mentioned above, macrophage-derived apoE normalizes serum cholesterol levels and prevents development of atherosclerosis in apoE (-/-) mice (Linton MF *et al*, 1995; Boisvert WA *et al*, 1995; Van Eck M *et al*, 1997). Shi and colleagues performed a study to determine the effect of macrophage-derived apoE on established atherosclerosis in 8-week-old apoE (-

/-) mice (Shi W *et al*, 2000b). The mice were transplanted with apoE (+/+) bone-marrow and plasma cholesterol levels were normalized four weeks after transplantation. A group of these mice were killed and their aortic lesions were measured and considered as a baseline. Aortic lesion areas were not significantly different from the baseline mice in another group of mice that were killed 12 and 20 weeks post-transplantation. On the other hand, a group of mice (8-week-old) that were transplanted with apoE (-/-) bone-marrow developed severe atherosclerotic lesions indicating the involvement of macrophage-derived apoE in preventing progression of atherosclerosis, but unable to induce regression of established atherosclerosis in apoE (-/-) mice (Shi W *et al*, 2000).

As explained in *Section* 1.3.4, apoE2 (a common variant of apoE) has reduced binding ability to the LDL-R. Another variant of apoE with such a defect is apoEcys142. Yoshida and co-workers transplanted 5 weeks of age apoE (-/-) mice with apoE (-/-) bone marrow cells transduced with apoE3, apoE2, or apoEcys142 retroviral vectors (Yoshida H *et al*, 2001). Human apoE was detected in the serum of all the treated mice four weeks post-transplantation. In addition, cholesterol levels increased with age in all the three groups without being affected by the level of apoE expression. Lesion area in apoE3 mice were 40 % smaller than the control animals. ApoE2 mice showed a lesion area similar to the control group, while apoEcys142 had a remarkable increase in lesion size (Yoshida H *et al*, 2001). This data demonstrated that anti-atherogenic effects of macrophage-derived apoE were dependent on the receptor-binding ability of this protein.

1.6.2.2 ApoE Gene Transfer via Viral Vectors

ApoE (-/-) mouse is a relevant animal model of atherosclerosis (*Section* 1.6.1.1). Systemic delivery of human apoE3 to liver of apoE (-/-) mice by adenoviral vectors driven by a Rous Sarcoma virus (RSV) demonstrated reduction of cholesterol-rich VLDL and IDL and an increase in beneficial HDL over a period of 21 days (Stevenson SC *et al*, 1995). However, the phenotypic corrections were transient as human apoE3 levels declined and plasma cholesterol levels increased 35 days post-transfection. This might have been due to an immune response against the viral proteins and/or the transgene products (Tripathy SK *et al*, 1996). In a similar study, Kashyap *et al* used a CMV-driven adenoviral vector for apoE3 gene transfer to apoE (-/-) hepatocytes and demonstrated a similar phenotypic change. In

addition, they observed a reduction of the mean atherosclerotic lesion area four weeks after injection (Kashyap VS *et al*, 1995).

Using a second generation adenoviral vector, Tsukamoto and colleagues studied the effect of different apoE isoforms in liver cells of apoE (-/-) mice on a western diet (Tsukamoto K *et al*, 1997a). Results showed hepatocytes that expressed adenovirally transduced apoE3 and apoE4 had a higher reduction in their cholesterol levels compared with apoE2 in apoE (-/-) mice. In addition, expression of all the apoE isoforms was still detectable three months post-injection. This study demonstrated long-term transgene expression by second generation adenoviruses compared to first generation adenoviral vectors (Stevenson SC *et al*, 1995; Kashyap VS *et al*, 1995). In a different study, the same group used a second generation adenoviral vector for treating older mice (already had developed different stages of atherosclerotic lesions) with the aim of quantifying the lesion areas (Tsukamoto K *et al*, 1999). Lesion regression was observed for mice expressing apoE4 but to a lesser extent than mice expressing apoE3 that showed a remarkable regression of lesion both at the early and advanced stage. On the other hand, an adenoviral vector bearing apoE2 cDNA did not induce lesion regression even though lesion progression was prevented. Consequently, apoE3 synthesized by hepatocytes in apoE (-/-) mice is able to reduce the area of established lesions despite the absence of macrophage-derived apoE (Tsukamoto K *et al*, 1999).

As the LDL-R is important for clearing apoE-containing lipoproteins, LDL-R (-/-) mice are expected not to show a dramatic alteration in cholesterol levels (Willnow TE *et al*, 1995). However, to study possible effects on atherogenesis, LDL-R (-/-) mice were on a western diet for 14 weeks allowing them to develop advanced lesions. The animals were subsequently injected by a second generation adenoviral vector encoding apoE3 (Tangirala RK *et al*, 2001). Six weeks post-injection, regression of the pre-existing advanced lesions was induced by apoE3 without any reduction in plasma cholesterol. This atheroprotection might reflect anti-oxidant properties of apoE due to reduction of an isoprostane in the aortic intima. This study also indicates therapeutic benefits of liver-derived apoE in the absence of macrophage-derived apolipoprotein confirming the findings of Tsukamoto and colleagues (Tsukamoto K *et al*, 1999).

Even though second generation adenoviruses result in a prolonged expression of the transgene compared to first generation vectors, they are still immunogenic. In a study that aimed to overcome this problem, apoE (-/-) mice was crossed with nude or nu (+/+) mice that lack mature T lymphocytes and thus are able to avoid cytotoxic T cell rejection of hepatocytes that express the viral proteins in addition to responses against the human transgene. The generated apoE (-/-)/nu (+/+) mice retained the same plasma lipoprotein profile and developed the same atherosclerotic lesions as the apoE (-/-) animals. This new mouse model was injected with a first generation adenoviral vector containing human apoE3 (Desurmont C *et al*, 2000). Over a period of five months, complete regression of plaques and reduction in cholesterol level was observed, showing the therapeutic potential of gene therapy in the absence of an immune response (Desurmont C *et al*, 2000).

Another study with second generation adenoviral vectors was performed in immunocompetent apoE (-/-) mice comparing intravenous injection and intramuscular injection of viruses (Harris JD *et al*, 2002a). The intramuscular injection resulted in very low apoE levels and offered no protection against atherosclerosis. A few days after the intravenous injection, however, high levels of apoE were detected in plasma accompanied by reductions in plasma cholesterol. ApoE levels then declined 70 days post-injection indicating a possible shutdown of the CMV promoter used in the trial, which is known to be silenced by nuclear factor kappaB (NFκB) activation in the liver (Loser P *et al*, 1998). In a later study, the same group (Harris JD *et al*, 2002b) demonstrated retardation of atherosclerotic plaque density in aortas of apoE (-/-) mice following muscle transduction with an AAV vector expressing human apoE3. Such a reduction was not observed after AAV-mediated apoE2 expression from muscle cells, but nevertheless demonstrated the potential atheroprotective ability of apoE3 expressed from muscles transduced with AAV.

1.6.2.3 ApoE Plasmids (Naked DNA) & Endothelial-Derived ApoE

In addition to viral-mediated gene transfer, intramuscular injection of plasmid DNA is a suitable candidate for apoE delivery. Yoshida rat models have LDL-R deficiency and hypercholesterolaemic phenotypes. Skeletal muscle of these animals was subjected to injection of naked DNA encoding human apoE2, the isoform defective in LDL-R binding, under the control of CMV promoter. Forty five days post-injection, plasma accumulation of

apoE2 was observed. In the contrary, expression of apoE3 injected into the muscle of normal rat, was only observed in the area of injection (Fazio VM *et al*, 1994).

Rinaldi and co-workers reported a remarkable reduction of hypercholesterolaemia in apoE (-/-) mice after intramuscular injection of a CMV-deriven plasmid vector encoding human apoE3 (Rinaldi M *et al*, 2000). Transgene expression was demonstrated for 16 weeks and cholesterol redistribution was observed between lipoprotein fractions; the cholesterol content of VLDL, IDL and LDL was reduced compared to control animals, while that in HDL was increased. Another group used intramuscular injection of plasmids encoding human apoE2 and apoE3 isoforms into apoE (-/-) mice and reported detectable levels of apoE2, but not apoE3, in plasma (Athanasopoulos T *et al*, 2000). One reason for the undetectable apoE3 might be its rapid uptake by cells (mainly hepatocytes) compared to apoE2, following secretion, although they observed no alteration of total cholesterol and triglyceride levels in treated animals compared to control mice (Athanasopoulos T *et al*, 2000). Nevertheless, when the apoE2 vector was used in a long-term study, reductions in xanthoma and atherosclerotic lesions were observed even though hyperlipidaemia was again not lowered (Athanasopoulos T *et al*, 2000).

The efficacy of endothelial cells as gene delivery vehicles was tested by stable transfection of endothelial cells derived from murine yolk sac with a plasmid containing human apoE3 cDNA (Cioffi L *et al*, 1999). The cultured cells were then grafted subcutaneously into apoE (-/-) mice. Three months post-transplantation, cholesterol levels of treated mice were lower than in control animals. In addition, atherosclerotic lesions were reduced in the treated animals (Cioffi L *et al*, 1999). This study emphasizes the potential of cultured cells as an efficient system for secretion of important proteins *in vitro* that could be employed as somatic gene delivery vehicles.

1.6.3 APOAI AND GENE THERAPY FOR ATHEROSCLEROSIS

HDL permits transfer of cholesterol from intimal macrophages to the liver and facilitate its excretion in bile (Oram JF *et al*, 1996). Thus, the progressive formation of sterol-rich lesions in the artery wall is retarded by this plasma lipoprotein. Being the principle constituent of HDL, apoAI is a potential protein for atheroprotection. ApoAI knock-out mice are characterized by very low plasma HDL levels, but no increased susceptibility to

atherosclerosis has been reported (Li H *et al*, 1993). However, absence of apoAI enhances the progression of lesions in human apoB transgenic mice though not in wild-type animals subjected to high-fat diet (Voyiaziakis E *et al*, 1998). This mouse model provides evidence for anti-atherogenic properties of apoAI. As explained previously, apoE (-/-) mice are prone to spontaneous atherosclerosis independent of diet (*Section* 1.6.1.1). Hepatic overexpression of human apoAI in apoE (-/-) mice (the C57BL/6 strain) has been shown to be a potent suppressor of diet induced atherosclerosis (Rubin EM *et al*, 1991). In a similar study, introduction of human apoAI transgene in C57BL/6 mice resulted in a three-fold increase in plasma HDL and six-fold decrease in aortic lesion area (Paszty C *et al*, 1994). Furthermore, crossing transgenic mice overexpressing human apoAI with apoE (-/-) mice, doubled HDL cholesterol levels and reduced atherosclerosis (Plump AS *et al*, 1994). In a similar study, transgenic overexpression of human apoAI in the liver of WHHL (Watanabe heritable hyperlipidaemic) rabbits delayed the development of aortic atherosclerosis (Duverger N *et al*, 1996). These studies in transgenic animals indicate the importance of apoAI gene transfer as a therapeutically useful tool for atheroprotection. A variant form of apoAI, apoAI-M is also recognized as a potential anti-atherogenic agent as discussed in *Section* 1.6.3.2.

1.6.3.1 ApoAI

De Geest and co-workers demonstrated increased neointima formation, a pro-atherogenic process, after endothelial denudation in apoE knock-out mice (De Geest B *et al*, 1997). Adenoviral-mediated transfer of human apoAI increased HDL-cholesterol and significantly reduced neointima formation suggesting an indirect vascular protective role for apoAI. Similarly, adenoviral gene transfer of human apoAI to apoE (-/-) mice reduced the progression of atherosclerosis (Benoit P *et al*, 1999). Several other animal studies have confirmed that injection or expression of apoAI inhibits the initiation and progression of atherosclerosis. One line of evidence was provided by intravenous injection of purified rabbit apoAI, which reduced progression of atherosclerotic lesions in cholesterol-fed rabbits even though HDL-cholesterol levels remained unchanged (Miyazaki A *et al*, 1995).

Regarding the ability of apoAI to induce regression of pre-existing atherosclerotic lesions, Badimon and co-workers demonstrated regression of established lesions in cholesterol-fed rabbits after weekly intravenous administration of human HDL (Badimon JJ *et al*, 1990).

HDL consists of other proteins such as apoE (*Section* 1.6.2) and apoAII. In order to show that apoAI alone is able to induce regression of pre-existing lesions, Rader and his team constructed a second generation adenoviral vector encoding human apoAI, which was injected intravenously to LDL-R (-/-) mice. They demonstrated prolonged apoAI expression (Tsukamoto K *et al*, 1997b) and a significant regression of established lesions in LDL-R (-/-) mice fed a western diet (Tangirala RK *et al*, 1999).

Even though macrophages do not secrete apoAI, they respond to it by increased cholesterol efflux (Mazzone T *et al*, 1994) and are believed to have protective effects against atherosclerosis. In a study by Ishiguro *et al* when apoE (-/-) bone marrow was retrovirally transduced with human apoAI and then transplanted into apoAI (-/-) mice, there were less atherosclerotic lesions compared to control apoAI (-/-) mice that received apoE (-/-) bone marrow transduced with a control retrovirus (Ishiguro H *et al*, 2001). To investigate whether the observed protective effect was due to lack of circulating apoAI in apoAI (-/-) mice, apoE (-/-) bone marrow expressing human apoAI was subsequently transplanted into apoAI transgenic mice. This also resulted in marked reduction of atherosclerotic lesions compared to recipients of apoE (-/-) marrow (Ishiguro H *et al*, 2001). Consequently, gene therapy by apoAI expressed from macrophages has anti-atherogenic effects as this could potentially protect vessel walls.

1.6.3.2 ApoAI-M

The first described mutant form of apoAI, apoAI-M, differs by a Cys to Arg substitution at position 173 (Sirtori CR *et al*, 1999). It confers to carriers a significant level of protection against atherosclerosis and vascular disease despite elevated triglycerides and low plasma levels of the main proteins involved in RCT (i.e. HDL, apoAI, LCAT and CETP) (Bekaert ED *et al*, 1993). The therapeutic potential of this mutant against atherosclerosis has been assessed in a range of *in vitro* and *in vivo* experiments using recombinant apoAI-M produced in *E.coli* (Calabresi L *et al*, 1999).

It was suggested that apoAI-M HDL is highly efficient in removing cellular cholesterol and that the subsequent improvement in RCT might explain the low susceptibility of apoAI-M carriers to atherosclerosis development (Franceschini G *et al*, 1999). Repeated injections of

apoAI-M to rabbits reduced intimal thickening induced by various arterial injuries (Soma MR *et al*, 1995).

Like apoAI, the ability of apoAI-M to inhibit formation or induce regression of atheromatous lesions was investigated. Repeated apoAI-M injections induced regression of lesions in apoE (-/-) mice by reducing the accumulation of lipid and macrophage in arterial plaques (Shah PK *et al*, 1998). The same group later showed that a single high dose of recombinant apoAI-M injected in apoE (-/-) mice lowered plaque lipid and macrophage content (Shah PK *et al*, 2001). In a recent study, Chiesa and colleagues infused a single high dose of recombinant apoAI-M into the carotid artery of cholesterol-fed rabbits (Chiesa G *et al*, 2002). They reported enhanced lipid removal from arteries and the regression of the pre-existing plaques.

1.7 Aims of thesis

ApoE is a suitable candidate for prevention of atherosclerosis (*Section* 1.6.2) mainly because of its involvement in lipid transport and metabolism (*Section* 1.3.6.1). Additionally, macrophage-secreted apoE exerts protection against atherosclerosis induced by hypercholesterolaemia as has been demonstrated by BMT studies (Boisvert WA *et al*, 1995; Linton MF *et al*, 1995) (*Section* 1.6.2.1). Another atheroprotective plasma protein is apoAI as outlined in *Section* 1.4. The physical and biological functions of recombinant apoE and apoAI were studied in this thesis as well as aiming to demonstrate the feasibility of chimeraplasty for targeting of human *APOE3* gene *in vitro*.
The specific aims of my thesis were, therefore:

Aim 1: to develop individual sandwich ELISA assays for quantifying levels of apoE and apoAI secreted from cultured cells.

Aim 2: to establish recombinant CHO cells expressing apoAI (CHOAI). In addition, to compare biologically activities (cholesterol efflux and LCAT activation) of newly secreted apoE3- and apoAI-containing particles from CHOE3 (available in our laboratory) and CHOAI respectively.

Aim 3: to assess the feasibility of chimeraplasty for converting the *APOE3* gene to mutant *APOE2* and *APOE4* isoforms in cultured human hepatoblastoma and monocytic cell lines. Based on the success of this technique the aim was then to compare the biological activities of liver-derived and macrophage-derived apoE particles and to determine their isoform-dependent properties.

Chapter 2

2. MATERIALS AND METHODS

This chapter describes protocols that were used throughout this PhD project (*Section* 2.2) followed by specialized procedures performed in the three results chapters: *Chapter* 3 (*Section* 2.3), *Chapter* 4 (*Section* 2.4), and *Chapter* 5 (*Section* 2.5).

2.1 Materials

Sodium dodecyl sulphate (SDS) was purchased from National Diagnostics (Leicestershire, UK). All tissue culture plastic-ware unless indicated otherwise in the text were from Marathon Laboratory Supplies (London, UK). Tetra-methylbenzidine (TMB) substrate kit was supplied by Pierce (Chester, UK). Protein G Hitrap affinity column and enhanced chemiluminescence protein biotinylation kit (ECL^{TM}) were purchased from Amersham Biosciences (Buckinghamshire, UK). Linear PEI (L-PEI or ExGen 500) was purchased from TCS Biologicals Ltd. (Botolph Claydon, UK). All oligonucleotide primers were made to order by Sigma Genosys (Cambridge, UK). All restriction enzymes unless otherwise stated in the text, were purchased from Promega (Southampton, UK). Chloroform, diethyl ether, ethanol, glacial acetic acid, hexane, methanol, and Cocktail T scintillant were supplied by BDH Laboratory Supplies (Poole, UK). All other reagents, unless otherwise indicated in the text, were purchased from Sigma-Aldrich Company Ltd. (Poole, UK).

2.2 General Methods

2.2.1 PROTEIN MEASUREMENT

All protein quantification was performed using the 'Bio-Rad Protein Assay Kit' (Bio-Rad, Hemel Hempstead, UK), except for samples containing more than 0.1% (v/v) detergent, for which the 'BCA Protein Assay Kit' (Perbio Science Ltd., Cheshire, UK) was used.

2.2.1.1 The Bio-Rad (Bradford) Protein Assay

This assay is based on Bradford's observation that there is a shift from 465 nm to 595 nm of the acidic solution of Coomassie Brilliant Blue G-250 as a result of its binding to proteins (Bradford MM, 1976). It was established by Spector that a dye-albumin solution had a constant extinction coefficient over a 10-fold concentration range (Spector T, 1978).

Consequently, Beer's Law has been applied for accurate quantification of protein concentration having selected an appropriate ratio of dye volume to sample concentration.

A standard curve ranged from 0-20 μg protein/50 μl was used for every assay. This was performed by triplicate dilutions of an appropriate protein standard [usually bovine serum albumin (BSA) or immunoglobulin G (IgG)] in distilled water to a final volume of 50 μl. Triplicates of the unknown samples were also diluted in 50 μl of distilled water. The standards and the unknown samples were added to appropriate wells of a 96-well plate. To each well, 250 μl of freshly diluted Bio-Rad dye reagent (final concentration 20%, v/v) was added. After 10 min incubation at room temperature, the OD_{595} versus reagent blank was measured using a Dynex plate-reader (Jencons-PLS, East Sussex, UK). The concentration of the standards versus their OD_{595} was plotted, and the test sample concentrations were determined from the standard curve.

2.2.1.2 The BCA Protein Assay

In this assay, Cu^{2+} is reduced to Cu^{1+} in the presence of the protein in an alkaline environment, with the colorimetric detection of cuprous cations by BCA (bicinchoninic acid) (Smith PK *et al*, 1985). Two molecules of BCA chelate each generated cuprous ion forming a purple-coloured product that is water-soluble with a strong absorbance at 560 nm. This absorbance increases linearly with an increase in protein concentration over a broad range of 20 μg/ml to 2 mg/ml.

For every assay performed, the BSA standards were set up freshly as described for the Bio-Rad method (*Section* 2.2.1.1), except that the final volume was 100 μl. Triplicates of unknown samples were also made up to 100 μl with distilled water. BCA Reagent A was mixed with BCA Reagent B in a 50:1 ratio, and 900 μl of this working reagent was added to each tube of diluted standards and unknown samples. After 30 min incubation at 60 °C, the standards and samples were transferred to disposable 1 ml microcuvettes and their absorbances measured at 562 nm relative to a water blank reference using the UVIKON 930 spectrophotometer (Kontron Instruments). The concentration of the standards versus their OD_{562} was plotted, and the test sample concentrations were determined from the standard curve.

2.2.2 SDS-POLYACRYLAMIDE GEL ELECTROPHORESIS (SDS-PAGE)

SDS-PAGE is one of the most commonly used methods for fractionation and characterization of proteins. The advantages of SDS-PAGE over similar techniques are speed and simplicity, as well as using only micrograms of proteins (Hames BD, 1983). It dissociates all the proteins within a complex mixture into their individual polypeptide subunits due to the presence of the ionic detergent SDS. The presence of excess SDS in the buffer and the use of a reducing agent such as β-mercaptoethanol or dithiothreitol (DTT), denatures the proteins and facilitates their binding to SDS in a 1.4:1 ratio of SDS:protein weight (w/w) once the samples are heated to 100 °C. As a consequence, each polypeptide-SDS complex will have a constant negative charge per mass unit and moves towards the anode during electrophoresis (Hames BD, 1983). In addition, the mobilities of the complexes are inversely proportional to their molecular weights due to the molecular-sieving properties of the gels. Proteins with known molecular weights can therefore be used to determine the molecular weight of sample proteins.

Polyacrylamide gels are formed by polymerization of acrylamide followed by subsequent cross-linking with bisacrylamide (N,N'-methylenebisacrylamide) that provides rigidity to the gel and forms pores through which the polypeptide-SDS complexes pass. The size of the pores is inversely related to the bisacrylamide:acrylamide ratio. The most commonly used ratio is 1:29 as shown in Table 2.1. The linear range of polypeptide separation by these gels is mainly influenced by the amount of cross-linking and the percentage of acrylamide used in gel preparation. TEMED (N,N,N,N'-tetramethylethylenediamine) and ammonium persulphate are used to initiate the polymerization reaction as the former catalyses free radical formation by the latter compound.

There are two types of polyacrylamide gels, discontinuous and gradient. The former system is used in order to obtain a high resolution of polypeptide separation from a large, dilute sample applied to the gel. It comprises stacking and resolving gel layers that differ in pH, salt concentration, acrylamide concentration, or a combination of these. Samples are applied to the stacking gel that is normally made of 4% (w/v) acrylamide. The high porosity of the stacking gel concentrates the polypeptide-SDS complexes into a narrow zone at the top of the resolving gel. The resolving gel separates the complexes into sharp polypeptide bands

due to its greater molecular-sieving properties as a result of having a larger percentage of acrylamide. Gradient gels, however, have an increasing concentration of acrylamide through the resolving gel. They resolve proteins covering a wider range of molecular weights on a single gel as well as promoting the sharpening of protein bands during migration. Hence, gradient gels offer more advantages over discontinuous gels (Margolis J *et al*, 1967). In this thesis, SDS-PAGE was used to determine the size of a protein (*Section* 2.4.7.2), to estimate the purity of a protein in a solution (*Section* 2.3.1), and to fractionate a complex protein mixture prior to immunoblotting (*Section* 2.2.3).

2.2.2.1 SDS-Polyacrylamide Gel Preparation

The single percentage mini-gels were cast in Bio-Rad MiniProtean II electrophoresis cassettes. The resolving gel was made (see Table 2.2 for components and quantities) and poured immediately into the cassette, until the meniscus was at the correct distance from the top of the plate to allow for the comb length plus 0.5 cm. The acrylamide solution was then overlaid with water-saturated isobutanol in order to produce a level resolving gel. The gel was left to set for about 30 min after which the isobutanol was removed and the gel was washed a few times with distilled water. The acrylamide solution for the stacking gel was then prepared (Table 2.2) and added to the top of the resolving gel. The appropriate comb was inserted and the stacking gel was allowed to set (~10 min). The comb was subsequently removed and the wells were washed once with distilled water, followed by 1 X running buffer: 25 mM Tris (pH 8.3), 192 mM glycine and 0.1% (w/v) SDS. With regard to gradient percentage gels, pre-cast Tris-glycine gradient gels of 4-20% and 8-16% (Novex gels) were purchased from Invitrogen (The Netherlands) and prepared for electrophoresis as described above.

Acrylamide concentration % (w/v) (1:29 molar ratio of bisacrylamide:acrylamide)	Linear range of polypeptide separation (kDa)
3	95-400
5	57-212
7.5	36-94
10	16-68
15	12-43

Table 2.1 Effective range of polypeptide separation by SDS-polyacrylamide gels.

Solution components	4% Stacking	10% Resolving	15% Resolving
Water	6.1 ml	4.0 ml	2.3 ml
30% Acrylamide mix	1.3 ml	3.3 ml	5.0 ml
Tris buffer	2.5 ml	2.5 ml	2.5 ml
10% (w/v) SDS	100 µl	100 µl	100 µl
* 10% (w/v) APS	100 µl	100 µl	100 µl
* TEMED	10 µl	4 µl	4 µl

Table 2.2 Requirements for preparation of SDS-polyacrylamide gels. *Acrylamide mix consists of acrylamide and bisacrylamide mixed in a ratio of 29:1. The resolving gel Tris buffer is made of 1.5 M Tris.HCl (pH 8.8), where the stacking gel is 1.0 M Tris.HCl (pH 6.8). APS stands for ammonium persulphate. *Solutions were added last to initiate polymerization. The given quantities are enough for 1 X 10 ml gel.*

2.2.2.2 Electrophoresis

For all SDS-polyacrylamide gels, samples were prepared as follows: samples were mixed (3:1 ratio) with 4 X SDS-PAGE sample buffer [200 mM Tris.HCl (pH 6.8), 8% (w/v) SDS, 0.2% (w/v) bromophenol blue, and 20% (v/v) glycerol]. For reduced samples, β-mercaptoethanol was added to a final concentration of 2% (v/v). Both reduced and non-reduced samples were heated in a boiling water bath for 5 min. In addition, a broad range molecular weight marker (6-175 kDa; New England Biolabs, Hertfordshire, UK) was also heated for 3 min. The samples (maximum volume of 30 µl) and the marker (15 µl) were

loaded on to the gel, after which the electrophoresis chamber was filled with 1 X running buffer (*Section* 2.2.2.1). Mini-gels cast in the laboratory were run in the Bio-Rad MiniProtean II electrophoresis chamber at a constant voltage of 125 V. Electrophoresis using Novex gels was performed in the Mini-cell Xcell II gel tank (Invitrogen, The Netherlands), according to the manufacturer's instructions. When the dye front had migrated to the bottom of the gel, the gel was removed from its cassette and used for staining (*Section* 2.2.2.3) or Western blotting (*Section* 2.2.3).

2.2.2.3 Coomassie Staining of SDS-Polyacrylamide Gels

Coomassie blue staining has a sensitivity of 0.1-0.5 μg protein and is a technique that is commonly used to visualize protein bands on gels. The reagent reacts with any protein regardless of its biological activity. After polypeptide separation by SDS-PAGE, the gel was incubated on a shaker for 30 min at room temperature with 50 ml of Coomassie stain: 0.25% (w/v) Coomassie brilliant blue R-250, 50% (v/v) methanol, and 10% (v/v) glacial acetic acid. The gel was then destained using successive volumes of destaining solution: 30% (v/v) methanol and 10% (v/v) glacial acetic acid. The thoroughly destained gel was then washed in distilled water and dried in a GelAir Drying Frame (Bio-Rad).

2.2.3 WESTERN BLOTTING

Antigens present within a complex mixture of proteins are normally detected by specific antibodies. Some of the commonly used immunodetection methods include radioimmunoassay (RIA), enzyme-linked immunosorbent assay (ELISA), immunoprecipitation and immunoblotting. ELISA (*Chapter* 3) and immunoblotting (Western blotting) are the two protein detection methods used in this thesis. This section focuses mainly on immunoblotting, summarized in *Figure* 2.1.

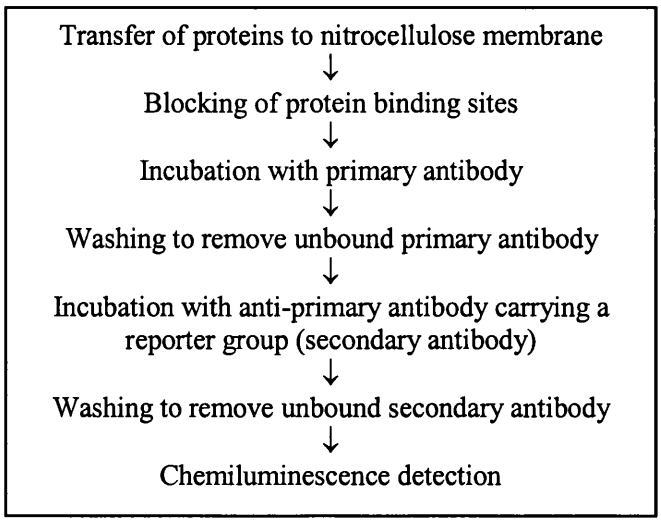

Figure 2.1 Steps required for immunoblotting technique.

In Western blotting, proteins are transferred to a nitrocellulose membrane after polyacrylamide gel electrophoresis. From the three basic methods for transferring proteins, namely capillary blotting, diffusion blotting, and electroblotting, the latter was mainly used in this thesis except when otherwise indicated. After transfer, the protein binding sites are then blocked on the membrane prior to exposure of the membrane to the specific primary antibody. Excessive washing is then required to remove any unbound primary antibody, after which the membrane is incubated with a secondary antibody directed against the primary antibody and carrying a reporter group such as horseradish peroxidase (HRP). Following another washing step, detection is carried out by chemiluminescence, which involves emission of light as a result of energy release from a substance in an excited state. In this thesis, the ECL detection system (Amersham Biosciences), which involves the oxidation of luminol by HRP in the presence of a chemical enhancer such as phenols (Whitehead TP *et al*, 1979) was used. The emitted light (438 nm) can be detected by a short exposure to blue-light sensitive autoradiograph film.

2.2.3.1 Buffers and Solutions for Immunoblotting

Transfer buffer: 25 mM Tris (pH 8.3), 192 mM glycine, 20% (v/v) methanol.

PBS (phosphate-buffered saline): 138 mM NaCl, 10 mM Na_2HPO_4, 1.75 mM KH_2PO_4, 7.2 mM KCl.

Washing buffer (PBS-T): PBS and 0.05% (v/v) Tween 20.

Marvel blocking buffer: 10% (w/v) Marvel milk powder in washing buffer.

Primary antibody dilution buffer: 5% or 10% (w/v) Marvel milk powder in washing buffer.
Secondary antibody dilution buffer: the washing buffer alone is used.

2.2.3.2 Sample Transfer for Immunoblotting

Nitrocellulose membrane was handled with gloves to prevent fingerprint staining. Proteins were transferred from a polyacrylamide gel to Hybond ECL nitrocellulose membrane (Amersham Biosciences) using either semi-dry blotting or wet blotting. In each case, one piece of the membrane and four sheets of 3MM absorbent paper (Whatman International Ltd., Maidstone, UK) were cut to the size of the gel and pre-soaked in transfer buffer for approximately 5 min before transfer. *Figure* 2.2 illustrates the cross-section of the transfer sandwich.

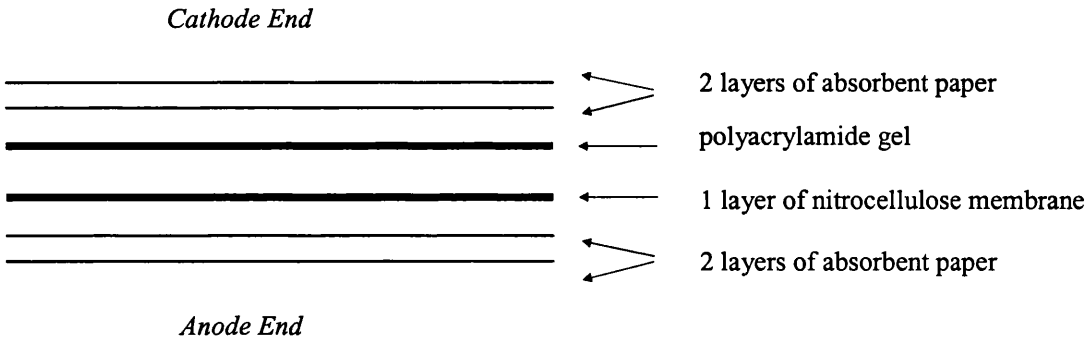

Figure 2.2 Cross-section of the transfer sandwich used for immunoblotting.

Air bubbles were removed by rolling a test tube over the transfer sandwich. For semi-dry blotting, the sandwich was placed in the bottom electrode (anode) of a Bio-Rad Trans-Blot Semi-Dry Transfer Cell and then the upper electrode was placed on the top of the stack. The electrodes were connected to a power pack and transfer was allowed to proceed for 90 min with a constant current of 1.5 mA/cm^2 of gel. For wet transfer, the transfer sandwich was placed in the centre of the Xcell II Blotting Module of a Novex Western Transfer Apparatus (Invitrogen), surrounded by sponges (pre-soaked in transfer buffer) provided in the kit. The inner chamber of the module was then filled with transfer buffer, while deionised water was poured in the outer chamber to prevent overheating. The electrodes were connected to a Novex power pack (Invitrogen) and blotting was carried out over 90 min at a constant current of 125 mA. A pre-stained protein marker was always present in the polyacrylamide gel to act as an internal control for protein transfer.

After transfer, the membrane was removed and its top right corner was cut for purposes of lane identification. The following incubation steps were performed on a shaker. The membrane was soaked in blocking buffer for 1 h at room temperature or overnight at 4 °C. Primary antibody was then diluted as shown in Table 2.3 and incubated with the membrane for 1 h at room temperature or overnight at 4 °C. The membrane was then thoroughly washed (3 x 10 min) with washing buffer before its incubation with the diluted secondary antibody (Table 2.3) at room temperature for 1 h. After repeating the washing step, an ECL substrate was used according to the manufacturer's instructions (Amersham Biosciences) and the blot was subsequently secured in a film cassette and exposed briefly to X-ray film (Hyperfilm ECL, Amersham Biosciences). Exposed films were developed in an automatic bench top processor (Compact X4, X-ograph Imaging Systems, Wiltshire, UK).

Antigen	1° antibody				2° antibody & dilution
	Name	Supplier	Dilution buffer	Incubation condition	
apoE	α-human apoE	Biogenesis	5% Marvel/PBS-T 1:2000	1 h @ RT	rabbit α-goat HRP 1:10,000 in wash buffer
apoAI	α-human apoAI	Chemicon	10% Marvel/PBS-T 1:10,000	overnight @ 4 °C	rabbit α-goat HRP 1:10,000 in wash buffer
LCAT	α-human LCAT (mAb)	monoclonal cells (T. Jowett, UCL, UK)	3% BSA/PBS 1:20	1 h @ RT	sheep α-mouse HRP 1:1000 in 10% Marvel/PBS-T

Table 2.3 Western blotting conditions used in this thesis for detecting the indicated antigens. *The symbols α and RT denote anti and room temperature, respectively. The secondary antibodies were purchased from Sigma-Aldrich Company Ltd. and diluted in the washing buffer or PBS-T. All antibodies were polyclonal, except for α-human LCAT, which was a monoclonal antibody (mAb).*

2.2.4 GENERAL CELL CULTURE AND CRYOPRESERVATION

CHOdhfr-, the mutant hamster cell line that is deficient in dihydrofolate reductase was chosen to be transfected and express human apoAI. HEK-293 (human embryonic kidney) cells, HepG2 (hepatoblastoma) cells and THP-1 (monocyte-macrophages) cells were the three human cell lines used in this thesis. HEK-293 cells had an epithelial-like morphology (Graham FL, 1977) and were kindly supplied by Dr I Graham (Department of Biological Sciences, Royal Holloway University of London, UK). CHOdhfr-, HepG2 and THP-1 cell lines were purchased from the European Collection of Animal Cell Culture (ECACC) (Wiltshire, UK) with ECACC numbers of 94060607, 85011430, and 88081201, respectively. HepG2 cells have an epithelial-like morphology and grow in monolayer. THP-1 cells are grown as single cells with a round morphology. Recombinant CHOdhfr- cells secreting human apoE3 (designated as CHOE3) were kindly supplied by Dr A Tagalakis (Department of Medicine, Royal Free & University College Medical School, London, UK).

2.2.4.1 Cell Maintenance

All cell types were cultured in 75 cm^2 and 175 cm^2 tissue culture flasks in a 37 °C incubator (Jencons Millenium CO_2 incubator, Jencons-PLS) with a humidified atmosphere of 5% CO_2 and 95% air. All cell culture work was performed in a class II microbiological safety cabinet (Envair Ltd., Lancashire, UK), using sterile, disposable plastic ware. All cell lines, except THP-1, were maintained as adherent cells in suitable growth medium supplemented as shown in Table 2.4. THP-1 cells were maintained as a suspension culture.

2.2.4.2 Passaging and Cryopreservation of Cell Lines

All adherent cell lines were passaged by trypsinisation; the cells were washed once in pre-warmed PBS, incubated with 0.25% (v/v) trypsin-EDTA (enough to just cover the cells) at 37 °C, and then neutralized by adding pre-warmed fresh medium. The cells were then re-suspended and split as indicated in Table 2.4. For HepG2 cells, resuspension was performed vigorously to ensure the formation of a single cell suspension prior to splitting. The only suspension cell line used in this thesis, THP-1, was passaged once a week ensuring its seeding density was 1 x 10^5 cells/ml and that it did not exceed 1 x 10^6 cells/ml.

Cryopreservation refers to storage of cells over a long period of time under liquid nitrogen. This was achieved by adding 1 ml freshly prepared cryoprotective solution [10% (v/v) dimethylsulphoxide (DMSO) in maintenance medium] to 1-5 x 10^6 cell suspension. The cryoprotective solution lowers the freezing point and allows for a slower cooling rate to limit the damage caused to cells by freezing. The whole mixture was immediately transferred to a 1.8 ml cryovial (Life Technologies, Paisley, UK) that was placed in a freezing chamber (Nalgene Cryo 1 °C Freezing Container, Fisher Scientific, Leicestershire, UK) and stored at -80 °C for about 5-6 h. The freezing chamber contained isopropanol that allowed the temperature to be reduced by 1 °C per minute at -80 °C. The cryovials were subsequently transferred to liquid nitrogen containers for long-term storage.

When required, the cells were rapidly thawed by immersing the bottom of the vial in a 37 °C water bath prior to transferring its content to an excess of pre-warmed maintenance medium. The cells were pelleted at 300 *g* for 5 min in a bench-top centrifuge (Heraeus Megafuge

1.0R) and then re-suspended in fresh medium in a 75 cm^2 flask. Cells were sub-cultured as described in Table 2.4.

2.2.4.3 Cell Counting

Trypan Blue exclusion was used for determining cell viability. The blue dye is only taken up by dead cells (non-viable cells) and this allows differentiation between viable and non-viable cells. A 40 µl aliquot of the single cell suspension was mixed with an equal volume (1:1 dilution) of 0.4% (w/v) Trypan Blue solution in a microfuge tube. The chambers of a haemocytometer with a fitted coverslip were filled with the mixture prior to observation under an inverted phase-contrast microscope (Nikon TMS, Jencons-PLS) using the x 10 objective lens. After counting the average number of viable cells in eight 1 mm^2 squares with a total volume of 10^{-4} cm^3, the concentration of cells per ml in the original cell suspension was calculated as follows:

$$\textit{Dilution factor x mean cell count per square x } 10^4 = \textit{Viable cell count/ml}$$

Cell line	Growth medium	Supplements added to growth medium						Passage
		FBS	dFBS	Glu	PS	HT	NAA	(split ratio)
CHOdhfr- (adherent)	Iscove's modified DMEM (Sigma)	—	10%	1%	1%	2%	1%	every 3-4 days (1:5)
CHOE3 (adherent)	Iscove's modified DMEM (Sigma)*	10%	—	1%	1%	—	1%	every 3-4 days (1:5)
CHOAI (adherent)	Iscove's modified DMEM (Sigma)*	10%	—	1%	1%	—	1%	every 3-4 days (1:5)
CHOHis6-LCAT (adherent)	Iscove's modified DMEM (Sigma)	5%	—	1%	1%	—	1%	every 5-6 days (1:5)
HEK-293 (adherent)	DMEM (Life Technologies)	10%	—	1%	1%	—	—	every 3-4 days (1:3)
HepG2 (adherent)	DMEM (Life Technologies)	10%	—	1%	1%	—	—	every 7 days (1:8)
THP-1 (suspension)	RPMI-1640 (Life Technologies)	10%	—	1%	1%	—	—	every 7 days (1:4)
CHOE3 CHOAI	CD-CHO (Life Technologies)	—	—	1%	1%	—	1%	—
CHOE3 CHOAI	CHO-SFM II (Life Technologies)	—	—	1%	1%	—	1%	—

Table 2.4 Cell lines frequently used in this thesis and their growth and maintenance conditions. *DMEM stands for Dulbecco's Modified Eagle's Medium. FBS denotes fetal bovine serum, dFBS is dialysed FBS, Glu is glutamine (2 mM), PS is penicillin (100 U/ml) and streptomycin (100 μg/ml), HT is hypoxanthine (0.1 mM) and thymidine (16 μM), and NAA is non-essential amino acids. All supplements were supplied from Life Technologies except for FBS (heat inactivated) that was purchased from Sigma. The media indicated by * are the maintenance media for CHOE3 and CHOAI and are referred to as selection medium in some parts of this thesis. However, CD-CHO or CHO-SFM II (indicated in the final two rows of this table) were used on confluent CHOAI or CHOE3 cells as indicated in appropriate sections of this thesis.*

2.2.5 PCR TECHNOLOGY

DNA amplification is achieved by using radioisotopes or by following a lengthy procedure involving the cloning of nucleic acids into vectors. The introduction of the polymerase chain reaction (PCR), however, enables molecular biologists to rapidly amplify DNA or

cDNA templates for further manipulation (Sambrook J *et al*, 1989c). A small portion of a nucleic acid target is amplified many million-folds generating sufficient material for subsequent experimental analysis. In this thesis, PCR technology was used as part of the analysis of apoE3 gene targeting (*Chapter* 5). The amplified PCR products were visualized on agarose gels (*Section* 2.2.6).

A basic PCR process amplifies ~100-500 bp segments of a longer DNA molecule using a typical reaction mixture comprising a DNA or cDNA template, two oligonucleotide primers, deoxynucleotide triphosphates (dNTPs), a thermostable DNA polymerase, reaction buffer and magnesium. The reaction components are mixed and placed in an automated instrument (a thermal cycler) that allows repetitive cycles of DNA denaturation, annealing and amplification (primer extension) through a series of various temperatures and times.

Each PCR cycle doubles the amount of template sequence in the reaction, and consists of three steps namely, denaturation, annealing and amplification. The two strands of target DNA are separated in the initial step by heating the reaction mix to at least 95 °C for up to 2 min. In the next step, stable association of oligonucleotide primers with the separated target DNA strands is performed by reducing the temperature to ~40-70 °C within 30-60 s. Finally, the thermostable polymerase begins DNA synthesis extending from primers on raising the temperature to ~72 °C, the optimal temperature for the polymerase. This extension normally lasts ~1-2 min depending upon the length of the target sequence. These steps should be optimized for each template and primer pair combination. The availability of advanced gradient thermocyclers can ease the optimization steps, in particular that of the annealing temperature by using a gradient of temperatures across the heating block. Having completed about 20-40 cycles, the amplified nucleic acid can be analysed for quantity, size and sequence, or used in further experimental methods such as cloning.

2.2.5.1 Basic PCR Protocol

For each PCR reaction, a master mix was prepared in 0.5 ml thin-walled PCR tubes by adding the following reagents in the order and amounts shown in Table 2.5. It was important to set up a negative control each time a PCR reaction was performed in order to ensure that no contaminants were present in the master mix. This was achieved by adding

all the components shown in Table 2.5 with the exception of the DNA template that was replaced with DEPC (diethylpyrocarbonate) water.

Components	Volume (µl)	Final concentration
Pfu buffer (10 X)	5	1 X
forward primer (10 µM)	2.5	0.5 µM
reverse primer (10 µM)	2.5	0.5 µM
DEPC water	29.5	-
dNTP mix (2 mM)	5	0.2 mM
DNA template or DECP water control	5	≤ 1 µg DNA
Pfu Turbo polymerase (2.5 U/µl)	0.5	1.25 U
Total volume including sample	50	-

Table 2.5 Requirements for setting up a PCR reaction. *Pfu Turbo polymerase was purchased from Stratagene Ltd. (Cambridge, UK).*

Two different thermal cyclers were used in this thesis depending on their availability, a Biometra cycler (PLS Ltd., UK), and a 40 Gradient Robocycler (Stratagene Ltd.) The tube contents were covered by 20 µl light mineral oil prior to incubation in the Biometra cycler. In the case of the Robocycler, the addition of oil was unnecessary as this thermal instrument has a heated lid, which prevents sample evaporation upon heating. The Robocycler was used for optimizing the annealing conditions for each primer pair combination based on the following general PCR programme:

95 °C	5 min	1 cycle
95 °C	1 min	30 cycles
54-68 °C	1 min	
72 °C	1min	
72 °C	10 min	1 cycle

If needed, the PCR protocol was also optimized by using a range of $MgCl_2$ concentrations (0.5-4 mg/ml). About 5 µl of the PCR product was run on an agarose gel (*Section* 2.2.6) in

order to ascertain how successful the PCR process was. The products were then either directly purified from the reaction mix (*Section* 2.2.7.1), or extracted from the agarose gel following electrophoresis (*Section* 2.2.7.2).

2.2.6 AGAROSE GEL ELECTROPHORESIS OF DNA

PCR products can be visualized by ultraviolet (UV) radiation of an agarose gel following electrophoresis and staining with ethidium bromide, which intercalates between adjacent base pairs (Sambrook J *et al*, 1989b). Agarose gel electrophoresis separates DNA strands according to their size. The separation range for commonly used gel concentrations are illustrated in Table 2.6.

DNA size (bp)	Percentage of agarose in gel (%)
1000-23000	0.75
400-1200	1.00
200-5000	1.50
150-4000	1.75
100-3000	2.00

Table 2.6 Separation ranges for common agarose gels.

Mini-gels analyses were generally performed in this thesis. The mini-gel apparatus (Horizon mini-gel apparatus, Life Technologies) was set up as recommended by the manufacturer. The required weight of agarose was added to the appropriate volume of 1 X Tris borate EDTA (TBE) buffer made from a 10 X stock (Life Technologies). TBE consists of 100 mM Tris (pH 8.4), 90 mM boric acid and 1 mM EDTA (ethylenediaminetetra-acetate). Agarose was dissolved in the buffer by heating, with mixing at regular intervals in a microwave oven until it was dissolved (~2 min). The solution was cooled to ~60 °C and, after adding 0.5 μg/ml ethidium bromide, poured into the cast. The gel was allowed to set for ~30 min at room temperature before removing the comb and blocks, and enough TBE buffer was added to cover the surface of the gel. PCR products were mixed with 10 X loading buffer; 10 mM Tris.HCl (pH 7.5), containing 50 mM EDTA, 10% (w/v) Ficoll 400,

0.25% (w/v) bromophenol blue, and 0.25% (w/v) xylene cyanol FF. An appropriate volume (10-40 µl) of each sample and 10 µl of a suitable DNA ladder (1 kb or 100 bp from Life Technologies) were loaded into the wells. Electrophoresis was performed at a constant voltage of 150 V for ~30 min until the dye front had migrated to 2 cm from the bottom of the gel. After electrophoresis, the gel was visualised and photographed under UV light using a gel documentation system (Epi Chemi II Darkroom, Ultra Violet prducts, Cambridge, UK).

2.2.7 PURIFICATION AND SEQUENCING OF PCR PRODUCTS

DNA was extracted either directly from the PCR product (*Section* 2.2.7.1) or after running the PCR product on an agarose gel (*Section* 2.2.7.2) as described above. The purified DNA was then prepared for automated sequencing by mixing ~500 ng of the DNA with 32 pmol of one of the primers used for PCR amplification in a final volume of 10 µl. Sequencing was carried out commercially by Babraham Institute (Cambridge, UK).

2.2.7.1 Direct Purification of PCR Products

Promega's Wizard PCR Preps DNA Purification Kit was used for direct purification of DNA from PCR reactions. The entire PCR reaction (50 µl) was mixed by vortexing with 100 µl of the provided Direct Purification Buffer. Once 1 ml of resin was added, the mixture was vortexed three times over a 1 min period allowing binding of DNA to the resin and formation of a slurry. The slurry was then pushed down a mini-column with a syringe and washed with 2 ml of 80% isopropanol. Traces of wash buffer were removed by centrifuging the mini-column for 2 min at 16,060 *g*. DNA elution was achieved by the addition of 30 µl of deionised water and centrifuging the mini-column for another 1 min. The concentration of the eluted DNA was estimated by measuring the optical density at 260 nm (OD_{260}) with a UVIKON 930 Spectrophotometer (Kontron Instruments) and using this equation:

$$DNA\ concentration\ (\mu g/ml) = OD_{260} \times dilution\ factor \times 50\ \mu g/ml$$

The DNA was either used immediately or stored at -20 °C.

2.2.7.2 DNA Extraction from Agarose Gels

The relevant DNA bands were extracted from agarose gel using the QIAquick gel extraction kit (Qiagen, Crawley, UK). Using UV light and a clean scalpel, the DNA band was excised and weighed before adding 3 volumes of QG solution from the kit to 1 volume of gel slice (eg. 100 mg gel = 300 µl QG solution). The mixture was placed at 50 °C for 10 min (with occasional vortexing) allowing the buffer to solubilize the gel. Next, one gel volume of isopropanol was added to the sample before it was transferred to a QIAquick spin column and centrifuged at 16,060 *g* for 1 min allowing the binding of DNA. The flow-through was discarded and the column was washed with 0.75 ml of PE buffer and re-centrifuged as before. DNA elution was performed by placing the column in a clean 1.5 ml microfuge tube, adding 30 µl of deionised water to the column, and centrifuging for 1 min at 16,060 *g*. The DNA concentration was estimated using the equation given in *Section* 2.2.7.1. The DNA was either used immediately or stored at -20 °C.

2.2.8 RESTRICTION ENZYME DIGESTION OF PCR PRODUCTS

Restriction endonucleases are bacterial restriction enzymes that recognize and cut specific and short nucleotide sequences within DNA (Sambrook J *et al*, 1989a). Typically, restriction sites comprise palindromes of 4, 5, 6, 7, or 8 bp each with an axis of rotational symmetry. The majority of enzymes are unable to cut DNA methylated on one or both strands of their recognition site. Six base cutters are generally used for cloning purposes as they cleave the DNA so that overhanging 'sticky' ends are formed, which are used in DNA ligation reactions (*Section* 2.4.2.4).

Manufacturer recommended buffer and instructions were used to digest up to 2 µg of DNA from the purified PCR product or plasmid vector. The reaction buffers contained varying concentrations of Tris.HCl (pH 7.5), NaCl, and $MgCl_2$. A master mix for digestion was prepared in a 1.5 ml microfuge tube, using the reagents in the volumes and order shown in Table 2.7. The tubes were incubated at the optimum temperature for at least 1 h.

All the enzymes used in this thesis and their required conditions are defined in Table 2.8. If the reaction buffer and conditions were matched, two enzymes could be used in the same reaction mix, otherwise a purification step was required in between (*Section* 2.2.7.1). The

DNA fragments obtained after digestion were separated on an agarose gel (*Section* 2.2.6) or on a TBE gel (*Section* 2.5.4.2).

Component	Volume (µl)
Appropriate 10 X buffer	2.0
DEPC water	7.0
DNA sample (in water)	10
Appropriate restriction enzyme (2U)	1.0

Table 2.7 Components and volumes required for setting up a restriction digest reaction.

Enzyme	Cleavage Site	Reaction conditions for optimal activity
BamHI	G/GATC C C CTAG/G	Buffer E @ 37 °C for 1 h
CfoI	G/CG C C GC/G	Supplied buffer @ 37 °C overnight or at least for 3 h
EcoRI	G/AATT C C TTAA/G	Buffer H @ 37 °C for 1 h
HindIII	A/AGCT T T TCGA/A	Buffer B or E @ 37 °C for 1 h

Table 2.8 Restriction enzyme cleavage sites and reaction conditions. *The enzymes used in this thesis are listed here. They were all purchased from Promega with the exception of CfoI, which was supplied by Life Technologies.*

2.2.9 BLOOD SAMPLING

Fifty millilitres of blood was taken from the antecubital vein of a donor, and added to tubes containing 0.8 ml of 0.2 M EDTA (pH 7.4) and 1.4 ml of 0.3 M sodium chloride (pH 7.4). The blood was immediately centrifuged for 20 min at 2,000 *g* and 4 °C using a bench-top centrifuge (Heraeus Megafuge 1.0R) in order to separate the plasma from the blood cells. Plasma was then stored in aliquots at – 80 °C. Fresh aliquots were used when required

without re-freezing any remainders. If heat-inactivated plasma was needed, an aliquot was heated in a water bath at 60 °C for 20 min.

2.2.10 STATISTICAL ANALYSIS

Values in text, tables and figures were expressed as the mean ± S.D when appropriate. Statistical differences between means were determined using 2-tailed unpaired Student's *t*-test and considered significant if $P<0.05$. Analysis was performed using Microsoft Excel (Microsoft Office 2000).

2.3 ApoE and ApoAI ELISAs

One of the aims of this thesis (*Chapter* 4) involved studying some of the biological activities of newly synthesised apoE3 particles secreted from recombinant CHOE3 cells (available in our laboratory). Recombinant CHO cells secreting apoAI (CHOAI) were generated and used as a positive control in the biological studies described in *Chapter* 4. In order to accomplish this aim, it was necessary to determine the quantities of secreted apolipoproteins. Levels of apoE and apoAI secreted in culture medium have been measured by a range of immunoassays including radioimmunoassay (RIA) and ELISA (Blum CB *et al*, 1980; Weisweiller P *et al*, 1983). It was decided to establish direct sandwich ELISAs for quantifying apoE and apoAI secreted by recombinant cells (*Chapter* 3). This section describes the methods used to establish these assays. For apoE ELISA, the coating antibody was purified (*Section* 2.3.1) and the detection antibody was biotinylated (*Section* 2.3.2). Initially, preliminary experiments confirmed that there was no cross-reactivity between the two antibodies, and either of the antibodies and streptavidin horseradish peroxidase (S-HRP) (*Chapter* 3). Titration assays were subsequently carried out in order to determine optimal concentrations of the coating antibody, the detection antibody, and the S-HRP complex (*Chapter* 3). In addition, the assay was further optimized as described in detail in *Chapter* 3.

2.3.1 AFFINITY COLUMN PURIFICATION OF COATING ANTIBODY FOR APOE ELISA

Anti-human apoE antibody (Diasorin, #82943) supplied in PBS solution supplemented with BSA, was used as the coating antibody for the apoE ELISA developed in this project. The antibody was purified using a protein G column. The tubing (1.6 mm) of a peristaltic pump (Bio-Rad, Watford, UK) was washed and primed with 10 ml PBS in order to remove a 20%

(v/v) ethanol preservative. One ml of the stock antibody (1.318 mg/ml) was mixed with 1 ml PBS and 200 µl of 1 M Tris.HCl (pH 7.4). This mixture was applied to the column at a rate of 1 ml/min. Any non-specifically bound material was eluted with 5 ml PBS, collecting 500 µl of eluate every 30 s. The bound antibody was thus eluted with 0.1 M glycine.HCl (pH 2.7) into 1.5 ml microfuge tubes each having 150 µl of 1 M Tris.HCl (pH 9.0). After collecting each fraction, the solutions were agitated manually to neutralize the low pH and prevent antibody denaturation. Any remaining unbound antibody was eluted with 0.1 M glycine.HCl (pH 2.0) into 150 µl of Tris.HCl (pH 9.0). All the collected eluates were stored on ice.

Each eluted fraction was assayed for protein by a Bio-Rad spot test. This was performed by mixing 5 µl of each fraction with 25 µl of freshly diluted Bradford dye reagent (final concentration 20%, v/v) on a sheet of laboratory Parafilm. A color change (brown → blue) indicated the presence of protein. All the fractions containing protein were pooled and subsequently dialysed against 5 litres of PBS buffer at 4 °C, changing the buffer every few hours. The concentration of the dialysed protein and the fractions of the PBS washes were determined using Bradford protein assay (*Section* 2.2.1.1). The original unpurified antibody and fractions from the column were subjected to SDS-PAGE to verify removal of BSA from the antibody and the success of the purification step. The purified antibody was stored in aliquots at -20 °C.

2.3.2 BIOTINYLATION OF DETECTION ANTIBODY FOR APOE ELISA

The goat anti-human apoE antibody (Biogenesis, Poole, UK, #0650-1904), hereafter referred to as the detection antibody, was biotinylated prior to use following the protocol in the ECL Protein Biotinylation Kit (Amersham Biosciences). The protein was diluted to 1 mg/ml in a freshly prepared 40 mM sodium bicarbonate buffer (pH 8.6). 40 µl of biotinylation reagent (biotinamidocaproate N-hydroxysuccinamide ester supplied in dimethylformamide) was added to the diluted protein, and the mixture was incubated at room temperature for 1 h with constant agitation. A Sephadex G25 column was equilibrated with 5 ml PBS containing 1.0% BSA (pH 7.5) followed by PBS (pH 7.5). The protein mixture was applied to the column and the antibody eluted with 5 ml of PBS (pH 7.5). Fractions containing the biotinylated antibody were pooled and the total protein

concentration was determined using the Bradford Protein Assay (*Section* 2.2.1.1). The biotinylated antibody was stored in small aliquots at 4 °C in the presence of 0.2% sodium azide.

2.3.3 DIRECT SANDWICH ELISA FOR APOE QUANTIFICATION

2.3.3.1 Buffers and Solution

Blocking Buffer: 50 mM Tris.HCl (pH 7.4), 150 mM NaCl, 1 mM $MgCl_2$, and 1% (w/v) BSA.

Washing Buffer: 10 mM Tris.HCl (pH 7.4), 150 mM NaCl, and 0.05% (w/v) Tween-20.

Assay Buffer: 50 mM Tris.HCl (pH 7.4), 150 mM NaCl, 0.01% (v/v) Tween-40, 0.05% (w/v) gamma-globulin, and 0.5% (w/v) BSA.

Tetra-methylbenzidine (TMB) Substrate: equal volumes of 0.004% (v/v) H_2O_2 (substrate) and TMB (dye).

2.3.3.2 ELISA Methodology

96-well microtitre plates were coated with 100 µl per well polyclonal anti-human apoE antibody (2.5 µg/ml in PBS, pH 7.4) and left covered at 4 °C overnight. At each step of the assay, the plates were covered securely with sealing tapes. In addition, the incubation steps performed at room temperature were all carried out on a shaker, and washing steps were repeated five times sequentially with a Dynex plate washer (Dynex Technologies, West Sussex, UK) at each step. Excess antibody was decanted and 350 µl/well of blocking buffer was added to block non-specific binding sites on the plastic solid phase. After 1 h incubation at 37 °C, the plates were washed five times with 350 µl/well washing buffer using the plate washer. The plates were incubated for 1 h at room temperature with 50 µl/well of samples or standards added in triplicate and diluted as required in assay buffer. After washing the plates, 50 µl biotinylated goat anti-human apoE (1 µg/ml in assay buffer plus 1% goat serum) was added to each well. The plates were incubated for 1 h at room temperature, before another washing step.

One hundred microlitres of S-HRP (1:2000 in assay buffer) was added to each well. After 30 min incubation at room temperature, the plates were washed as before. ApoE quantification was determined by adding 100 µl/well of freshly prepared TMB substrate.

The colour reaction (colorless → blue) was allowed to proceed for exactly 10 min with the plates gently shaken. The reaction was stopped by adding 100 µl/well of 2 M H_2SO_4. The absorbance at 450 nm was immediately measured using a Dynex microplate reader (Dynex Technologies). The described ELISA methodology is summarized in *Figure* 2.3.

2.3.4 APOAI ELISA

A direct sandwich ELISA for future experiments with recombinant CHO cells (*Sections* 2.4.5, 2.4.6, and 2.4.7) was needed to quantify the apoAI levels secreted by cultured CHOAI cells. It was decided to follow the same principle and method used for developing the apoE ELISA (*Section* 2.3.3). Goat polyclonal anti-human apoAI (Chemicon International, CA, USA, #AB740) and sheep polyclonal anti-human apoAI (Biogenesis, Poole, UK, #0650-0180) were used as coating and detection antibodies, respectively. The detection antibody was biotinylated following the method described in *Section* 2.3.2. Initially, preliminary experiments confirmed there was no cross-reactivity between the two antibodies, and either of the antibodies and S-HRP (*Chapter* 3). This was followed by titration curves to determine the optimal working concentrations of each antibody and S-HRP (*Chapter* 3). The buffers used for apoAI ELISA were the same as those for apoE ELISA (*Section* 2.3.3.1). The coating and detection antibodies were diluted in PBS and assay buffer (supplemented with 1% sheep serum) respectively. Pure apoAI (delipidated apoAI purified from human plasma, generously provided by Dr G Sperber, Department of Medicine, Royal Free & University College Medical School, London, UK) was used for establishing a suitable standard curve. Even though efforts were made to establish and optimize this ELISA procedure, the protocol proved unsuccessful as described further in *Chapter* 3. It was decided to pursue quantification of apoAI by Western blot followed by scanning densitometry (*Section* 2.4.4).

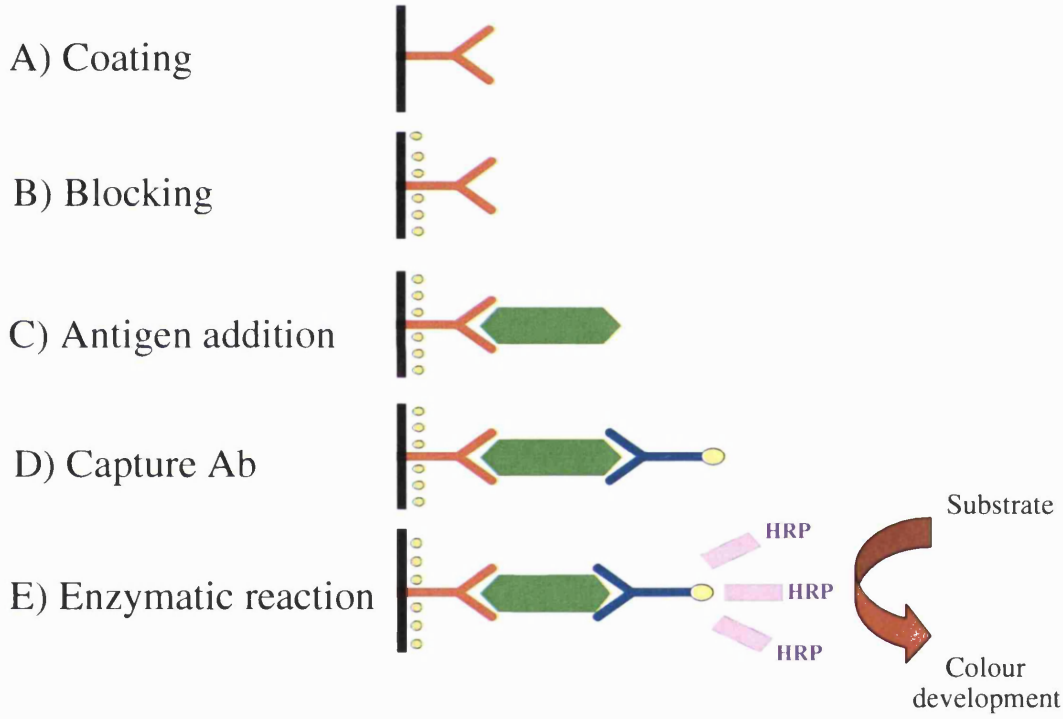

Figure 2.3 Schematic presentation of steps involved in direct sandwich ELISA. *A) Capture antibody is attached to the solid phase. B) Excess antibody is decanted and blocking buffer is added. C) After washing, antigen is added. D) Another washing step followed by the addition of biotinylated detection antibody. E) After washing, incubation with streptavidin-HRP is followed by the last washing step. Enzymatic colour development is achieved by adding TMB substrate, and stopping the reaction with 2 M* H_2SO_4.

2.4 Recombinant Chinese Hamster Ovary (CHO) Cells

Recombinant CHO cells expressing human apoE3 (CHOE3) were kindly provided by Dr A Tagalakis (Department of Medicine, Royal Free & University College Medical School, London, UK). The apoE3 sequence was checked by sending PCR products from the extracted DNA for sequencing. The aim was to use recombinant CHO cells expressing apoAI as a positive control for the characterization studies of CHOE3. In this section, the methods used for generation and characterization of recombinant CHOAI cells are described.

2.4.1 SITE-DIRECTED MUTAGENESIS OF APOAI IN pcDNA3.1.AI

The *full-length* human apoAI cDNA sequence in a pcDNA3.1 vector (pcDNA3.1.AI) was kindly provided by Prof. L. Fan (Department of Biochemistry, Royal Holloway University of London, Egham, UK). The first step involved checking the sequence of apoAI, which was achieved by excising the apoAI fragment with *HindIII* and *EcoRI* enzyme to obtain the predicted 806 bp product on an agarose gel, followed by gel purification and sequencing (*Sections* 2.2.6, 2.2.7.2, and 2.2.7). The sequence chromatogram of this product showed a correct orientation of the apoAI sequence within the vector, but unexpectedly revealed a mutation at position 354 bp of the sequence (chromatogram not shown). The mutation was corrected by using the 'QuikChange Site-Directed Mutagenesis Kit' from Stratagene Ltd. This procedure uses a double stranded DNA vector and two synthetic oligonucleotides that are complementary to opposite strands of the sequence of interest and contain the desired mutation. After primer annealing, *Pfu* Turbo DNA polymerase is used for primer extension, which incorporates the mutation into the linearised vector sequence. Following polymerization in a thermal cycler, the parental DNA template is digested with *DpnI* endonuclease. This enzyme is specific for methylated and hemi-methylated DNA and allows selection of mutation-containing synthesized DNA. The nicked vector sequence containing the desired mutation is then transformed into *E. coli* that re-ligates the two ends of linear DNA and generates circular plasmids. The presence of the desired mutation is subsequently confirmed by analyzing bacterial clones. The potential for random mutations throughout this procedure is reduced through the use of a small quantity of starting DNA

template, a low number of PCR cycles and the high fidelity of the *Pfu* Turbo DNA polymerase.

The point mutation in pcDNA3.1.AI caused an amino acid change from a lysine (AAG) to an asparagine (AAT). To correct T to G, the following synthetic oligonucleotide primers were designed so that they contained the correct bases:

Forward primer: 5' AT CTG GAG GAG GTG AAG GCC AAG GTG CAG C 3'
Reverse primer: 5' TA GAC CTC CTC CAC TTC CGG TTC CAC GTC G 3'

The vector containing the mutated sequence was purified from bacteria using the miniprep extraction protocol (*Section* 2.4.2.5). The reaction mixture was made up using 5, 20, or 40 ng of DNA template and the following components in a final volume of 50 µl:

125 ng forward primer
125 ng reverse primer
1 X cloned *Pfu* reaction buffer
200 µM dNTP mix
2.5 U *Pfu* Turbo DNA polymerase

The cycling parameters were as listed below considering Stratagene's recommendation to use 12 cycles for point mutations and 2 min for the extension step per every kb of plasmid length.

denaturation (one cycle):	95 °C	30 s
annealing & extension (12 cycles):	95 °C	30 s
	55 °C	1min
	68 °C	12 min

Following temperature cycling, the reaction mix was placed on ice for 2 min to cool the reaction. Ten µl of the amplified products were run on a 1% agarose gel (*Section* 2.2.6), and confirmed that sufficient amplification was achieved. The next step was to digest the parental DNA by adding 10 U of *DpnI* enzyme to each amplified reaction and incubating it at 37 °C for 1 h. Transformation of 1 µl *DpnI*-treated DNA into *E. coli* JM109 cells was

then carried out (*Section* 2.4.2.5) followed by sequencing of plasmids extracted from bacterial clones to verify the success of the mutagenesis.

2.4.2 CONSTRUCTION OF p7055 VECTOR ENCODING APOAI

2.4.2.1 Preparation of p7055 Expression Vector

p7055 contains two *BamHI* sites (*Chapter* 4), making it difficult for cloning apoAI obtained from pcDNA3.1.AI (after cut with *BamHI* and *HindIII*). Thus, p7055 was initially digested by two separate reaction mixtures (reaction A, and B) as indicated in Table 2.9. Both reactions were incubated at 37 °C for 50 min (reaction A) and 20 min (reaction B) prior to electrophoresis on 1% agarose gel (*Section* 2.2.6). The gel photograph obtained is shown in *Figure* 2.4 (Panel a). The ~6.8 kb band from reaction B (partial digestion with *BamHI*) that is the same size as the linear plasmid (corresponding to the band from reaction A) was excised and gel purified, eluting the plasmid in 40 µl of elution buffer in the final step of the procedure (*Section* 2.2.7.2). Partial digestion with *BamHI* resulted in obtaining a linear plasmid randomly cut in both *BamHI* sites as marked in *Figure* 4.2. This was followed by setting up four digestion reactions (reactions C, D, E, and F) as shown in Table 2.9. Each of these reactions was incubated at 37 °C for 75 min prior to separation of the digestion products on 1% agarose gel (*Section* 2.2.6). As shown in *Figure* 2.4, the linear vector with IL-2 cDNA excised, was obtained from reaction F (band of ~6.3 kb). This ~6.3 kb band was excised and gel purified as described in *Section* 2.2.7.2 (*Chapter* 4). The vector was then dephosphorylated (*Section* 2.4.2.2) and used for cloning the apoAI cDNA (*Section* 2.4.2.4).

Reagents	Digestion reactions					
	A	B	C	D	E	F
Uncut p7055	1.0 µl	3.0 µl	1.0 µl	1.5 µl	1.0 µl	–
Linear p7055 (from reaction B)	–	–	–	–	–	40 µl
10 X NEB2 buffer	1.5 µl	6.0 µl	1.5 µl	1.5 µl	1.5 µl	5.0 µl
BamHI (dilution in water)	–	3.0 µl (1/50)	1.0 µl (1/25)	1.0 µl (neat)	–	–
HindIII (dilution in water)	1.0 µl (neat)	–	–	1.0 µl (neat)	1.0 µl (neat)	5.0 µl (neat)
Nuclease-free water	11.5 µl	48 µl	11.5 µl	10.0 µl	11.5 µl	–
Total volume	15 µl	60 µl	15 µl	15 µl	15 µl	50 µl

Table 2.9 Requirements for setting up endonuclease digestion reactions used for preparation of p7055 vector.

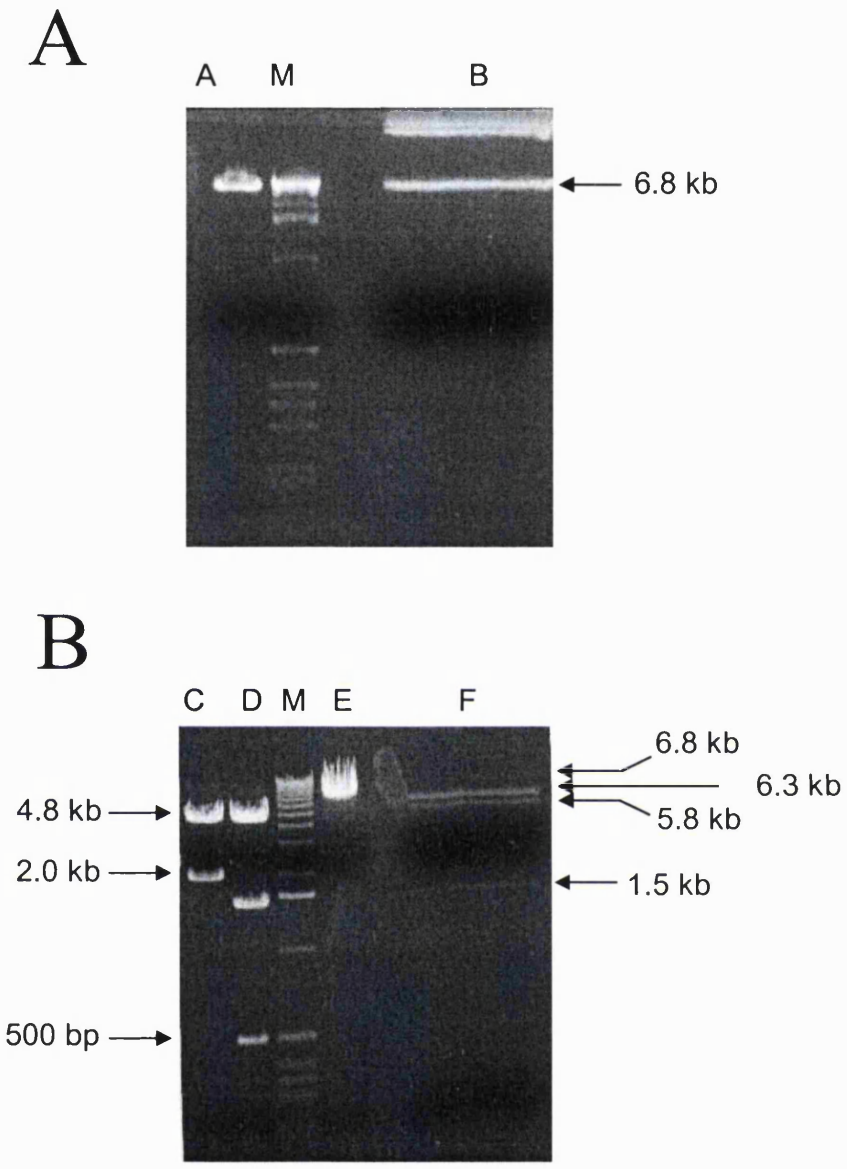

Figure 2.4 Preparation of p7055 for subsequent cloning. *The p7055 vector bears two BamHI restriction sites that makes it difficult for the cloning of apoAI cDNA that is obtained from pcDNA3.1.AI as a result of a digest with BamHI and HindIII (Section 4.2.1.2). Thus the vector was subjected to different digestion reactions as described in Section 2.4.2.* ***Panel A,*** *gel photograph (1% agarose gel) of the p7055 vector after digestion with reaction A (A on gel) and B (B on gel) as described in text. The ~6.8 kb band from B (corresponds to the linear vector from A) was excised and gel purified.* ***Panel B,*** *four digestion reactions were set up as described in Section. All the digestion products were separated using a 1% agarose gel. The 6.2 kb from reaction F (F) was excised and gel purified as it corresponds to the p7055 vector with IL-2 cDNA excised. The vector was now ready for subsequent cloning of apoAI cDNA. M = 1kb ladder.*

2.4.2.2 Dephosphorylation Reaction

Restriction endonucleases produce 'sticky ends' that facilitate binding of most vectors to DNA fragments (*Section* 2.2.8). During ligation, the phosphate groups left at the 5' end form phosphodiester bonds with the adjacent nucleic acids linking the vector with the incoming nucleic acid sequence. The vector could potentially re-circularise instead of ligating to the inserted fragment. Consequently, it is essential to remove terminal 5' phosphates by the process of dephosphorylation that uses calf intestinal alkaline phosphatase (CIP; purchased from Roche Diagnostics, East Sussex, UK).

One microgram of the p7055 vector was subjected to endonuclease digestion (*Section* 2.2.8) with *BamHI* and *HindIII* after which the vector was purified and eluted in 30 µl of deionised buffer (*Sections* 2.2.7.1 and 2.2.7.2). Dephosphorylation was then performed by preparing the following reaction mix with a final volume of 40 µl:

Component	**Volume (µl)**
Purified cut vector (eluted in 30 µl)	30
10 X alkaline phosphatase buffer	4
Sterile water	4
CIP (1 U/µl)	2
Total Volume	**40**

The reaction mix was incubated for 1 h at 37 °C prior to addition of another 1 µl of CIP and a further incubation at 37 °C for 30 min. The reaction was stopped by the addition of 2 µl 0.5 M EDTA and incubation at 65 °C for 20 min. The plasmid was then subjected to ethanol precipitation.

2.4.2.3 Ethanol Precipitation

Ethanol precipitation is generally used for purification and concentration of plasmids or DNA. The dephosphorylated p7055 vector was purified and concentrated using ethanol precipitation. For this procedure, one-tenth of the volume of 3 M sodium acetate (pH 5.2) was added to the reaction mix, followed by 2.5 times the combined volume of 100 % ethanol. After mixing, the tube was left overnight at -20 °C before centrifuging for 20 min at

4 °C. The supernatant was removed and the pellet was washed by adding 100 µl of 70% ethanol and centrifuged for 15 min at 4 °C. Following another wash, the ethanol was removed and the dephosphorylated and concentrated vector was re-suspended in 10 µl of sterile water.

2.4.2.4 Ligation

Complementary sticky ends of vector and insert are ligated by T4 DNA ligase that catalyses the formation of phosphodiester bonds between neighbouring 3'-hydroxyl and 5'-phosphate ends in double-stranded DNA (Weiss B *et al*, 1968). For p7055 ligation, a vector DNA:insert DNA molar ratio of 1:3 was used. The following equation was used to calculate the appropriate amount of vector and inserts for the ligation reaction:

ng insert = [(ng vector x kb size of insert)/kb size of insert] x molar ratio (insert:vector)

The reaction mix was composed of the following:

Components	**Volume (µl)**
Vector (< 1 µg/10µl)	1
Cut PCR Product	5 or 15
T4 DNA Ligase (1 U/µl; Roche Diagnostics)	1
10 X DNA Ligase Buffer	2
Final Volume	**Made up to 20 µl with deionized water**

The ligation took place at 4 °C for 16 h. The next step involved transformation of the ligated plasmid DNA (p7055.AI) into competent bacterial cells (*Section* 2.4.2.5).

2.4.2.5 Transformation of p7055.AI into Competent *E. coli* Cells

The ability of bacterial cells to take up recombinant DNA vectors is enhanced when the cells are in a 'competence' state (Hanahan D, 1983). This can be achieved by treating bacteria with an ice-cold solution of 50 mM calcium chloride prior to heating them briefly. The

transformation efficiency of DH5α strain of *E. coli* (kindly provided by Dr A Manzano, Department of Medicine, Royal Free & University College Medical School, London, UK) was assessed by transforming the bacteria with a circular plasmid and then calculating the number of colony forming units/μg DNA. The cells were regarded to be competent as more than 1 x 10^8 colony forming units/μg DNA was observed.

Fifty microlitres aliquots of competent cells were thawed out on ice and gently mixed with 5μl of ligation mix (1-50 ng of DNA is required) in pre-chilled tubes. After 10 min incubation on ice, the tubes were transferred to a 42 °C water-bath for exactly 45 s before being replaced in ice for another 5 min. LB (Luria-Bertani) broth was warmed to 37 °C and 125 μl was added to each tube, which was then shaken at ~200 rpm for 1 h at 37 °C. Different volumes (10 μl, 20 μl or 100 μl) from the content of each tube were then spread onto LB agar plates (containing 100 μg/ml ampicillin), which were left for 1 h at room temperature before being placed inverted in a dry 37 °C incubator overnight. The plasmid vector contained an ampicillin resistant gene. Therefore, successful transformants exhibit ampicillin resistance and will grow on the selection plates. For a negative control, the same procedure was repeated without using DNA in the transformation reaction. If the ampicillin selection is successful, then the plates containing the negative control mix should contain no colonies.

Colony growth was found in all plates except the negative controls, as expected. A total of three colonies were picked from the plates using sterile pipette tips, and cultured overnight in 50 ml tubes containing 6 ml LB broth (containing 100 μg/ml ampicillin) at 37 °C with shaking (~200 rpm). The bacterial clones can then be stored permanently at -80 °C as glycerol stocks. Glycerol stocks are prepared by mixing an equal volume of the overnight culture with sterile glycerol prior to storing them at -80 °C. After storage, the exponential growth of bacteria can be prompted by removing the stocks from freezer, spreading them onto LB plates and incubating the plates at 37 °C.

2.4.2.6 Plasmid Extraction from Bacterial Host Cells

In order to isolate successful transformants, plasmids should be extracted from the clones that were picked from the agar plates before being analysed by endonuclease digestion and

agarose gel electrophoresis. Small or large scale extraction procedures were used. In a small scale extraction, 3 ml of the overnight cultures and the Wizard Plus Minipreps DNA Purification System (Promega) were used. The cells were pelleted by spinning at 16,060 *g* for 2 min prior to resuspension in 200 µl TB buffer: 50 mM Tris.HCl (pH 7.5) and 10 mM EDTA. Two hundred microlitres of cell lysis buffer [0.2 M NaOH and 1% (w/v) SDS] was subsequently added to each tube and the contents were mixed by inversion. After the addition of 200 µl neutralisation solution (1.32 M potassium acetate), the cell debris were removed by 5 min centrifugation at 16,060 *g*. One millilitre of the provided DNA-binding resin was added to the supernatant and the resulting slurry was passed through a mini-column. Column wash solution (2 ml) was used to wash the DNA before it was dried by centrifuging the column at 16,060 *g* for 2 min. DNA plasmids were subsequently eluted with 50 µl deionised water and collected by brief centrifugation. The plasmids were either analysed immediately or stored at -20 °C for later analysis.

Twenty microlitres of miniprep DNA extracted from each cultured colony (*Section* 2.4.2.5) were subjected to restriction digest with *BamHI* and *HindIII*. The digest products were then run on a 1% agarose gel to check for the presence of successful transformants. Two of the analysed clones had the correct p7055.AI plasmid (*Chapter* 4). A large-scale plasmid preparation for one of these clones was then performed using its remaining cell pellets. This required 100 ml of the overnight cultures and the Qiagen's EndoFree Plasmid Maxi kit. This protocol was similar to the steps described above, except for being on a large scale and yielded 240 µg of plasmid as calculated by OD measurements at 260 nm. This plasmid was again checked by restriction digest and agarose gel electrophoresis to confirm direct orientation of apoAI inserted in p7055 vector (data not shown).

2.4.3 TRANSFECTION AND SELECTION OF STABLE CLONES

As described above (*Section* 2.4.2) human apoAI cDNA was cut from pcDNA3.1.AI and cloned into p7055 vector. This plasmid (p7055.AI) was then used to transfect CHOdhfr- cells as follows:

2.4.3.1 Transfection of CHOdhfr- Cells

CHOdhfr- cells were seeded 1 day prior to transfection in a 6-well plate and incubated in the growth medium overnight to produce a monolayer at ~70% confluency. On the day of transfection, 2 μg of p7055.AI was diluted in 100 μl of culture medium free of serum or antibiotics. This was then incubated with 10 μl Superfect Transfection Reagent from Qiagen (see *Section* 2.5.2 for more information on Superfect) for 10 min at room temperature. The growth medium was aspirated from CHOdhfr- cells and they were washed with 2 ml of pre-warmed medium. The transfection complexes were subsequently mixed with 600 μl fully-supplemented maintenance medium, and added to the cells. Cellular uptake of DNA was allowed by incubating the plate for 3 h at 37 °C (and 5% CO_2) before removing the transfection mixture, washing the cells twice with 4 ml PBS, and adding fully-supplemented growth medium. The cells were then incubated overnight. The cytotoxicity of the protocol was also tested in parallel by performing the same transfection protocol in two different wells with Superfect Transfection Reagent alone, and DNA alone, respectively. pcDNA3 plasmid encoding the green fluorescent protein (pGFP) was kindly provided by Dr A Manzano. As a positive control for the Superfect Reagent, 2 μg of pGFP plasmid was transfected into cells of another well following the same protocol. After 24 h, GFP fluorescence was detected with an inverted fluorescent microscope (Nikon Eclipse TE200) at 20 X magnification using incident light of wavelength 465-495.

2.4.3.2 Selection of Transfected Cells

The mutant CHOdhfr- cells lack the *DHFR* gene, therefore, they are defective in endogenous purine and pyrimidine base synthesis. As a consequence, they require the addition of hypoxanthine and thymidine (HT) to their normal growth medium (Table 2.4). In any transfection, only a small percentage of transfected cells have the DNA integrated into the host genome. In order to select these cells, which have long-term and stable transgene expression, a selectable marker such as *DHFR* gene can be used. Thus, twenty four hours after transfection as described above, selection of successfully transfected cells began by removing HT supplement from the growth medium. These cells expressed DHFR as well as human apoAI and were thus expanded and maintained under selection pressure. Selection was continued over 2-3 weeks and the cells obtained were referred to as the 'mixed population of cells'. They were cryopreserved (*Section* 2.2.4.2) and production of

apoAI was confirmed by SDS-PAGE (*Section* 2.2.2.1) and Western blotting (*Section* 2.2.3). This was followed by quantification of secreted apoAI by scanning densitometry (*Section* 2.4.4).

2.4.3.3 Isolation and Analysis of Clones and Sub-Clones

The mixed population of cells obtained after the addition of selection medium to the transfected cells were cloned. Cloning allows the production of a genetically homogenous population of cells resulting from a single cell by mitosis. Two cloning procedures were used in this thesis as follows:

Cloning in 90-mm dish

Recombinant CHOAI cells were trypsinised from a confluent 25cm^2 flask, followed by suspension in maintenance medium. A cell count was performed and the suspension then serially diluted in six 15 ml tubes to give final concentrations of 320, 160, 80, 40, 20, and 10 cells/10 ml in each individual tube. The content of each tube was then emptied in a 90-mm dish. Once the cells had adhered to the plates overnight, the position of single cells were marked on the underside of each plate using an inverted light microscope. The cells were allowed to undergo about five cell divisions (2-4 days) before being removed gently by trypsinisation (*Section* 2.2.4.2) using an inverted light microscope and a 20 µl Gilson pipette containing a few microlitres of media. The tip of the pipette was used to gently detach each clone that appeared spherical under the microscope. This was followed by applying suction so that a few cells were picked up and then transferred to a well of a 12-well plate. Two ml maintenance medium was added to each well. The medium was changed every 4 days and the cells were allowed to expand.

Cloning in 96-well plate

A cell suspension of recombinant CHOAI cells was prepared and counted as described earlier for cloning in 90-mm dish. Wells of a 96-well plate were filled with 100 µl of maintenance medium. 100 µl of diluted cell suspension were seeded in each well so that there was 1 cell/well. After 3-4 days, clones were apparent in some of the wells checked under an inverted light microscope. After about a week, medium was changed every 3 days and the cells were kept in culture at 37 °C for another 2-3 weeks until clones were large

enough to be picked up by trypsinising each well and transferring its content to a 24-well plate.

Clones isolated by both methods were expanded gradually until they were ready for cryopreservation and analysing the transgene expression by SDS-PAGE and Western blotting using conditioned medium (*Sections* 2.2.2, 2.2.3, and 2.4.4.1). Two of the high-producer CHOAI clones were selected and further sub-cloned as described above in order to increase the possibility of selecting a pure clone. After choosing one of the high-producer CHOAI sub-clones, continuous secretion of apoAI was tested by passaging the cells a few times and examining their recovery following cryopreservation. The quantity of apoAI secreted was also determined by scanning densitometry of immunoblots (*Section* 2.4.4.2). The best apoAI-producer sub-clone was then used as a positive control for determining some of the physical and biological characteristics of apoE3 secreted by recombinant CHO cells (*Sections* 2.4.5, 2.4.6, and 2.4.7).

2.4.3.4 Methotrexate (MTX) Amplification

MTX is a common agent for amplification of stably-integrated DNA. It is believed that resistance to MTX toxicity can occur with an increased level of dhfr expression (Schimke RT, 1988). This can be achieved in the stably-transfected cells as they express both the desired and *DHFR* gene. Once the stably-transfected CHOAI clones were isolated and expanded (*Section* 2.4.3.3), two of the best-apoAI producers were subjected to growth in maintenance medium with the addition of 2nM MTX. The amount of added MTX was doubled gradually (up to 32 nM) after each subculture. Conditioned medium (24 h collection) was analysed for apoAI production after each MTX addition.

2.4.4 SCANNING DENSITOMETRY FOR APOAI QUANTIFICATION

2.4.4.1 Preparation of CHOAI Conditioned Medium

It was necessary to produce CHOAI conditioned medium for scanning densitometry as well as for future physical and biological characterisation experiments. For scanning densitometry, CHOAI and control cells (CHOdhfr-) were grown overnight in 6-well plates to 80% confluency in maintenance medium (Table 2.4) before being washed with pre-warmed PBS. They were then incubated with their corresponding serum-free maintenance medium (Table 2.4) for 24 h conditioning. Conditioned medium was then sterile-filtered

using a 0.2 μm filter. For experiments requiring more concentrated apoAI, conditioned media was collected from confluent 175 cm^2 flasks. The medium was subsequently centrifuged at 300 x *g* for 3 min to remove cell debris. This was followed by concentrating the medium 40 X in Vivaspin 15 ml concentrators (10,000 MWCO or molecular weight cut-off) (Vivascience Ltd., Binbrook, UK) at 2,500 *g* for 15-30 min. Control CHOdhfr- cells were treated similarly.

2.4.4.2 Scanning Densitometry

The conditioned media from 6-well plates of CHOAI and control cells were subjected to SDS-PAGE and immunoblotting (*Sections* 2.2.2 and 2.2.3). Known quantities of pure apoAI (delipidated apoAI purified from human plasma, kindly provided by Dr G Sperber, Department of Medicine, Royal Free & University College Medical School, London, UK) were run on the same gel. The generated autoradiograph was used to determine levels of apoAI secretion using the bands from pure apoAI for establishing a standard curve by the aid of scanning densitometry (Bio-Rad Imaging Densitometer, Model GS-670). The local background was subtracted from each of the values and the mean 'adjusted volume' was calculated by the densitometer. It was necessary to obtain a standard curve for each apoAI quantification carried out throughout this thesis.

2.4.5 BASIC CHARACTERISATION OF CHO CELL-DERIVED APOE3- AND APOAI-CONTAINING PARTICLES

2.4.5.1 Agarose Gel Electrophoresis

Fresh samples of conditioned medium (containing ~2 μg of apoE3 and apoAI) from CHOE3, CHOAI (used as a positive control) and control CHOdhfr- cells were analysed by electrophoresis on alkaline-buffered (pH 9.2) 0.8% agarose gels using the HYDRAGEL LIPO + Lp(a) kit from Sebia (Issy-les-Moulineaux, France) according to the manufacturer's instructions. Samples of fresh plasma (2 μl per lane) were used as controls to monitor lipoprotein migration in the gel. The migration pattern of the main plasma lipoproteins classes that can be visualized by agarose gel electrophoresis is illustrated in *Figure* 2.5. HDL particles migrate to the alpha position; at the pre-beta position VLDL particles can be seen; LDL particles migrate lower than VLDL particles at the beta position; and chylomicrons remain at the application point. If sufficient amounts of lipoprotein (a) or

Lp(a) are present in the plasma, then a band between HDL and VLDL represents the migration of these particles.

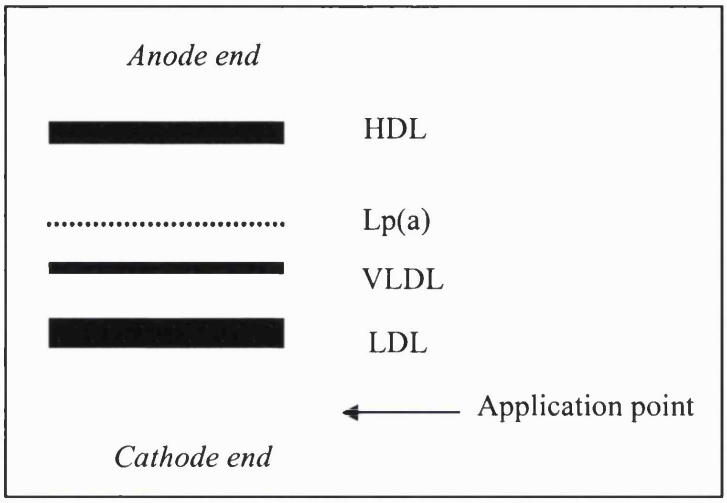

Figure 2.5 Migration pattern of plasma lipoproteins on agarose gel.

The prepared conditioned media and a sample of fresh plasma were applied to the agarose gel and allowed to diffuse into the gel, which was then placed in the electrophoresis chamber (Sebia K20) containing 300 ml of the supplied Tris-barbital (pH 9.2) running buffer. Electrophoresis was carried out for 2 h at a constant voltage of 50 V. One lane of plasma was subsequently cut from the rest of the gel and subjected to 15 min staining with freshly prepared Sudan black staining solution (0.044% w/v in 53% ethanol). After destaining with 45% ethanol (v/v), the migration pattern of the lipoprotein bands was revealed. The particles on the remainder of the gel were transferred to Hyperfilm ECL nitrocellulose for immunoblotting using diffusion blotting as a mode of transfer. The nitrocellulose was cut to size, pre-soaked in PBS and placed on top of the gel followed by two sheets of PBS-soaked filter paper (Whatman International Ltd.) removing any trapped air bubbles by rolling a test tube over the sandwich. This was followed by 6 sheets of dry filter paper and a glass plate was then placed on the top to distribute a 100 g weight. After 1 h of transfer, the gel was dried and stained with Sudan black to check the efficiency of transfer, while the membrane was subjected to immunoblotting (*Section* 2.2.3) with the relevant antibodies (Table 2.3).

2.4.5.2 Non-Denaturing Gradient Gel Electrophoresis (NDGGE)

Unlike SDS-PAGE (*Section* 2.2.2.1), NDGGE is used when the protein is to be maintained in its native state. In addition, it is based on mixing two acrylamide gel solutions of different percentages forming a gradient up the gel. The gradient starts with a higher concentration of cross links at the bottom, which form very small pores, all the way to a low concentration of cross links at the top, which form relatively large pores. The NDGGE technique allows effective separation of molecules depending on their size without losing the very small molecules by running them off the gel.

Conditioned medium (24 h collection) from CHOE3, CHOAI (containing ~2 μg of apoE3 and apoAI), and CHOdhfr- were subjected to NDGGE. A 4-25% TBE polyacrylamide gel was pre-focused with a constant voltage of 125 V for 30 min at 4 °C. The samples were diluted (1:1) in sample buffer (10% sucrose/0.016% bromophenol blue) before being loaded onto the pre-focused gel alongside 15 μl of pre-stained molecular marker (50 μg, Pharmacia). Electrophoresis was then carried out in a Novex chamber using the following conditions at 4 °C:

25 V for 15 min
50 V for 15 min
75 V for 15 min
250 V for 24 h

The region of the gel containing the marker was cut and stored in PBS for later use. The proteins in the rest of the gel were then transferred to a nitrocellulose membrane using the wet transfer system as explained in *Section* 2.2.3.2. Transfer was allowed to occur with a constant voltage of 200 mA for 12-16 h at 4 °C. Immunoblotting (*Section* 2.2.3) was subsequently carried out in order to determine the particle size distribution of apoE3 and apoAI.

2.4.6 MEASURING CELLULAR FC EFFLUX BY CHO CELL-DERIVED APOE3- AND APOAI-CONTAINING PARTICLES

Radioisotopes are commonly used as tracer molecules in metabolic investigations. One such isotope is tritium (^3H) with an unstable atomic nucleus emitting an electron during its decay. Tritium is thus known as a β-emitting radioisotope. The number of radioactive atoms present is directly proportional to the number of decay events in a given time interval. Consequently, the total number of radioactive atoms present in a sample can be determined by measuring the number of decay events by means of liquid scintillation counting (LSC). This method uses a fluorescent organic compound as a scintillant. The photons of light emitted upon the excitation of the scintillant with radiation or electrons is captured by photomultiplier tubes and quantified. In order to determine whether secreted apoE3 particles by recombinant CHOE3 cells are biologically active in promoting FC efflux, conditioned medium from the cells was incubated with labelled [^3H]-cholesterol human macrophages (used as cholesterol donor) and the amount of radioactivity effluxed into the medium was measured using LSC. Conditioned media from CHOAI and CHOdhfr- cells were also used as positive and negative controls, respectively. The first step was to prepare differentiated macrophages.

2.4.6.1 Monocyte Differentiation into Macrophages

The phorbol ring in phorbol 12-myristate 13-acetate (PMA) is known to bind to cell membranes activating a signal transduction pathway and thus generating adherent THP-1 cells by preventing cell proliferation (Tsuchiya S *et al*, 1982). As a result, PMA was used in this thesis to differentiate THP-1 monocytes into macrophage-like cells. These cells mimic human monocyte-derived macrophages in different ways: a) accumulation of cholesteryl esters, b) secretion of apoE and lipoprotein lipase, and c) induction of scavenger receptors (Tajima S *et al*, 1985; Hara H *et al*, 1987). THP-1 cells were seeded into 12-well plates (0.35×10^6 cells/2 ml/well). For each experimental condition, triplicate or quadruplicate wells were seeded. PMA (1mM in DMSO) was added to each well at a final concentration of 250 nM, and the plates were incubated at 37 °C in a humidified atmosphere (95% air and 5% CO_2) for seven days. The medium containing PMA was replaced every two days. Thus, differentiated macrophages were developed with a characteristic morphology of irregular shaped nuclei and phagocytotic vacuoles.

2.4.6.2 Cholesterol Labelling of Macrophages and Efflux Experiments

Medium was aspirated from differentiated macrophages (*Section* 2.4.6.1) and the cells were labelled with 1 ml/well normal growth medium containing 5% (v/v) FBS and 1 μCi [^{3}H]-cholesterol. The cells were incubated at 37 °C for 24 h to allow uptake of radiolabelled cholesterol. At day 2, the labelling medium was removed and the cells were washed twice with maintenance medium free from serum (serum-free medium). The cells were then incubated for 16 h at 37 °C with equilibration medium (1 ml/well); serum-free medium with the addition of 1% fatty acid-free (w/v) BSA. At day 3, the cells were washed twice with serum-fee medium and incubated with 1 ml conditioned serum-free medium collected from CHOAI (~6 μg of apoAI) with/without 5% (v/v) HDL-plasma (plasma depleted of the apoB-containing lipoproteins), or 1 ml conditioned serum-free medium collected from CHOE3 (~6 μg of apoE3) with/without 5% (v/v) HDL-plasma, or 1 ml conditioned serum-free medium collected from CHOdhfr- cells with/without 5% (v/v) HDL-plasma (*Section* 2.4.4.1 explains preparation of conditioned medium).

Serum-free Iscove's modified DMEM was chosen for preparation of conditioned medium following preliminary cholesterol efflux experiments using CHOdhfr- cells incubated with a range of serum-free media (*Section* 4.2.5). Efflux was allowed to take place by incubating the cells at 37 °C for 4 h, or a time course (1, 2, 4, 8, and 24 h) was performed. Efflux was terminated by removing the medium from the cells and centrifuging it for 2 min at 16,060 *g*. A 800 μl aliquot of supernatant was used for LSC. In addition, cell monolayers were washed once with PBS and lysed in 1.0 ml of 0.1 M NaOH, taking an aliquot of 800 μl from each cell lysate for LSC. Both aliquots (supernatant and cell lysate) were mixed thoroughly with 8 ml of Cocktail T scintillation fluid in separate vials. As the medium and the cells contained [^{3}H]-cholesterol, the number of decay events occurring in each vial was measured over a time length of 5 min/vial with the aid of a liquid scintillation counter (Beckman LS 6500, Beckman Coulter Ltd.). The values were recorded in disintegrations per minute (dpm) that were subsequently used to calculate percentage FC efflux using the following equation:

$$\% \, FC \, efflux = A/(A + B) \, x \, 100$$

A = [^{3}H]-cholesterol in media (dpm)

B = [^{3}H]-cholesterol in cells (dpm)

The abilities of apoE3 and apoAI particles to efflux FC were then compared. The effect of HDL-plasma (generously provided by Dr J Mulcahy, Department of Medicine, Royal Free & University College Medical School, London, UK) on efflux was also compared since HDL is an extracellular cholesterol acceptor that promotes FC efflux (Fielding CJ *et al*, 1997). The methodology described for the measuring FC efflux was based on a protocol described by Gu *et al* (Gu X *et al*, 2000).

2.4.7 ABILITY OF CHO CELL-DERIVED APOE3- AND APOAI-CONTAINING PARTICLES TO ACTIVATE RECOMBINANT LCAT

Initially, a labelled cholesterol/albumin emulsion (*Section* 2.4.7.1) was prepared and tested to ensure its functionality and suitability for future LCAT assays. The LCAT used for experiments in this part of the thesis was prepared (*Section* 2.4.7.2) from recombinant CHO cells secreting human LCAT, referred to as CHOHis6-LCAT, kindly provided by Mr. J. Low (Department of Medicine, Royal Free & University College Medical School, London, UK). It was necessary to produce CHOHis6-LCAT conditioned medium for LCAT activity experiments. In addition, the presence of recombinant LCAT in the medium needed to be confirmed, for which anti-LCAT (α-LCAT) antibodies were prepared as described in *Section* 2.4.7.2.

2.4.7.1 Preparation of Labelled Cholesterol/Albumin Emulsion

The first step of LCAT activity assay was to prepare [^{3}H]-cholesterol/albumin emulsion based on a protocol described by Gillett *et al* (Gillett MPT *et al*, 1992). One millilitre of 5% BSA (w/v) in 0.2 M sodium phosphate buffer (pH 7.4) was prepared and heated in a 56 °C water bath for 30 min to destroy any endogenous LCAT activity. The solution was centrifuged at 500 x *g* for 15 min and the supernatant was transferred to a clean tube recording the weight of the tube and its contents. During this time, 5 μCi [^{3}H]-cholesterol was transferred to a tube containing a few drops of ethanol and the solvent evaporated under a stream of N_2.

The labelled cholesterol was re-dissolved in 100 μl acetone before being added drop-wise to the BSA solution whilst vortexing. The BSA tube was then placed in a 20 °C heating block

and a stream of N_2 was directed onto the surface of the solution to remove the acetone, whilst vortexing the tube every few minutes. After 30 min, the tube and contents was weighed again and compared to the original weight to determine the volume of water loss. The volume of lost water was then added drop wise to the tube while vortexing before passing the solution through a 0.2 μm filter. The emulsion was tested in an LCAT assay using human plasma (*Chapter* 4) and was ready to be used as a substrate in performing LCAT assays or stored at 4 °C for up to four days before use.

2.4.7.2 Preparation of Recombinant LCAT and α-LCAT Antibody

Recombinant LCAT preparation

CHOHis6-LCAT cells were grown overnight to 80% confluency in maintenance medium (Table 2.4) before being washed with pre-warmed PBS. They were then incubated with their maintenance medium without serum (serum-free maintenance medium) for 24 h conditioning. Conditioned medium was centrifuged at 300 x *g* for 3 min to remove cell debris. The medium was subsequently concentrated 100 X in Vivaspin 15 ml concentrators with 30,000 MWCO (Vivascience Ltd.) at 2,500 *g*. This stock of conditioned medium (for simplicity referred to as recombinant LCAT) was stored in aliquots at -80 °C. In order to confirm the presence of recombinant LCAT in the medium, it was necessary to prepare anti-LCAT antibody (α-LCAT) from LCAT hybridomas.

α-LCAT preparation

Six different sub-clones of LCAT hybridomas (suspension cultures) were generously provided by Dr T Jowett (Monoclonal Antibody Unit, Windeyer Institute of Medical Science, UCL, London, UK). Each batch was grown [RPMI supplemented with 1% Pyruvate, 0.5% Hepes, and 0.5% penicillin (100 U/ml)/streptomycin (100 μg/ml)] to confluency in two 75 cm^2 flasks and kept for 2-3 weeks in the humidified incubator at 37 °C until the cells were almost dead, determined by a morphological loss of round shape and becoming adherent to the plate. Once they were centrifuged for 3 min at 400 x g, the supernatants were concentrated 50 X and used as an antibody for detection of human LCAT. In a Western blot experiment (*Chapter* 4) using conditioned media from recombinant CHO cells (described above) and the prepared α-LCAT antibodies, it was demonstrated that the recombinant cells secrete LCAT and all the batches of prepared antibody were functional.

The secreted recombinant LCAT in the conditioned medium was subsequently shown to be active following an LCAT assay experiment using human plasma and heat-inactivated human plasma (*Chapter* 4). This experiment was also used to calculate the concentration of the recombinant LCAT. The stock of recombinant LCAT was subsequently used as the enzyme source in LCAT activity assays (*Section* 2.4.7.3).

2.4.7.3 LCAT Activity Assay

Conditioned media from recombinant CHOE3 or CHOAI (containing ~6 μg of apolipoproteins) or control cells (CHOdhfr-) were incubated in glass tubes with 50 μl of [^{3}H]-cholesterol/albumin emulsion adjusting the final volume to 450 μl with PBS if required. Human plasma was used as a positive control for the experiment. Following an overnight incubation on ice at 4 °C, 50 μl of recombinant LCAT (*Section* 2.4.7.1) was added to each tube before placing them in a 37 °C water bath and testing the activation of LCAT over 1 h or in a time course study (0.5, 1, 2, and 4 h). The reaction was terminated by taking a 100 μl of each sample and transferring it to a glass tube containing 4 ml pre-chilled chloroform/methanol (1:1). The reaction mix should be stored on ice if it is not immediately used.

Water (1.2 ml) was subsequently added to the tube and the mixture was vortexed thoroughly before centrifuging (MSE Mistral Centrifuge) at 500 *g* for 10 min at 4 °C. The lower organic phase was transferred carefully using a plastic micropipette to a clean glass tube containing 5-6 drops of methanol. The samples were then dried in heating block (40 °C) under N_2 before adding 200 μl of chloroform/methanol (1:1) per tube, rinsing the walls and repeating the drying step. The dried samples were dissolved thoroughly in 50 μl chloroform and transferred alongside 10 μl of lipid standard (Sigma) onto the application zones of TLC (thin layer chromatography) plates (Silica gel 60 Å; 20 x 20 cm, layer thickness 250 μm; Whatman, USA).

The gel was allowed to dry in air for a few minutes and subsequently transferred to a thin layer chromatography chamber containing ~50 ml solvent (sufficient to cover a few mm from the bottom of gel); hexane/diethylether/acetic acid in a 90:20:1 ratio. Lipid separation was terminated by removing the gel once the solvent had reached the top. The gel was air-

dried briefly followed by staining in a chamber containing iodine crystals. The pattern obtained after staining of human plasma is shown in *Figure* 2.6. Bands were generally stronger in plasma and marker lanes as they have a high lipid content compared to samples from the recombinant CHO cells. The gel was removed from the chamber and the CE and UC regions were marked with a pencil before being sprayed with water, scraped and transferred to scintillation vials containing 8 ml of the scintillation fluid. The vials were vortexed thoroughly and taken for LSC where dpm values were recorded over a period of 1 min. The percentage of [^{3}H]-cholesterol esterified by the recombinant LCAT was calculated using the following equation:

$$\% \text{ cholesterol esterified} = CE/(CE + UC) \times 100$$

CE = esterified cholesterol (dpm)

UC = unesterified cholesterol (dpm)

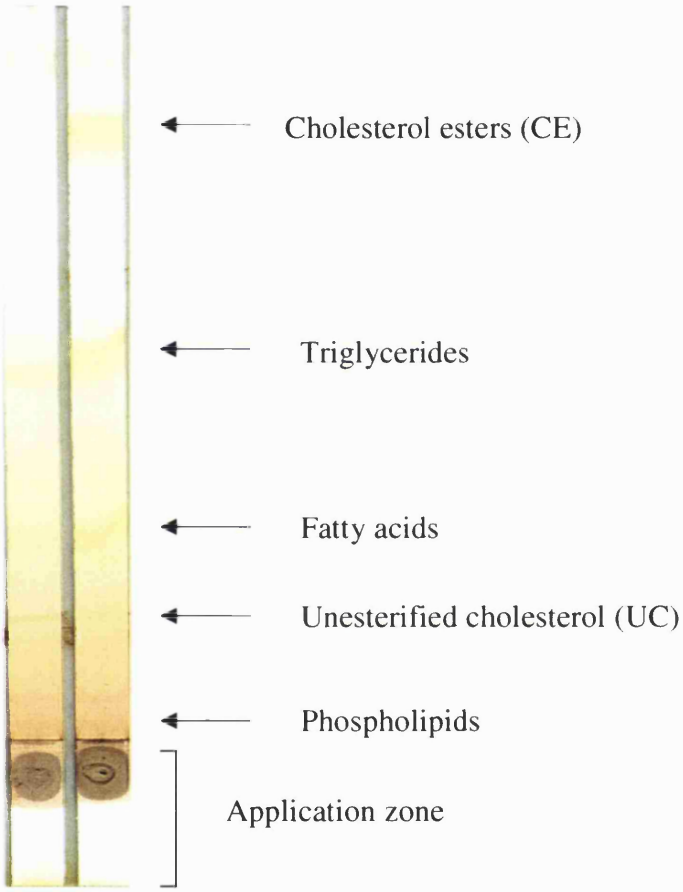

Figure 2.6 Separation of UC from CE by TLC plate. *Fifty microliters of labelled cholesterol/BSA emulsion (Section 2.4.7.2) was mixed with 100 ml of human plasma. Lipid separation was carried out on a TLC plate as described in Section 2.4.7.3. This figure illustrates the pattern of lipid separation after staining with iodine vapour.*

2.5 *APOE3* Gene Targeting

A range of different techniques are underway to target genes of interest for functional and therapeutic purposes. Efforts are focused to overcome a number of hurdles including effective delivery of genes or targeting vectors to desired tissues, and maintaining appropriate levels of required effect(s). RNA-DNA oligonucleotides (RDOs), also known as chimeraplasts, and single stranded oligonucleotides (SSOs) are relatively new approaches in gene targeting field with capacities to induce significant genotypic and phenotypic conversions (*Section* 1.5.6). These techniques were employed in this thesis in order to target *APOE3* gene in human cell lines.

THP-1 cells used in transfection experiments described in *Chapter* 5 were not treated with PMA to fully differentiate to macrophages, although, they are referred to as macrophages as they have macrophage-like properties such as expression of the mannose receptor (Rivera-Marrero CA *et al*, 2002). Human liver (HepG2) and macrophage (THP-1) cell lines were genotyped to confirm that they are from homozygous apoE3/E3 donors (*Section* 5.2.1). They were subsequently targeted by specific RDOs and SSOs in order to convert the *APOE3* gene to *APOE2* and *APOE4*. The ultimate aim was to demonstrate the feasibility of gene targeting by chimeraplasty (using RDOs). If chimeraplasty had proved successful, then biological studies will be performed to determine isoform specificity of liver-derived and macrophage-derived apoE particles. In addition, the *APOE3* gene was also targeted with SSOs.

2.5.1 DESIGN AND CONCENTRATIONS OF RDOs AND SSOs

2.5.1.1 Design of RNA-DNA Oligonucleotides (RDOs)

RDOs are complex double stranded molecules, typically 68 nucleotides in length (*Section* 1.5.6.1). Two 68-mer RDOs were designed for gene targeting of *APOE3* with the addition of a control RDO molecule. ApoE3-to-apoE2 RDOs were supplied by MWG (Germany) and Oswel (Southampton, UK), whereas the only apoE3-to-apoE4 RDO described in this thesis was provided by MWG. *Figure* 2.7, Panel A shows the structure of the synthetic apoE3-to-apoE2 RDO aligned with its homologous sequence in human *APOE3* gene. As described in *Section* 1.5.6.1, the top strand is known as the chimeric strand containing modified RNA residues (shown in lower case) and the bottom strand is referred to as the all-

DNA strand. The DNA nucleotides in the all-DNA strands are underlined. They are complementary to the sequence of apoE3 cDNA with the exception of a mismatched base (T) in the middle that is highlighted. This mismatched base has its complementary base (A) highlighted in the middle of the pentameric DNA region in the chimeric strand. Control apoE2-to-apoE3 RDO was designed in a similar way with the exception of the mismatched base being C in the all-DNA strand and G in the chimeric strand. The structure of the designed apoE3-to-apoE4 RDO molecule aligned with human apoE3 cDNA is shown in *Figure* 2.7, Panel B.

2.5.1.2 Design of Single-Stranded Oligonucleotides (SSOs)

The sequence of an SSO is homologous to the target DNA except for a mismatched base that causes the desired DNA base substitution. The mismatched base is complementary to the base that is to be introduced into the target DNA. The SSOs are end protected from endonuclease degradation by phosphothiorate linkages. Each of the SSOs for apoE3-to-apoE2 conversions were either provided by Dr L Kowarz (ValiGen, Paris, France) or purchased from Oswel. In each case, two SSOs were supplied, namely coding and non-coding as shown in *Figure* 2.8.

2.5.1.3 Estimating Concentrations of Oligonucleotides

Upon receiving the RDOs (supplied lyophilized), the tubes were briefly spun in a table-top centrifuge. Reconstitution was performed with endotoxin-free water before determining RDO concentration by measuring the absorbance at 260 nm and using the following equation recommended by MWG:

$$Concentration\ (pmole/\mu l) = OD_{260} \times 100/(1.54A + 0.75G + 1.17C + 0.92T\ or\ U)$$

A, G, C, T, U = number of each nucleotide

They were then stored at -80 °C in small (10-20 µl) aliquots. All SSOs were provided in liquid form, and after measuring their concentrations (as above), they were stored in the same manner as RDOs. Table 2.10 details the RDOs and SSOs used in this project.

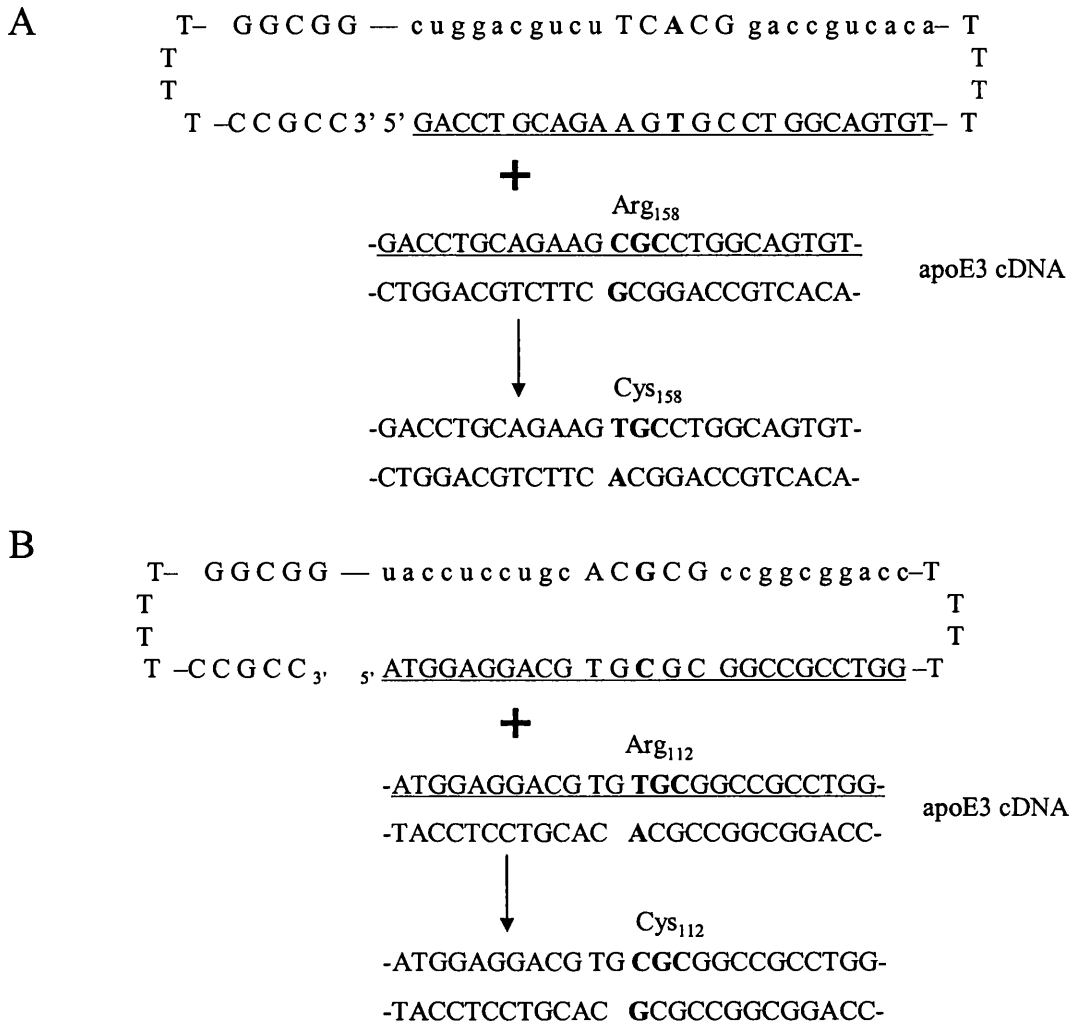

Figure 2.7 Structure of RDOs designed for *APOE3* gene targeting. *Sequences of the chimeric oligonucleotides for apoE3-to-apoE2* ***(Panel A)****, and apoE3-to-apoE4* ***(Panel B)*** *conversions, are aligned with homologous sequence of human apoE3 cDNA respectively. In each diagram,, DNA residues are in capitals and the 2'-O-methyl RNA residues are in lower case. The G:C clamp in the left is identified by an artificial break in the sequence complementary to the 3' to 5' bridge. The poly (T) hairpin loops are also indicated with artificial breaks at each side of the sequence. The targeted nucleotides in apoE3 cDNA are singly underlined. The DNA nucleotides in the all-DNA strand are complementary to the targeted nucleotides with the exception of a single mismatched base (highlighted) in the centre. The base complementary to this mismatched base is (highlighted) in the middle of the mutator region. With regard to the control apoE2-to-apoE3 RDO, the structure was designed in the same way as apoE3-to-apoE2 with the exception of the mismatched base being C in the all-DNA strand and so having its complementary base (G) in the chimeric strand.*

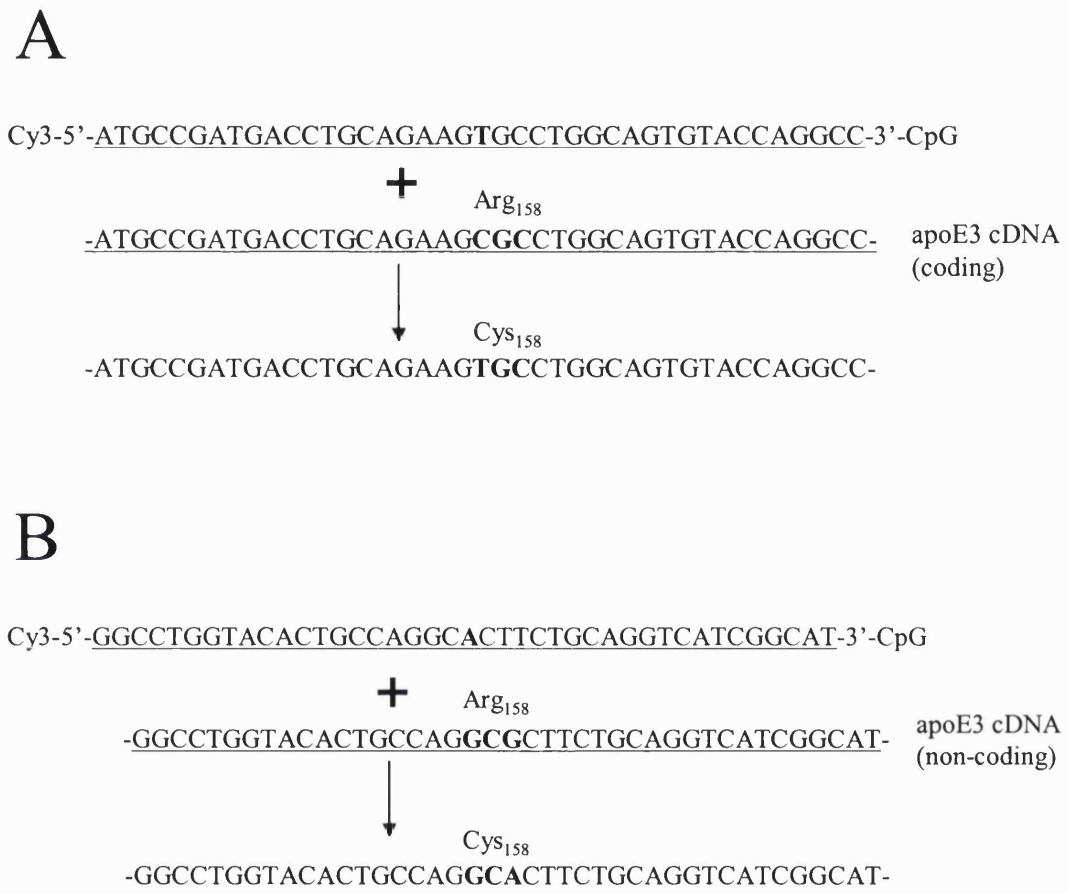

Figure 2.8 Structure of SSOs designed for *APOE3* to *APOE2* gene conversion. *Showing the sequence of the coding **(Panel A)** and non-coding **(Panel B)** SSOs aligned with human apoE3 cDNA, respectively. Each SSO consists of 41 DNA nucleotides that are homologous to the target DNA with the exception of a central mismatched base that is highlighted in above figures. Cy3 is a dye in the 5' end of the molecule protecting it from endonuclease degradation. This dye fluoresces red under an inverted fluorescent microscope. Inverted 3'CpG nucleotides refer to a cytosine followed by a guanosine base that are linked in a 3'-3' manner to the hydroxyl group of the 3' end nucleotide. They also protect the SSO from endonuclease degradation.*

ApoE3-to-apoE2	Supplier	Concentration (μg/ μl)
RDO1	MWG	2.5
RDO2	MWG	2.5
RDO3	MWG	2.4
RDO4	MWG	2.4
RDO5	Oswel	0.75
SSO1 (coding)	Oswel	0.6
SSO2 (non-coding)	Oswel	0.58
SSO3 (coding)	Valigen	2.5
SSO4 (non-coding)	Valigen	2.5
ApoE3-to-apoE4 RDO	*MWG*	*2.4*

Table 2.10 Oligonucleotide concentrations. *Concentrations of all the batches of apoE3-to-apoE2 RDOs and SSOs and the only batch of apoE3-to-apoE4 RDO with their supplier are shown here. Concentrations were calculated using an average of two OD_{260} and the equation shown in Section 2.5.1.3. These concentrations were used for designing transfection experiments throughout this thesis.*

2.5.2 TRANSFECTIONS WITH OLIGONUCLEOTIDES

A range of synthetic polycations have been reported for non-viral gene therapy (*Section* 1.5.4.2). These molecules differ in the number of their repeating units, their chemical structure and the architecture of the polymer backbone (e.g. linear or branched). Among them, PEIs have been mainly used in this report. PEIs have high cationic-charge density that makes them excellent reagents for DNA condensing and gene delivery (Godbey WT *et al*, 1999). Two members of this family, branched PEI (B-PEI) and linear PEI (L-PEI) were used in the transfection experiments. B-PEI (25 kDa) is a randomly branched molecule with equivalent portions of primary, secondary, and tertiary nitrogen atoms, while L-PEI (22 kDa) is a linear molecule mainly containing secondary nitrogen atoms. The presence of nitrogen atoms makes these molecules weak bases conferring upon them their buffering property. This led to the proton sponge hypothesis, which implies that after the endocytosis of PEI/DNA complexes, the cationic polymer buffers the endosomes. This in turn initiates a proton accumulation followed by passive chloride influx into the endosome and the resulting

osmotic swelling. As a consequence, endosome is disrupted and the endocytosysed complexes can escape degradation and reach the nucleus ensuring high transgene expression (Boussif O *et al*, 1995) (*Figure* 2.9).

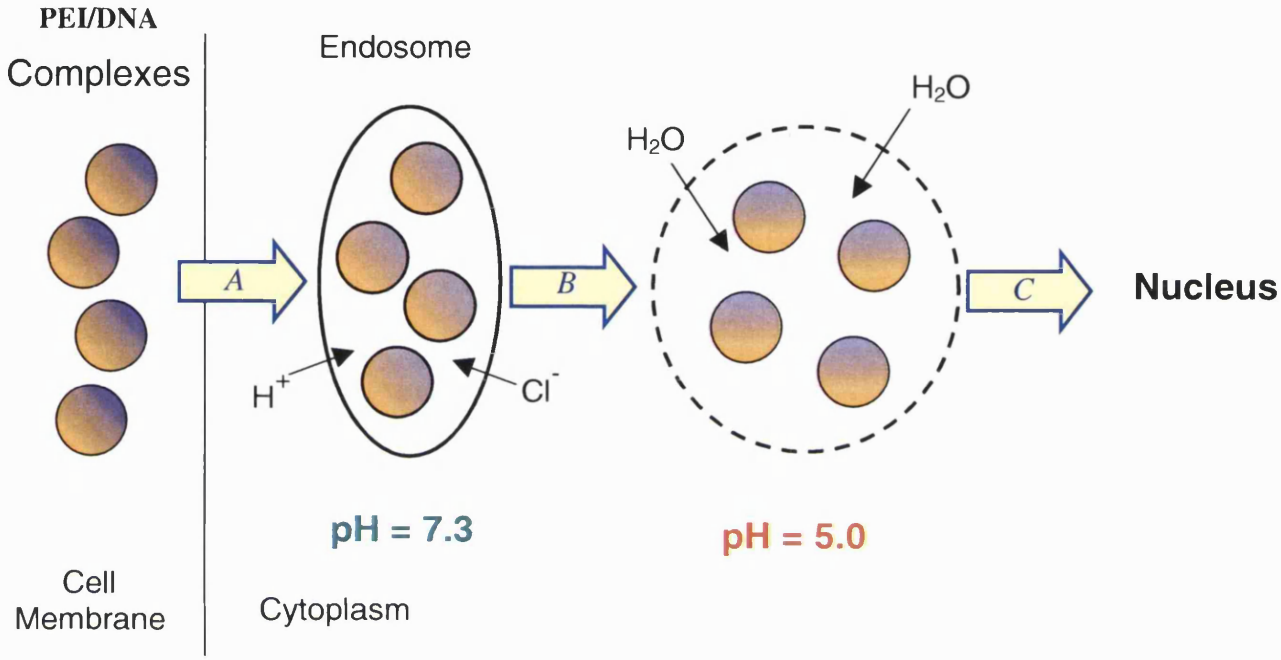

Figure 2.9 Schematic presentation of the 'proton sponge hypothesis' of PEI. *This is a modified figure taken from Kichler et al, 2001. It shows the ability of PEI to deliver intact DNA molecules to the nucleus and thus be an efficient gene transfer vehicle. A) PEI/DNA complexes enter the cytoplasm via endocytosis. The presence of nitrogen atoms that can be protonated in PEI leads to proton accumulation followed by influx of chloride ions. B) Osmotic swelling of the endosomes is followed by escape of complexes from degradation and C) their journey is continued towards the nucleus.*

The ability of PEI to transfect 25 different cell types including 18 mammalian cell lines as well as pig and rat primary cells have been documented (Boussif O *et al*, 1996). In addition, experiments of PEI-mediated gene transfer in newborn and adult mice and Sprague-Dawley rats have been reported (Boussif O *et al*, 1995). Furthermore, PEI can be conjugated to a variety of ligands such as sugars (discussed in *Section* 5.4.1), transferring, and antiCD3 (Ogris M *et al*, 1998). Provided the targeting ligand is recognized by the cell, this type of cell targeting is believed to improve transfection efficiency. PEI has been

successfully used in condensing RDO molecules for specified nuclear targeting (Bandyopadhyay *et al*, 1999; Kren BT *et al*, 1998).

PEI covalently conjugated with melittin (Mel-PEI) has been used in transfections carried out in this project (*Section* 2.5.2.2). Melittin is a 26-amino acid cationic peptide obtained from the venom of the European honey bee that can lead to membrane disruption (Dempsey CE *et al*, 1990). Transgene's expression as a result of melittin's ability to disrupt membranes has been previously reported (Legendre JY *et al*, 1997). Mel-PEI has been shown to improve release of DNA-carrier complexes from endosomes into the cytoplasm (Ogris M *et al*, 2001).

Superfect is an example of a polycation with a dendrimeric architecture, with branches radiating from a central core that terminate at charged amino groups (Gebhart CL *et al*, 2001). The Superfect-DNA complexes possess a net positive charge that allows them to bind to negatively charged receptors (e.g. sialylated glycoproteins) on the surface of eukaryotic cells. In addition, Superfect promotes the delivery of DNA into the cytoplasm by buffering the lysosome and inhibiting DNA degradation by lysosomal nucleases. LipofectAMINE^{TM} belongs to another group of delivery vehicles known as lipid transfection reagents. It associates with DNA via charged interactions to form a complex with an overall positive charge. The entry of the complex to the cell is achieved following the same path as described for PEI.

In preliminary experiments, three different transfection reagents (LipofectAMINE^{TM}, Superfect, and L-PEI) were tested in recombinant CHOE2 cells. A normal transfection procedure was used and the synthetic apoE2-to-apoE3 RDO (*Section* 2.5.1.1) was complexed with each reagent individually. Data (*Section* 5.2.2.1) supported the literature that L-PEI is the best transfer reagent (Boussif O *et al*, 1995). Hence, L-PEI was used for transfection trials with my synthetic 68-mer RDOs and 41-mer SSOs.

2.5.2.1 Transfections with Linear PEI

The normal transfection procedure was as follows. Cells were seeded into 6-well culture plates so that they would be 50-70% confluent the next day. Transfection mixture was freshly prepared by mixing 22 kDa L-PEI with increasing amounts of RDO (to give final

concentrations of 200-1000 nM), usually at a 5:1 amine (residues of L-PEI) to phosphate (residues of DNA) molar ratio (N:P). This was adjusted to a final volume of 50 µl by adding 150 mM NaCl. The mixture was incubated for 10 min at room temperature. The cells were first washed twice with 2 ml/well PBS before adding 0.5 ml of serum-free medium (maintenance medium without FBS) (*Section* 2.2.4.1) followed by the addition of the transfection mixture. Control cells received the same treatment except for the addition of the RDO molecule. Four-to-eight hours post-transfection, 1.5 ml of maintenance culture medium was added to each well. Cellular or genomic DNA was extracted (*Section* 2.5.4.1) after 24-48 h and analyzed by PCR-RFLP (PCR-restriction fragment length polymorphism) (*Section* 2.5.4.2). In some experiments, half of the cells were maintained and passaged four times before a second targeting with chimeraplast and/or cloning by limited dilution. The appropriate volume of L-PEI for each transfection was calculated using the following equation:

$$\textit{Volume of L-PEI (µl)} = \textit{(N:P ratio x 3 x µg of DNA)/}N^{+}$$

N:P ratio = molar ratio of nitrogen atoms in L-PEI to phosphates in DNA

3 = Need this number since 1 µg of DNA has 3 nmol of phosphate

N^{+} = Concentration (mM) of N^{+} residues in L-PEI (see Table 2.11)

For instance, the volume of L-PEI required for transfection with 1 µg of RDO and N:P ratio of 5:1, was calculated as shown:

$$\textit{Volume of L-PEI} = \textit{(N:P ratio x 3 x µg of DNA)/}N^{+}$$
$$\textit{Volume of L-PEI} = \textit{(5 x 3 x 1)/5.5}$$
$$\textit{Volume of L-PEI} = \textit{2.7 µl (as shown in Table 2.11)}$$

2.5.2.2 Transfections with Modified PEI and Other Reagents

Transfection experiments were prepared as described above for L-PEI transfections. Dr M Ogris (Institute of Biochemistry, University of Vienna, Vienna, Austria) kindly provided the modified PEI reagents. Table 2.11 shows the concentration of each reagent and the amount required per transfection. Volumes were calculated using the same equation explained for L-PEI in *Section* 2.5.2.1

DNA transfer reagent	Concentration of N^+ residues (mM)	Concentration of transfer reagent (mg/ml)	µl of transfer reagent/ µg oligonucleotide for shown N:P ratios		
			5:1	7:1	9:1
L-PEI	5.5	0.23	2.7	3.8	4.8
B-PEI	23	1.0	0.65	0.90	1.2
Mel-PEI	23	0.92	0.70	1.0	1.2
Gal4-PEI	50	0.19	0.30	0.40	0.60
Man-PEI	40	1.72	0.40	0.60	0.75

Table 2.11 Concentrations and volumes of DNA transfer reagents used in transfections. *The N^+ concentrations are used for determining how much DNA transfer reagent is required for each transfection considering the N:P ratio and using the equation given in Section 2.5.2.1. The symbols L-PEI, B-PEI, Mel-PEI, Gal4-PEI, and Man-PEI denote linear-PEI, branched-PEI, melittin-PEI, galactose4-PEI, and mannose-PEI, respectively. All the named reagents with the exception of L-PEI and B-PEI were prepared by chemical modifications of L-PEI (gifts from Dr M Ogris). In addition, Dr M Ogris also provided the B-PEI, while L-PEI was purchased from TCS Biologicals Ltd. (Section 2.1).*

2.5.3 MICROINJECTION OF RDOs

Direct delivery of RDOs into the nucleus by microinjection was also performed in order to ensure that DNA circumvents any obstacles that might hinder its delivery to the nucleus. Several coverslips were dipped in 70% ethanol and flamed before placing them into wells of a 12-well plate (1 coverslip/well). About 180 cells were seeded per coverslip in a final volume of 30 µl. The cells were then allowed to adhere for 4 h by incubation in a cell culture incubator before adding 1 ml of maintenance medium to each well. The following day, cells were transferred to a 90-mm dish, which was placed into an enclosed Perspex chamber of an inverted microscope (Zeiss-Axioscop) that was heated to 37 °C. Injection pipettes of 0.5 µm tip diameter were pulled with glass pipettes (1.2 mm bore) using a programmed pipette puller system. ApoE3-to-apoE2 RDO1 was diluted in PBS to a final volume of 2.5 µl, and ~1.28×10^{-11} µg of the diluted RDO1/cell was kindly microinjected by Dr M Dos Santos. The RDO solution was loaded into an injection pipette and the cells were microinjected individually. About 100 cells were microinjected per coverslip. The cells were maintained on the coverslips in 12-well plates for about one week prior to their transfer

to a 24-well plate. They were maintained and expanded for two weeks before being harvested (*Section* 2.5.4.1) and analysed by a PCR-RFLP method (*Section* 2.5.4.2).

2.5.4 PCR-RFLP ANALYSIS OF ALL TRANSFECTIONS

Several different methods have been described in the literature for determining the three different apoE isoforms (*Section* 1.3.4), apoE2, apoE3 and apoE4, which are encoded by Cys-Cys, Cys-Arg, and Arg-Arg at amino acid positions 112 and 158, respectively. These methods are either based on phenotyping or genotyping of apoE. Isoelectric focusing (IEF) is a common way of phenotyping apoE even though prolonged storage of the media or serum can cause artefactual results (McDowell IF *et al*, 1989). It was decided to use a genotyping analysis for determining any possible changes in the *APOE3* gene after treatment with RDOs and SSOs, as this method is based on using DNA that is stable when stored at -80 °C. In addition, it bypasses misclassification of apoE phenotypes caused by post-translational modification of the apoE protein (Lahoz C *et al*, 1996).

Determining the three apoE isoforms at the DNA level can be performed by a number of techniques, including single strand confirmation polymorphism or SSCP (Tsai MY *et al*, 1993), allele specific nucleotide probes or ASO (Weisgraber KH *et al*, 1988), and amplification refractory mutation system or ARMS (Wenham PR *et al*, 1991). SSCP and ASO require the use of radioisotopes for labelling oligonucleotides and are time-consuming techniques. Even though ARMS is not dependent on radiolabelling, four PCR reactions should be performed per analysed sample. As a consequence, it was decided to use RFLP, which involves digestion of a PCR product with a suitable enzyme that creates a unique pattern for each point mutation.

2.5.4.1 DNA Extraction from Cells

The first step in analysis involved the extraction of DNA from transfected and control cells. Cellular or genomic DNA was extracted using a DNeasy Tissue Kit (Qiagen) following the manufacturer's protocol. After trypsinisation, the cell pellet was re-suspended in 200 µl PBS followed by addition of 20 µl proteinase K and 200 µl buffer AL. The samples were mixed thoroughly by vortexing and incubated at 70 °C for 10 min before adding 200 µl ethanol and re-vortexing. The solution was then transferred into a DNeasy spin column and

centrifuged for 1 min at 16,060 *g*. Flow-through was discarded and after addition of 500 µl buffer AW1 to the column, the centrifugation was repeated as above. The flow-through was discarded, 500 µl of buffer AW2 was added and the column was centrifuged for 3 min at 16,060 *g*. DNA was eluted into a clean microfuge tube by adding 200 µl buffer AE to the column and centrifuging for 1 min. The concentration of purified DNA was estimated as described in *Section* 2.2.7.1. The DNA fragment was used immediately, or stored at –20 °C.

2.5.4.2 PCR-RFLP Analysis of Transfected Cells

The PCR-RFLP method (*Figure* 2.10) used for apoE genotyping after transfection experiments was based on the protocol described by Hixson *et al* (Hixson JE *et al*, 1990). 24-48 h post-transfection, cells were harvested for DNA extraction as described above, followed by PCR-RFLP analysis of the DNA to determine the apoE genotype in each sample. The PCR was set up as shown in Table 2.12. G:C rich regions possess strong secondary structure that often fails to denature during the first step of the PCR, thereby preventing primer annealing and amplification (Chenchik A *et al*, 1996). The first 200 bp of apoE are rich in guanines or cytosines and so PCR utilises DMSO to help weaken base pairing in G:C rich sequences and create single strands of cDNA for primer annealing (Pomp D *et al*, 1991).

Components	Volume (µl)	Final concentration
Pfu buffer (10 X)	5	1 X
DMSO(100 %)	5	10 %
TF sense primer (10 µM)	2.5	0.5 µM
TR anti-sense primer (10 µM)	2.5	0.5 µM
DEPC water	24.5	-
dNTP mix (2 mM)	5	0.2 mM
DNA (or DEPC water control)	5	≤ 1 µg DNA
Pfu Turbo polymerase (2.5 U/µl)	0.5	1.25 U
Total volume including sample	50	

One cycle	30 cycles			One cycle
	Denaturation	Annealing	Elongation	
96 °C for 5 min	96 °C for 1 min	62 °C for 1 min	72 °C for 1 min	72 °C for 10 min

Table 2.12 Requirements and programme for PCR reaction of extracted DNA from transfected cells. *A master mix for amplification was prepared by adding the reagents in the order and proportions shown in the top table to 0.5 ml thin-walled PCR tubes. Tube contents were covered with 20 µl light mineral oil to prevent evaporation of reaction mix and incubated in a Biometra thermocycler. Alternatively, tubes were incubated in a Robocycler without the addition of mineral oil as it has an integrated heated lid. In each case, the thermocycler programme that was followed (lower table) would commence with 5 min at 96 °C followed by 30 cycles of 1 min at 96 °C, 1 min at 62 °C and 1 min at 72 °C. The program ended with a final elongation step of 10 min at 72 °C.*

The 5' to 3' sequences of the forward (TF) and reverse (TR) primers were as follows:

TF TCCAAGGAGCTGCAGGCGGCGCA

TR ACAGAATTCGCCCCGGCCTGGTACACTGCCA

Primers were based on protocol by Hixson *et al* (Hixson JE *et al*, 1990) and were ordered from Sigma Genosys. Using *Pfu* Turbo DNA polymerase and a Biometra thermocycler or a

RoboCycler 40 Gradient Cycler, the primers amplified a 227 bp fragment. Direct digestion of the PCR product (*Section* 2.2.7.1) was found to be unsatisfactory for identifying the apoE genotypes as extra bands appeared after the digest leading to misclassification of apoE genotype. Therefore, the template DNA was purified (*Section* 2.2.7.2) from PCR products following separation by an agarose gel electrophoresis (*Section* 2.2.6). The purified DNA was subsequently digested with excess *Cfo*1 (Life Technologies) as the following digest mix indicates:

Component	**Volume (μl)**
Purified PCR product	10
10 X React 1 buffer	2.0
Sterile water	7.0
CfoI (10 U/μl)	1.0
Total Volume	**20**

Digestion was carried out at 37 °C for at least 3 h prior to electrophoresis at either 250 V for 1 h in 4% agarose gels or 200 V for 2 h in 20% TBE polyacrylamide gels (Novex, Invitrogen). Each apoE genotype was distinguished by a unique combination of *CfoI* fragment sizes (*Figure* 2.10, Panel B, Table 2.13). In some experiments, a subset of purified PCR products were subjected to automatic DNA sequencing (*Section* 2.2.7) in one or both directions following purification on 1% agarose gel.

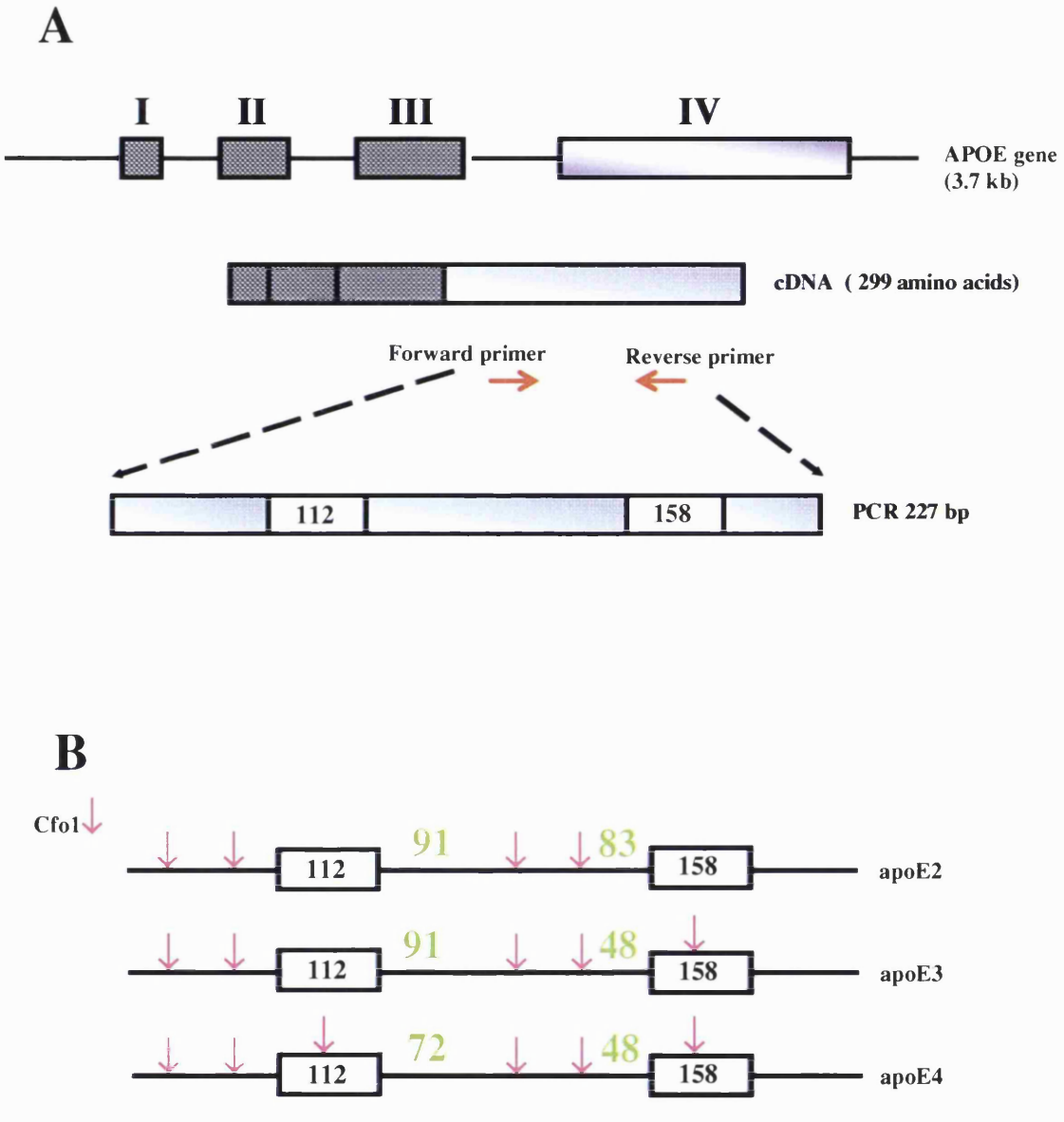

Figure 2.10 ApoE genotyping by PCR-RFLP. *The human APOE gene contains four exons separated by three introns (Section 1.3.3). Genotyping was achieved by amplifying a 277 bp PCR product from exon IV* ***(Panel A)****, followed by restriction isotyping with Cfo1* ***(Panel B)****. The cleavage maps for apoE2, apoE3, and apoE4 are shown with the cleavage sites depicted as downward arrows. The filled boxes indicate codons 112 and 158.*

ApoE genotypes	Diagnostic fragment sizes after *Cfo1* digests (bp)
ApoE2/E2	91, 83
ApoE3/E3	91, 48
ApoE4/E4	72, 48
ApoE2/E3	91, 83, 48
ApoE2/E4	91, 83, 72, 48
ApoE3/E4	91, 72, 48

Table 2.13 Diagnostic fragment sizes of different apoE genotypes after *Cfo1* digest. *After digesting the purified PCR product with Cfo1 enzyme (Section 2.5.4.2, Figure 2.10, Panel B), the above expected bands were used to distinguish between the various apoE genotypes.*

2.5.5 CLONING OF TRANSFECTED CELLS

After analysis of transfected cells, some of the HepG2 (treated with RDO1, and apoE3-to-apoE4 RDO) and THP-1 (treated with ROD1 only) cells that showed a successful conversion of *APOE3* to *APOE2* or *APOE4* were passaged four times before being stored in liquid nitrogen (*Section* 2.2.4.2). Once the cells were thawed, they were cloned in 90-mm dishes or 96-well plates as described in *Section* 2.4.3.3. Single clones were kept in culture and expanded in 6-well plates. Half of the cells were then harvested and analysed by PCR-RFLP (*Section* 2.5.4), while the remainder were further expanded and either cryopreserved or discarded (if transfection was unsuccessful).

2.5.6 OLIGONUCLEOTIDES RESOLVED ON TBE-UREA GELS

RDOs and SSOs were analyzed on 15% TBE-Urea gels in order to assess the purity of the synthesized oligonucleotides. This was performed by adding 2 X TBE loading buffer and 1% β-mercaptoethanol to 1 μg of each oligonucleotide. The mix was boiled at 95 °C for 10 min before running it on a 15% Novex TBE-Urea gel, using a Novex gel tank that was filled with TBE buffer. After electrophoresis at 180 V for 75 min, or until bromophenol blue reached the bottom of the gel, staining with ethidium bromide (0.5 μg/ml in TBE buffer) was performed and the gel was subsequently visualised and photographed under a UV light.

Chapter 3

3. DEVELOPMENT OF ENZYME-LINKED IMMUNOSORBENT ASSAYS (ELISAs) FOR APOE & APOAI QUANTIFICATION

3.1 Introduction

ApoE is one of the protein moieties of several plama lipoprotein subclasses (*Section* 1.3). ApoE plays an important role in lipid metabolism through interactions with lipoprotein receptors of hepatic and extrahepatic tissues (*Section* 1.3.6.1). ApoAI is the major protein component of HDL (*Section* 1.4). It plays an important role in reverse cholesterol transport (RCT) and acts as a cofactor for LCAT (*Sections* 1.4.3.1 and 1.4.3.2).

ApoE and apoAI secreted in cell culture media have been measured by a number of different techniques including radioimmunoassay (RIA), radial immunodiffusion, immunonephelometry, and ELISA (Blum CB *et al*, 1980; Marcovina S *et al*, 1986). Methods such as immunonephelometry require relatively high concentrations of antibody, which renders them expensive assays. Radioimmunoassays have the disadvantage of involving radioactive materials and are time-consuming with regard to preparing radiolabelled reagents. In addition, almost all apolipoprotein assays are based on antibodies, which are either specific to specialised laboratories or are not readily available. The results obtained by these various methods are difficult to compare because of the different protocols and reagents utilised.

One of the objectives of this project was to investigate the biological activities of newly synthesised apoE3 particles secreted from recombinant CHO cells using recombinant apoAI (generated as described in *Chapter* 4) as a positive control (*Chapter* 4) since both proteins share a number of functions such as facilitating cholesterol efflux. Another aim was to use chimeraplasty (*Chapter* 5) for gene targeting of apoE3 secreting cell lines (HepG2 and THP-1). Had this technique proven to be successful, the next step would have involved characterization of liver- and macrophage-derived apoE particles. To achieve these objectives, a method for accurate and reproducible quantification of both apoE3 and apoAI levels was required. This chapter describes the establishment of an ELISA for human apoE and attempts to develop an ELISA for human apoAI. The established apoE ELISA has been

successfully applied to projects in our laboratory that have required accurate estimation of levels of apoE secreted in cell culture medium as well as some *in vivo* studies (Tagalakis AD *et al*, 2001; Harris JD *et al*, 2002b).

A number of different ELISA techniques are described in the literature such as sandwich and competitive ELISA, with further subdivisions. Direct sandwich ELISA using polyclonal antibodies seemed to be a suitable method as pre-coating with antibody allows efficient capture of the desired antigen. In addition, cross-reactivity is reduced between the two antibodies by having the antigen sandwiched between them. The major factors to consider when developing a sandwich ELISA are:

- Correct type of solid-phase support.
- Correct type of antibodies.
- Suitable type of enzyme-labelled detector and substrate.
- Buffers for blocking non-specific binding, washes between each steps, and dilutions of test samples and standards.

Normally two antibodies "coating and detection antibody" are required for a sandwich ELISA. The coating antibody as the name suggests is used to coat a solid phase such as a 96-well plate, and is the mechanism by which the antigens are trapped. The detection antibody is usually labelled and added after antigen incubation so that the antigen is sandwiched between the two antibodies. Possible cross-reactivity problems between these reagents should be monitored. In addition, antibodies might require purification by a suitable system such as affinity chromatography or protein A or G columns.

Intrinsic to ELISA is the addition of reagents conjugated to enzymes and chromatogenic substrates. Assays are then quantified by the level of coloured product measured spectrophotometrically. The most commonly used enzymes in ELISA are horseradish peroxidase (HRP), alkaline phosphatase (AP), and β-D-galactosidase (β-GAL). There is a range of commercially available substrates and their corresponding dye, such as the combinations of hydrogen peroxide (H_2O_2) and ortho-phenylene diamine (OPD); H_2O_2 and tetra-methylbenzidine (TMB); and, urea and bromocresol. Each of the enzyme-substrate

systems has its own stopping conditions and develops a coloured product with an absorbance that is measured at a specific wavelength and expressed as optical density (OD). Having chosen suitable reagents and buffers, a sandwich ELISA was developed for quantifying apoE. The coating antibody needed to be purified to remove the BSA in which the manufacturers supplied the antibody, while the detection antibody was biotinylated. Initially, pilot experiments were carried out to test for any cross-reactivity between different reagents used in the ELISA. This was followed by titration experiments to elucidate empirically the optimum assay conditions. The precision profile of the established ELISA was then determined by calculating the coefficient of variation. The established assay was subsequently used for quantifying levels of apoE3 secreted by recombinant CHOE3 cells. Efforts were made to develop an ELISA for apoAI based on the same principles applied to apoE ELISA.

3.2 Results

3.2.1 AFFINITY COLUMN PURIFICATION OF COATING ANTIBODY FOR APOE ELISA

Polyclonal anti-human apoE antibody (Diasorin, #82943) was purified using a protein G affinity column in order to remove the BSA that was added to the antibody by the manufacturers. One milliliter of the unpurified antibody (1.3 mg/ml) was mixed with 1 ml PBS and 200 µl Tris.HCl (pH 7.4) before loading on the column and collecting the flow-through, bound antibody fractions, and any remaining unbound antibody as explained in *Section* 2.3.1. The concentrations of the flow-through and purified antibody (after dialysis) were determined using the Bradford protein assay (*Section* 2.2.1.1). *Figure* 3.1 shows a typical standard curve of IgG concentration plotted against $OD_{595\ nm}$ that was used to determine the concentrations of samples prior to electrophoresis (*Section* 2.2.2).

Two µg of each sample (unpurified antibody, unpurified antibody plus PBS and Tris.HCl pH 7.4, flow-through, and dialyzed purified antibody) and 7 µl of a pre-stained molecular weight marker in a separate lane (New England Biolabs) were applied to a 1.5 mm thick SDS-polyacrylamide gel casted with 12% resolving gel and 4% stacking gel (*Section* 2.2.2.1). After electrophoresis, the gel was stained with Coomassie blue for 1 h followed by

an overnight destaining step (*Section* 2.2.2.3). A photograph of the dried gel is shown in *Figure* 3.2 indicating the presence of BSA (66 kDa) in the flow-through and the heavy (50 kDa) and light chain (25 kDa) of IgG in the purified and dialyzed polyclonal anti-human apoE antibody. The concentration of purified coating antibody was 0.64 mg/ml as determined from the Bradford assay using IgG standards.

3.2.2 BIOTINYLATION OF DETECTION ANTIBODY FOR APOE ELISA

The detection polyclonal anti-human apoE antibody (Biogenesis, #0650-1904) was biotinylated using Sigma's Biotinylation kit, following the manufacturer's instructions as explained in *Section* 2.3.2. The final concentration of the biotinylated antibody was 0.2 mg/ml as determined by the Bradford assay using IgG standards (*Section* 2.2.1.1).

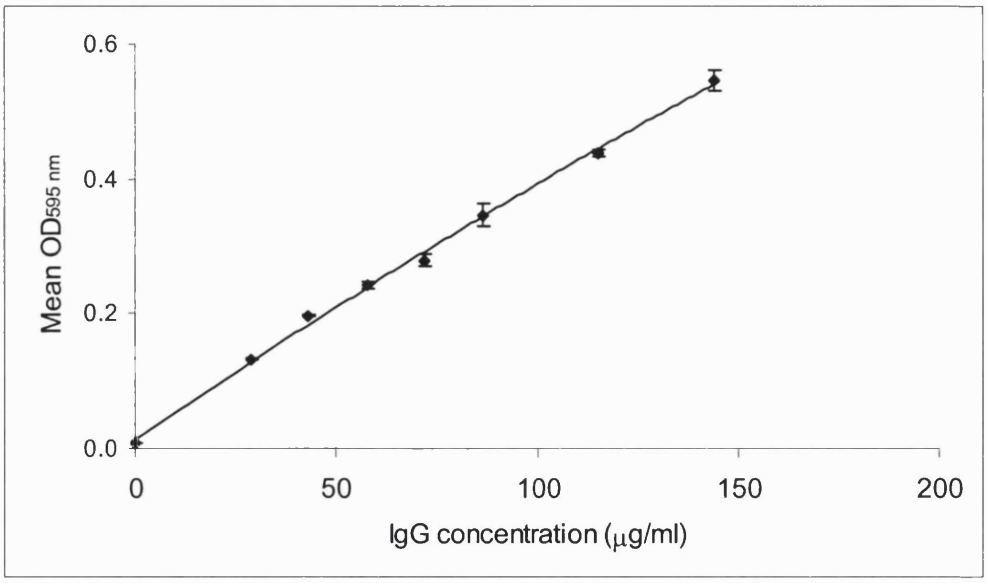

Figure 3.1 A typical standard curve obtained by Bradford assay using IgG standards. *The assay was performed as described in Section 2.2.1.1 using IgG in the range of 0-144 μg/ml. The mean of absorbances at 595 nm ± S.D from triplicate wells in a single assay were plotted versus IgG concentrations. The generated curve was fitted to a quadratic equation using Microsoft Excel.*

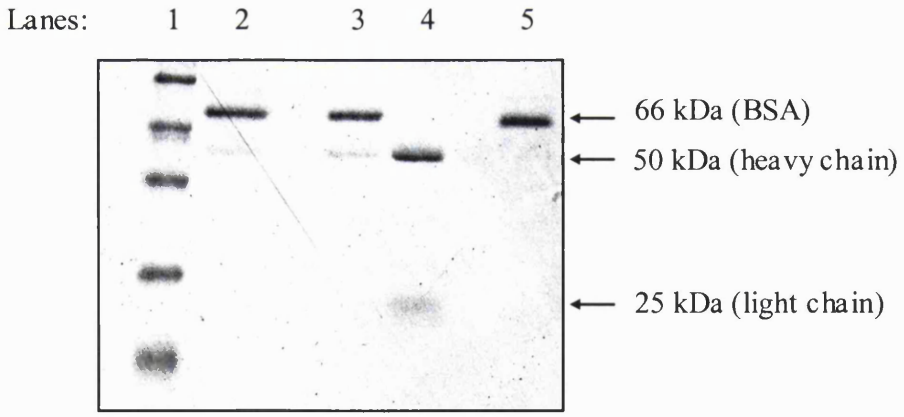

Figure 3.2 Photograph of a SDS-polyacrylamide gel after Coomassie blue staining showing the samples from affinity column purification of coating anti-apoE antibody used in apoE ELISA. *Lane 1 = molecular weight marker, Lane 2 = unpurified antibody, Lane 3 = diluted unpurified antibody (antibody + PBS + Tris), Lane 4 = purified and dialyzed antibody, Lane 5 = flow-through. Two micrograms of each indicated sample were loaded per lane of a 1.5 mm thick SDS-polyacrylamide gel casted with 12% resolving and 4 % stacking gel. After electrophoresis (Section 2.2.2.2), the gel was stained with Coomassie blue stain as described in Section 2.2.2.3. Removal of BSA (66 kDa) in the purified antibody was evident (lane 4) as compared to the unpurified antibody (lanes 2 and 3).*

3.2.3 TITRATION CURVES OF ANTIBODIES AND STREPTAVIDIN-HORSERADISH PEROXIDASE (S-HRP) FOR APOE ELISA

Preliminary experiments were carried out in order to rule out possible cross-reactivity between the two antibodies and either of the antibodies and S-HRP. Initially cross-reactivity between the two antibodies was tested by performing an ELISA without the addition of antigens. The coating antibody was used at a concentration of 1 μg/ml in all wells. The detection antibody was used at a starting concentration of 0.5 μg/ml in triplicates in the first row and then diluted serially 1:3, 1:9, and 1:27 down the columns. S-HRP was used at a dilution of 1:1000 in all wells. Results demonstrated no cross-reactivity between the two antibodies (data not shown). In the next experiment, 1 μg/ml of coating antibody was used in all wells. No antigen or detection antibody was added. S-HRP was added at 1:1000 in triplicates in the first row and then diluted serially 1:3, 1:9, and 1:27 down the columns. Results showed no cross-reactivity between the coating antibody and S-HRP conjugate (data not shown). In a third assay, no antigen or coating antibody were used. The detection antibody was used at a concentration of 0.5 μg/ml in all wells. S-HRP was added at 1:1000 in triplicates in the first row and then diluted serially 1:3, 1:9, and 1:27 down the columns. Results of this assay confirmed no cross-reactivity between the detection antibody and S-HRP (data not shown).

Three titration assays were carried out sequentially in order to determine the optimum working concentration of the coating anti-apoE antibody, the detection biotin-conjugated antibody and the S-HRP conjugate. In all the titration assays, 8 ng/50 μl (8 ng/well) of Technoclone apoE standard (Technoclone, Kent, UK) was used as antigen. While the concentrations of detection antibody (0.5 μg/ml) and S-HRP (1:1000) were kept fixed (based on preliminary experiments), coating antibody was diluted in a 10-fold serial manner starting from 25 μg/ml until 25 x 10^{-5} μg/ml. Quadruplicate wells of each dilution was used and the optimum dilution of the coating antibody was judged as being 2.5 μg/ml (*Figure* 3.3). This optimal value was used in the proceeding experiment where S-HRP was fixed and a range of serial dilutions of the detection antibody (in doubling dilutions starting from 8 μg/ml until 0.0625 μg/ml) were used each in quadruplicate wells. As shwon in *Figure* 3.4, the optimum dilution of the detection antibody was judged as being 1 μg/ml. Similarly, using the optimum dilutions of both antibodies, S-HRP was serially diluted (in doubling

dilutions from 1:1000 until 1:32000) in a third assay and its optimal working dilution was judged to be 1:2000 (*Figure* 3.5). Background could be defined in two ways; from a well where all the reagents are used in the absence of antigen, or from a well where a known negative sample (an antigen known not to be recognized by capture/detection antibodies) is used. In this chapter, background was determined using the former method.

For each reagent, the "titre" was defined as the highest dilution of the reagent that resulted in optimum specific signal (OD $\leq$ 1-1.5) with a low background. This was 2.5 μg/ml (1:256 dilution) for the coating antibody, 1 μg/ml (1:200 dilution) for the detection antibody and 1:2000 dilution for S-HRP as indicated by a dashed line in *Figures* 3.3, 3.4, and 3.5, respectively. The data on the x-axis of these figures was plotted on a logarithmic scale because a wide range of concentrations (dilutions) of each named reagent was used in setting up the titration curves. The three titration assays were repeated independently to confirm the obtained data.

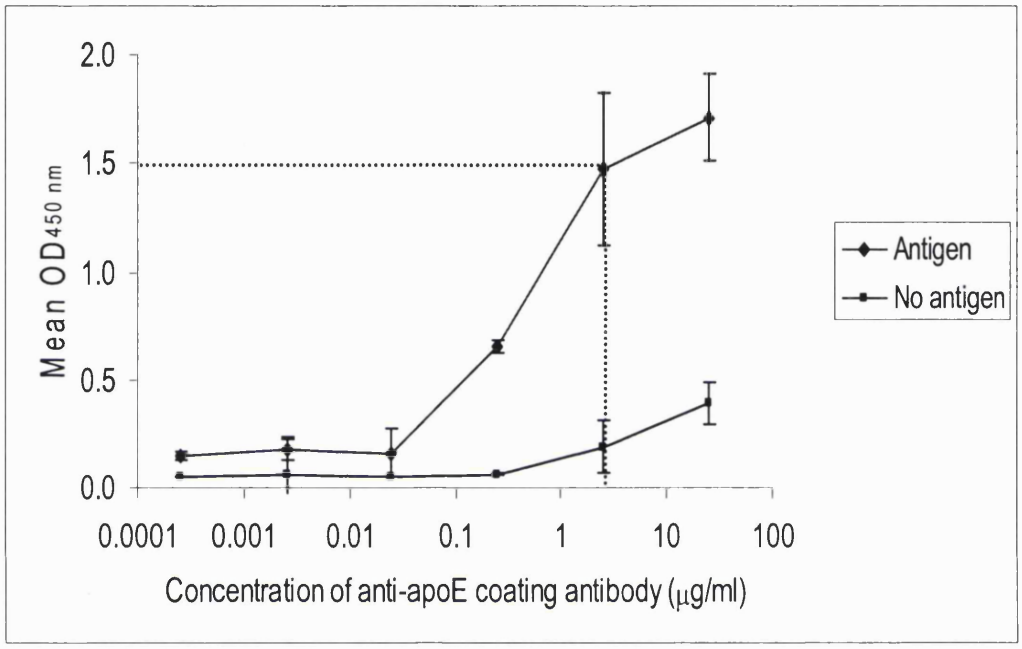

Figure 3.3 Titration curve and optimum concentration for the coating antibody in apoE ELISA. *The purified and dialyzed goat polyclonal anti-apoE coating antibody (stock concentration of 0.64 mg/ml) was progressively diluted in tenfold stages, starting from 25 μg/ml. Based on preliminary studies, the detection antibody and S-HRP were used at 0.5 μg/ml and 1:1000 dilutions respectively. Technoclone apoE standard at a concentration of 8 ng/50 μl (8 ng/well) was used as antigen for the ELISA, which was carried out as explained in Section 2.3.3. In the key, 'No antigen' refers to an ELISA carried out without the addition of the antigen. The antibody concentrations are shown on the x-axis log scale against the mean absorbance values at 450 nm (A_{450} in OD units) ± S.D for triplicate wells in a single ELISA. The chosen optimal concentration (2.5 μg/ml) that is indicated by the dashed line was confirmed in a second independent experiment and used in subsequent assays.*

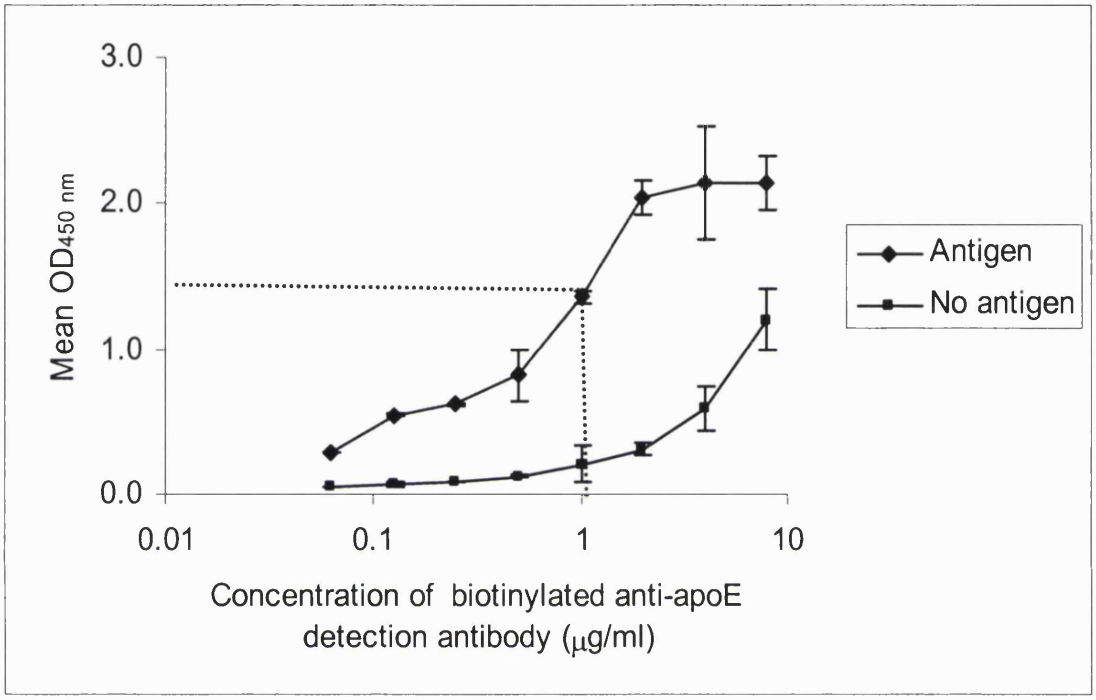

Figure 3.4 Titration curve and optimum concentration for the detection antibody in apoE ELISA. *The biotinylated goat polyclonal anti-apoE coating antibody (stock concentration of 0.2 mg/ml) was serially diluted in doubling dilutions, starting from 2.8 μg/ml. Coating antibody was used at its optimal concentration of 2.5 μg/ml (1:256) (see Figure 3.3). Based on preliminary studies, S-HRP was used at 1:1000 dilution respectively. Technoclone apoE standard at a concentration of 8 ng/50 μl (8 ng/well) was used as antigen for the ELISA, which was carried out as explained in Section 2.3.3. In the key, 'No antigen' refers to an ELISA carried out without the addition of the antigen. The antibody concentrations are shown on the x-axis log scale against the mean absorbance values at 450 nm (A_{450} in OD units) ± S.D for triplicate wells in a single ELISA. The chosen optimal concentration (1.0 μg/ml) that is indicated by the dashed line was confirmed in a second independent experiment and used in subsequent assays.*

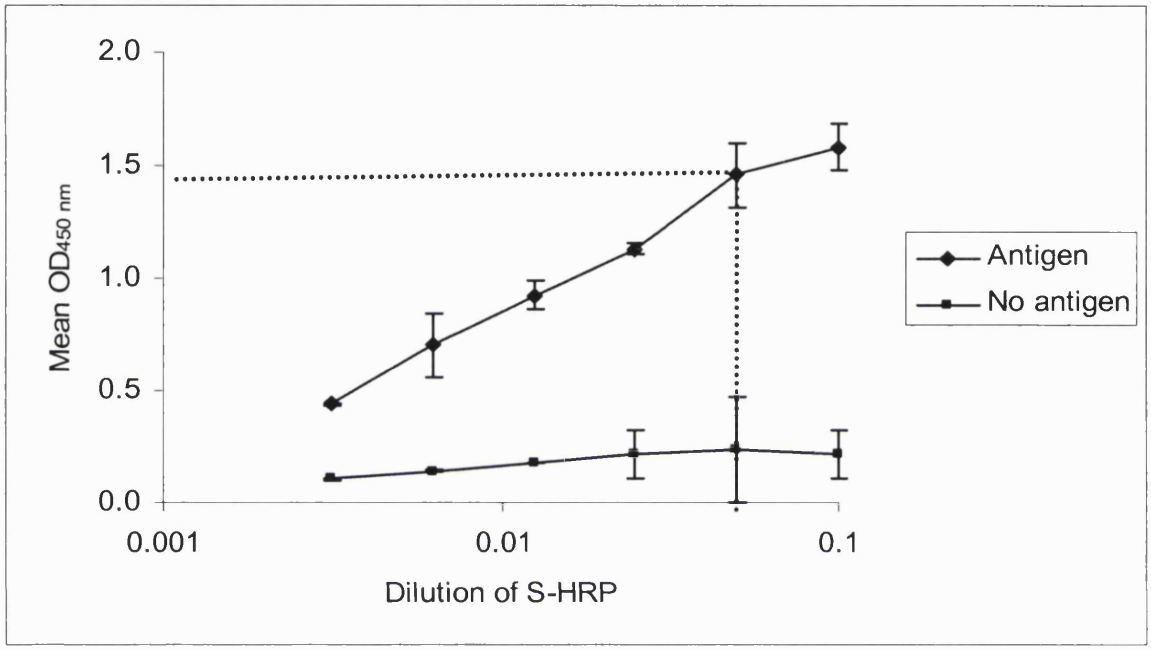

Figure 3.5 Titration curve and optimum concentration for the S-HRP in the apoE ELISA. *S-HRP complex was serially diluted (in doubling dilutions) starting from 1:1000. Coating and detection antibodies were used at their optimal concentrations, 1:256 and 1:200 dilutions, respectively. Technoclone apoE standard at a concentration of 8 ng/50 µl was used as antigen for the ELISA, which was carried out as explained in Section 2.3.3. In the key, 'No antigen' refers to an ELISA carried out without the addition of the antigen. Dilutions of the stock S-HRP are shown as decimals x 100 (e.g. 1:1000 plotted as 0.1), and plotted against the mean absorbance values at 450 nm (A_{450} in OD units) $\pm$ S.D for triplicate wells in a single ELISA. The chosen optimal dilution (1:2000 dilution) that is indicated by the dashed line was confirmed in a second independent experiment and used in subsequent assays.*

3.2.4 SELECTING THE BEST STANDARD CURVE FOR APOE ELISA

Reference curves (standard curves) are essential for each run of the ELISA as one cannot be certain that the amount of color generated and the concentration of the sample used will follow a linear relationship. Four different standards each of a known apoE concentration were used to choose the best standard curve for apoE ELISA. Assays were carried out using the optimized concentrations of coating and detection antibodies and S-HRP (*Section* 3.2.3). The standards were as listed below:

- ApoE standard provided in a commercial apoE ELISA kit (Perimmune Inc., Maryland, USA) that was previously used in our laboratory. The kit was discontinued from manufacture, but excess standards were stored in -80 °C.
- ApoE human plasma from Calbiochem (Merck Biosciences Ltd., Nottingham, UK) provided kindly by Dr C Dobson (Department of Optometry and Neuroscience, UMIST, Manchester, UK).
- ApoE standard provided in a kit for apoE hydragels (Sebia, France). They were prepared from a pool of human sera and used previously in our laboratory for establishment of calibration curves for human apoE quantification by electroimmunodiffusion technique.
- ApoE human plasma from Technoclone (Kent, UK) that had been newly purchased and was used in setting up the titration curves explained in *Section* 3.2.3.

All the above standards were used in triplicates in a range of 0-10 ng/50 µl (0-10 ng/well) and ELISA was carried out as before. Pooled human plasma from seven volunteers (*Section* 2.2.9) was used as an internal control and the experiment was independently repeated. The results (*Figure* 3.6) demonstrated that the calibrated plasma from Technoclone was the best performing antigen for this ELISA, giving highest $OD_{450\ nm}$ of 1.5 and apoE content of 61 $\pm$ 1.5 mg/l for pooled human plasma that is within the expected range (50-90 mg/l for normolipidaemic subjects). This result was confirmed in a second independent assay. The standard curve obtained from Perimmune's kit was very poor persumably due to loss of antigenic activity of the diluted standards after their prolonged storage at -80 °C. The

highest $OD_{450\ nm}$ from the Calbiochem and Sebia antigens were 0.7 and 0.9 respectively, which were poor signals as compared to Technoclone apoE standard, which was the standard of choice (*Figure* 3.6). The assay conditions could potentially be optimized for the Calbiochem and Sebia antigens if they were to be used as suitable standards.

3.2.5 DETECTION RANGE OF APOE ELISA

Following the standard ELISA methodology (*Section* 2.3.3) with the optimized concentrations of the coating and detection antibody and the S-HRP, a typical standard curve was obtained with 0–10 ng/50 µl of Technoclone apoE as antigens (*Figure* 3.6). The sensitivity limit of the assay was determined from a standard curve with 0-2 ng/50 µl of the antigen (*Figure* 3.7). The sensitivity limit refers to the smallest quantity of the antigen that can be detected by the assay. A sensitivity limit of ~0.2 OD units above background is normally considered to be reliable (Kemeny DM, 1991). These calibration curves allowed the assessment of apoE concentration from 1 ng/well (20 ng/ml) to 8 ng/well (160 ng/ml). Thus, the sensitivity limit of the assay, being almost twice the background value, is 20 ng of apoE per ml.

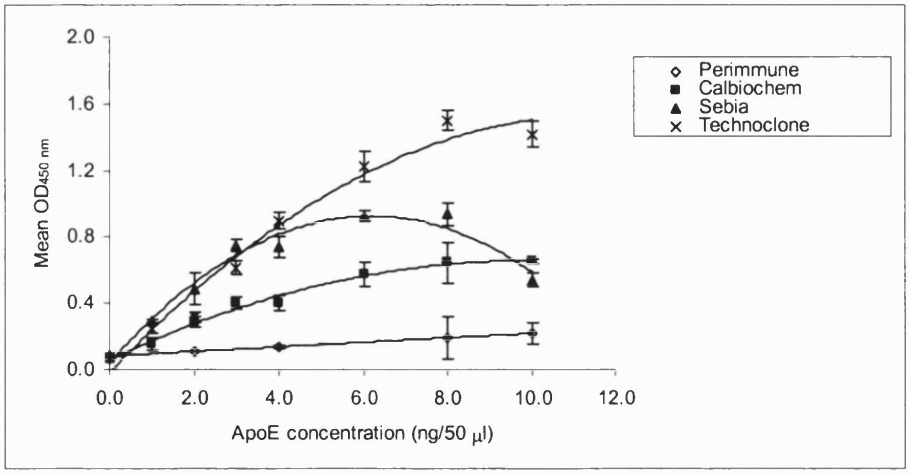

Figure 3.6 Comparison of four different commercial apoE standards. *Using the optimal concentrations/dilutions of antibodies and S-HRP, an ELISA (Section 2.3.3) was performed with four different sets of commercially available apoE standards; Perimmune, Calbiochem, Sebia, and Technoclone. Perimmune gave the poorest standard curve, while Technoclone provided the best curve with a large window for apoE measurements over a range of apoE concentrations. The mean of absorbances at 450 nm ± S.D from triplicate wells in a single assay are plotted versus antigen concentrations. The generated curve was fitted to a quadratic equation using Microsoft Excel.*

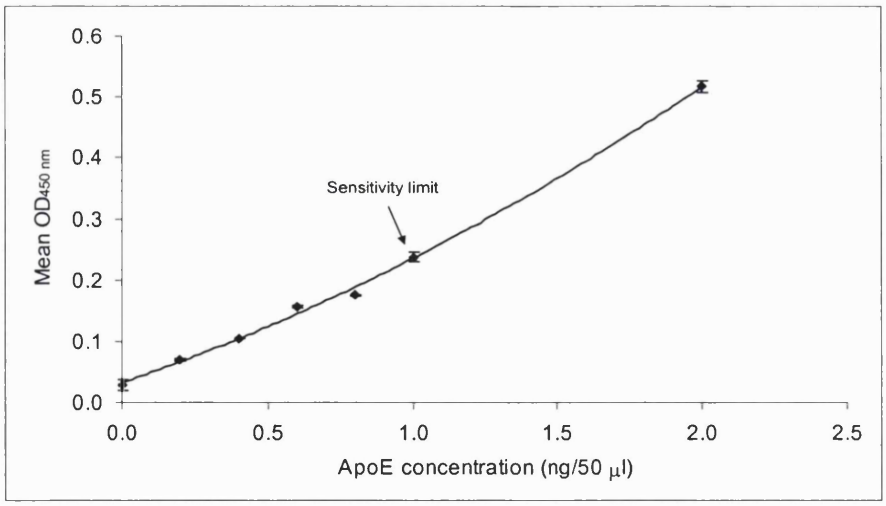

Figure 3.7 Standard curve obtained using Technoclone apoE as antigens to show the sensitivity limit of apoE ELISA. *The assay was performed as described in Section 2.3.3 using the Technoclone apoE standard in a range of 0-2 ng/50 µl. The mean of absorbances at 450 nm ± S.D from triplicate wells in a single assay were plotted versus antigen concentrations. The generated curve was fitted to a quadratic equation using Microsoft Excel. This curve showed that the sensitivity limit of the developed apoE ELISA was 1 ng of apoE per well (20 ng/ml).*

3.2.6 OPTIMISATION OF APOE ELISA

3.2.6.1 Optimal Reaction End Point Time

The final step of the ELISA involves an enzymatic reaction, which is stopped by adding the "stopping reagent", 2 M sulphuric acid. The optimal reaction end point time is a "stopping time" made when the relationship between the enzyme-substrate-product is in the linear phase. An ELISA was carried out as explained in *Section* 2.3.3 using optimal concentrations of reagents (*Section* 3.2.3). Standards (Technolone, 0-10 ng/50 µl) were added in duplicate wells across the rows of a 96-well plate. In each duplicated row, the stopping reagent was added at a different time (3-10 min) after the addition of the TMB substrate. The optimal reaction time (maximal absorbance for a minimal blank value) was chosen to be 10 min according to the plotted standard curves (*Figure* 3.8) as it gave the largest window for apoE quantification, although the curve was only linear up to about 8 ng apoE /well. This reaction time was used for all subsequent assays.

3.2.6.2 Storage of plates after the addition of coating antibody

Coating antibody (2.5 µg/ml) was added to two 96-well plates that were subsequently stored at 4 °C overnight. Next day, the antibody was decanted and the plates sealed securely by plastic films and stored at 4 °C and –20 °C, respectively. After one week both plates, and a third plate prepared as in the standard procedure (overnight incubation of the coating antibody at 4 °C), were used to set up apoE ELISA assays using triplicate wells of standards (Technoclone, 0-8 ng/50 µl) as described previously (*Section* 2.3.3) with all the determined optimal conditions (*Sections* 3.2.3-3.2.6.1). Standard curves plotted from the obtained data indicated that an overnight incubation of the coating antibody at 4 °C (*Figure* 3.9, curve A) provides a better window for estimating apoE concentration when compared to that of storage for one week at 4 °C (*Figure* 3.9, curve B) or at –20 °C (*Figure* 3.9, curve C). In addition, curve A had the best line of fit while in the other two curves (curves B & C), the points were scattered.

As shown in *Figure* 3.9, curves B and C gave generally higher $OD_{450\ nm}$ values compared to curve A. The reason for this remains unclear. Based on these findings, preparing plates with coating antibody (overnight at 4 °C) and storing them for convinient future use was not deemed advisable for this ELISA. However, there have been reports of apoE ELISAs that

have been developed whereby after incubation with coating antibody plates were stored at 4 °C (up to one month) until ready to use (Gracia V *et al*, 1994).

3.2.6.3 Precision profile of the Assay

The ELISA was validated by measurement of apoE in a pooled plasma sample from seven normal volunteers (*Section* 2.2.9). The plasma sample was diluted 2000-fold and assayed ten times in the same ELISA and thirteen times on different days over a course of three months. Coefficients of variation (CVs) were calculated using the following equation:

$$CV = (SD/mean) \times 100$$

CVs determine the level of variation within and between assays. The intra- and inter-assay coefficients of variation (7.2% and 9.6% as shown in Table 3.1) were similar to those previously reported in the literature and are well within acceptable limits for ELISA (Tozuka M *et al*, 1991; Gracia V *et al*, 1994).

	% Mean (SD)	% CV
Intra-assay (n = 10)	51.5 mg/l (2.8)*	7.2
Inter-assay (n = 13)	58.2 mg/l (1.9)*	9.6

Table 3.1 Intra- and inter-assay reproducibility of apoE ELISA. *A sample of pooled plasma from seven normal volunteers (Section 2.2.9) was diluted 1:2000 and assayed ten times in the same assay and thirteen times on different days using the apoE ELISA assay explained in Section 2.3.3. The coefficients of variation of the average data for intra- and inter-assay variability were calculated from the equation CV = (SD/mean) x 100. *Values were expressed as percent of mean value (mg apoE/l) for a pooled specimen of normal plasma from seven donors.*

3.2.7 ESTIMATING THE CONCENTRATION OF CHO CELL-DERIVED APOE3

In order to determine the amount of apoE3 secreted by CHOE3 cells, conditioned medium was collected after 24 h from four confluent wells of a 6-well plate as described in *Section* 2.4.4.1. The collected medium was analyzed by ELISA as explained in *Section* 2.3.3. This was repeated two more times and the amount of apoE3 secreted was calculated to be 12.3 $\pm$ 0.17 μg/mg cell protein/24 h.

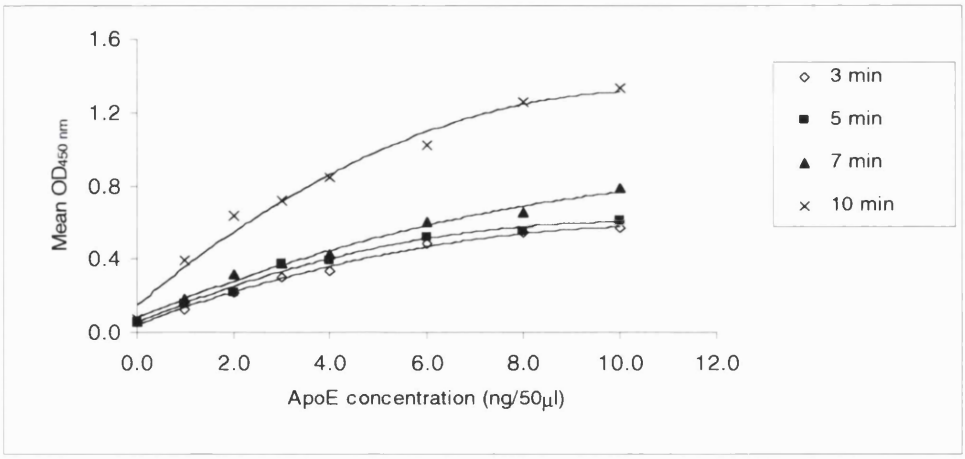

Figure 3.8 Determination of the optimal reaction time for apoE ELISA. *The assay was performed as described in Section 2.3.3 using antigens (Technoclone standard) in a range of 0-10 ng/50 µl. The mean of absorbances at 450 nm from duplicated wells in a single assay were plotted versus antigen concentrations. The generated curves were fitted to a quadratic equation using Microsoft Excel. Results showed that the optimal reaction time for the apoE ELISA was 10 min.*

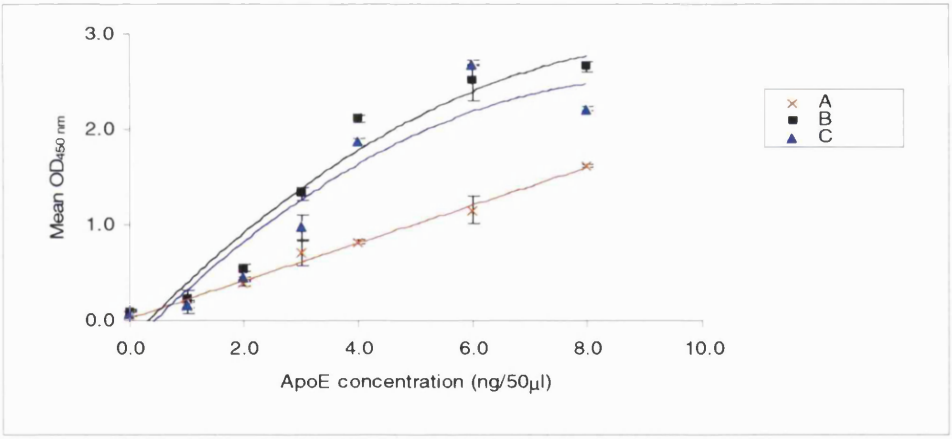

Figure 3.9 Storage of plates after incubation of coating antibody is not advisable for apoE ELISA. *Three different assays were performed using antigens (Technoclone standard) in a range of 0-8 ng/50 µl. The mean of absorbances at 450 nm ± S.D from triplicate wells in a single assay are plotted versus antigen concentrations. The generated curves were fitted to a quadratic equation using Microsoft Excel.* ***Curve A,*** *ELISA was performed as described in Section 2.3.3.* ***Curve B,*** *a second plate was incubated overnight with coating antibody. The antibody was then decanted, and the plate was sealed in cling film and stored at +4 °C for one week. The remainder steps of the ELSIA was then continued as before.* ***Curve C,*** *a third plate was treated in a similar way to that in Curve B, however this time the plate was stored at –20 °C for one week. Curve A is the best indicating that the ELISA should be performed without prior storage of plates.*

3.2.8 ATTEMPTS TO DEVELOP AN APOAI ELISA

Goat anti-human apoAI polyclonal antibody (Chemicon International Inc., CA, USA, #AB740) and sheep anti-human apoAI polyclonal antibody (Biogenesis, Poole, UK, #0650-0180) were used as the coating and detection antibody, respectively. Unlike apoE ELISA, there was no need to purify the coating antibody as there was no BSA added by the manufacturers. However, the detection antibody was biotinylated following the same protocol used for apoE detection antibody (*Section* 2.3.2). The final concentration of the biotinylated antibody was 0.6 mg/ml as determined by the Bradford assay using IgG standard (*Section* 2.2.1.1). Pure apoAI (delipidated apoAI purified from human plasma, generously provided by Dr G Sperber, Department of Medicine, Royal Free & University College Medical School, London, UK) was used as antigen for establishing suitable standard curves. Using the BCA Protein Assay (*Section* 2.2.1.2), the concentration of pure apoAI was determined to be 3.4 mg/ml.

Initially, cross-reactivity between the two antibodies was tested by performing an ELISA without the addition of antigens. The coating antibody was used at a concentration of 1 mg/ml in all wells. The detection antibody was used, however, at a starting concentration of 0.01 mg/ml in triplicates in the first row and then diluted serially 1:3, 1:9, and 1:27 down the columns. S-HRP was used at a dilution of 1:1000 in all wells. Results demonstrated no cross-reactivity between the two antibodies. Next, 1 mg/ml of coating antibody was used in all wells. No antigen or detection antibody was added. S-HRP was added at 1:1000 in triplicates in the first row and then diluted serially 1:3, 1:9, and 1:27 down the columns. Results showed no cross-reactivity between the coating antibody and S-HRP conjugate. Similarly, another experiment confirmed no cross-reactivity between the detection antibody and S-HRP.

Following these preliminary experiments, titration of coating antibody was carried out starting with a concentration of 50 μg/ml diluted 1:10 down to 5 x 10^{-4}μg/ml. The ELISA method was carried out as for apoE (*Section* 2.3.3), using 8 μg/ml of the detection antibody and 1:1000 dilution of S-HRP in all wells. Pure apoAI was used as antigen at a concentration of 8 ng/50 μl (8 ng/well). As shown in *Figure* 3.10, the optimum concentration of the coating antibody, which provided a large window for measurements and

low background signal, was 5 μg/ml. This concentration of coating antibody was used in all wells in the next experiment, while the detection antibody was used at doubling dilutions from 16 μg/ml to 0.5 μg/ml. S-HRP and pure apoAI were used as before. *Figure* 3.11 showed that the detection antibody never reached a plateau phase indicating that possibly higher concentrations of this antibody were required.

Microtitre plates have a limited capacity to bind proteins. At high concentrations of coating antibody, protein-protein interactions can take place as the space is limited on the surface of the plate. Dissociation of supposedly bound proteins might occur during the assay as protein-protein interactions are weaker than protein-plastic interactions. Thus, one should not go beyond the zone of independent binding, which refers to the range of protein concentrations where there is no interference with the binding of protein to the plastic. Normally, concentrations higher than 5 μg/ml of coating antibody should be avoided to prevent protein-protein bindings (Kemeny DM, 1991). Therefore, the titration curve of the detection antibody was repeated using 5 μg/ml of the coating antibody in all wells and starting with a higher concentration of the detection antibody (starting at 64 μg/ml in each of the first two wells and then doubling dilutions down to 4 μg/ml, followed by 1, 0.5 and 0.05 μg/ml of the antibody). The S-HRP and pure apoAI were kept as before, but it was not possible to determine the optimum concentration of the detection antibody as the graph never reached a plateau phase again (*Figure* 3.12). In fact the shallow curve shown in *Figure* 3.11 might indicate that the detection antibody has quite a low affinity for apoAI. Affinity is defined as the strength of the interaction between antigen and antibody.

In order to ensure that the antigen is not the limiting factor, the second titration trial of the detection antibody was repeated (as per the concentrations of *Figure* 3.12) whilst using a range of pure apoAI (20, 10, and 5 ng/50 μl). It was not possible to determine the optimum concentration of the detection antibody from this experiment as the curves never reached a plateau (data not shown). Where there is no plateau, it is possible to choose a concentration close to the highest recorded OD reading. Considering the practicality and expense of using high concentrations of detection antibody, 16 μg/ml was chosen as the optimal concentration of this antibody (indicated by a dashed line in *Figure* 3.12). Using optimal coating (5 μg/ml) and detection (16 μg/ml) antibody concentrations, 1:1000 dilution of S-HRP, and

pure apoAI in a range of 0-10 ng/50 µl, it was not possible to obtain a reasonable standard curve as the highest $OD_{450\ nm}$ was only ~0.22 units (*Figure* 3.13). For an effective ELISA, one requires the highest $OD_{450\ nm}$ to be at least 1-1.5, which provides a large window within the limits of accurate spectrophotometric detection.

The low color development at the final stage of the apoAI ELISA could not have arisen from the TMB substrate, as the same substrate provided a strong color in the apoE ELISA. In addition, color development was not intensified by extending the reaction end point time (i.e. the stopping time of the enzymatic reaction of ELISA at the final step of the assay) from 10 to 60 min (data not shown). Furthermore, using 1:500 dilution of S-HRP did not improve the $OD_{450\ nm}$ readings (data not shown). Therefore, it was not possible to set up an accurate and sensitive ELISA for measuring apoAI levels secreted by recombinant CHO cells (*Chapter* 4) and it was decided to use Western blotting and scanning densitometry instead (*Section* 2.4.4).

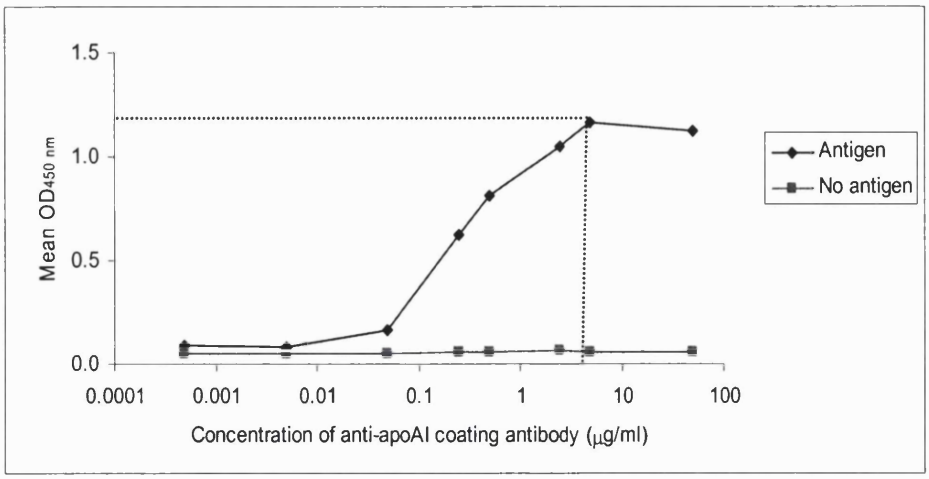

Figure 3.10 Titration curve and optimum concentration for the coating antibody in the apoAI ELISA. *The goat polyclonal anti-apoAI was used in a range of concentrations (starting from 50 μg /ml). The detection antibody and S-HRP were used at 8 μg/ml and 1:1000 dilution, respectively. Pure apoAI (antigen) was used at a concentration of 8 ng/50 μl and the ELISA was carried out as explained in Section 2.3.3. The antibody concentrations are shown on the x-axis log scale against the mean absorbance values at 450 nm (A_{450} in OD units) for duplicate wells in a single ELISA. The chosen optimal concentration that is indicated by the dashed line was confirmed in a second independent experiment and used in subsequent assays.*

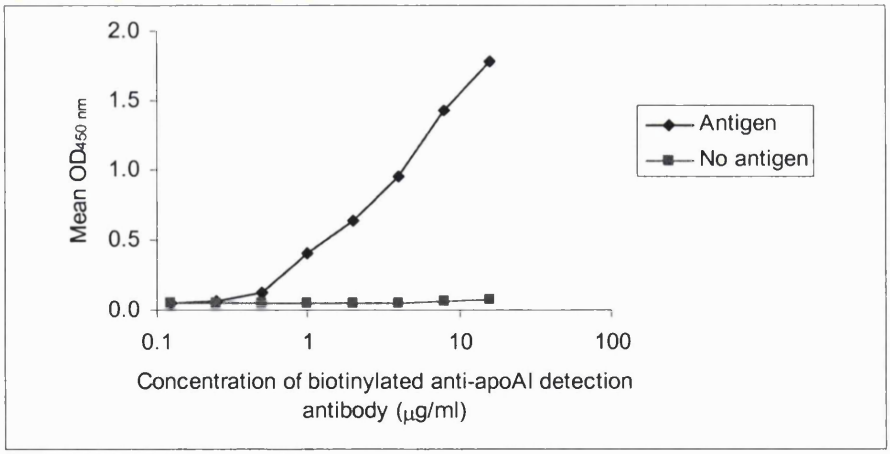

Figure 3.11 Titration curve for the detection antibody in the apoAI ELISA. *The sheep polyclonal anti-apoAI was serially diluted in doubling dilutions, starting from 16 μg/ml. The coating antibody and S-HRP were used at 5 μg/ml and 1:1000 dilution, respectively. Pure apoAI (antigen) was used at a concentration of 8 ng/50 μl and the ELISA was carried out as explained in Section 2.3.3. The antibody concentrations are shown on the x-axis log scale against the mean absorbance values at 450 nm (A_{450} in OD units) for duplicate wells in a single ELISA. As the graph never reached a plateau, it was difficult to determine the optimal concentration of the detection antibody and so this titration curve was repeated using different dilutions of the antibodies as shown in Figure 3.12.*

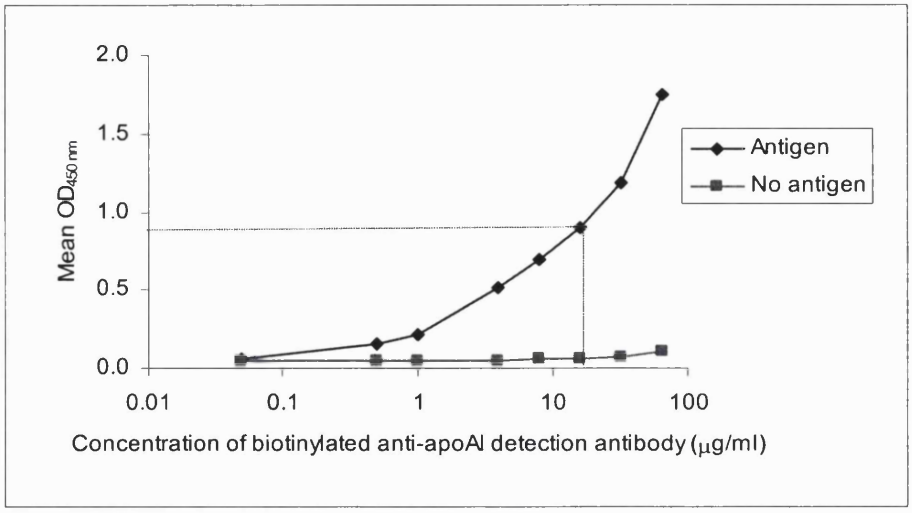

Figure 3.12 A second titration curve and optimum concentration for the detection antibody in apoAI ELISA. *The stock sheep polyclonal anti-apoAI was serially diluted in doubling dilutions starting from 64 µg/ml, down to 4 µg/ml, followed by 1, 0.5 and 0.05 µg/ml of the antibody. The coating antibody and S-HRP were used at 5 µg/ml and 1:1000 dilution, respectively. Pure apoAI (antigen) was used at a concentration of 8 ng/50 µl and the ELISA was carried out as explained in Section 2.3.3. The antibody concentrations are shown on the x-axis log scale against the mean absorbance values at 450 nm (A_{450} in OD units) for duplicate wells in a single ELISA. The chosen optimal concentration that is indicated by the dashed line was used in subsequent assays.*

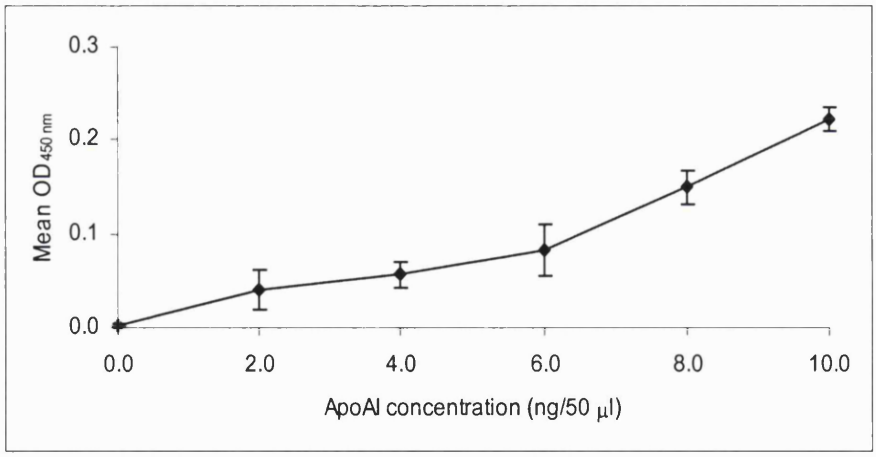

Figure 3.13 Standard curve for apoAI ELISA. *The assay was performed as described in Section 2.3.3 using optimal concentrations of coating antibody (5 µg/ml), detection antibody (16 µg/ml), and S-HRP (1:1000). Purified apoAI was used as the antigen in a range of 0-10 ng/50 µl. The mean of absorbances at 450 nm ± S.D from triplicate wells in a single assay were plotted versus antigen concentrations. The generated curve was fitted to a quadratic equation using Microsoft Excel. This curve showed that the highest antigen concentration (10 ng/50 µl) gave a very low OD_{450} value (0.22 units).*

3.3 Discussion

The apoE ELISA described in this chapter was established as a sensitive and accurate technique to quantify apoE levels secreted by cultured cells in addition to plasma apoE concentration. The ultimate aim was to use this immunoassay to quantify apoE3 secreted by recombinant CHO cells (CHOE3). A number of functional analyses on newly-secreted apoE3 were subsequently carried out as described in *Chapter* 4. Furthermore, if the *APOE3* to *APOE2* or *APOE4* gene conversion by chimeraplasty (*Chapter* 5) were successful in HepG2 and THP-1 cells, the amount of apoE isoforms secreted by these cell lines could have been quantified using the established apoE ELISA.

Knowing that protein charge and hydrophobicity might be some of the factors involved in protein binding to a solid phase, optimum conditions for a coating antibody can thus be determined by using buffers of varying pH, since this affects the overall charge of a protein. In the case of the apoE ELISA, PBS (pH 7.4) seemed to be the correct diluent for the coating antibody and thus trials with other recommended buffers such as carbonate/bicarbonate (pH 9.6) (Starck M *et al*, 2000; Tozuka M *et al*, 1990) were not attempted. Another important factor is the temperature of incubation step that can be chosen to give some flexibility to the assay. For instance, coating antibody can be incubated at room temperature for one hour as higher temperatures increase coating efficiency (Crowther JR, 1995). However, incubating this antibody at 4 °C overnight usually has the same effect. The volume of reagents used in setting up an ELISA can be anywhere between 50-300 µl dependent on the capacity of microtitre plates. Therefore, it is not difficult to choose a suitable volume considering the expense of reagents and the range of volumes of test samples.

It is important to freshly prepare apoE standards for each ELISA in order to prevent a decrease in the immunoreactivity of the standards due to the formation of apoE aggregates in diluted samples overtime (Bury J *et al*, 1986). Accessibility of the antigenic determinant of apoE to the antibodies is essential for an accurate measurement of this plasma protein. This was achieved in the described apoE ELISA by using a non-ionic detergent, Tween-40, in the sample dilution buffer (assay buffer). The assay buffer also contained BSA, which has been reported to stabilize apoE by acting as an apoE carrier-protein (Bury J *et al*, 1986).

In addition, BSA minimizes background signals ensuring that signal-to-noise ratios are maximized (Cianflone K *et al*, 1994). The washing buffer contains Tween-20, which is thought to decrease the non-specific interactions between the coating and detection antibodies (Feng M *et al*, 1995). This detergent is also useful for stabilizing adsorbed proteins on micro-well surfaces.

The detection antibody was biotinylated in the developed apoE ELISA. Biotinylation is an easy and rapid procedure, while the biotin tag remains stable over a long period of time with little or no effect on the biological activity of the antibody (Underwood PA *et al*, 1991). Avidin is a glycoprotein present in egg white with a molecular weight of 66 kDa. Streptavidin (from *Streptomyces avidinii*) has an affinity to biotin similar to that of avidin. However, streptavidin is less basic than avidin and has no carbohydrate residues, and thus prevents non-specific reactions with acidic groups (Underwood PA *et al*, 1991). There are a number of enzymes and substrates to choose for the final stage of ELISA. The rate of color development and consistency are major factors to consider. In the established apoE ELISA, HRP was used as it has a reasonably fast turn over time (the time taken by the enzyme to catalyze the conversion of the substrate) and is the most cost-effective when compared with other commonly used enzymes such as alkaline phosphatase and β-D-galactosidase (Kemeny DM, 1991). Consequently, detection was easily achieved in the developed apoE ELISA by use of streptavidin-HRP (S-HRP) conjugate.

The apoE ELISA was optimized in several ways. With regard to the antibodies, the optimal concentrations were evaluated from titration curves indicating a coating antibody concentration of 2.5 μg/ml, and a detection antibody concentration of 1 μg/ml. A conjugate (S-HRP) dilution of 1:2000 was also chosen for maximal color development and minimal blank value. To check for repeatability and reproducibility of the ELISA, a pooled human plasma sample (from seven donors) was used as an internal control in each assay. The apoE concentration in pooled human plasma from volunteers obtained over three months was 58.2 $\pm$ 1.9 mg/l, which was in good agreement with most reported values (Weisweiller P *et al*, 1983; Leroy A *et al*, 1988). This indicates that the antigenic epitopes of apoE in tested plasma sample were fully exposed to the antibodies used in the ELISA. However, there are reports showing a large discrepancy in reported apoE concentrations in normal plasma, for

example values as low as 25 mg/l (Holmquist L, 1980) and as high as 246 mg/l (Kushwaha RS *et al*, 1977) have been reported. This may be due to the use of differing apoE standards and methods. Indeed from my experience not all types of apoE standards (possibly depending on their sources) were suitable for ELISA as demonstrated in *Figure* 3.6.

An attempt to set up a similar sandwich ELISA for apoAI was undertaken applying the same principles used to establish the apoE ELISA. The apoAI ELISA would be required later on in this project once recombinant CHOAI cells (*Chapter* 4) had been generated. Even though the literature has references to apoAI ELISAs set up in different laboratories (Francone OL *et al*, 1997), our attempts were unsuccessful. This could be attributed to a poor choice of antibodies or to the fact that not all apoAI antigenic epitopes are always expressed and easily accessible (Pruvot I *et al*, 1987). However, in described attempts to set up an apoAI ELISA, polyclonal antibodies were used reducing the possibility of apoAI epitopes not to be recognized. The choice of antibodies (polyclonal or monoclonal) is discussed in *Section* 6.2. In addition, lipids can mask antigenic determinants of apolipoproteins (Albers JJ *et al*, 1989) not allowing their recognition by antibodies, which is unlikely the case since delipidated apoAI was used in the described ELISA in this project. Being unable to develop an ELISA for apoAI, this protein was quantified by Western blotting and scanning densitometry as described in *Chapter* 4.

In conclusion, during this work I developed a sensitive and precise sandwich ELISA (detection limit of 20 ng apoE/ml) that is suitable for apoE quantification in plasma and medium from different cultured cells. It has the advantage of using standard and specific antibodies of commercial grade that can recognize different apoE isoforms from cultured cells and animal models (Tagalakis AD *et al*, 2001; Harris JD *et al*, 2001b). Consequently, the ELISA would be reproducible in other laboratories with a relatively low cost as reagents are stable when stored under the recommended conditions. Furthermore, this ELISA is ideal for infrequent assays and small batches.

Chapter 4

4. CHARACTERIZATION OF RECOMBINANT CHO CELL-DERIVED APOE3 USING CHO CELL-DERIVED APOAI AS A POSITIVE CONTROL

4.1 Introduction

As outlined in *Chapter* 1 (*Sections* 1.3 and 1.4), apoE and apoAI are plasma proteins that serve a protective role against atherogenesis. The anti-atherogenic property of apoE has been attributed to its ability in promoting cholesterol efflux from peripheral cells and lipid clearance from plasma (Mahley RW *et al*, 1989; Mahley RW *et al*, 1999). ApoAI is the major constituent of HDL. HDL can be separated into particles containing apoAI only (HDL-AI) and those containing both apoAI and apoAII (HDL-AI/AII) (Cheung MC *et al*, 1984). It has been postulated that HDL-AI might represent the anti-atherogenic fraction of HDL since the concentration of this particle is decreased in coronary heart disease (CHD) patients (Cheung MC *et al*, 1991).

CHO cells, a well-established cell line, have emerged as the vehicle of choice for synthesis of recombinant human proteins (Zeng S *et al*, 1997). This chapter describes generation of recombinant CHO cells expressing human apoAI and the quantification of secreted protein by immunoblotting and scanning densitometry after unsuccessful attempts at development of an ELISA for apoAI (*Chapter* 3). The generated cell line was used as a control for some functional analyses of newly-secreted apoE3 particles (from available recombinant CHOE3 cells) since apoE and apoAI share a number of biological functions such as enhancement of cholesterol efflux and activation of LCAT. The size distribution of the secreted apoE3- and apoAI-containing particles and their mobility in agarose gel were examined in this chapter. In addition, the effect of these particles in promoting cholesterol efflux from macrophages and activating recombinant LCAT (prepared from available recombinant CHOHis6-LCAT) was studied. LCAT is a key enzyme in lipoprotein metabolism since it accounts for the synthesis of most of the plasma cholesteryl esters (CEs) (*Section* 1.4.3.2). It was intended to use the biological assays developed in this chapter for comparing the different apoE isoforms (apoE2, apoE3, and apoE4) secreted by HepG2 and THP-1 cells, if chimeraplasty was successful for *APOE3* gene conversion in these cell lines (*Chapter* 5).

4.2 Results

4.2.1 GENERATION OF EXPRESSION VECTOR ENCODING HUMAN APOAI

The aim was to use recombinant CHO cells expressing apoAI as a positive control for studying the biological activities of CHO cell-derived apoE3-containing particles. This section describes steps taken in generation of recombinant CHO cells secreting human apoAI.

4.2.1.1 Confirming ApoAI Sequence in pcDNA3.1 Expression Vector

Human apoAI cDNA in pcDNA3.1 vector (pcDNA3.1.AI) was kindly provided by Prof L. Fan (Department of Biochemistry, Royal Holloway University of London, UK) (*Figure* 4.1). The first step was to check the sequence of apoAI. This was done by excising apoAI fragment with *HindIII* and *BamHI* enzyme and obtaining the predicted 806 bp product on a 1% agarose gel. Sequencing data from this product revealed a mutation at position 354 bp of the sequence. The mutation, a T to G conversion, was corrected by using the Site-directed Mutagenesis Kit from Stratagene (*Section* 2.4.1) (sequence not shown).

4.2.1.2 Construction of p7055.AI

p7055 contains the selectable marker gene, dihydrofolate reductase (*DHFR)*, of mouse origin, which is weakened by a downstream insertion of a sequence rich in A and T. In addition, it contains the SV40 enhancer-promoter reinforced by the hepatitis B virus X transactivator (HBV-X) that allows high expression of the desired gene and makes this vector suitable for selection assays of mammalian cell lines (*Figure* 4.2). It was decided to insert apoAI (excised from pCDNA3.1.AI as shown in *Figure* 4.3, Panel A) in the p7055 so that it replaces the IL-2 cDNA. The p7055 vector has a *BamHI* and *HindIII* restriction site in the region of IL-2 cDNA. In addition, it possesses another *BamHI* site, which makes it difficult for preparation before ligating with apoAI cDNA. Therefore, p7055 was prepared following a series of digestion reactions as described in *Sections* 2.4.2.1-2.4.2.3.

The double digest of pCDNA3.1.AI with *BamHI* and *HindIII* enzymes gave the predicted bands of 5 kb, and 806 bp as shown by 1% agarose gel separation (*Figure* 4.3,

panel A). The 806 bp band corresponding to full size apoAI cDNA was excised and gel purified (*Section* 2.2.7.2). The cDNA was now ready for ligation.

Some of the purified p7055 vector (ready for ligation) and a few μl of the apoAI cDNA were separated on a 1% agarose gel to confirm the correct sizes of each fragment (*Figure* 4.3, Panel B). p7055.AI was constructed by ligating p7055 and apoAI in a 2-way ligation using a vector DNA:insert DNA molar ratio of 1:3 (*Section* 2.4.2.4). Following transformation of competent bacteria (*E.coli* DH5α cells) (*Section* 2.4.2.5), plasmids were purified from three bacterial clones (*Section* 2.4.2.6) and analyzed by restriction digest for correct apoAI sequence insertion. Analysis was necessary as the expression vector has two *BamHI* sites, allowing apoAI cDNA to be cloned in two different orientations. The digestion products (*BamHI* and *HindIII* cut) were subsequently separated on an agarose gel revealing that only clones 1 and 2 contained the apoAI sequence inserted into the p7055 vector in the correct orientation (*Figure* 4.3, Panel C). The constructed plasmid was then used to transfect CHOdhfr- cells as described in *Section* 2.4.3.

4.2.2 SCANNING DENSITOMETRY FOR FUTURE QUANTIFICATION OF CHO CELL-DERIVED APOAI

Prior to transfection of CHOdhfr- cells with p7055.AI, selection and cloning, an assay was needed to monitor and quantify levels of secreted apoAI. This would also be used for subsequent physical characterization (*Section* 4.2.5) and studies of biological functions of apoAI and apoE3 (*Sections* 4.2.6 and 4.2.7). It was decided to use Western blotting and densitometric analysis (*Section* 2.4.4) since an attempt to establish an ELISA for this protein was unsuccessful (*Chapter* 3). The concentration of a pure apoAI standard was determined by BCA protein assay (*Section* 2.2.1.2), and then known quantities run on a 4-20% SDS-polyacrylamide gel (*Section* 2.2.2) to obtain a standard curve for apoAI measurements. At the end of Western blotting, film saturation was ascertained by exposing the nitrocellulose membrane to X-ray film for varying lengths of time (5 s-5 min). *Figure* 4.4, Panel A shows the autoradiograph generated from a 1 min exposure. This was repeated twice (data not shown) and the bands obtained on the three autoradiographs were measured by densitometry. The local background was subtracted from each of the values and the mean 'adjusted volume' for each was calculated and plotted versus pure apoAI concentrations (*Figure* 4.4, Panel B). The calibration curve showed that saturation of film was reached after using 99 ng of pure apoAI at 1 min

exposure time. Standard curves (0-99 ng of apoAI) were produced throughout this study whenever there was a need to quantify levels of secreted apoAI, taking care to ensure that standards and test samples were applied to the same gel and treated under the same conditions.

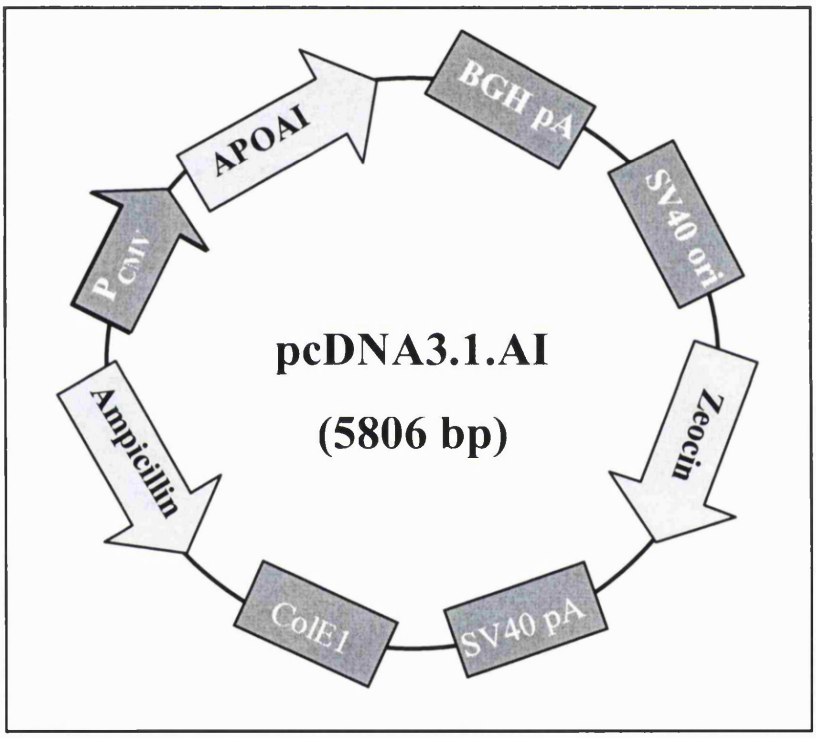

Figure 4.1 Simplified plasmid diagram showing the main features of pcDNA3.1.AI. *This figure shows a functional map of pcDNA3.1.AI that was kindly provided by Prof L Fan. It contains cytomegalovirus (CMV) enhancer-promoter for high-level expression of apoAI, bovine growth hormone (BGH) polyadenylation signal and transcription termination sequence to enhance mRNA stability. The ampicillin resistance gene and ColE1 origin, select and maintain the plasmid in E.coli, whereas the zeocin- selectable marker confers rapid selection in zeocin-containing medium. This plasmid is ~ 5 kb in size and carries a single copy of full-size human apoAI cDNA that was excised after digestion with BamHI and HindIII. Direct sequencing of the PCR product identified a T to G mutation that was subsequently corrected with the Site-directed Mutagenesis kit (Section 2.4.1).*

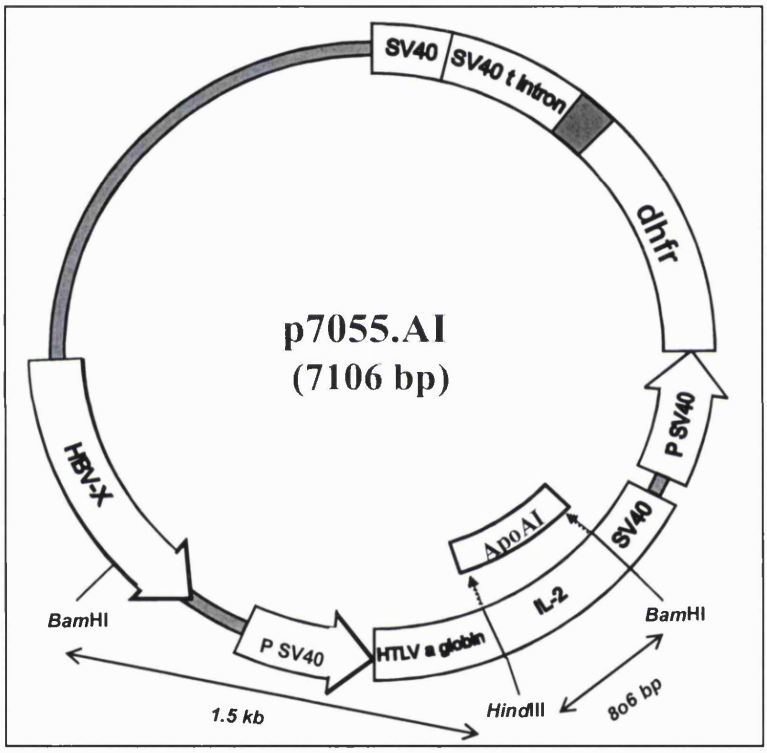

Figure 4.2 Simplified plasmid diagram showing the main features of p7055.AI. *The expression plasmid p7055 (~6.8 kb) was supplied by Dr D. Vinogradov. The location of both BamHI and the HindIII site is marked on the diagram. These restriction sites were used in preparing the p7055 vector for cloning as described in Section 2.4.2.1. The apoAI cDNA was excised (BamHI and HindIII) from pcDNA3.1.AI and ligated into this vector in the location of IL-2 cDNA as described in Section 2.4.2.4. The length of the cloned apoAI was 806 bp.*

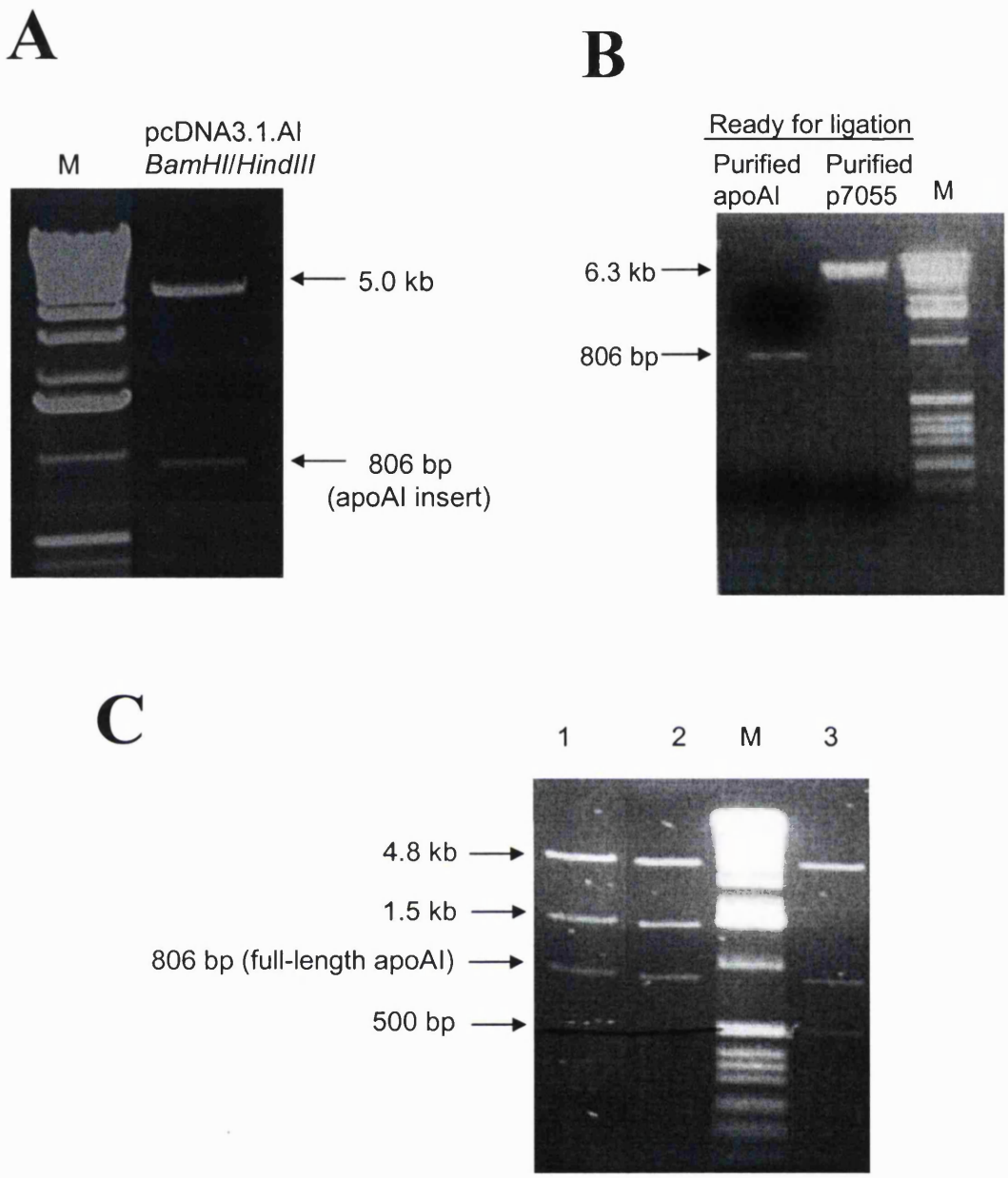

Figure 4.3 Successful transfer of apoAI cDNA into the p7055 expression vector. ***Panel A,*** *photograph of a 1% agarose gel showing an ~806 bp band corresponding to apoAI cDNA excised (BamHI and HindIII) from pcDNA3.1.AI. This band was excised and gel purified (Section 2.2.7.2).* ***Panel B,*** *The purified apoAI band from Panel A, and the purified p7055 that was ready for ligation (Section 2.4.2.1-2.4.2.3) were separated on a 1% agarose gel to confirm the correct size of each fragment.* ***Panel C,*** *following the ligation of the two fragments (Panel B) as described in the text, transformation of competent bacterial cells was performed (Section 2.4.2.5). Three bacterial clones were analysed (Section 4.2.1.2) by extracting plasmids from each clone and subjecting it to restriction endonuclease digestion with BamHI and HindIII. The digestion products were separated using a 1.0 % agarose gel. Only clones 1 and 2 contained the apoAI sequence inserted in the correct orientation.*

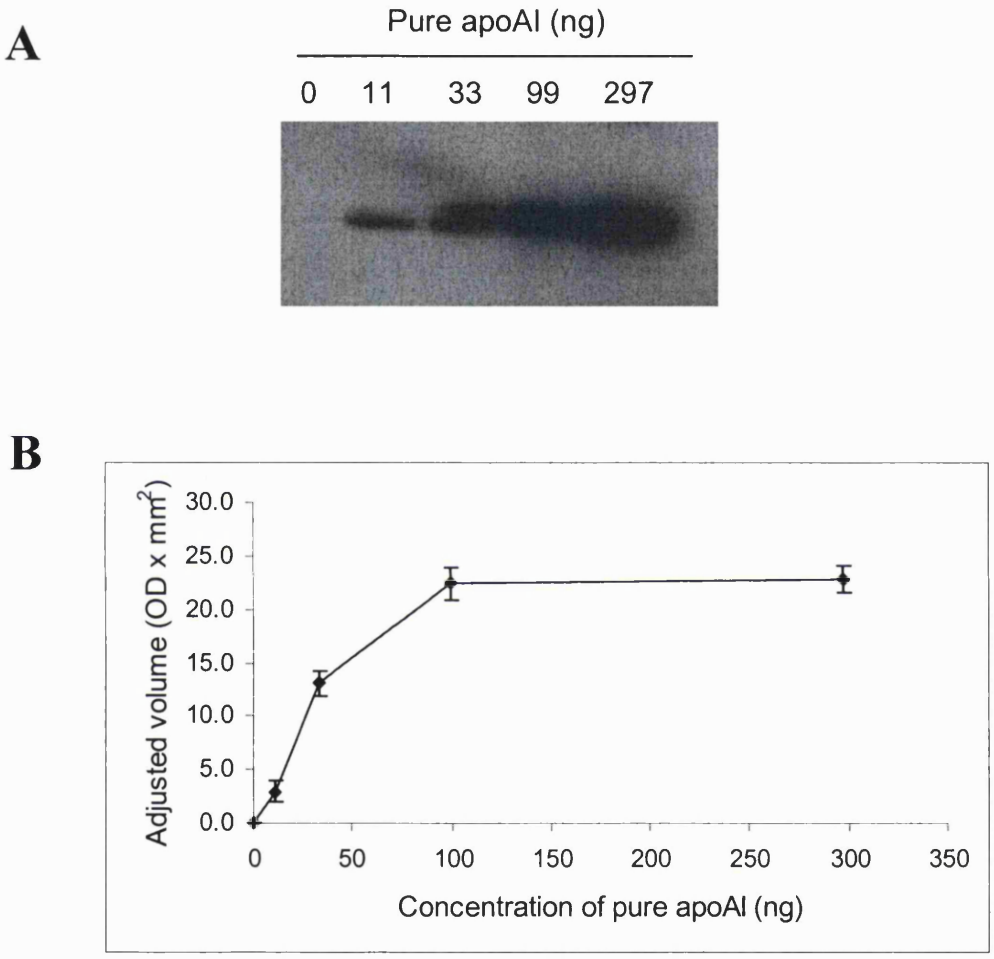

Figure 4.4 Western blotting and densitometry to determine levels of apoAI secreted by recombinant CHO cells. ***Panel A,*** *known quantities of pure apoAI (pureAI) were separated on a 4-20 % SDS-polyacrylamide gel. The autoradiograph shows results of Western blotting (1 min exposure).* ***Panel B,*** *the pure apoAI bands from Panel A, were analysed by scanning densitometry. Average scanning densitometry data from Panel A and two other repeat experiments are shown in Panel B. Having subtracted the local background from each of the values, the mean adjusted volume ± S.D. for each band was calculated and plotted versus pure apoAI concentration. The obtained curve indicated saturation after using 99 ng of pure apoAI. A similar standard curve was produced throughout this study when there was a need to quantify levels of apoAI secreted from recombinant CHO cells.*

4.2.3 CLONING AND SUB-CLONING OF CHOdhfr- CELLS TRANSFECTED WITH HUMAN APOAI

p7055 expression vector containing human apoAI cDNA (p7055.AI) was isolated from a large-scale bacterial culture using the 'EndoFree Plamid Maxi' kit (Qiagen) (*Section* 2.4.2.6). The endotoxin-free plasmid (240 μg) extracted by this procedure was then used to transfect eukaryotic CHOdhfr- cells.

4.2.3.1 Transfection and Selection of Transfected Cells

The mutant CHO cell line, CHOdhfr-, is deficient in the dihydrofolate reductase (*DHFR*) gene which makes it defective in endogenous purine and pyrimidine base synthesis. Consequently, it requires hypoxanthine and thymidine for growth. CHOdhfr- cells were transfected with 2 μg of p7055.AI plasmid using Superfect as described in *Section* 2.4.3.1. Another batch of CHOdhfr- cells were also transfected with pGFP plasmid (*Section* 2.4.3.1), which was used as a positive control for the experiment. Twenty-four hours post-transfection, approximately 15% of the cells fluoresced green, as observed by phase-contrast microscopy and fluorescent microscopy using incident blue light, indicating that the transfection with the pGFP plasmid had been successful (*Figure* 4.5). The quantity of secreted apoAI from the transiently-transfected cells was verified by scanning densitometry (*Section* 2.4.4). The presence of a 28 kDa band, absent in control cells, indicated that apoAI was secreted by transiently-transfected cells (*Figure* 4.7, Panel A). The quantity of secreted apoAI was calculated to be 0.5 $\pm$ 0.07 μg/mg protein/24 h (*Figure* 4.7, Panel B).

After transfection, the cells were harvested and seeded in a new flask. The maintenance medium for CHOdhfr- cells was then replaced with selection medium (Table 2.4) (*Figure* 4.6, Panel A). This medium lacks hypoxanthine and thymidine and, thus, only cells successfully transfected with p7055.AI, which contains the *DHFR* gene, continue to grow (*Figure* 4.6, Panel B). The surviving cells were expanded, some were cryopreserved, while the rest were maintained under selection pressure. They are referred to as the 'mixed population' of cells. Non-transfected CHOdhfr- cells were used as control for this selection procedure. In this case, all the cells died by 2-3 weeks after the addition of the selection medium (*Figure* 4.6, Panel C).

It was necessary to confirm that the mixed population of cells secretes apoAI protein. This was performed as explained earlier. ApoAI was detected in conditioned medium

from the mixed population of cells (*Figure* 4.7, Panel A). Scanning densitometry determined the mean quantity of secreted human apoAI as 1.1 + 0.22 μg/mg protein/24 h (*Figure* 4.7, Panel B).

4.2.3.2 Isolation of CHOAI Clones and Sub-Clones

The aim of this cloning section was to ensure sufficient amounts of apoAI protein were secreted by recombinant CHOAI cells to match them with cells secreting recombinant CHOE3 (*Section* 3.2.7). Cloning was performed by limiting dilution in a 96-well plate (*Section* 2.4.3.3) in order to isolate individual CHOAI cells. Each marked cell was allowed to undergo 4/5 cell divisions prior to picking 30 clones and expanding them under selection pressure. Twelve of the fastest growing CHOAI clones were analyzed by Western blotting using equal volumes of media obtained from a 24 h collection of confluent cells in 6-well plates. As shown in Panel A of *Figure* 4.8, the majority of clones secreted varying levels of apoAI, with the remaining clones no apoAI secretion was detected. Subsequently, two of the best apoAI-producer clones (# 2 and # 9) were chosen to undergo MTX amplification (*Section* 2.4.3.4) starting with addition of 2 nM MTX to the selection medium and then doubling the concentration up to 32 nM after each subculture. MTX-containing medium did not affect the normal growth of both clones. However, instead of increasing, the level of secreted apoAI was gradually reduced after adding 2 nM of MTX to both # 2 and # 9 subcultures (*Figure* 4.8, Panels B & C respectively). It was therefore, decided to stop the MTX treatment.

The selected best producer clones (# 2 and # 9) were then subcloned to ensure isolation of pure clones, which were expected to secrete more apoAI. Twelve sub-clones were expanded and analyzed by Western blotting only, as scanning densitometry was time-consuming. It was established that not all the sub-clones from # 2 secreted equal amounts of apoAI (data not shown), indicating that pure clones had not been isolated in the first cloning step. However, all the sub-clones from # 9 were secreting almost identical amounts of apoAI (*Figure* 4.9, Panel A). Sub-clone # 2B was chosen and the quantity of secreted apoAI was monitored. Initially, this sub-clone was passaged 12 times (1:10 split). In addition, after passage 12, the cells were cryopreserved for a week and then thawed out and maintained in culture up to passage 16. Testing conditioned media from passages 4, 8, and 12 prior to freezing in liquid nitrogen, and passages 13 and 16 after thawing out the cells, demonstrated that apoAI secretion was not affected by freezing or passaging of the recombinant cells (*Figure* 4.9, Panel B). Having

demonstrated a consistent secretion of apoAI, # 2B was expanded and cryopreserved for future use. Scanning densitometry demonstrated 9.8 $\pm$ 0.19 μg/mg protein/24 h of secreted apoAI, which was higher than the amount secreted by the initial stably-transfected clones.

4.2.4 CONFIRMING THE GENOTYPE OF RECOMBINANT CHOE3 CELLS

Recombinant CHO cells expressing human apoE3 (CHOE3) were kindly provided by Dr A Tagalakis (Department of Medicine, Royal Free & University College Medical School, London, UK). Using recombinant CHOE2 cells (previously genotyped) as a positive control (for the genotyping method), apoE genotyping was performed on recombinant CHOE3 cells by DNA extraction followed by PCR-RFLP analysis (*Section* 2.5.4). The expected 227 bp PCR product (*Figure* 4.10, Panel A) was excised from the gel and used for *Cfo1* digest (*Section* 2.5.4.2) as well as sequencing (*Section* 2.2.7). A photograph of RFLP products separated on a 20% TBE gel (*Figure* 4.10, Panel B) demonstrated the presence of diagnostic bands (91 and 48 bp) for the *APOE3* gene (Table 2.13). Sequencing data indicated the presence of a C at position 170 confirming the presence of the *APOE3* gene (*Figure* 4.10, Panel C). Similarly, the control cell line (CHOE2), showed the diagnostic bands (91 and 83 bp) for *APOE2*, and presence of a T at position 169 (*Figure* 4.10, Panels B & C).

A

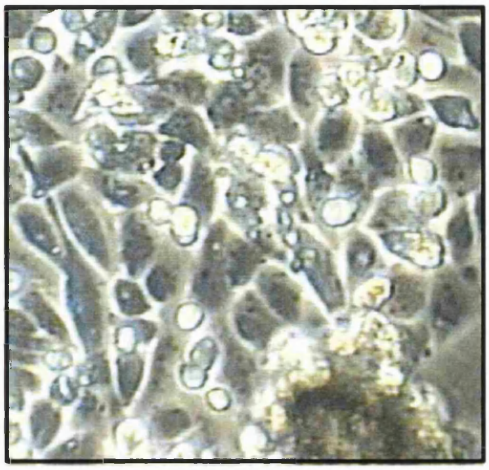

B

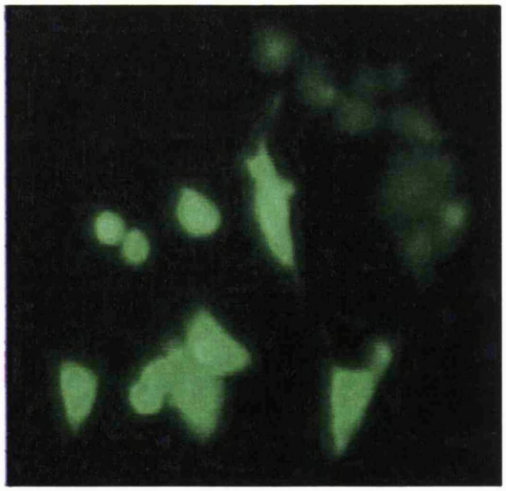

Figure 4.5 Successful transfection of CHOdhfr- cells with pGFP. *CHOdfhr- cells (50-70 % confluent) were transfected with a pGFP expression plasmid using Superfect as described in section 2.4.3.1. Twenty-four hours post-transfection, the cells were observed by phase-contrast microscopy* ***(Panel A)****, or by fluorescent microscopy with blue light of wavelength 465-495 nm* ***(Panel B)****. Both images are 20X magnification.*

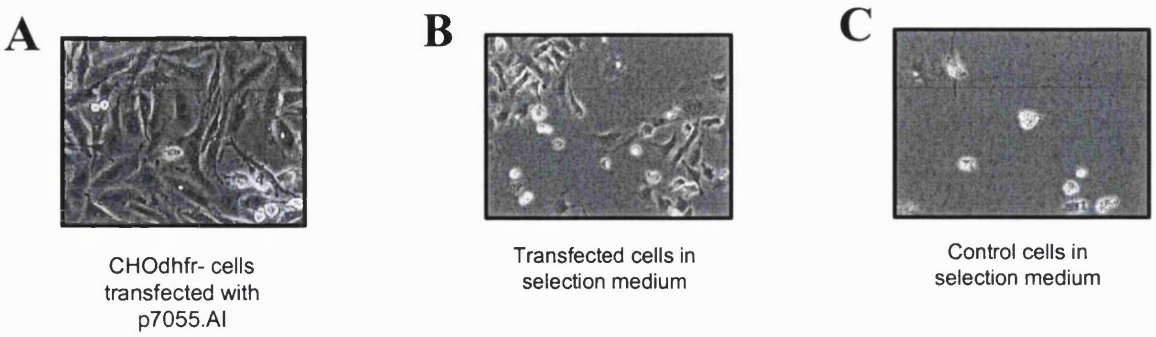

Figure 4.6 Transfected and control CHOdhfr- cells in selection medium. *Phase-contrast microscopy of CHOdhfr- cells transfected with the p7055.AI vector as described in the text* ***(Panel A)****. After addition of selection medium (Table 2.4), the cells that were stably transfected survived* ***(Panel B)****, while the control cells (not transfected with the plasmid) died 2-3 weeks after the addition of selection medium* ***(Panel C)****.*

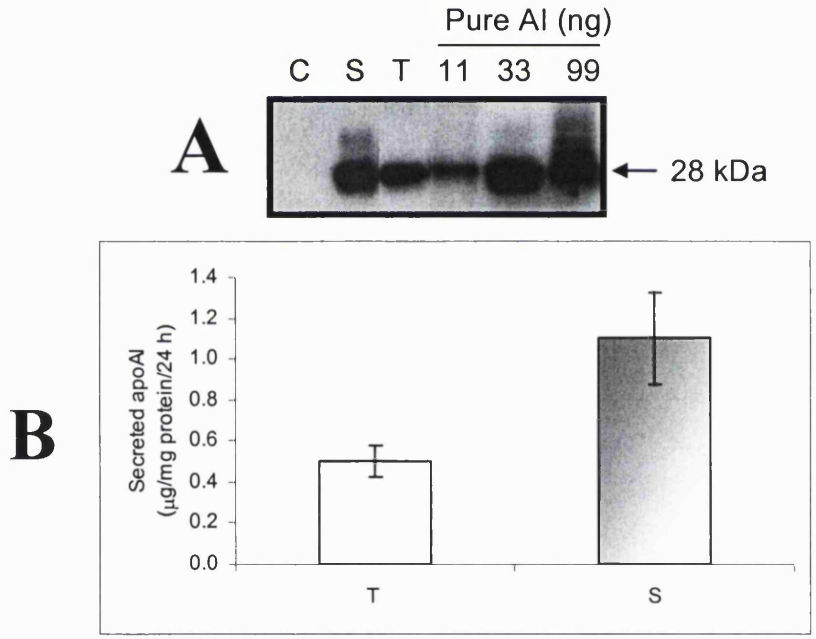

Figure 4.7 ApoAI secretion from transiently- and stably-transfected CHO cells. *Conditioned media from untransfected CHOdhfr- and recombinant CHOAI cells (after transient and stable transfection) were collected after 24 h incubation. Proteins were separated by 4-20 % SDS-PAGE, followed by immunoblotting with anti-apoAI antibody. In addition, known quantities of apoAI were subjected to electrophoresis and immunoblotting* ***(Panel A)****. Presence of the 28 kDa bands indicated presence of apoAI in all samples except for control. Scanning densitometry using known quantities of pure apoAI was used for quantifying levels of secreted apoAI (Section 2.4.4). Stably-transfected cells secreted more apoAI than the transiently-transfected ones (1.1 ± 0.22 µg/mg protein/24 h versus 0.5 ± 0.07 µg/mg protein/24 h)* ***(Panel B)****. C, T, and S denote medium from control (CHOdhfr-), transiently-transfected, and stably-transfected cells.*

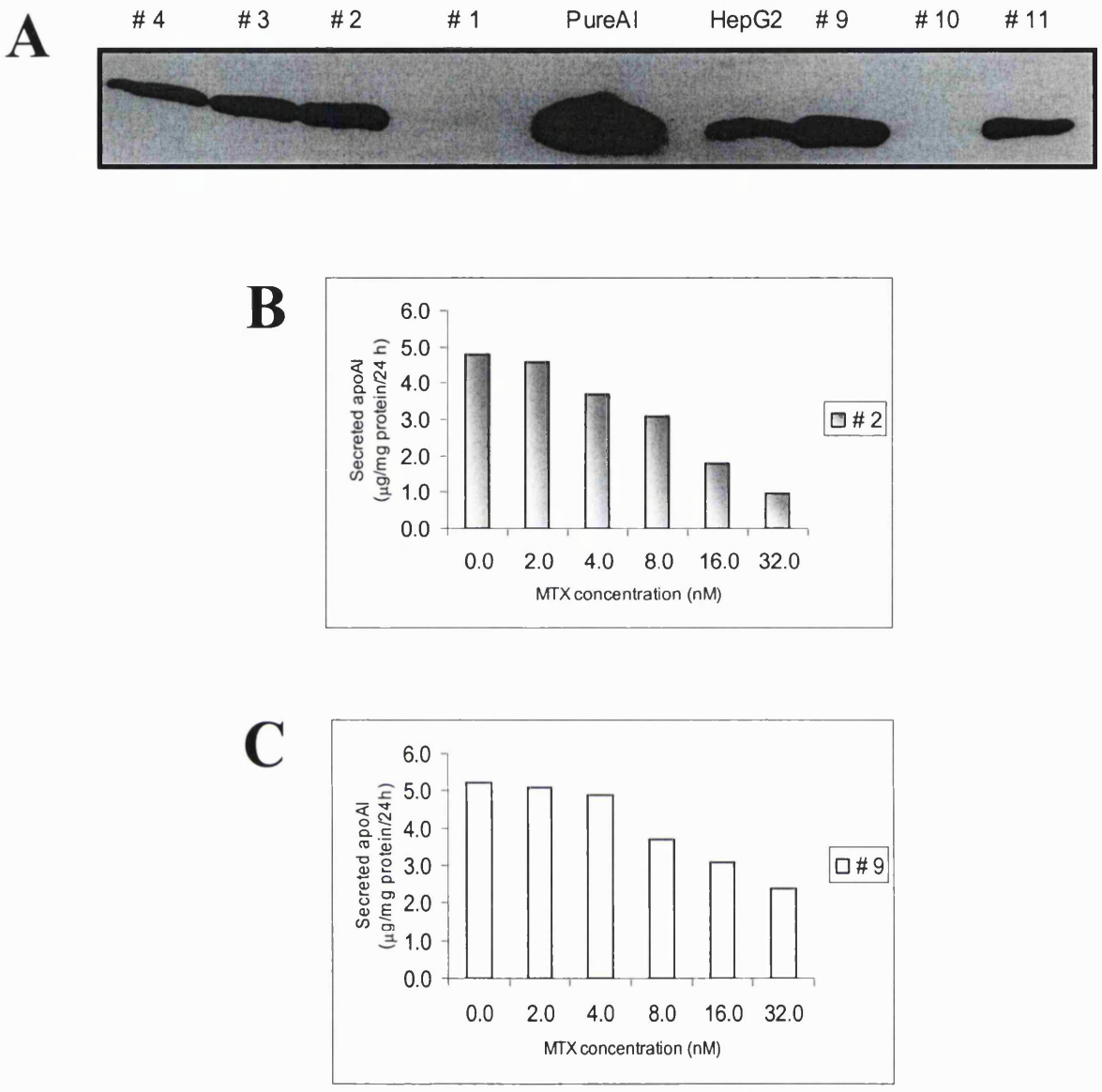

Figure 4.8 Identification of recombinant CHOAI clones and MTX amplification of the two best apoAI-producer clones. ***Panel A,*** *Media from twelve confluent CHOAI clones were analyzed for apoAI secretion by separating 20 µl of medium from each clone on 4-20 % SDS-polyacrylamide gels and immunoblotting. Results of some of the clones are shown, demonstrating a range of apoAI production from the majority of the clones while with the remaining clones (# 1 and # 10) no apoAI production was detected. The two best apoAI-producer clones (# 2 and # 9) were subsequently subjected to increasing concentrations of MTX in their selection medium to increase the amount of secreted apoAI. MTX was added at a concentration of 2 nM followed by doubling its concentration after each subculture. Concentrations of apoAI in conditioned media were determined by scanning densitometry (Section 2.4.4). Graphs indicated a gradual reduction of apoAI secretion for # 2* ***(Panel B)*** *and # 9* ***(Panel C)*** *after culture in 2 nM MTX when compared to conditioned media without any MTX.*

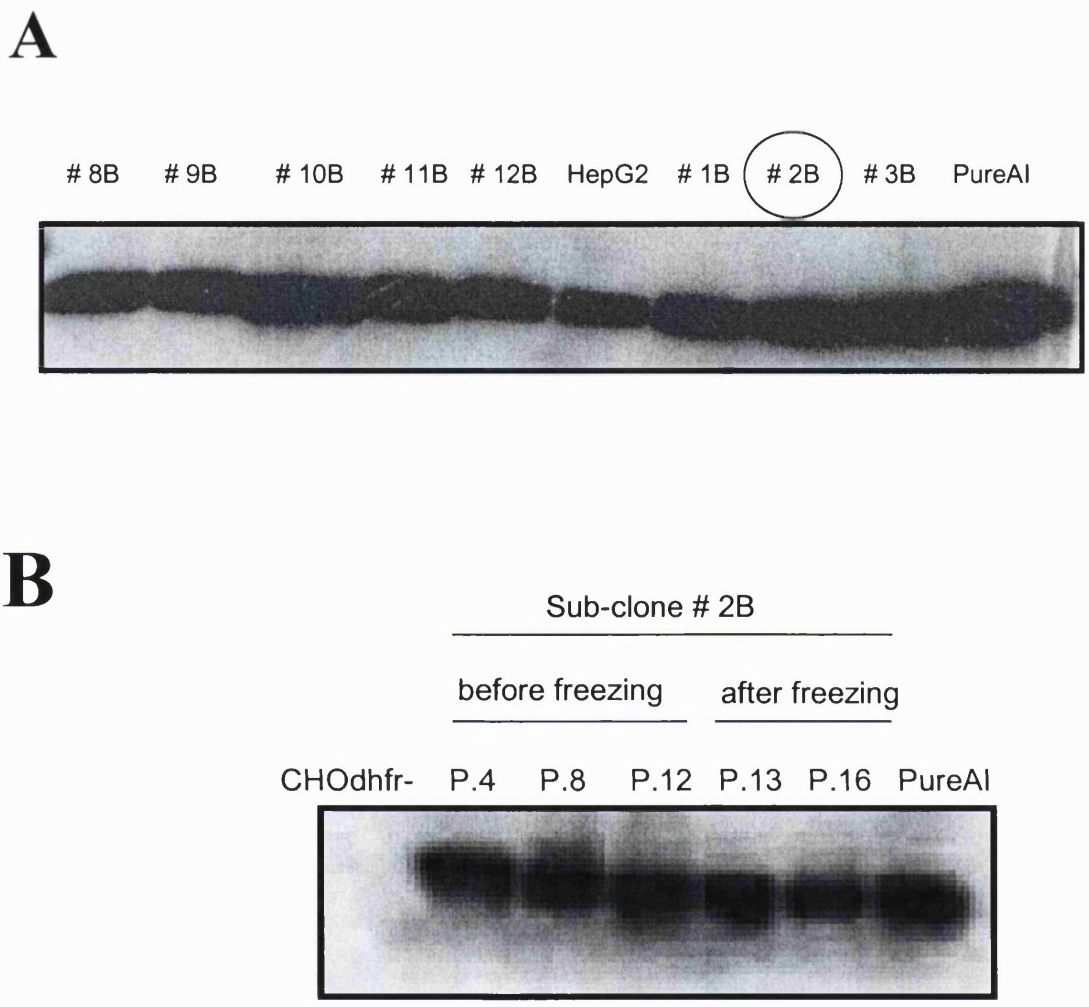

Figure 4.9 Identification of the best apoAI-producer sub-clone and confirmation of its stability following freeze-thaw experiments. ***Panel A,*** *This shows some of the twelve sub-clones of # 9 that were expanded and analyzed by Western blotting. Purified apoAI (PureAI) and medium from confluent cells in a well of a 6-well plate of HepG2 cells (HepG2) were used as positive controls.* ***Panel B,*** *The circled sub-clone from panel A (# 2B) was chosen and subjected to passaging and freeze-thawing to ensure continual secretion of apoAI. Passages 4, 8, and 12 prior to freezing and 13, and 16 after thawing out were tested by Immunoblotting. Results demonstrated that apoAI secretion was maintained through passaging prior and after cryopreservation. As a consequence, this sub-clone (# 2B) was expanded for future cell characterization studies.*

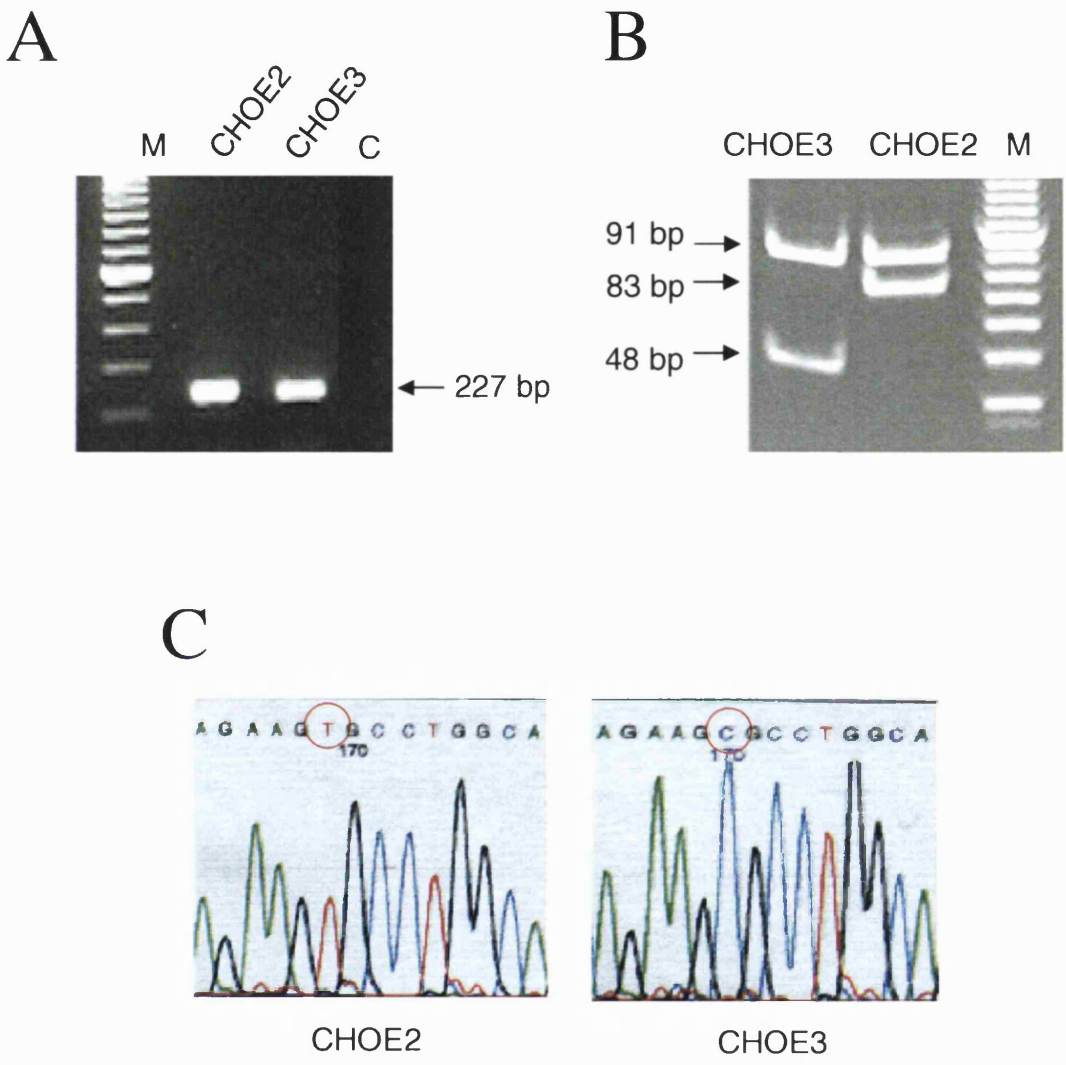

Figure 4.10 Confirming the genotype of recombinant CHOE3 cells. *Recombinant CHOE3 cells were trypsinised from a confluent well of a 6-well plate (Section 2.2.4.2). DNA was extracted (Section 2.5.4.1) and apoE genotyping was carried out by PCR-RFLP analysis (Section 2.5.4.2). Direct sequencing of the PCR product was also performed to confirm the genotype. Previously genotyped CHOE2 cells were treated in the same way and used as a positive control for the genotyping procedure.* ***Panel A,*** *indicates the expected 227 bp PCR product after electrophoresis on a 1% agarose gel. C denotes water negative control of PCR reaction. M = 100 bp ladder.* ***Panel B,*** *indicates the final Cfo1 digest of RFLP analysis separated using a 20% TBE gel. Both cell lines showed the expected bands: CHOE3 (91 and 48 bp), CHOE2 (91 and 83 bp). M = 10 bp ladder.* ***Panel C,*** *apoE genotypes were confirmed by direct sequencing of the purified PCR products. ApoE3 had a C nucleotide, and apoE2 a T nucleotide at positions 170 and 169 respectively (circled bases).*

4.2.5 PHYSICAL CHARACTERIZATION OF CHO CELL-DERIVED APOE3- AND APOAI-CONTAINING PARTICLES

Some of the physical properties of apoE3 and apoAI secreted by recombinant CHO cells were determined by agarose gel electrophoresis and non-denaturing gradient gel electrophoresis (NDGGE) using ~2 μg of each particle and following the protocols described in *Section* 2.4.5. Separation of serum-free conditioned media by agarose gel electrophoresis and immunoblotting for the presence of immunoreactive apoE3 and apoAI demonstrated that both particles had mainly preβ-mobility on the gel (*Figure* 4.11).

Serum-free conditioned medium from both cell lines was also separated by NDGGE and subsequently analyzed by Western blotting in order to determine diameter of the secreted particles. *Figure* 4.12 shows the autoradiographs of apoE3 and apoAI generated from 3 min and 5 min exposure times, respectively. As indicated, the predominant apoAI particle size is ~9.4 nm, which is quite similar to small HDL particles in plasma, with a smaller population of ~7.0 nm. ApoE3 had a prominent band at ~9.4 nm and a fainter one at ~10.4 nm.

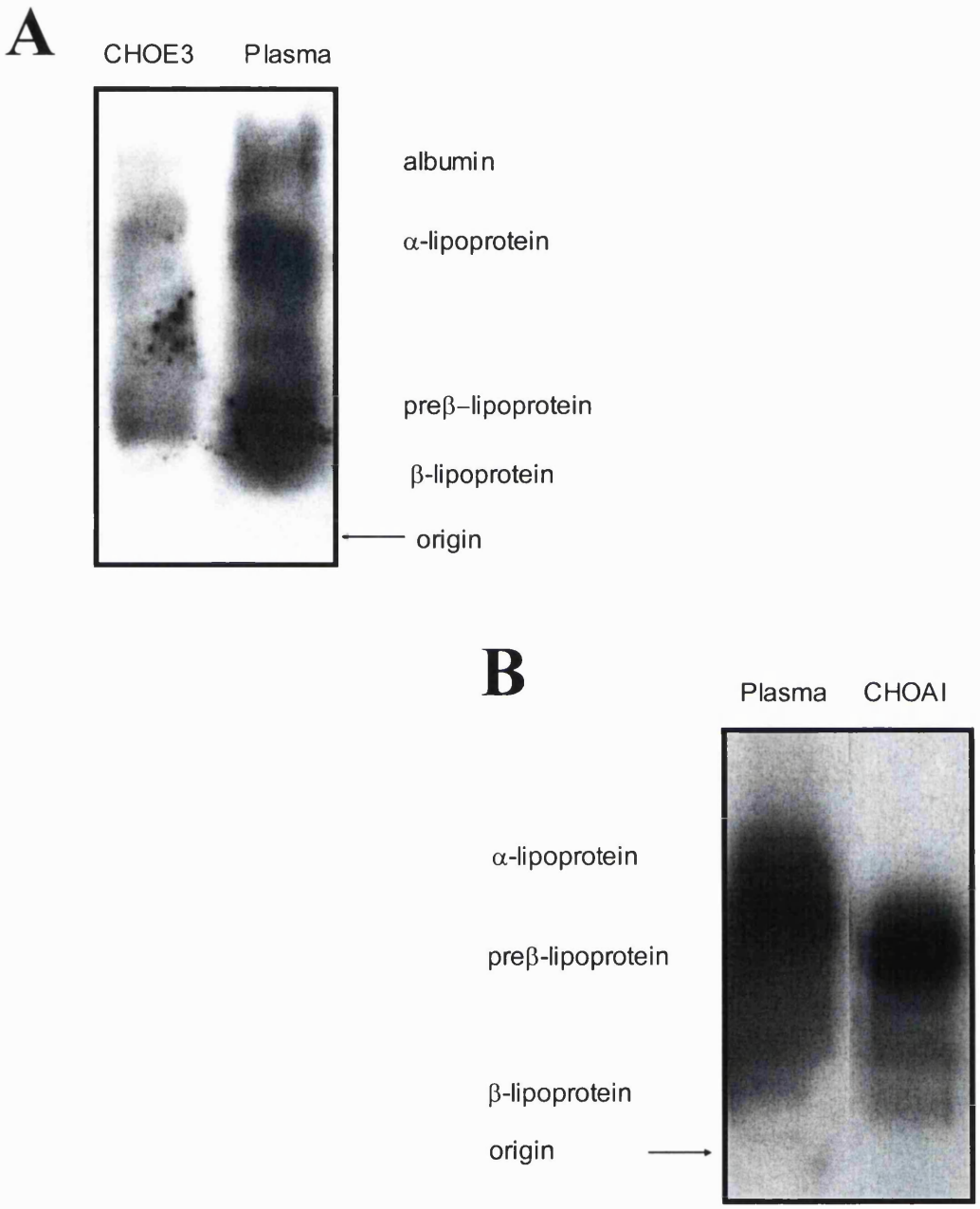

Figure 4.11 Mobility of CHO cell-derived apoE3- and apoAI-containing particles in agarose gel. *Serum-free selection medium was added to confluent CHOE3 and CHOAI cells. Media were collected after 24 h, filtered, and concentrated about 50 X using 30,000 MWC and 10,000 MWC concentrators for CHOE3 and CHOAI respectively. About 2μg of each prepared medium was then subjected to agarose gel electrophoresis (Section 2.4.5.1) and immunoblotted for apoE3* ***(Panel A)*** *and apoAI* ***(Panel B)****, separately. As shown, both particles are heterogeneous having mainly pre-β mobility on agarose gel.*

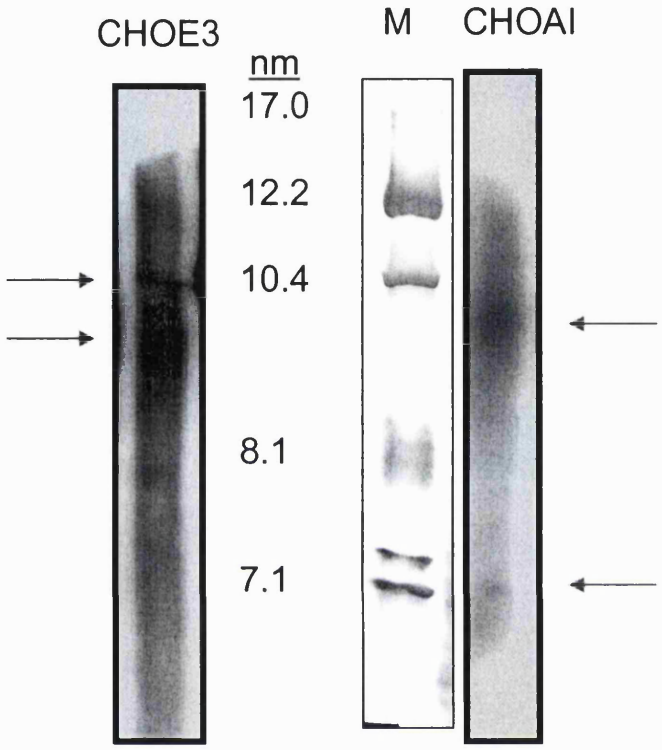

Figure 4.12 Size distribution of CHO cell-derived apoE3- and apoAI-containing particles determined by NDGGE. *Serum-free selection medium was added to confluent CHOE3 and CHOAI cells. Media were collected after 24 h, filtered, and concentrated about 50 X using 30,000 MWC and 10,000 MWC concentrators for CHOE3 and CHOAI respectively. About 2 μg of each prepared medium was then subjected to NDGGE followed by Western blotting (Sections 2.4.5.2 & 2.2.3). The size distribution of the apoE3-containing particles was ~9.4 nm and ~10.4 nm (arrowed). The apoAI particle size distribution was ~9.4 nm and ~7.0 nm (arrowed). M, indicates the marker that includes thyroglobulin (17.0 nm), ferritin (12.2 nm), catalase (10.4 nm), lactate dehydrogenase (8.1 nm), and BSA (7.1 nm).*

4.2.6 CHO CELL-DERIVED APOE3- AND APOAI-CONTAINING PARTICLES PROMOTE FREE CHOLESTEROL (FC) EFFLUX FROM LABELLED MACROPHAGES

The aim of these experiments was to determine whether the apoE3-containing particles secreted by the recombinant CHOE3 cells were biologically active in promoting FC efflux. ApoAI particles secreted by recombinant CHOAI cells were used as positive controls. THP-1 cells were used as cholesterol donors because they have an active lipoprotein-mediated efflux pathway (Kritharides L *et al*, 1998).

Initially, THP-1 cells were seeded into 12-well plates and stimulated with PMA (over seven days) to become adherent macrophages. They were then radiolabelled with [^{3}H]-cholesterol (*Sections* 2.4.6.1 and 2.4.6.2) and incubated with different conditioned media from CHOdhfr- control cells to determine the medium which gave the lowest background efflux. The cells were incubated with each of the following serum-free media (Table 2.4): Iscove's modified DMEM, RPMI-1640, CHO-SFM II, CD-CHO, and standard efflux medium (Iscove's modified DMEM + 1% (w/v) fatty acid-free BSA or FFA-BSA). Conditioned media were collected after 24 h and treated as explained in *Section* 2.4.4.1 prior to its incubation with the radiolabelled macrophages (1ml/well). Cholesterol efflux experiment was performed as described in *Section* 2.4.6.2. As illustrated in *Figure* 4.13, the medium with the lowest background reading was serum-free Iscove's modified DMEM (1.46% efflux) and, therefore, this medium was used for further efflux studies.

The next FC efflux experiment was performed comparing the abilities of particles secreted from CHOE3 and CHOAI cells to efflux cholesterol from labelled macrophages over a 24 h time-course. Initially the cellular FC pool of macrophages was successfully labelled with [^{3}H]-cholesterol (42% uptake) for 24 h and equilibrated a further 16 h with equilibration medium (*Section* 2.4.6). Conditioned media were collected from confluent CHOE3 and CHOAI cells and concentrated 40 X (*Section* 2.4.4.1). Macrophages were stimulated with 6 μg/ml of apoE3- and apoAI-enriched conditioned medium. Conditioned medium from CHOdhfr- cells was similarly treated and used as a negative control. Radioactivity in an aliquot of the medium and cell lysate was assessed by LSC (*Section* 2.4.6.2). The mean percentage cholesterol efflux values from quadruplicate wells $\pm$ S.D (from a single experiment) were calculated and plotted versus time for each cell type (*Figure* 4.14).

A substantial difference between the abilities of conditioned medium from CHOdhfr- control and recombinant cells (CHOE3 and CHOAI) to efflux FC was revealed from this experiment; the percentage of FC efflux from the recombinant cells was significantly higher than control cells at every time point measured ($P<0.05$ or greater) except for the initial 1 h time point when efflux was almost the same for all the cell lines (CHOdhfr- conditioned medium: 1.53 $\pm$ 0.13% efflux, CHOAI conditioned medium: 1.9 $\pm$ 0.07% efflux, CHOE3 conditioned medium: 1.80 $\pm$ 0.20% efflux; $P>0.05$ at 1 h). As shown in *Figure* 4.14, the effluxing ability of conditioned medium from control cells reaches a plateau after 1 h. However, efflux by conditioned medium from CHOE3 remains linear through out the time-course study with approximately a five-fold increase in percentage efflux at 24 h (9.13 $\pm$ 0.51%) compared to that at 1 h (1.80 $\pm$ 0.20%). Similarly, percentage efflux by CHOAI conditioned medium remained linear between 1-8 h and then doubled from 8 to 24 h. Most importantly, at each time point, there was no significant difference between the FC efflux values from conditioned media of recombinant cells (for example at 24 h, CHOAI conditioned medium: 13.8 $\pm$ 1.46% efflux, CHOE3 conditioned medium: 9.13 $\pm$ 0.51% efflux; $P>0.05$). The explained statistical conclusions were confirmed in a second independent experiment.

In a different experiment, the effect of HDL-plasma (plasma depleted of the apoB-containing lipoproteins) on the effluxing abilities of recombinant apoE3 and apoAI particles was assessed. Cellular FC of macrophages was labelled with [^{3}H]-cholesterol (37% uptake from the labelling medium). Conditioned media were collected from confluent CHOE3, CHOAI and CHOdhfr- control cells after 24 h and concentrated 40 X as described previously. In this experiment macrophages were additionally stimulated with conditioned medium from CHOE3 or CHOAI (containing 6 μg/ml of apoE3 and apoAI) or control cells supplemented with 5% (v/v) HDL-plasma. Efflux was carried out for 24 h, and the level of [^{3}H]-cholesterol in the media and the cells was determined by LSC. The mean percentage cholesterol efflux values from quadruplicate wells $\pm$ S.D (from a single experiment) were calculated and plotted for each cell type (*Figure* 4.15).

This experiment revealed that firstly, all the three cell lines (recombinant CHOE3 and CHOAI, and CHOdhfr-) showed increased ability to FC efflux on addition of HDL-plasma compared to conditioned medium alone. For example, at 24 h, conditioned medium from CHOE3 cells plus HDL-plasma stimulated THP-1 cells to efflux 24% of their radiolabelled FC, which was significantly higher than when conditioned medium

was used alone (CHOE3 conditioned medium alone: 11.1 ± 0.87% efflux, CHOE3 conditioned medium plus HDL-plasma: 24 ± 1.81% efflux; P<0.001). This indicated that HDL-plasma stimulated FC efflux ability of the examined cell lines. Secondly, FC effluxing ability of conditioned medium from CHOAI (13.1 ± 0.55% efflux) was significantly higher (P<0.001) than that from CHOdhfr- control cells (1.7 ± 0.17% efflux). This difference in efflux remained significant upon the addition of HDL-plasma to conditioned media from both cell lines (CHOAI conditioned medium plus HDL-plasma: 26.5 ± 0.63% efflux, CHOdhfr- conditioned medium plus HDL-plasma: 18.5 ± 3.58% efflux; P<0.001). Furthermore, these conclusions were applicable to conditioned media from CHOE3 and CHOdhfr- when media were used alone (CHOE3 conditioned medium: 11.1 ± 0.87% efflux, CHOdhfr- conditioned medium: 1.7 ± 0.17% efflux; P<0.001) or when HDL-plasma was added to the media (CHOE3 conditioned medium plus HDL-plasma: 24.0 ± 1.81% efflux, CHOdhfr- conditioned medium plus HDL-plasma: 18.5 ± 3.58% efflux; P<0.01).

Thirdly, there was no significant difference (P>0.05) at effluxing FC between conditioned medium from CHOE3 (11.1 ± 0.87% efflux) and CHOAI (13.1 ± 0.55% efflux) cells. Similarly, addition of HDL-plasma to conditioned media from both cells had no significant effect in percentage FC effluxing abilities between cells (CHOE3 conditioned medium plus HDL-plasma: 24.0 ± 1.81% efflux, CHOAI conditioned medium plus HDL-plasma: 26.5 ± 0.63% efflux; P>0.05). When this experiment was repeated on a separate occasion, the same statistical conclusions were obtained. The data explained here indicated that newly secreted apoE3 and apoAI particles are capable of effluxing labelled FC from THP-1 macrophages albeit to a lesser extent than when HDL-plasma is present in the conditioned media.

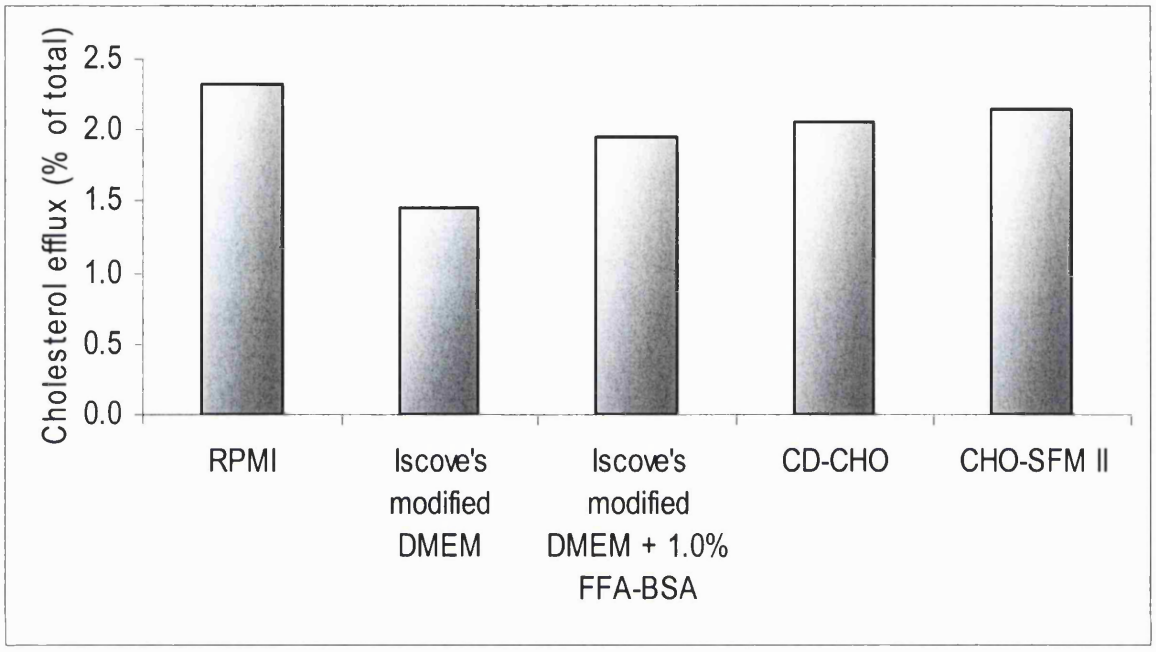

Figure 4.13 The lowest background for FC efflux from THP-1 is obtained by using serum-free Iscove's medium from control CHOdhfr- cells. *Confluent CHOdhfr- control cells were each incubated with one of the following serum-free medium: RPMI, Iscove's modified DMEM, Iscove's modified DMEM + 1.0% FFA-BSA (fatty acid-free BSA) , CD-CHO and CHO-SFM II (Table 2.4). Each medium was collected after 24 h incubation, briefly centrifuged and concentrated 40 X (Section 2.4.4.1). Equal volumes (800 μl) of each prepared medium were subsequently used in experiments of cholesterol efflux from human THP-1 macrophages (Section 2.4.6.2) to determine the medium with the lowest background for future efflux studies. Results demonstrated that serum-free Iscove's modified DMEM gives the lowest background (1.46 % efflux), and thus this medium was used for subsequent efflux studies.*

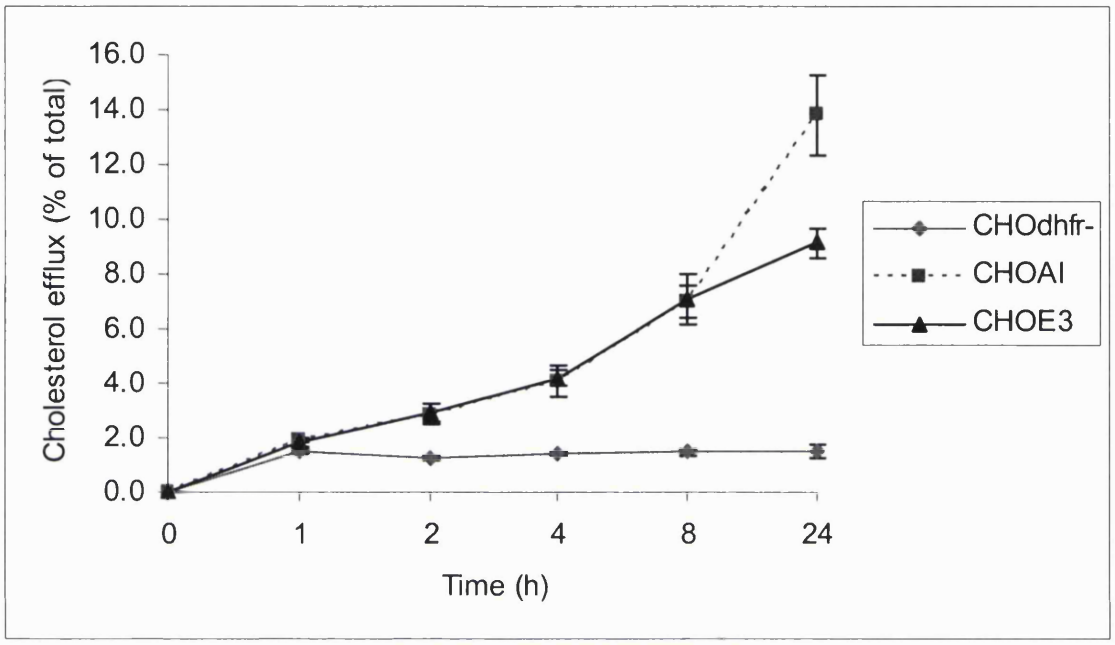

Figure 4.14 FC effluxing ability of conditioned medium from recombinant CHOE3 or CHOAI. *Conditioned media were collected from confluent CHOE3, CHOAI and CHOdhfr- control cells 24 h after the cells were incubated with serum-free Iscove's modified DMEM medium. Media were briefly centrifuged and concentrated 40 X (Section 2.4.4.1). These media were subsequently used to study cholesterol efflux from labelled human THP-1 macrophages (Section 2.4.6.2) over a 24 h time-course. FC efflux was expressed as a percentage of radioactivity in the medium compared to the total in both medium and cells. Mean percentage cholesterol efflux values from quadruplicate wells ± S.D (from a single experiment) were calculated and plotted versus time.*

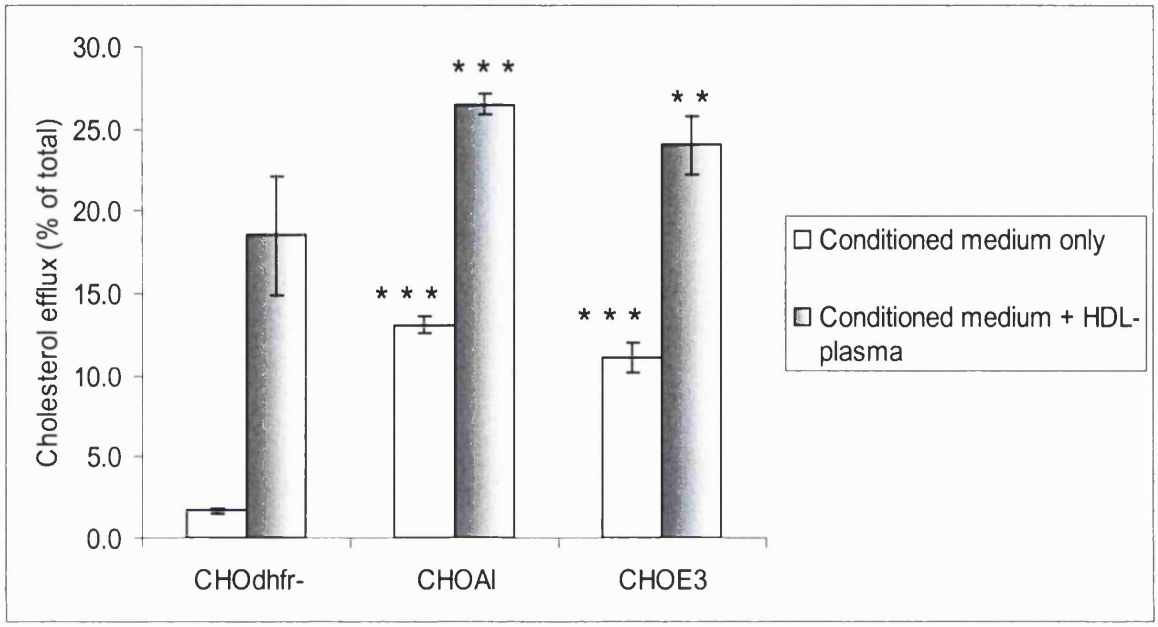

Figure 4.15 The effect of HDL-plasma on FC effluxing ability of conditioned medium from recombinant CHOE3 and CHOAI cells. *Conditioned media were collected from confluent CHOE3, CHOAI and CHOdhfr- control cells 24 h after the cells were incubated with serum-free Iscove's medium. Media were briefly centrifuged and concentrated 40 X (Section 2.4.4.1). These media were subsequently used for 24 h efflux experiments with cholesterol-labelled human THP-1 macrophages (Section 2.4.6). Conditioned media were either used alone or with the addition of HDL-plasma. FC efflux was expressed as a percentage of radioactivity in the medium compared to the total in both medium and cells. Mean percentage cholesterol efflux values from quadruplicate wells ± S.D (from a single experiment) were calculated and plotted versus time. The difference between the means of the recombinant cells compared to control cells for each time point was assessed by Student's t-test (**P<0.01, and ***P<0.001).*

4.2.7 CHO CELL-DERIVED APOE3- AND APOAI-CONTAINING PARTICLES ACTIVATE LCAT

Prior to starting experiments to compare the effect of newly-secreted apoE3 and apoAI from recombinant CHO cells on activation of LCAT, substrate (labelled cholesterol/albumin emulsion) was tested to ensure its suitability and functionality for the assay. In addition, it was necessary to have a stock source of LCAT, to estimate its concentration, and to verify that the enzyme was active.

The LCAT activity of an aliquot of frozen human plasma (not previously thawed) was measured during a 1 h time-course, using a preparation of labelled cholesterol/albumin emulsion as the substrate (*Section* 2.4.7.1) following the protocol described in *Section* 2.4.7.3. The mean percentage [^{3}H]-cholesterol esterification of duplicate samples plotted versus time is shown in *Figure* 4.16. Based on the data plotted, plasma LCAT activity was linear up to 30 min, after which there was a small increase up to 45 min with the curve reaching a plateau passed this time point. Plasma LCAT activity being linear in the first 30 min of incubation at 37 °C has been reported in the literature (Francone OL *et al*, 1995). It was concluded that the prepared [^{3}H]-cholesterol/albumin emulsion was suitable to use in future LCAT activity assays.

The next step involved preparing a source of LCAT with a known mass for future experiments. Conditioned medium from recombinant CHOHis6-LCAT cells (referred to as recombinant LCAT through out this report) were prepared as described in *Section* 2.4.7.2. The presence of recombinant LCAT in the medium was confirmed using monoclonal α-LCAT antibodies that were obtained from six different sub-clones of LCAT hybridomas (*Section* 2.4.7.2). Recombinant LCAT was subjected to SDS-PAGE and the expected bands (~65 kDa) were visualized by Western blotting, utilizing each of the prepared α-LCAT antibodies (*Figure* 4.17). Molecular weight of plasma LCAT estimated with SDS-PAGE ranges from 59-68 kDa (Chung J *et al*, 1979; Albers JJ *et al*, 1976). A stock of recombinant LCAT was prepared and stored in aliquots at -80 °C (*Section* 2.4.7.2).

Having confirmed recombinant LCAT secretion by the CHOHis6-LCAT cells, an LCAT activity assay (*Section* 2.4.7.3) was performed using the labelled cholesterol/albumin emulsion as substrate (*Section* 2.4.7.1) and human plasma or the stock recombinant LCAT plus heat-inactivated human plasma as enzyme sources (*Figure* 4.18). The

percentage of [^{3}H]-cholesterol esterified by heat-inactivated plasma plus recombinant LCAT was 6.3% at 0.5 h, and 10.6% at 1 h. This confirmed that CHOHis6-LCAT cells secrete an active enzyme. In the same experiment, human plasma gave percentage efflux values of 6.5% at 0.5 h, and 7.4% at 1 h. Using the percentage esterification values at 0.5 h (since the values are comparable for plasma and heat-inactivated plasma plus recombinant LCAT) and knowing that normal human plasma contains on average ~6 μg LCAT/ml (Hoeg JM *et al*, 1996), it was calculated that the recombinant cells secrete approximately 5.8 μg/mg protein/24 h of the enzyme.

The first LCAT activity assays using CHO cell-derived apoE3 particles were performed over a 4 h time-course. Conditioned media from recombinant CHOE3, CHOAI (~6 μg of each apolipoprotein), or control cells (CHOdhfr-), were incubated with the labelled cholesterol/albumin emulsion. After an overnight incubation on ice to allow equilibration, the stock recombinant LCAT (*Section* 2.4.7.2) was added and the enzymatic activity followed at 37 °C over a range of times. Once the reaction was terminated, free and esterified cholesterol were separated by TLC followed by isolation of the separated lipid zones for LSC. For each cell type, the mean percentage cholesterol esterification from triplicate wells ± S.D was calculated and plotted versus time (*Figure* 4.19).

Based on the obtained data, a clear difference is revealed between the abilities of medium from CHOdhfr- control cells and that from recombinant cells (CHOE3 and CHOAI) to activate recombinant LCAT: the percentage esterification by medium from each of the recombinant cells was higher than control cells at every time point measured ($P<0.001$ at all time points). As shown in *Figure* 4.19, control cells esterified cholesterol moderately from 0-0.5 h (4.23 ± 0.33 at 0.5 h), after which percentage esterification reached a plateau between 0.5-2 h. However, the curve declined after 2 h. The patterns of esterification by media from recombinant cells were as follows; a sharp rise from 0-0.5 h, then gradual increase from 0.5-2 h, with a sudden drop after 2 h. However, the percentage esterified cholesterol values were generally higher for CHOAI medium compared to CHOE3 medium with significant differences only at 0.5 h (CHOAI medium: 21.1 ± 0.75% esterification, CHOE3 medium: 17.4 ± 0.05% esterification; $P<0.05$) and 1 h (CHOAI medium: 25.6 ± 0.29% esterification, CHOE3 medium: 21.5 ± 0.31% esterification; $P<0.001$). Consequently, newly secreted apoAI particles were significantly better than apoE3 particles at activation of recombinant LCAT at 0.5 h or 1

h time points. The reason for a drop in LCAT activity observed in all the curves (*Figure* 4.19) after 2 h could be attributed to substrate depletion.

Subsequently, one further experiment was performed in quadruplicates to confirm that CHO cell-derived apoAI was significantly better at activating LCAT than CHO cell-derived apoE3. Using conditioned medium from each of the three cell lines (labelled with the cholesterol/albumin emulsion) as substrate and stock recombinant LCAT as enzyme, the experiment was repeated measuring the cholesterol esterification after 1 h. *Figure* 4.20 shows a bar diagram of the mean percentage cholesterol esterification $\pm$ S.D for each cell line. This confirmed that after 1 h of incubation, CHOAI exerted a significantly higher effect on cholesterol esterification than CHOE3 (CHOAI medium: 23.6 $\pm$ 0.57% esterification, CHOE3 medium: 20.8 $\pm$ 0.79 esterification; $P<0.001$ at 1 h). In addition, the effect of both cell lines on activating LCAT was markedly higher than that of the control cells ($P<0.001$ at 1 h).

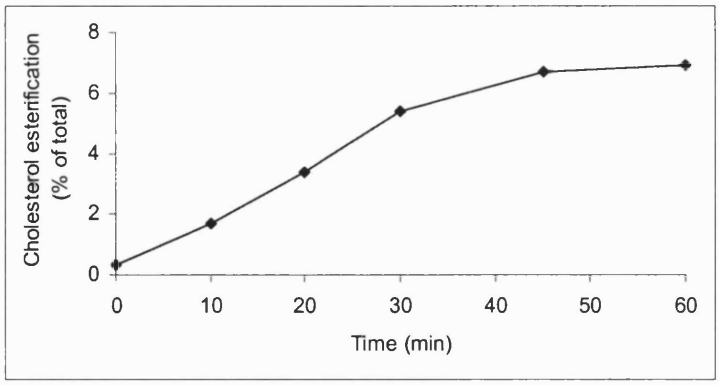

Figure 4.16 Labelled cholesterol/albumin emulsion is functional in LCAT activity assays. *Plasma from a normal volunteer (Section 2.2.9) was used for performing cholesterol esterification studies over a 1 h time-course. The LCAT assay was carried out as described in Section 2.4.7.3 using labelled cholesterol/albumin emulsion as substrate (Section 2.4.7.1). Esterified cholesterol was expressed as a % of radiolabelled cholesteryl ester (CE) compared to the total radiolabelled CE plus unesterified cholesterol (UC). Mean percentage cholesterol esterification values from duplicate tubes were calculated and plotted versus time.*

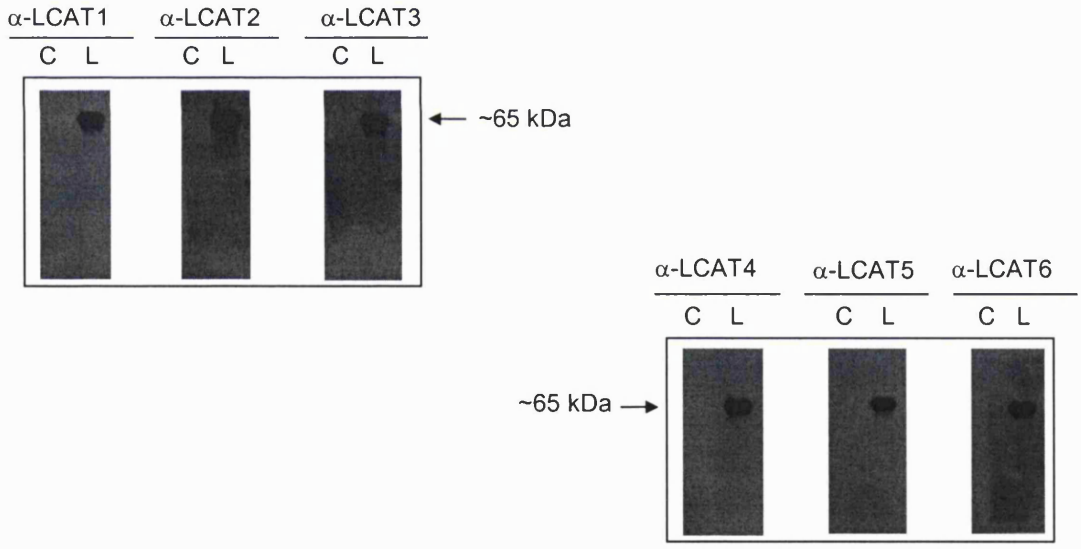

Figure 4.17 Immunoblotting of conditioned medium from recombinant CHOHis6-LCAT cells using α-LCAT antibody obtained from hybridoma cells. *Conditioned medium was collected from confluent CHOHis6-LCAT cells and CHOdhfr- control cells 24 h after their incubation with serum-free Iscove's modified DMEM medium. Media were briefly centrifuged and concentrated 100 X (Section 2.4.7.2). These media were screened for LCAT by Western blotting with a-LCAT monoclonal antibodies (labelled a-LCAT1 to a-LCAT6) obtained from six different hybridoma cell lines (Section 2.4.7.2). The appearance of ~65 kDa bands demonstrated the presence of LCAT in the conditioned medium from recombinant cells. C and L denote medium from control cells and CHOHis6-LCAT cells respectively.*

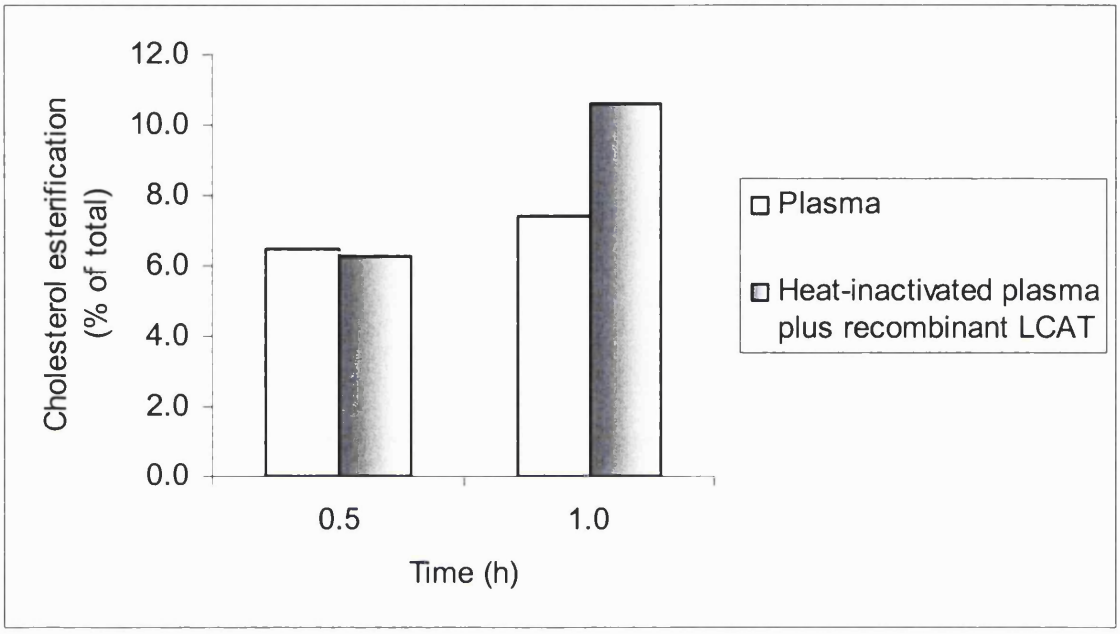

Figure 4.18 LCAT activity assay confirms that recombinant CHOHis6-LCAT cells secrete an active enzyme and allows estimation of its concentration. *Conditioned medium (recombinant LCAT) was collected from confluent CHOHis6-LCAT cells 24 h after the incubation of cells with serum-free Iscove's modified DMEM medium. Medium was briefly centrifuged and concentrated 100 X (Section 2.4.7.2). LCAT assay was performed over a 1 h time-course (Section 2.4.7.3) using labelled cholesterol/albumin emulsion (Section 2.4.7.1) as substrate and human plasma from a normal volunteer (Section 2.2.9) or heat-inactivated human plasma plus recombinant LCAT as the source of enzyme. Esterified cholesterol was expressed as a % of radiolabelled cholesteryl ester (CE) compared to the total radiolabelled CE plus unesterified cholesterol (UC). Mean percentage cholesterol esterification values from duplicate tubes were calculated and plotted versus time. Knowing normal human plasma content of LCAT (~6 μg/ml) and considering the esterification values at 0.5 h (comparison is possible between plasma and heat-inactivated plasma plus recombinant LCAT) the concentration of the recombinant LCAT was calculated to be ~5.8 μg/mg protein/24 h.*

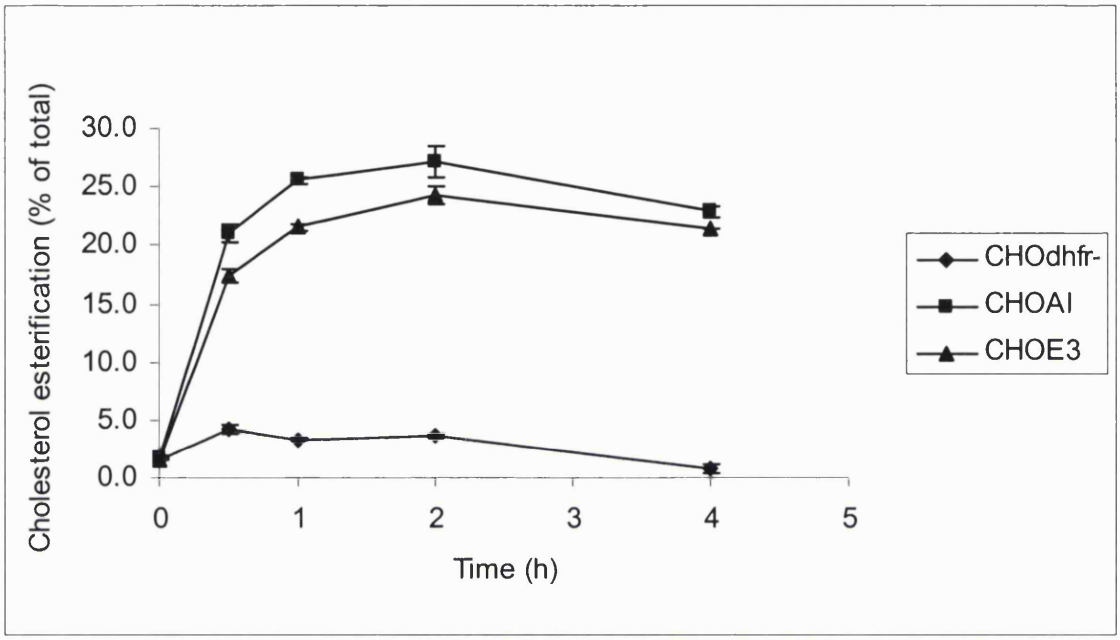

Figure 4.19 Ability of conditioned medium from CHOE3 or CHOAI cells to activate LCAT. *Conditioned medium was collected from confluent CHOE3, CHOAI and CHOdhfr- control cells 24 h after the incubation of cells with serum-free Iscove's modified DMEM medium. Media were briefly centrifuged and concentrated 40 X (Section 2.4.4.1). These media were labelled with [^{3}H]-cholesterol/albumin emulsion (Section 2.4.7.1) and used as a substrate for LCAT activity assays over a 4 h time-course (Section 2.4.7.3) using stock recombinant LCAT as the source of enzyme. Enzyme stock was prepared as described in Section 2.4.7.2; conditioned medium (recombinant LCAT) was collected from confluent CHOHis6-LCAT cells 24 h after the incubation of cells with serum-free Iscove's modified DMEM medium. Media were briefly centrifuged and concentrated 100 X. Esterified cholesterol was expressed as a % of radiolabelled cholesteryl ester (CE) compared to the total radiolabelled CE plus unesterified cholesterol (UC). Average percentage cholesterol esterification values $\pm$ S.D from triplicate wells were calculated and plotted versus time. The difference between the means of the control and recombinant cells was assessed by Student's t-test (see text).*

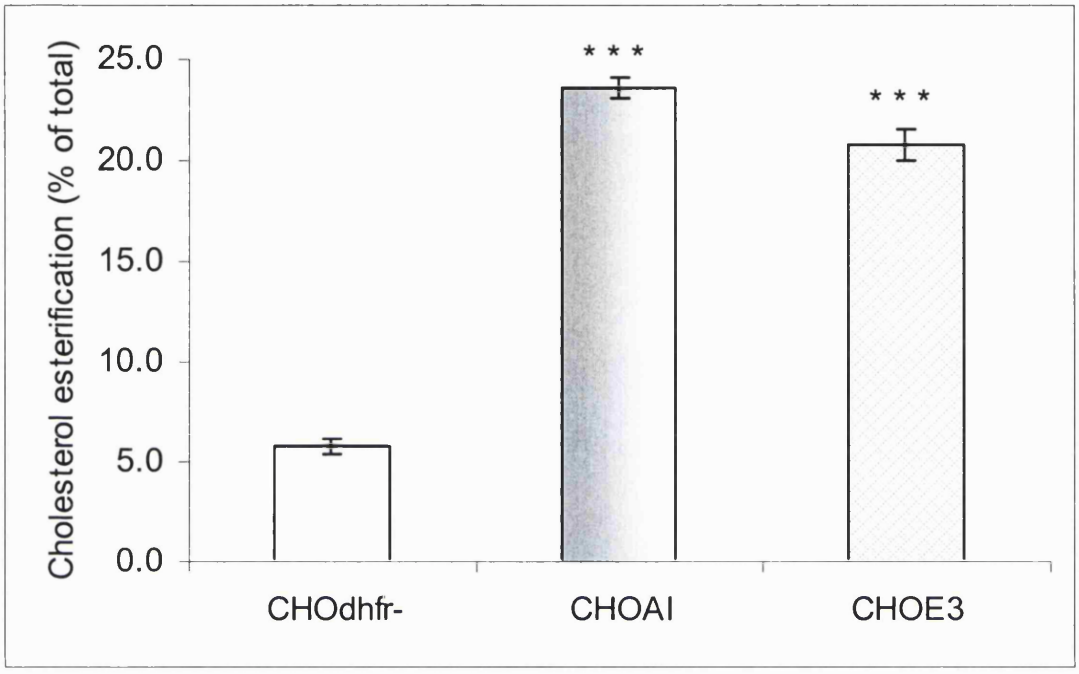

Figure 4.20 Conditioned medium from CHOAI cells stimulates LCAT activation to a higher extent compared to that of CHOE3 cells. *Medium was collected from confluent CHOE3, CHOAI and CHOdhfr- control cells 24 h after the incubation of cells with serum-free Iscove's medium. Media were prepared as described in Section 2.4.4.1 and used for LCAT activity experiment after 1 h incubation (Section 2.4.7.3) using labelled cholesterol/albumin emulsion (Section 2.4.7.1) and stock recombinant LCAT (Section 2.4.7.2). Esterified cholesterol was expressed as a % of radiolabelled cholesteryl ester (CE) compared to the total radiolabelled CE plus unesterified cholesterol (UC). Average percentage cholesterol esterification values $\pm$ S.D from quardruplicate wells were calculated. The difference between the means of the control and recombinant cells was assessed by Student's t-test (***$P < 0.001$).*

4.3 Discussion

4.3.1 PHYSICAL CHARACTERIZATION OF CHO CELL-DERIVED APOE3- AND APOAI-CONTAINING PARTICLES

The first part of this chapter described work undertaken to generate stably-transfected CHO cells secreting human apoAI. Firstly, a mutation in the human apoAI sequence in pcDNA3.1.AI was corrected and the sequence was transferred to another expression vector (p7055) that was used previously in our laboratory for generating recombinant CHOE3 cells. The generated p7055.AI vector was subsequently used to transfect CHOdhfr- cells. As a consequence, the apoE3 and apoAI proteins studied in this chapter were generated from recombinant CHO cells following similar procedures and this should enable a reasonable comparison of their biological functions.

Some eukaryotic proteins have been expressed efficiently in prokaryotic hosts. However, proteins synthesized in bacteria exhibit low biological activities due to incorrect folding and post-translational modifications, including no glycosylation (Grabenhorst E *et al*, 1999). To overcome these hurdles, mammalian cell expression systems such as CHO and COS cells have been developed (Levinson AD *et al*, 1990; Weikert S *et al*, 1999). In addition, CHO cells adapt easily to growth in the absence of serum and can grow as adherent cells or in suspension (Kim EJ *et al*, 1998). CHOdhfr- cells have been described by Urlaub and Chasin (Urlaub G *et al*, 1980) and they have been employed for expressing various therapeutic human proteins (Baez JM *et al*, 2002; Laitinen S *et al*, 2002). There are a number of successful reports of recombinant apoAI (Lindholm EM *et al*, 1998; Schmidt HH *et al*, 1997; Bielicki JK *et al*, 1997) and apoE (Ye SQ *et al*, 1993; Choi SY *et al*, 1994; Yang DS *et al*, 1997) expression in CHO cells.

ELISA was the preferred method for accurate quantification of secreted apoAI. However, as described in *Chapter* 3, the development of a functional ELISA for this protein proved unsuccessful. Consequently, a more time-consuming methodology was employed, namely immunoblotting followed by scanning densitometry to determine the level of CHO cell-derived apoAI. This has been utilised by other researchers for quantification of apoAI (Haghpassand M *et al*, 1995), apoE (Dean B *et al*, 2003), and other proteins (Kimura N *et al*, 2003; Szymanski PT *et al*, 2002). This technique demonstrated that the recombinant cells secrete 9.8 $\pm$ 0.19 μg apoAI/mg protein/24 h. Literature has reports of recombinant apoAI secretion from stably-transfected CHO cells,

but they cannot be easily compared with our production as the units of apoAI concentration are not the same. For instance Schmidt and co-workers achieved 20-30 μg/ml of cultured medium of apoAI, while Brissette *et al* reported a concentration of 0.5 μg/ml medium/48 h (Schmidt HH *et al*, 1997; Brissette L *et al*, 1991). ApoE3 production (by our CHOE3 cell line) of 12.3 ± 0.17 μg/mg protein/24 h was confirmed by ELISA (*Chapter* 3). This is about 9-12 times higher than apoE secreted (1.4 μg/mg protein/24 h or 1 μg/mg protein/24 h) by stably-transfected J774 macrophage cells from two different studies (Mabile L *et al*, 2003; Lin CY *et al*, 1999). However, the apoE secreted in media from the cells used in this thesis is about half of that (1.25 μg/mg protein/h) reported by Choi *et al* from recombinant CHO cells (Choi SY *et al*, 1994).

ApoAI cDNA was inserted into recombinant CHO cells as described in *Section* 4.2.1, leading to synthesis and secretion of apoAI protein. If that continuous cell line had not been cloned, there was a risk of loosing the inserted DNA (possibly due to mutations) as cells without the insert would have become preferentially cultured, eventually leading to an absence of the DNA insert from the progeny (Ferrero RL *et al*, 1993). As a consequence, cloning, a process whereby single cells are isolated in culture, was carried out. These cells were subsequently propagated into a population of identical cells. Cloned cells are advantageous due to minimal genetic diversity. To ensure that true clones were isolated, sub-cloning was also carried out during the production of CHOAI cells in this project. It is essential to assay selected sub-clones for existence of inserted DNA and presence of the corresponding protein in the cultured medium. These can be readily achieved by Western blotting analysis, which in the present study confirmed the continual secretion of apoAI in the medium even when the chosen sub-clone was subjected to freeze-thaw studies. As a consequence, the selection process was not sequential and, thus, was achieved in one step. Furthermore, amplification with MTX (an anti-proliferative agent) was carried out on chosen clones as will be discussed in *Section* 6.2.

With regard to physical characterizations, our recombinant apoE3- and apoAI-containing particles are heterogeneous as shown by electrophoretic characterization. In addition, the NDGGE gels demonstrated that both particles have major bands less than 10 nm, which may indicate a discoidal structure (De Pauw M *et al*, 1995). It remains to be seen if collecting media at different time points and performing NDGGE will produce a pattern of apolipoproteins from lipid-free and lipid-poor, to lipid-rich particles.

4.3.2 CHO CELL-DERIVED APOE3- AND APOAI-CONTAINING PARTICLES ARE BIOLOGICALLY ACTIVE

Serum-free conditioned media were used throughout the experiments in this chapter. The absence of FBS in the media ensured that the secreted apolipoproteins did not bind to HDL particles, which are the predominant lipoprotein class in FBS. Indeed, apoE2 (an isoform of apoE) interacts preferentially with HDL in FBS (Weisgraber KH, 1990). ApoE conformation is dependent on its lipid environment, which can influence the helical content and ordering of apoE (Weisgraber KH, 1994b) and affect its biological activities. The state of lipidation of apoAI influences its ability to mediate cellular cholesterol efflux (Phillips MC *et al*, 1998). Lipid-free or lipid-poor apoAI induces cholesterol efflux via a membrane-microsolublization process, whereas lipid-rich apoAI (found in mature HDL_2 and HDL_3) removes cholesterol from cells by the aqueous diffusion mechanism (Phillips MC *et al*, 1998).

The apoE3- and apoAI-containing particles used for all experiments in this chapter were not subjected to purification procedures. The inherent characteristics of newly-synthesized apolipoproteins may contribute highly to their biological activity. Various purification procedures (e.g. ultracentrifugation or delipidation) might alter the oxidation state of apolipoproteins and affect their endogenous conformation (LaDu MJ *et al*, 1995). ApoE secreted from recombinant cells has been demonstrated to have biological activities similar to that of native apoE (Lin CY *et al*, 1998). Thus, the use of unpurified apoE-containing particles in the present study, which have minimal conformational alterations (La Du MJ *et al*, 1995), is a more physiological way of studying the effects of apoE. Therefore, results showing sequestering of cholesterol from labelled THP-1 macrophages by apoE3- and apoAI-containing particles at a low concentration (~6 μg/ml) were interesting. The dosage of apoE3 used is similar to the levels of apoE in circulation (~10% of total plasma apoE) that is primarily contributed by macrophages (Boisvert WA *et al*, 1995; Linton MF *et al*, 1995). CHO cell-derived apoAI (13.8 $\pm$ 1.46% efflux) also facilitated cholesterol efflux with no significant difference from that of newly-synthesized apoE3-containing particles (9.13 $\pm$ 0.51% efflux). Time permitting, it would have been interesting to study the effect of endogenously secreted apoE3 in sequestering cellular pools of cholesterol, which is discussed in *Section* 6.2.

Human monocyte-macrophages (Basu SK *et al*, 1982) and HepG2 cells (Zannis VI *et al*, 1981), both secrete functionally active apoE that contains excess residues of sialic acid on its carbohydrate chain when compared with plasma apoE. Similarly, apoE derived from astrocytes in brain has a higher level of sialylation (Pitas RE *et al*, 1987). In addition, recombinant CHO cells are unable to glycosylate their secreted proteins (Jenkins N *et al*, 1994), but they can synthesize multiple sialylated forms of apoE (Wernette-Hammond ME *et al*, 1989). Further investigations are required in order to test if the degree of sialylation is essential for the effect of our recombinant apoE3-containing particles in promoting cholesterol efflux and activating LCAT. One way to achieve this would be to compare the effect of particles secreted from CHOE3 cells with that synthesized by CHOldlD cells, which do not sialylate secreted proteins (Zanni EE *et al*, 1989). Alcohol-mediated desialylation of apoE in peritoneal macrophages of rats, impaired apoE binding to HDL and, thus, resulted in a defective RCT (Ghosh P *et al*, 2000).

Basu *et al* reported that apoE and cholesterol secretion from macrophages occur via independent pathways (Basu SK et al, 1983). Cholesterol efflux from cultured mouse macrophages is promoted by apoE, and a similar effect is exerted by exogenous apoE and apoAI. In fact, human apoE associates with α-migrating HDL and increases its capacity to accept more cholesterol. Based on the results explained in this chapter, stimulation of conditioned media from recombinant CHOE3 and CHOAI cells with HDL-plasma increased the ability of newly-secreted particles in sequestering cellular cholesterol by 116.2% and 102.3%, respectively. However, there was still no significant differences between the ability of particles in effluxing labelled cholesterol from macrophages. Cholesterol efflux from macrophages is dependent on apoE even though it can be performed in the absence of exogenously added cholesterol acceptors such as apoAI or discoidal HDL (Zhang WY *et al*, 1996). ApoAI may act as an extracellular cholesterol acceptor and induce macrophage apoE secretion and cholesterol efflux. Exposure of macrophages from wild-type mice to lipid-free or lipid-poor apoAI increases their apoE production (Rees D *et al*, 1999). In addition, apoE and apoAI can have concerted anti-atherogenic effects as demonstrated by *in vitro* studies in the arterial wall (Benoit P *et al*, 1999). *In vivo* studies by Boisvert *et al*, confirmed that apoE and apoAI-containing HDL protect the vessel wall from hypercholesterolaemic effects (Boisvert WA *et al*, 1999).

ApoAI-containing particles from recombinant CHOAI cells had the capacity to activate recombinant LCAT in experiments presented in this chapter. Indeed, the main physiological activator of LCAT is apoAI (Fielding CJ *et al*, 1995). ApoAI activation of LCAT depends directly upon the binding of apoAI to the lipid surface (Chung J *et al*, 1979). In addition, it was demonstrated that small HDL particles (HDL_{3bc}) (*Section* 1.2.3.1) and apoAI-phospholipid discs have the most active surface configuration for cholesterol esterification by LCAT (Barter PJ *et al*, 1985; Sparks DL *et al*, 1999), while large HDL (HDL_{2b}) molecules might inhibit the enzymatic reaction (Karpe F *et al*, 1990). In addition to apoAI, other apolipoproteins such as apoE can also activate LCAT *in vitro* even though to a lesser extent (Jonas A, 1991). Indeed from our experience, recombinant LCAT was activated by conditioned medium from CHOE3 (20.8 $\pm$ 0.79% esterification) to a significantly lower extent than that from CHOAI cells (23.6 + 0.57% esterification) at 1 h time point.

To summarize, recombinant CHOAI cells that secrete bioactive apoAI were produced. This cell line was used as a positive control for physical and biological characterization of CHO cell-derived apoE3 particles. Both recombinant particles were shown to have heterogeneous mobility on agarose gel. Furthermore, the unpurified newly-secreted particles were biologically active as they promoted cholesterol efflux from [^{3}H]–cholesterol labelled macrophages and activated recombinant LCAT *in vitro*.

Chapter 5

5. THE FEASIBILITY OF CHIMERAPLASTY TO PERMANENTLY CONVERT THE *APOE3* GENE TO *APOE2* OR *APOE4* IN HUMAN LIVER AND MACROPHAGE CELLS

5.1 Introduction

Over the last decade a variety of gene therapy strategies have been developed based on our understanding of the genetic basis of disease and the endogenous DNA repair machinery. A commonly used approach among conventional strategies involves correcting the phenotype by the addition of a functional gene. A wide range of viral vectors have been studied for gene addition with a range of limitations (Kay MA *et al*, 2001) (*Section* 1.5.3). Another approach is based on homologous recombination and is known as targeted gene repair, which can potentially be achieved by a number of methods, each associated with its own advantages and limitations (Kmiec EB, 1999) (*Section* 1.5.5 and 1.5.6).

In our laboratory, we have been exploiting the radical new technology of chimeraplasty-mediated gene repair (*Section* 1.5.6), to develop realistic gene therapeutic strategies with the potential to regress atherosclerotic plaques and, hence, treat pre-existing arterial disease. Tagalakis *et al* reported that synthetic RNA-DNA oligonucleotides (RDOs or chimeraplasts) could achieve ~30% conversion of *APOE2*, the gene associated with recessive hyperlipidaemia, to *APOE3* in CHO cells expressing human apoE2 (CHOE2) (Tagalakis AD *et al*, 2001).

This chapter describes investigations into the feasibility of chimeraplasty for targeting the *APOE3* gene in HepG2 (hepatoblastoma) and THP-1 (monocyte-macrophages) cells in order to produce new homozygous cell lines secreting apoE2 and apoE4. If successful, these cells will be invaluable resources to compare the isoform dependency of the biological functions of liver-derived and macrophage-derived apoE particles. An additional aim was to compare the relative efficiency of chimeraplasts or RNA-DNA oligonucleotides (RDOs) in mediating gene conversion to that of SSOs (single-stranded oligonucleotides), which has the potential to be a better alternative for gene repair due to ease of its synthesis and purification.

5.2 Results

5.2.1 APOE GENOTYPING OF CELL LINES

The ultimate aim was to target the *APOE3* gene in HepG2 and THP-1 cells. However, the chimeraplasty experiments were initially tried on HEK-293 (human embryonic kidney) cells, which are known to be easy to transfect (previously tested in our laboratory), and recombinant CHOE3 cells. HEK-293, HepG2, and THP-1 cells were available from homozygous apoE3 donors. ApoE genotyping was performed on these cell lines in order to confirm their genotype using recombinant CHOE3 and CHOE2 cells as positive controls for the genotyping procedure. DNA was extracted from one confluent well of a 6-well plate (~ $5x10^6$ cells/well) using the method described in *Section* 2.5.4.1. PCR-RFLP analysis was followed as described in *Section* 2.5.4.2. The final result is shown in *Figure* 5.1, which confirmed that all the three cell lines were derived from apoE3 homozygous donors.

5.2.2 TRANSFECTIONS WITH APOE3-TO-APOE2 RDO1

5.2.2.1 Preliminary Experiment to Choose the Best Delivery Reagent

CHOE2 cells, a cell line that our laboratory has successfully targeted previously using an apoE2-to-apoE3 RDO, were used in a preliminary transfection in order to choose the best delivery vehicle for subsequent experiments. This cell line was transfected (*Section* 2.5.2.1) with the apoE2-to-apoE3 RDO (400 nM) complexed with linear-polyethylenimine (L-PEI) or LipofectAMINE™ or Superfect (*Section* 2.5.2). It was concluded that L-PEI was the best reagent since it was only with this vehicle that an *APOE2* to *APOE3* conversion was detected (appearance of the diagnostic 48 bp band and loss of intensity of the 83 bp band in cells treated with L-PEI compared to untreated CHOE2 cells as shown in *Figure* 5.2). In addition, CHOE3 cells were transfected with L-PEI in the same experiment following the same conditions used for treated CHOE2 cells. There was no gene conversion in treated CHOE3 cells indicating that the RDO molecule was functional in a specific manner.

5.2.2.2 Initial Transfections in HEK-293 & CHOE3 Cells

The first batch of apoE3-to-apoE2 RDO (RDO1) from MWG (Table 2.9) was initially tested in HEK-293 and recombinant CHOE3. The cells were plated in 12-well plates to reach 50-70% confluency the next day. After 24 h, a transfection mix was prepared (*Section* 2.5.2.1) by mixing 400 nM of the apoE3-to-apoE2 RDO1 with L-PEI at a nitrogen to phosphate ratio

(N:P) of 5:1, and 150 mM NaCl. The transfection mix was incubated for 10 min at room temperature and added to the cells. After incubation for 6 h, the cells were washed twice with PBS and 1 ml pre-warmed maintenance medium (Table 2.4) was added to each well. Cells were harvested after 48 h and DNA was extracted as described in *Section* 2.5.4.1. PCR-RFLP analysis was carried out as before (Section 2.5.4.2). The appearance of the 83 bp band in the treated samples as shown in *Figure* 5.3 (Panels A and B) was a clear indication of *APOE3* to *APOE2* conversions in both HEK-293 and CHOE3 cells at 400 nM RDO concentration. However, the percentage of conversion was higher in CHOE3 (22.4%) compared to HEK-293 (5.6%) cells as calculated by densitometric analysis. The results of this experiment revealed that the RDO1 molecule is functional and, furthermore, that it may be possible to obtain the desired *APOE* gene conversion in HepG2 cells. Consequently, transfections with RDO1 in HepG2 cells were subsequently carried out as described in the next section.

5.2.2.3 Transfections in HepG2 Cells

In contrast to the above success in HEK-293 and CHOE3 cells, a preliminary transfection of HepG2 cells under the same conditions showed no conversion (data not shown). This failure might have been related to inability of the transfection complex to reach the nucleus without prior lysosomal degradation or poor entry of the complex into the cells, which might be related to L-PEI not being the best vehicle for RDO1 delivery in human hepatoma cells. As a consequence, it was decided to improve the efficiency of transfection by the following three methods:

1) Microinjection of the RDO1 molecule without a carrier directly into the nucleus to ensure that the intact oligonucleotide reaches the nucleus of HepG2 cells and thus, be able to assess the functionality of this chimeraplast in liver cells.
2) Centrifugation of the 12-well plate after addition of the transfection mix in order to improve contact between cells and the transfection complex and hence, aid the successful entry of the RDO1 into the cells. This might lead to successful conversions in HepG2 cells.
3) Use of branched PEI (B-PEI) and melittin-PEI (Mel-PEI) as alternative delivery vehicles and their comparison with L-PEI that was shown not to be efficient in

introducing the desired point mutation in HepG2 cells when the standard protocol was carried out as previously described (*Section* 5.2.2.2).

Results obtained from all the above are explained in the following sections.

5.2.2.4 Microinjection of RDO1 in HepG2 cells

Microinjection was carried out to ensure that if the RDO1 molecule was active it would generate the desired gene conversion once it has reached the nucleus of HepG2 cells. CHOE3 cells were used as a positive control since previous transfection with RDO1 proved successful in this cell line (Section 5.2.2.2). One coverslip of CHOE3 cells and three coverslips of HepG2 cells were prepared in order to microinject about 100-120 cells per coverslip with RDO1 as described in *Section* 2.5.3. HepG2 cells were more difficult to microinject, as they tended to grow on top of each other instead of forming a monolayer. Post-injection, the cells were grown on coverslips in a 12-well plate and transferred to wells of a 24-well plate prior to analysis by PCR-RFLP (*Section* 2.5.4.2). Results (*Figure* 5.4) indicated a modest conversion in HepG2 cells (~5.8% of the total microinjected cells) whereas CHOE3 cells showed ~20% conversion (of the total microinjected cells) as quantified by densitometry. Conversions are shown in *Figure* 5.4 by the appearance of the diagnostic 83 bp bands in the treated cells.

5.2.2.5 Centrifugation of Plates for HepG2 Transfections

Transfections were carried out in order to see whether the addition of a centrifugation step will improve transfection efficiency in HepG2 cells as compared to the standard protocol without any centrifugation. HepG2 cells were plated in two 12-well plates (one well of cells/plate) such that they reached 50-70% confluency the next day. The following day, the transfection mix was prepared as before (*Section* 2.5.2.1) using 400 nM of the RDO1. Transfection conditions were as described previously for one of the plates, but the second plate was centrifuged for 3 min at 400 x *g* after the addition of the transfection mix. This improved protocol (an additional centrifugation step added to the standard protocol) resulted in some conversion in HepG2 cells as compared to the cells where the plate was not centrifuged (*Figure* 5.5). The conversion is shown in *Figure* 5.5 by the appearance of the diagnostic 83 bp band.

5.2.2.6 Use of B-PEI and Mel-PEI for HepG2 Transfections

The aim of this experiment was to compare the effect of B-PEI and Mel-PEI (*Section* 2.5.2) with that of L-PEI on HepG2 transfections using the improved protocol described in *Section* 5.2.2.5. HepG2 cells were plated in two 12-well plates so that they would reach 50-70% confluency the next day. The following day, plate one was used for transfections with a pcDNA3 plasmid encoding the green fluorescent protein (pGFP), while plate two was used for transfections with RDO1. pGFP was used as a positive control to test the efficiency of transfections with each of the named delivery reagents (L-PEI, B-PEI, and Mel-PEI). For plate one, the transfection mix was prepared for each of the individual transfer reagents as described in *Section* 2.5.2.1, but using 1 μg of pGFP instead of RDO1. After adding each transfection mix to the appropriate well, the plate was centrifuged as before. Twenty-four hours following transfection, the cells were observed using phase-contrast microscopy and fluorescent microscopy with the excitation light of wavelength 465-495 nm (*Figure* 5.6, Panels A and B, respectively). In each case some of the cells fluoresced green compared to control cells (received pGFP alone) that showed no fluorescence (data not shown), indicating that L-PEI, B-PEI and Mel-PEI all aided in successful transfections of HepG2 with pGFP. L-PEI demonstrated the highest percentage of cells fluorescing green at ~30%, Mel-PEI displayed ~25%, and B-PEI demonstrated ~2%. Consequently, L-PEI was the best transfection reagent when compared to Mel-PEI and B-PEI. With regard to the second plate of HepG2 cells, the transfection mix was prepared (*Section*s 2.5.2.1 and 2.5.2.2) using each delivery vehicle with 400 nM of RDO1 at a 5: 1 molar ratio of nitrogen atoms in the delivery vehicle to phosphates in the oligonucleotide (N:P ratio) (Table 2.11). In the case of L-PEI, the RDO was also used at 1000 nM. PCR-RFLP analysis (*Figure* 5.6, Panel C) indicated a greater percentage of *APOE3* to *APOE2* conversion when 400 nM of RDO1 was complexed with L-PEI (18.1%) as compared to Mel-PEI (12%) or B-PEI (5.8%). Therefore, it was decided to use L-PEI combined with a centrifugation step (improved protocol) for subsequent HepG2 transfections with RDO1.

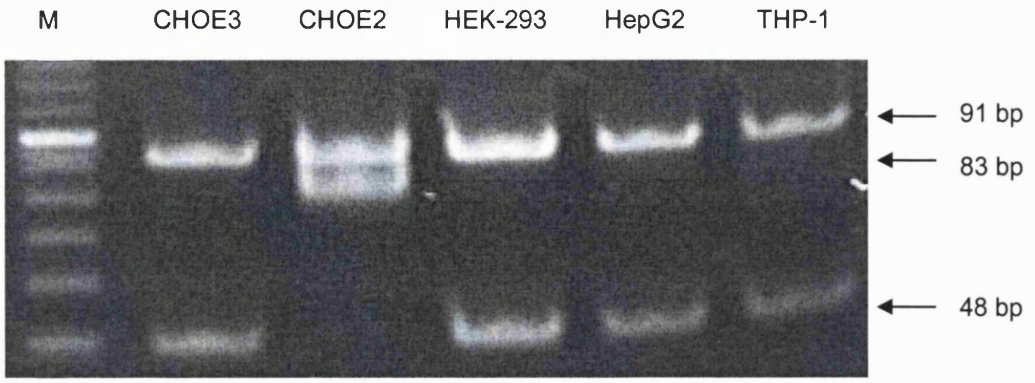

Figure 5.1 ApoE genotyping of HEK-293, HepG2, and THP-1 cells. *HEK-293, HepG2, and THP-1 cells were collected from a confluent well of a 6-well plate. DNA was extracted and analysis was carried out by PCR-RFLP (Section 2.5.4). CHOE3 and CHOE2 cells (previously genotyped in our laboratory) were treated in the same way and used as positive controls for the genotyping protocol. The final digestion products were separated using a 20% TBE gel. M = 10 bp ladder. The diagnostic 91 bp and 48 bp bands confirmed that HEK-293, HepG2, and THP-1 cells were derived from apoE3 homozygous donors.*

Figure 5.2 L-PEI is the best delivery reagent compared to Superfect and LipofectAMINE™. *CHOE2 cells were treated with 400 nM of an apoE2-to-apoE3 RDO mixed with Superfect (SU), LipofectAMINE™ (LI) or linear-PEI (L-PEI). CHOE3 cells were treated with L-PEI following the same protocol and thus were used as a negative control for the transfection protocol. Forty eight hours post-transfection, cells were harvested and their DNA was extracted (Section 2.5.4.1). PCR-RFLP analysis (Section 2.5.4.2) was carried out and the CfoI digestion products were separated using 20 % TBE gels. M = 10 bp ladder. L-PEI was the best vehicle for converting APOE2 to APOE3 as shown by the appearance of the diagnostic 48 bp band and loss of intensity of the 83 bp band.*

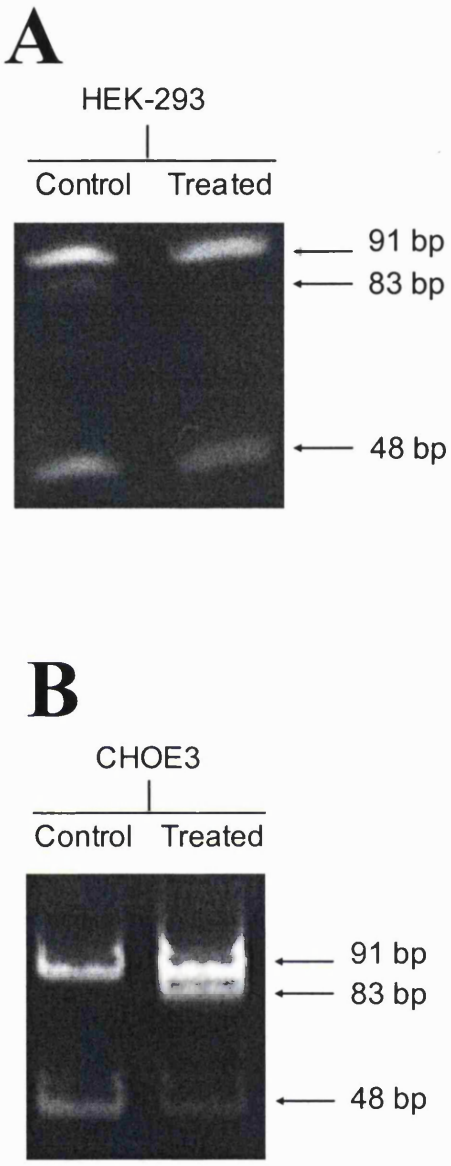

Figure 5.3 Successful *APOE3* gene conversion in HEK-293 and CHOE3 cells treated with apoE3-to-apoE2 RDO1. *HEK-293 cells **(Panel A)** and CHOE3 cells **(Panel B)** were treated with 400 nM of apoE3-to-apoE2 RDO1 mixed with L-PEI at a N:P ratio of 5:1. In each case, DNA extraction followed by PCR-RFLP analysis (Section 2.5.4) was carried out and the CfoI digestion products were separated using 20 % TBE gels. The appearance of the 83 bp bands in the treated cells was a clear indication of APOE3 to APOE2 conversion in both HEK-293 (22.4% conversion) and CHOE3 (5.6% conversion) cells.*

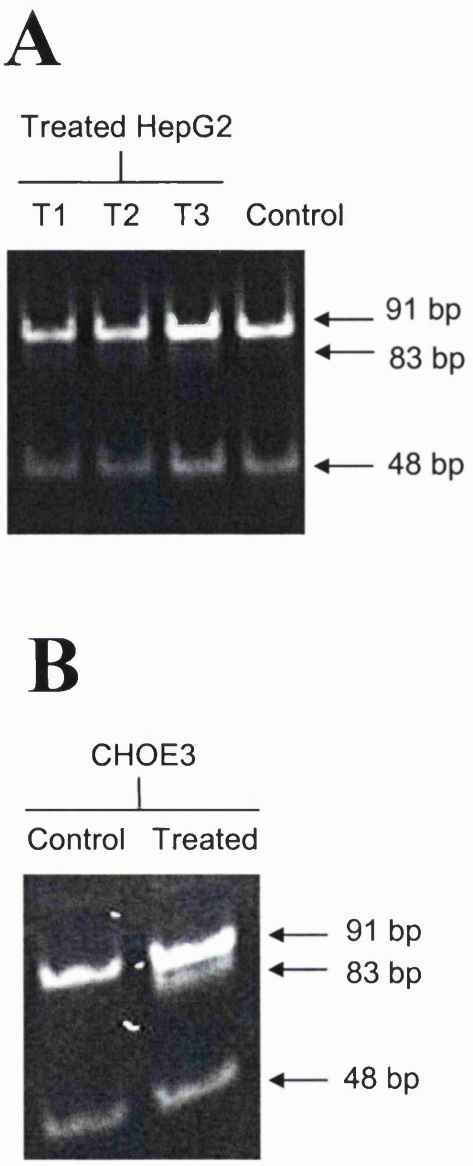

Figure 5.4 Successful *APOE3* gene conversion in HepG2 and CHOE3 cells after microinjection with apoE3-to-apoE2 RDO1. *One coverslip of CHOE3 cells and three coverslips of HepG2 cells were prepared as described in Section 2.5.3. RDO1 was microinjected directly into the nucleus of about 100-120 cells per cover slip (Section 2.5.3). The cells were grown on cover slips for 6 days before being transferred to wells of a 24-well plate. They were then kept growing for another 10 days prior to DNA extraction followed by PCR-RFLP analysis (Section 2.5.4). The final CfoI digestion products of microinjected HepG2* ***(Panel A)*** *and CHOE3* ***(Panel B)*** *cells were separated using 20 % TBE gels. In Panel A, the three preparations of microinjected HepG2 cells are indicated by T1, T2 and T3. Appearance of the diagnostic 83 bp bands indicated successful APOE3 to APOE2 conversions in HepG2 (average of 5.8% conversion) and CHOE3 (20% conversion) cells.*

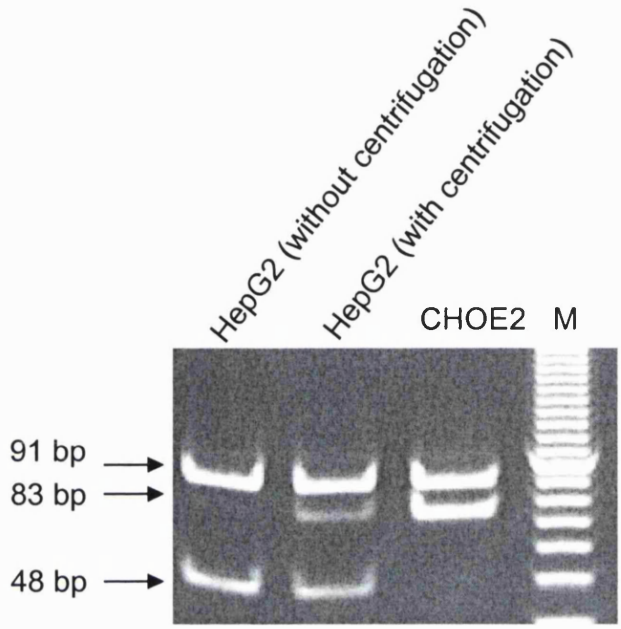

Figure 5.5 ***APOE3*** **gene conversion in HepG2 cells treated with apoE3-to-apoE2 RDO1 is achieved by addition of a centrifugation step.** *HepG2 cells were plated in two 12-well plates (one well/plate) the day before transfection. The cells in both plates were treated with 400 nM apoE3-to-apoE2 RDO1 mixed with L-PEI at a N:P ratio of 5:1. For one plate, the transfection procedure was carried out as in Section 2.5.2.1, but for the other, method was slightly modified by centrifuging (3 min at 400 x g) the plate after addition of the transfection mix. In both cases, DNA extraction followed by PCR-RFLP analysis (Section 2.5.4) were carried out and the CfoI digestion products were separated on a 20 % TBE gel. CHOE2 cells were used as a positive control for the analysis steps. M = 10 bp ladder. Only HepG2 cells transfected with the addition of the centrifugation steps showed some conversion of APOE3 to APOE2 as indicated by the appearance of the diagnostic 83 bp band. Therefore, addition of a centrifugation step to the standard transfection protocol (Section 2.5.2.1) was essential for subsequent transfections of HepG2 cells with the RDO1 molecule.*

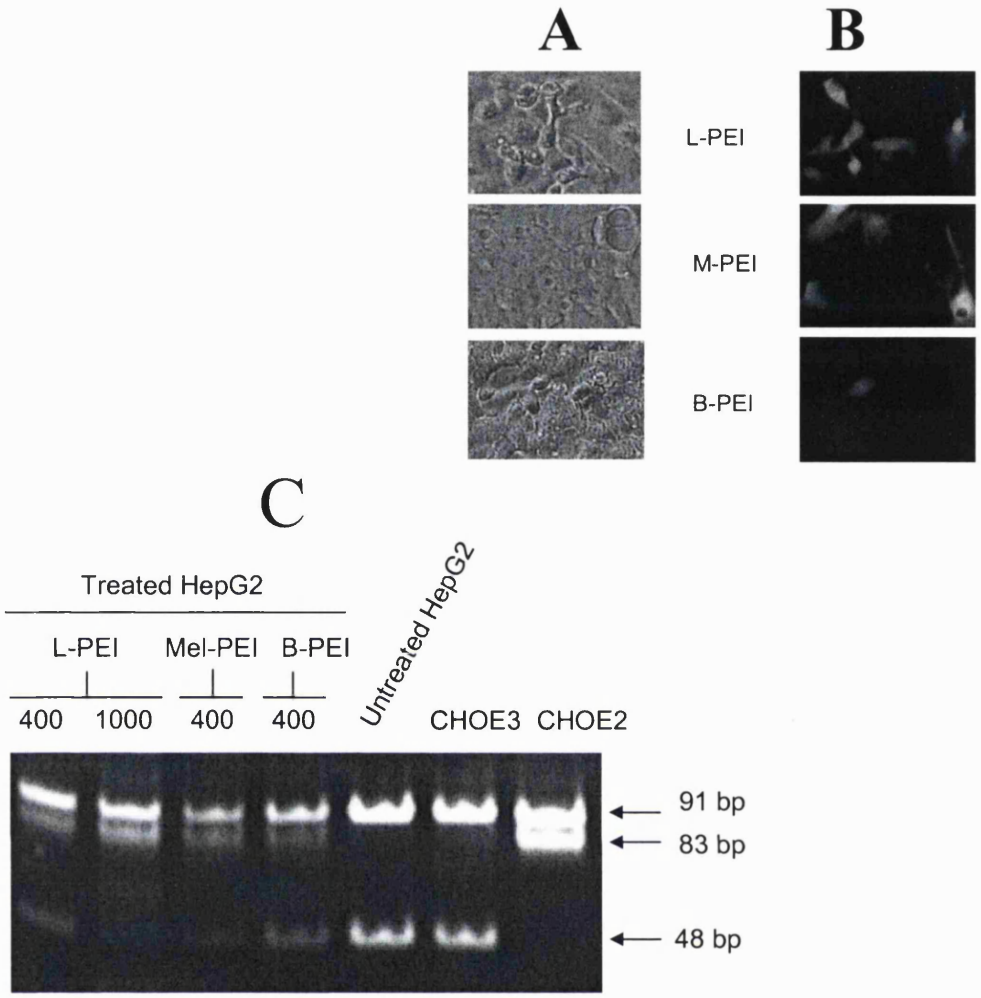

Figure 5.6 Comparing the efficiency of three different transfection vehicles (L-PEI, B-PEI, and Mel-PEI) in HepG2 cells using pGFP and apoE3-to-apoE2 RDO1. *HepG2 cells from a 12-well plate were transfected with 1 μg of the pGFP expression plasmid using linear-PEI (L-PEI), branched-PEI (B-PEI), or melittin-PEI (Mel-PEI) as described in text. The cells were observed 24 h post-transfection by phase-contrast microscopy* ***(Panel A)*** *and fluorescent microscopy, with incident blue light of 465-495 nm wavelength* ***(Panel B)****, both at 20 X magnification. Additional HepG2 cells (from a second 12-well plate) were treated with 400 nM RDO1 mixed with L-PEI, B-PEI, or Mel-PEI at a N:P ratio of 5:1 (Sections 2.5.2.1 and 2.5.2.2). In the case of L-PEI, RDO1 was also used at 1000 nM concentration. DNA from CHOE3 and CHOE2 cells were used as positive controls for the analysis steps. DNA extraction followed by PCR-RFLP analysis (Section 2.5.4) were carried out and the CfoI digestion products were separated on a 20 % TBE gel* ***(Panel C)****. Appearance of the diagnostic 83 bp band in cells treated with L-PEI, Mel-PEI, or B-PEI indicated successful APOE3 to APOE2 conversion. The highest percentage of conversion (at 400 nM RDO1) was, however, achieved by using L-PEI (18.1%) compared to Mel-PEI (12%) and B-PEI (5.8%). Thus, L-PEI was chosen for subsequent HepG2 transfections with the RDO1.*

5.2.2.7 Increasing the Concentration of RDO1 for HepG2 Transfections

RDO1 from MWG was used at a range of concentrations (200-1000 nM) in HepG2 transfections following the improved protocol described earlier (*Section* 5.2.2.6). PCR-RFLP analysis confirmed a clear conversion of *APOE3* gene to *APOE2* as indicated by the gain of 83 bp band and loss of intensity of 48 bp band in treated cells (*Figure* 5.7, Panels A). Scanning densitometry analysis confirmed a dose-dependent conversion starting with 4.2% for cells treated with 200 nM RDO1, increasing to 16.5% for cells treated with 400 nM RDO1, and finally reaching 30.7% conversion in cells treated with 1000 nM of the same chimeraplast (*Figure* 5.7, Panel A). Similar percentage of conversions of *APOE3* to *APOE2* were obtained from a second independent experiment for HepG2 cells as shown in *Figure* 5.7, Panel B (3.6% for 200 nM RDO1, 19.1% for 400 nM RDO1, and 33.4% for 1000 nM RDO1). In this experiment, CHOE2 cells (in a separate plate) were also treated with 400 nM RDO1 following the same protocol used for HepG2 cells. They were used as a negative control for the improved transfection protocol. *Figure* 5.7 (Panel B) showed that apoE3-to-apoE2 RDO1 was not functional in CHOE2 cells.

5.2.2.8 Sequencing of the Treated HepG2 Cells

Sequencing was performed for some of the HepG2 samples in which positive conversions to the *APOE2* gene were demonstrated. The PCR reaction for DNA samples analyzed in *Figure* 5.7, Panel B, was prepared using all the components in twice the stated volumes in *Section* 2.5.4.2. Half of each PCR product was used for *CfoI* digestion as described previously. The other half was run separately on a 1% agarose gel and the DNA was extracted from the gel as explained in *Section* 2.2.7.2, but in this case, the elution was carried out in about 12 µl instead of 30 µl of de-ionized water. The eluted PCR product with the addition of TF primer (*Section* 2.5.4.2) was sent for automated sequencing (*Section* 2.2.7). The sequencing chromatograms showed *APOE3* to *APOE2* (C → T) conversions in the treated samples indicated by a mixed population of blue (C) and red (T) peaks in the area of the circled bases (*Figure* 5.8, Panels A, B, and C) as compared to control cells that only had *APOE3* (blue peak in the area of the circled base as shown in *Figure* 5.8, Panel D). Moreover, as the RDO1 concentration was increased from 200 to 400 and finally 1000 nM, the relative size of the red peaks was enhanced. This might have indicated a step-wise

increase in the percentage of conversions, which was in agreement with the PCR-RFLP data of the same treated cells shown in *Figure* 5.7, Panel B.

5.2.2.9 Transfections in THP-1 Cells

THP-1 cells were seeded in a 12-well plate on the day of transfection. The normal transfection procedure (*Sections* 2.5.2.1 and 2.5.2.2) was carried out using L-PEI, B-PEI, Mel-PEI and mannose-PEI (Man-PEI) complexed with 400 nM apoE3-to-apoE2 RDO1 at a 5:1 ratio of N:P. In addition, a centrifugation step was also included (improved protocol for HepG2 cells, *Section* 5.2.2.6). No conversions were obtained (data not shown). As THP-1 cells have the mannose receptor, it was decided to use Man-PEI in another trial with a higher concentration (800 nM) of RDO1 and following the improved protocol that was deduced for HepG2 cells. Successful conversion (12.4%) was obtained by using Man-PEI as indicated by the appearance of the 83 bp band and a reduced intensity of the 48 bp band in treated THP-1 cells (*Figure* 5.9).

5.2.3 TRANSFECTIONS WITH APOE3-TO-APOE4 RDO

A single batch of an apoE3-to-apoE4 RDO was ordered from MWG (Table 2.11). HepG2 and THP-1 cells were treated with a range of concentrations (200-1000 nM) of this chimeraplast complexed with L-PEI, B-PEI, or Mel-PEI at a 1:5 ratio of P:N. In addition, Man-PEI was used for THP-1, and Gal4-PEI for HepG2 cells (Table 2.10) due to the presence of the mannose receptor and the asialoglycoprotein receptor (ASGPR) in these cell lines, respectively. All the transfections were accompanied by the centrifugation step. No obvious conversions of *APOE3* to *APOE4* were detected in either HepG2 or THP-1 cells (data not shown). In subsequent experiments for HepG2 cells, the RDO molecule (800 nM) was complexed with a 1:1 ratio of Gal4-PEI and L-PEI. This resulted in an *APOE3* to *APOE4* gene conversion indicated by the appearance of two extra bands (83 and 72 bp) in the treated cells compared to untreated HepG2 cells that were subjected to the same protocol except for the addition of the RDO molecule (*Figure* 5.10). For THP-1, however, no conversion of *APOE3* to *APOE4* was achieved even when a 1:1 ratio of Man-PEI and L-PEI were tested following the same procedure as for HepG2 cells (data not shown).

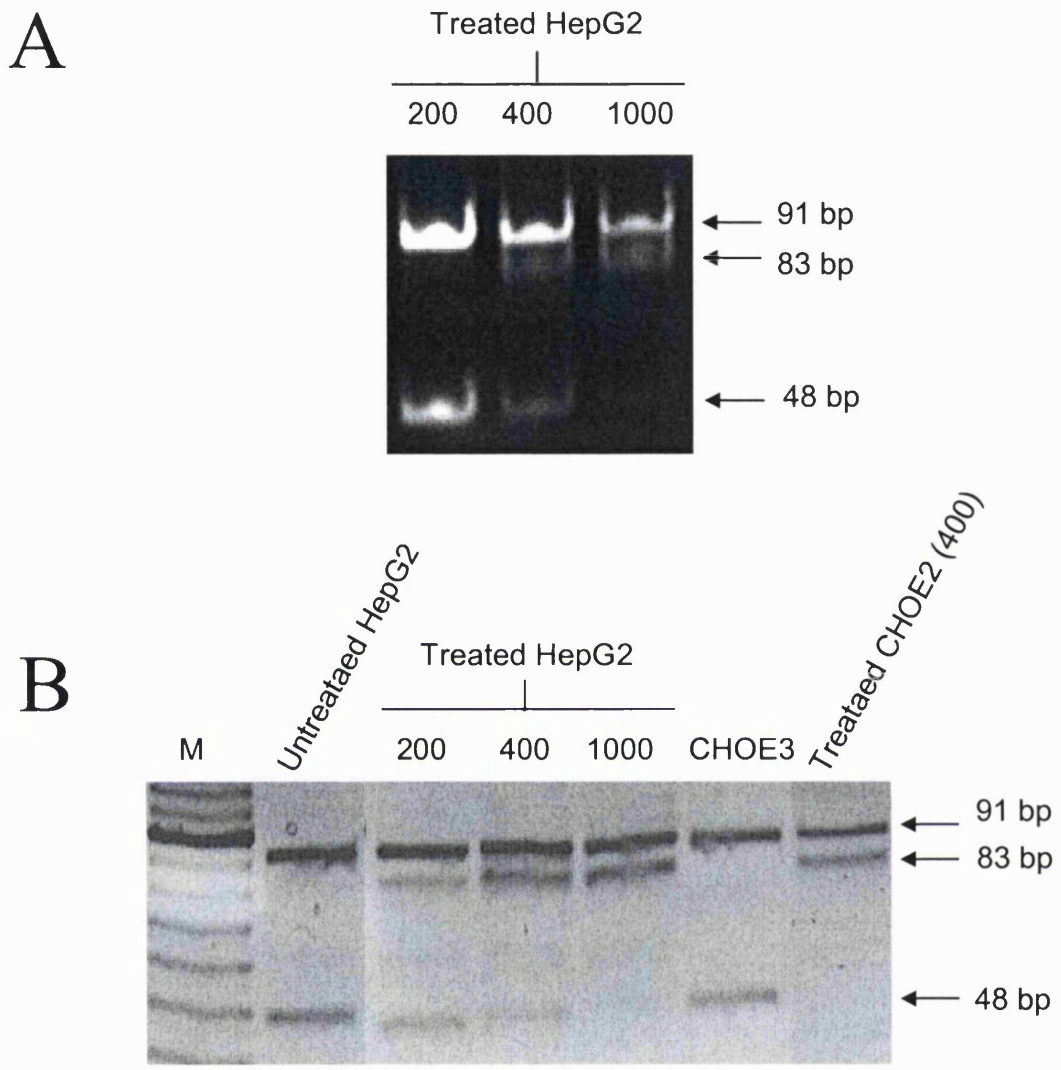

Figure 5.7 Dose-dependent *APOE3* to *APOE2* gene conversion in HepG2 cells. *Cells in two 12-well plate were transfected (Section 2.5.2.1) with a range of concentrations (200-1000 nM) of apoE3-to-apoE2 RDO1 complexed with L-PEI at a N:P ratio of 5:1. The plates were briefly centrifuged (improved protocol, Section 5.2.2.6) and PCR-RFLP analysis was carried out 48 h post-transfection. The final CfoI digest was separated on a 20 % TBE gel in* ***Panel A****, while a 4 % agarose gel (Section 2.5.4.2) was used in* ***Panel B****. Panles A and B refer to two independent experiments, both showing successful gene conversions in treated HepG2 cells indicated by the appearance of the 83 bp bands. Additionally, in Panel B, CHOE2 cells (in a separate plate) were targeted with 400 nM RDO1 following the same protocol as for HepG2 cells. CHOE2 cells were thus used as a negative control for the transfection protocol Moreover, DNA from CHOE3 cells was used as a positive control for the analysis steps. Untreated HepG2 cells were subjected to the same protocol used for treated cells except for the addition of the RDO1 molecule. M = 10 bp ladder.*

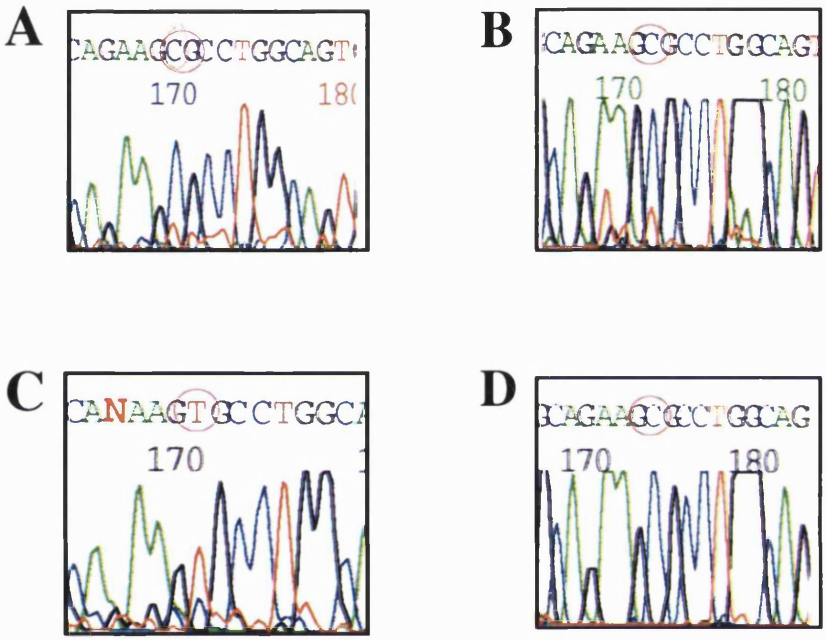

Figure 5.8 Direct sequencing of PCR products confirms *APOE3* to *APOE2* conversion in HepG2 cells. *PCR products from samples genotyped in Figure 5.7 (Panel B) were sent for automated sequencing (Babraham Institute, Cambridge). Mixed blue (C) and red (T) peaks in the region of circled base indicated the presence of both APOE3 and APOE2 in samples treated with 200, 400, and 1000 nM of RDO1 (**Panels A, B, & C** respectively). In addition, a gradual increase in the size of the red peaks was evident by increasing the RDO1 concentration possibly indicating an enhanced % of gene conversion. Sequence of control cells (only blue peak in the area of circled base) is shown in **Panel D**. These results confirmed a dose-dependent conversion of APOE3 to APOE2 (C → T) in HepG2 cells, which was in agreement with the PCR-RFLP data of the same treated cells (Figure 5.7, Panel B).*

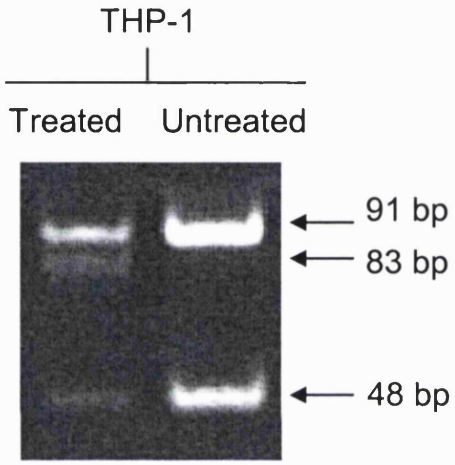

Figure 5.9 Successful *APOE3* gene conversion in THP-1 cells treated with apoE3-to-apoE2 RDO1 complexed with Man-PEI. *The transfection mix was prepared as described in Section 2.5.2.2, using Man-PEI and 800 nM of the chimeraplast at a 5:1 ratio of N:P. Cells were seeded in a 12-well plate on the day of transfection and the plate was centrifuged (improved protocol, Section 5.2.2.6) for 3 min at 400 x* g *after the addition of the transfection mix. Forty eight hours post-transfection, DNA extraction followed by PCR-RFLP analysis (Section 2.5.4) were carried out as shown by separating the final CfoI digests on a 20 % TBE gel. Successful conversion (12.4%) was indicated in treated cells by the appearance of the 83 bp band. Untreated cells were subjected to the same protocol used for treated cells except for the addition of the RDO1 molecule.*

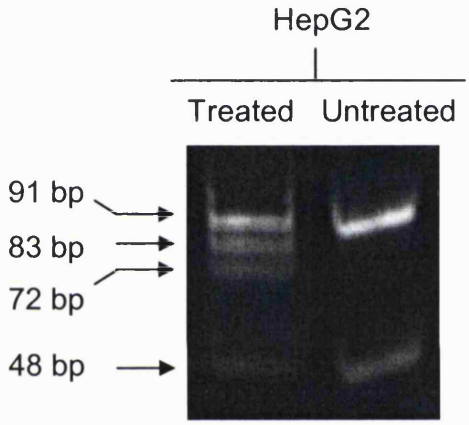

Figure 5.10 Successful *APOE3* to *APOE4* gene conversion in HepG2 cells treated with apoE3-to-apoE4 RDO complexed with Gal4-PEI & L-PEI. *The transfection mix was prepared as described in Section 2.5.2.2 using Gal4-PEI & L-PEI (1:1) and 800 nM of the apoE3-to-apoE4 RDO at a 5:1 ratio of N:P. The 12-well plate containing cells and the transfection mixture was centrifuged for 3 min at 400 x* g. *Forty eight hours post-transfection, the cells were analyzed by DNA extraction followed by PCR-RFLP (Section 2.5.4). The final CfoI digests were separated on a 20 % TBE gel. Successful APOE3 to APOE4 conversion was indicated by the presence of two extra bands (83 bp and 72 bp) in the treated cells compared to the untreated cells that were subjected to the same protocol except for the addition of the RDO molecule.*

5.2.4 CLONING OF RDO-TREATED HepG2 AND THP-1 CELLS

Some of the HepG2 and THP-1 cells that were successfully treated with RDO1 (*Figures* 5.7 and 5.9) were kept growing after half of the cells were harvested for analysis (48 h post-transfection). These cells were passaged four times until they were confluent in a 75 cm^2 flask. In order to start cloning of all the cells at the same time under similar experimental conditions, the treated cells were cryopreserved until transfections with the apoE3-to-apoE4 RDO were completed. Once it was confirmed that this RDO was functional, although only in HepG2 cells (*Figure* 5.10), the treated HepG2 cells also underwent four passages in culture and cryopreserved. After one week, one vial of each cell line (two sets of HepG2 cells treated with 1000 nM or 400 nM RDO1, THP-1 treated with 800 nM RDO1, and HepG2 treated with 800 nM apoE3-to-apoE4 RDO) was thawed out followed by cloning of the cells as described in *Section* 2.5.5. Fifty clones of each cell line were analyzed by DNA extraction followed by PCR-RFLP as before, and final results of some of the analyzed clones are shown in *Figure* 5.11. Left hand side of Panel A in *Figure* 5.11 shows some of the clones of HepG2 treated with 1000 nM RDO1, while right hand side of the same panel shows some of the clones of HepG2 treated with apoE3-to-apoE4 RDO. Results of some of clones of THP-1 treated with RDO1 are presented in Panel B of *Figure* 5.11. All the analyzed clones had no evidence of the appearance of a 83 bp indicating that they were all homozygous for *APOE3*. Four clones from each set of cells were also passaged three times and analyzed by PCR-RFLP showing no presence of any mixed population of cells (data not shown).

As a large number (50) of original clones and passaged ones were analyzed from each set of treated cells, the absence of a clone(s) with *APOE2* or *APOE4* gene only or those with mixed *APOE3/APOE2* or *APOE3/APOE4* might have been related to passaging and/or freezing of the treated cells. Consequently, it was decided to repeat the transfections and clone some of the converted cells directly after transfection, while subject others to passaging and/or freezing. This would have enabled a comparison between different types of treatment of successfully converted cells as well as determining some of the underlying reason(s) for the loss of successfully converted cells. Having run out of both RDO molecules, more chimeraplasts were needed. However, this was limited to ordering apoE3-to-apoE2 only as this RDO had proved more functional than its counterpart, apoE3-to-apoE4 RDO. Table 2.10 shows a list of all the RDOs used in this thesis.

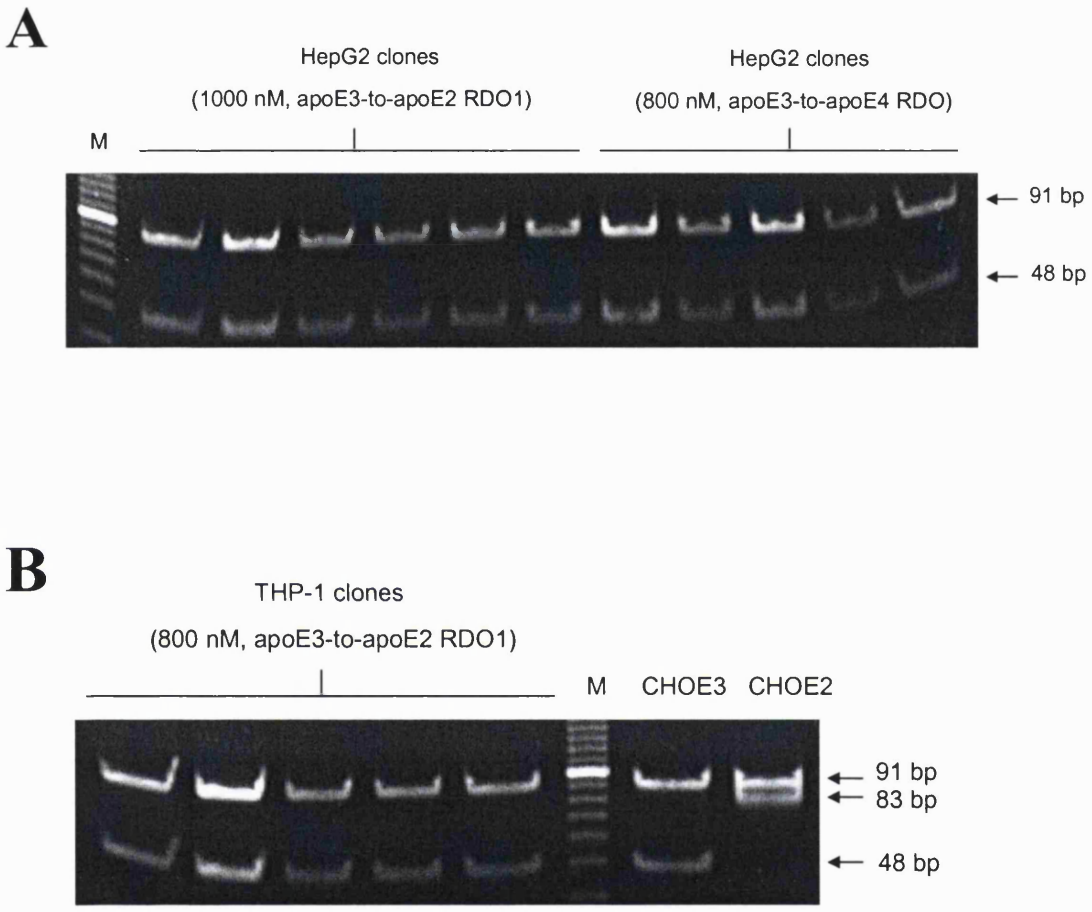

Figure 5.11 Cloning of RDO-treated HepG2 and THP-1 cells. *Some of the HepG2 (1000 nM or 400 nM) and THP-1 (800 nM) cells successfully-treated with apoE3-to-apoE2 RDO1 (Figures 5.7 and 5.9) as well as HepG2 cels (800 nM) treated with apoE3-to-apoE4 RDO (Figure 5.10) were passaged four times prior to cryopreservation. After one week, the cells were thawed out (Section 2.2.4.2) and cloned as described in Section 2.5.5. Fifty clones from each cell line were analyzed by DNA extraction followed by PCR-RFLP (Section 2.5.4) to determine whether the chimeraplasty-mediated gene conversion was permanent. The TBE gel photographs show some of the analyzed HepG2* ***(Panel A)*** *and THP-1* ***(Panel B)*** *clones. DNA extracted from CHOE2 or CHOE3 cells was used as positive control. M = 10 bp ladder.*

5.2.5 TRANSFECTION ATTEMPTS WITH NEW BATCHES OF APOE3-TO-APOE2 RDOs

A 2nd batch of RDO (RDO2) was ordered from MWG after RDO1 was almost used up in the previous experiments (*Section* 5.2.2). This batch was tested in HEK-293 and CHOE3 using L-PEI, B-PEI, or Mel-PEI and following the standard transfection protocols (Sections 2.5.2.1 and 2.5.2.2). There was no apparent conversion (data not shown) despite using various concentrations of RDO2 (200, 400, and 1000 nM) complexed with the delivery vehicles at P:N ratios of 1:5. In addition, RDO2 was not functional in HepG2 cells even though the improved transfection protocol (Section 5.2.2.5) and different transfer vehicles (L-PEI, B-PEI, Mel-PEI, and a mixture of Gal4-PEI and L-PEI in a 1:1 ratio) were employed. This was unexpected, and thus, new batches (RDO3 and RDO4) were ordered from MWG, while another company (Oswel) also supplied an additional batch of apoE3-to-apoE2 RDO (RDO5) in a separate order (Table 2.10). Unfortunately, the positive conversions achieved with RDO1 were never reproduced in either of the tested cell lines (HEK-293, CHOE3, or HepG2) with the new batches of RDOs (200, 400, and 1000 nM) even though several different transfer reagents were used and the P:N ratios were varied from 1:5 to 1:7 and 1:9 (data not shown). It was, therefore, decided to test some apoE3-to-apoE2 SSOs since they are cheaper and are expected to be synthesized and purified with more ease by the manufacturers due to their smaller size and simpler design, compared to RDOs.

5.2.6 TRANSFECTIONS WITH APOE3-TO-APOE2 SSOs

One set of SSOs for *APOE3* to *APOE2* conversion targeting both coding (CO) and non-coding (NCO) strand of *APOE3* gene were provided by Valigen. Another set of the same SSOs were purchased from Oswel (Table 2.10). Experiments were carried out in HepG2 cells following the same improved protocol used for RDOs (*Section* 5.2.2.5). Initially, the cells were treated with 550 or 1100 nM of each SSO molecule (from both MWG and Valigen) complexed with L-PEI at a P:N ratio of 1:5. Transfections were accompanied by a centrifugation step as previously described. Some of the cells were taken for analysis 48 h post-transfection, while the remainder was kept in culture for a second round of targeting with the same concentration of SSO molecules using L-PEI as a transfer reagent. After taking half of the cells for analysis, the remainder were kept in culture for a third targeting using the same

conditions as before. PCR-RFLP analysis of all the treated cells showed no clear conversion of *APOE3* to *APOE2*. The results of the treated cells after the 1st targeting with SSOs from Valigen and those after the 3rd targeting with SSOs from MWG are shown in the right-hand side and left-hand side of *Figure* 5.12 respectively. Results of 1st and 2nd targeting with SSOs from MWG and 2nd and 3rd targeting with SSOs from Valigen are not shown. These transfections were subsequently repeated without the addition of the centrifugation steps, but no obvious gene conversion was noticed (data not shown).

In subsequent experiments, a 1:1 mix of L-PEI and Gal4-PEI was complexed with each SSO at 550 0r 1100 nM and used for HepG2 transfections. Again, no obvious *APOE3* to *APOE2* conversions were obtained from SSO transfections, even at a high concentration of 1100 nM (data not shown). Additionally, two more successive attempts at targeting of the treated cells failed to show any gene conversion (data not shown).

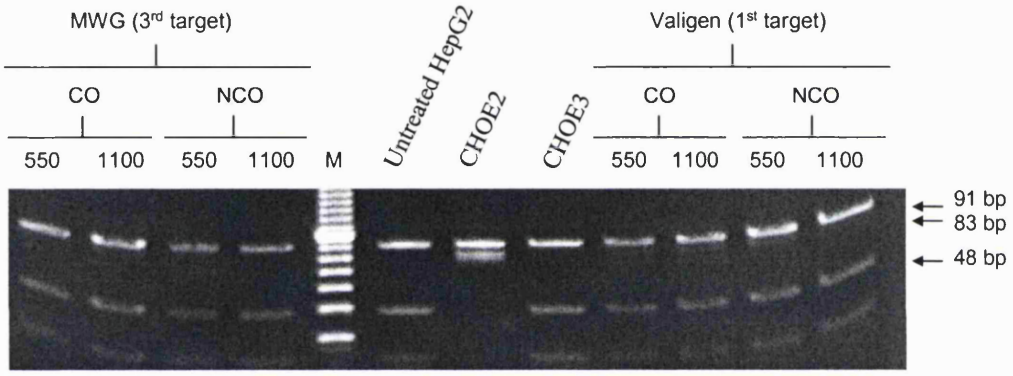

Figure 5.12 Gene conversion (attempts) in HepG2 cells using apoE3-to-apoE2 SSOs. *Cells were plated in a 12-well plate to be 50-70 % confluent on the day of transfection. The next day, a transfection mix was prepared as described in Section 2.5.2.1 using L-PEI complexed with 550 or 1100 nM of the SSOs (from MWG and Valigen, Table 2.10) at a 5:1 ratio of N:P. The plate was centrifuged as before (Section 5.2.2.5). Forty eight hours post-transfection, the cells were analyzed by DNA extraction followed by PCR-RFLP (Section 2.5.4). DNA from CHOE2 and CHOE3 cells were used as positive controls for the analysis steps. This figure shows the result of the 3rd targeting of HepG2 cells with SSOs from MWG, and the 1st targeting with SSOs from Valigen. M = 10 bp ladder. CO refers to coding and NCO to non-coding SSOs, respectively.*

5.2.7 ASSESSING OLIGONUCLEOTIDE QUALITY BY TBE-UREA ELECTROPHORESIS

The RDOs and SSOs used for transfection experiments in this chapter (Table 2.10) were analyzed on a 15% TBE-Urea gel (*Section* 2.5.6) in order to evaluate the quality of the synthesized oligonucleotides. *Figure* 5.13 shows all the RDOs and SSOs that have been used in the transfection studies described in this chapter, resolved on the gel. All the apoE3-to-apoE2 RDOs from MWG gave bands of the expected mobility. The active RDO1 had a more well-defined band compared to the others even though this batch contained a 2^{nd} band (with higher base pairs) that might indicate impurity of the synthesized RDO or incomplete denaturation or RDO1 dimer. The apoE3-to-apoE4 RDO that had some activity when used in HepG2 cells (*Figure* 5.10) had the correct mobility but was poorly defined, unlike the band observed for the more active RDO1. In addition, this RDO had only one single band unlike RDO1 that showed the presence of a second extra band as discussed above. Thus, it was concluded that the inactive or poorly-active MWG RDOs were possibly not as pure as the active RDO1. The Oswel apoE3-to-apoE2 chimeraplast (RDO5) appeared to have a correct mobility and a reasonably clear and defined band compared to MWG RDOs (RDO2, RDO3, and RDO4) even though all these RDO molecules were not functional based on previously explained experimental data. However, the band corresponding to the Oswel RDO (RDO5) was not as defined as the functional MWG RDO1.

With regard to SSOs, bands corresponding to coding and non-coding oligonucleotides from Valigen and that of non-coding SSO from Oswel seemed to have more impurities compared to that of coding SSO from Oswel. Furthermore, the bands corresponding to both SSOs from Valigen indicated the presence of a main band with a mobility less than the expected size (41 bp). The reason for this remains unclear, but might indicate lack of precision by the manufacturer in synthesizing the requested SSO molecules.

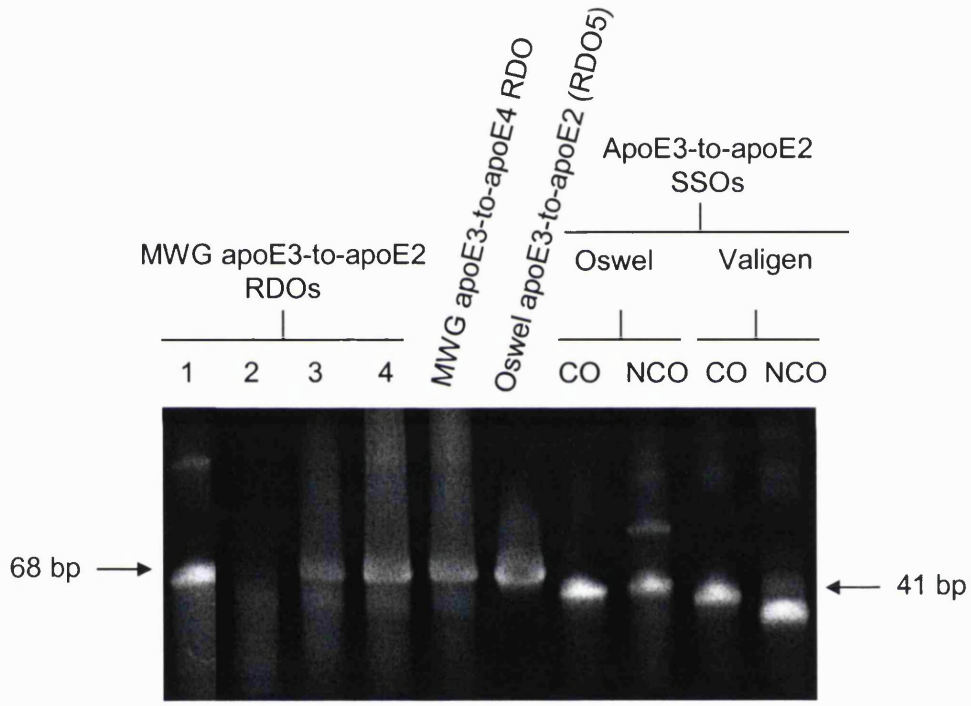

Figure 5.13 Assessing the purity of RDOs and SSOs by TBE-Urea gel electrophoresis. *Different batches of apoE3-to-apoE2 RDOs, the only batch of apoE3-to-apoE4 RDO, and the apoE3-to-apoE2 SSOs were separated on a 15 % TBE-Urea gel (Section 2.5.6). 1 μg of each oligonucleotide was boiled with sample buffer and 1 % β-mercaptoethanol for 10 min at 95 °C before being applied to the gel. The RDOs should all be 68 nt while the SSOs are smaller in length (41 nt). CO refers to coding and NCO to non-coding SSOs, respectively.*

5.3 Discussion

5.3.1 CHIMERAPLASTY-MEDIATED GENE TARGETING OF *APOE3* IN CULTURED HepG2 CELLS

Chimeraplasty was used to target *APOE3* gene in human THP-1 monocyte-macrophages and HepG2 hepatoblastoma cells in order to produce new cells secreting apoE2 or apoE4. If successful, these cell lines would be useful models for comparing the biological activities of liver- and macrophage-derived apoE particles and determining any isoform dependencies. This section deals with the results obtained from gene targeting of HepG2 cells. The outcome of targeting THP-1 cells is discussed later (*Section* 5.3.2).

Initial standard transfection experiments in HepG2 cells with the 68-mer apoE3-to-apoE2 chimeraplast (RDO1) complexed with L-PEI were unsuccessful. Three approaches were employed to improve transfection efficiency in HepG2 cells. Firstly, in order to ensure there was no barrier problem and that the chimeraplast reached the nucleus, direct microinjection of the synthetic RDO1 in individual HepG2 cells plated on coverslips was carried out. Microinjection was successful and 5.8% *APOE3* to *APOE2* conversion was obtained. Microinjection has the potential of being useful for *ex vivo* gene therapy of stem/progenitor cells especially since ultra-thin injection needles with improved flow properties became available (Davis BR *et al*, 2000). However, microinjection cannot be applied *in vivo*, and thus, the second approach involved improving the efficiency of standard transfection protocol without direct injection. The improved transfection procedure (addition of a centrifugation step) was successful in targeting the *APOE3* gene in HepG2 cells. This might be related to the ability of centrifugation to sediment chimeraplast-vehicle complexes onto target cells, allowing increased interaction with the cell surface and thus, facilitating internalization of the complex by cells. Additionally, the conversion was specific based on the following two points: a) the apoE3-to-apoE2 RDO1 did not work on CHOE2 cells; and b) the apoE2-to-apoE3 RDO was not functional in CHOE3 cells. Furthermore, a dose-dependent conversion of *APOE3* gene to the mutant isoform, *APOE2*, was achieved in HepG2 cells and this was confirmed by sequencing.

The choice of delivery reagent is important in transfection experiments even though short stretches of DNA molecules can enter the cell via endocytosis. L-PEI was the chosen delivery reagent after preliminary experiments with apoE2-to-apoE3 control RDO in CHOE2 cells indicated that L-PEI was the best vehicle compared to Superfect or LipofectAMINE^{TM}. Thus, the third approach involved optimizing the improved transfection protocol using different delivery vehicles. This was achieved by employing B-PEI and Mel-PEI that were available in our laboratory and comparing their efficiency in targeting HepG2 cells with that of L-PEI. Experiments with the apoE3-to-apoE2 RDO1 in HepG2 cells proved that L-PEI is indeed the best reagent for delivery of DNA, which was consistent with the data obtained by using pGFP (positive control for transfection efficiency). This agrees with a previous study in which L-PEI was shown to have a significantly higher transfection ability compared to B-PEI (Wightman L *et al*, 2001). Mel-PEI has been shown to be a better carrier than PEI alone (Ogris M *et al*, 2001). In fact, a dual function has been suggested for melittin; a) enhanced release of DNA-carrier complex from endosomes, and b) improved transport of complexes to the nucleus possibly due to the presence of a nuclear localization-like sequence (KRKR) near the C terminus of this peptide (Ogris M *et al*, 2001).

Despite achieving successful gene conversion with RDO1 in HepG2 cells by using L-PEI alongside centrifugation, apoE3-to-apoE4 RDO complexed with L-PEI had no effect in targeting the same cell line. B-PEI and Mel-PEI were also ineffective in targeting cultured liver cells with apoE3-to-apoE4 RDO. This failure suggested the need for targeted gene delivery to hepatocytes by means of receptor-mediated endocytosis of the chimeraplast-vehicle complexes. The field of glycotargeting has been successful in targeting liver cells via the asialoglycoprotein receptor (ASGPR) present on hepatocytes. PEI harbouring galactosyl residues has been used to transfer DNA through the ASGRP that allows it to undergo endocytosis (Zanta MA *et al*, 1997). Glycotargeting of liver via chimeraplasty-mediated gene transfer has been reported in primary hepatocytes *in vitro*, and rat liver *in vivo* (Bandyopadhyay P *et al*, 1999; Kren BT *et al*, 1998). Despite these successful reports, the apoE3-to-apoE4 RDO used in this project was still inactive in HepG2 cells even when it was complexed with Gal4-PEI (PEI harbouring 4 galactose residues). However, with the innovative idea of mixing Gal4-PEI with L-PEI in a 1:1 ratio, successful *APOE3* to *APOE4* conversion in cultured liver cells was demonstrated. Nevertheless, this required a higher

concentration of the synthetic apoE3-to-apoE4 RDO (800nM) compared to the apoE3-to-apoE2 RDO1 that was functional in the same HepG2 cells even at a concentration of 200nM. Future experiments are required to show whether an active apoE3-to-apoE4 RDO complexed with a mix of Gal4-PEI and L-PEI (1:1 ratio) will be functional in HepG2 cells at concentrations lower than 800 nM.

5.3.2 *APOE3* GENE TARGETING IN CULTURED THP-1 BY CHIMERAPLASTY

THP-1 cells were treated with apoE3-to-apoE2 RDO1, and apoE3-to-apoE4 RDO following the same protocol used for HepG2 cells. However, the *APOE3* gene proved more difficult to target in THP-1 cells. Both chimeraplasts proved inactive using the improved transfection protocol with L-PEI, B-PEI, or Mel-PEI. Thus, it was decided to use specific receptor-mediated targeting via surface bound mannose receptors that are expressed in THP-1 cells. DNA-delivery reagent complexes carrying mannosyl residues have previously been used for specific targeting of mannose receptor on macrophages (Erbacher P *et al*, 1996). This receptor recognizes glycoproteins with mannose, fucose and N-acetylglucosamine residues (Achord DT *et al*, 1977). Conversely, galactose-terminal glycoproteins are not recognized by the mannose receptor (Lennartz MR *et al*, 1987). Based on the results obtained in this chapter, Man-PEI aided in obtaining a clear *APOE3* to *APOE2* conversion when apoE3-to-apoE2 RDO1 was used, even though at a high concentration of 800 nM. The THP-1 cells used in transfections described in *Chapter* 5 were not treated with PMA to totally differentiate them into macrophages, though the mannose receptor is still present in the suspension of THP-1 cells.

It remains to be seen if percentage of gene conversion will be improved by targeting totally differentiated macrophages with Man-PEI. In the current study, targeting the *APOE3* gene in THP-1 at the other locus with apoE3-to-apoE4 RDO was not achieved despite using Man-PEI or a 1:1 ratio of Man-PEI and L-PEI. Glycotargeting in liver cells seemed to be easier than that of THP-1 possibly due to reduced expression of some of the proteins involved in repair machinery in THP-1 compared to HepG2 cells. In addition, both cell lines demonstrated that chimeraplasty-mediated gene conversion of *APOE3* to *APOE2* is more feasible than gene targeting at the other locus of human *APOE3* gene. This is further discussed in *Chapter* 6 (*Section* 6.3).

5.3.3 TARGETING *APOE3* GENE IN OTHER CELL LINES

Transfection trials on HEK-293 cells at a concentration of 400 nM of the 68-mer RDO1 molecule proved successful in converting *APOE3* to *APOE2*. This demonstrated that human *APOE3* gene can be targeted at the genomic level in cell lines other than liver and THP-1 monocyte-macropahges. In addition, the genomic apoE3 is a legitimate target not only when the protein is transcribed (i.e. in HepG2 and THP-1), but also in HEK-293 cells where apoE3 is not transcribed. RDO1 molecule was also functional in transfections performed on CHOE3 cells using the same conditions as that for HEK-293 cells. As a consequence, human *APOE3* gene can be targeted both at the cDNA and genomic level. It is interesting to note that unlike successful conversions in HepG2 and THP-1 cells, experiments on HEK-293 and CHOE3 cell lines were not accompanied by a centrifugation step and, thus, all the cell lines treated with RDO1 have the following order with regard to ease of conversion: CHOE3/HEK-293 > HepG2 > THP-1. Consequently, targeting each cell line is different and requires its own specific optimization steps with regard to the type of delivery reagent used and details of the transfection procedure.

5.3.4 CLONING THE SUCCESSFULLY RDO-TREATED CELL LINES AND TESTING NEW BATCHES OF APOE3-TO-APOE2 RDOs

In order to confirm that chimeraplasty-mediated targeting of the *APOE3* gene in cultured liver and THP-1 monocyte-macrophage cell lines was permanent, and to isolate individual clones secreting only one of the isoforms, it was decided to clone some of the converted cells. Unexpectedly, after testing 50 clones from each cell line, there was no clear indication of any converted cells in HepG2 cells treated with either the RDO1 or apoE3-to-apoE4 RDO, or in THP-1 cells treated with the RDO1 molecule. In addition, four clones from each cell line were passaged three times and analyzed indicating no conversion in any of the cells. Initially, this indicated that the conversion was not permanent, although there might be some alternative explanations for this finding. Firstly, in order to start cloning of the treated cells at the same time, RDO1-treated HepG2 and THP-1 cells were passaged four times until there were enough cells to freeze a few vials. During this stage transfection trials with the apoE3-to-apoE4 RDO were carried out and successfully converted HepG2 cells were also passaged four times prior to cryopreservation. Cloning was subsequently carried out after thawing out the frozen cells. Other reports of permanent conversions lasting for several passages do not include a freezing-thawing step. As a consequence, the loss of converted

cells in what was believed to be a mixed population of apoE3 and apoE2 (or apoE3 and apoE4) cells might have occurred either prior to freezing or after freezing. If cell death occurred prior to freezing, a possible explanation could be the cytotoxicity imposed upon the cells as a result of treating them with L-PEI. This was particularly apparent when the cells chosen for cloning were treated with high doses of RDOs (800 or 1000 nM) which in turn indicates their exposure to more L-PEI or modified L-PEI. Despite numerous reports of successful transfections with L-PEI, this reagent can potentially induce cytotoxicity due to its high positive charge even though the toxicity is reduced upon L-PEI binding to DNA (Godbey W *et al*, 1999). Gebhart *et al* have documented that polycations which are more active, such as L-PEI, are also more toxic than less active reagents such as B-PEI (Gebhart CL *et al*, 2001).

Another explanation for cell death prior to cryopreservation might be related to the fact that treated cells were not passaged enough times to allow them to recover from the stress of transfection prior to subjecting them to the freezing procedure. For instance, Tagalakis and co-workers reported passaging their chimeraplasty-treated cells for two months prior to isolating clones (Tagalakis AD *et al*, 2001). If death occurred after freezing, it could be attributed to the stress caused upon the cells during the freezing procedure. As yet there is no explanation for why only treated cells should be affected. Further stringent analyses are required to clarify the underlying reason and/or exact time of death of converted cells as discussed in *Chapter* 6 (*Section* 6.3). It remains to be seen whether cloning of HEK-293 or CHOE3 cells, which were easier to transfect (*Section* 5.3.3), could have given a different outcome. This unfortunately was not pursued as the remainder of the cells were discarded after harvesting some cells for the analysis steps mainly because the major aim of this chapter was successful gene conversion in HepG2 and THP-1 cells.

The cloning results described above were not enough to present a scientific conclusion, thus, it was decided to repeat the cloning, starting from the beginning (transfection with RDOs) and analyzing the cells at each passage. This required more synthetic RDO1 or apoE3-to-apoE4 chimeraplast, since the original batches had unfortunately finished as they were also used by other colleagues in our laboratory and elsewhere. Consequently, more RDOs were ordered, and this was limited to apoE3-to-apoE2 RDO based on my findings that *APOE3* conversion to *APOE2* was easier than that to *APOE4* and also due to the high expense of

these molecules. Despite ordering several new batches of the RDO from two different suppliers, reproducing the original success proved difficult in most of the available cell lines (HepG2, HEK-293, and CHOE3). This could be attributed to the quality of the replacement RDO molecules as well as their purity, which is discussed in *Chapter* 6 (*Section* 6.2).

5.3.5 *APOE3* TO *APOE2* GENE CONVERSION BY SSOs

Experiments designed to optimize the structure of RDO molecules led to the proposal that the all-DNA strand is responsible for gene conversion (Gamper HB *et al*, 2000a, Gamper HB *et al*, 2000b) and this was the basis of using SSOs for gene repair. There have been some reports indicating that SSOs are more active than RDOs, both *in vitro* (Rice MC *et al*, 2001a; Gamper HB *et al*, 2000a) and *in vivo* (Liu L *et al*, 2001; Parekh-Olmedo H *et al*, 2001). Thus, after unsuccessful attempts in using new batches of apoE3-to-apoE2 RDOs, it was decided to use SSOs synthesized by two different manufacturers for targeting both coding and non-coding strands of human *APOE3*. Despite using these oligonucleotides at two different concentrations (550 and 1100 nM) with L-PEI, or modified L-PEI vehicles when applicable, following the standard transfection protocol with and without the centrifugation step, no gene conversion was observed in HepG2 cells.

Re-targeting RDO-treated cells has been shown to substantially increase transfection efficiency (Tagalakis AD *et al*, 2001). Nevertheless, in our experiments, even targeting transfected cells three times with both sets of SSOs proved unsuccessful. Similar negative results were obtained after retargeting HepG2 cells treated with SSOs complexed with Gal4-PEI:PEI (1:1), which had been successful earlier in some of the difficult transfections with the apoE3-to-apoE4 RDO. In conclusion, SSOs are not as efficient as RDOs for targeting the *APOE3* gene in HepG2 cells. A reduced stability of SSOs due to their simpler design may be one explanation for this conclusion. However, confirmation will require a functional RDO, which can be tested under the same conditions alongside the SSOs, not only in HepG2 cells but also in all the other available cell lines, especially HEK-293 and CHOE3 that proved easier to transfect with the RDO1 molecule. In addition, using the SSO oligonucleotides at concentrations lower than 550 nM, such as 400 nM or 200 nM that proved successful in HepG2 cells with RDO1 transfections, may have resulted in a positive outcome.

Chapter 6

6. GENERAL DISCUSSION

6.1 Hypothesis

ApoE and apoAI are plasma proteins with a range of anti-atherogenic properties as described in *Chapter* 1 (*Sections* 1.3.6 and 1.4.3). Both proteins are important components of RCT. Lipid-poor apoAI (pre-β HDL), either secreted by liver or gut, or recycled from mature HDL, is the major acceptor of cellular cholesterol (Fielding CJ *et al*, 1997). This particle mediates fast cholesterol efflux by interaction with the recently described ABC-A1 transporter (Owen JS, 1999). Another acceptor for cellular cholesterol is apoE-containing particles (γ-LpE). These might be involved in clearing cholesterol from arteries since macrophages secrete apoE at lesion sites (O'Brien KD *et al*, 1994). Upon apoE and apoAI capture of cellular cholesterol, nascent HDL particles are generated that serve as substrates for LCAT. Furthermore, these apolipoproteins have intrinsic antioxidant activities; protecting LDL against oxidative effects (Parthasarathy S *et al*, 1990), inhibiting their uptake by macrophages and reducing foam cell formation (Steinberg D *et al*, 1989). ApoAI binds oxidized sterols (Kritharides L *et al*, 1995) and inhibits Cu^{+2}-mediated oxidation of lipoproteins (Miyata M *et al*, 1996), while lipid-free apoE protects cells against oxidative cytotoxicity, potentially reflecting an ability to bind metal ions (Miyata M *et al*, 1996). The three major isoforms of apoE (apoE2, apoE3, and apoE4) have antioxidant potential with the apoE2 being the most protective isoform as reported by Mabile *et al* from studies in a cell-free system (Mabile L *et al*, 2003).

One aspect of this thesis was to compare the biological activities of newly-secreted apoE3- and apoAI-containing particles. Recombinant CHO cells expressing human apoE3 (CHOE3) were already available in our laboratory, however, CHO cells secreting human apoAI needed to be generated. The levels of secreted apoE3 and apoAI were quantified by sandwich ELISA and densitometric analysis of Western blots, respectively. Experiments were carried out to compare the ability of apoE3- and apoAI-containing particles to sequester cellular cholesterol and activate LCAT. The final aim of this project was to test the hypothesis that: **'the *novel technology of chimeraplasty is capable of converting the APOE3 gene to mutants APOE2 and APOE4 in HepG2 and THP-1 cells.*'** These new cell lines would be suitable models for studying the biological activities of liver- and macrophage-derived apoE particles and determining their isoform-

dependency. Introducing permanent point mutations in the *APOE3* gene was investigated using both RDOs and SSOs and employing a range of suitable delivery reagents. Chimeraplasty has the potential to be an alternative to conventional approaches for treatment and prevention of atherosclerosis.

6.2 ApoE3- and ApoAI-Containing Particles Secreted by Recombinant CHO Cells are Biologically Active

Prior to a comparison of biological activities of newly-secreted apoE3 and apoAI from recombinant CHO cell lines, it was necessary to quantify levels of these apolipoproteins in cultured media. Due to there being no suitable commercially available immunoassay, quantification could only be achieved by establishing separate reproducible and accurate in-house assays for apoE and apoAI. An ELISA was chosen from a range of assays such as RIA, due to long-term reagent functionality and not being based on radioisotopes. A direct sandwich ELISA was developed for apoE using commercially available reagents. This assay permits inter-laboratory comparability of results, involves relatively low cost, and is adaptable for the measurement of low levels of apoE (as low as 20 ng/ml of apoE). Furthermore, the ELISA is pan-apoE sensitive, obviating the need for sensitive assays for the three apoE isoforms (Tagalakis AD *et al*, 2001; Sacre SM *et al*, 2003).

For apoAI quantification, densitometric analysis of Western blots was used after attempts to develop a sandwich ELISA proved to be unsuccessful. The poor choice of coating and detection antibody (both polyclonal) could be attributed to the unsuccessful attempts to develop this ELISA. Monoclonal antibodies are believed to be more suitable as coating antibodies for measurements of proteins since they bind to the antigen on a single epitope and thus reduce the chances of non-specific binding (Marcovina S *et al*, 1986). Such monoclonal antibodies, however, are not always available. Conversely, the detection antibody should be polyclonal (recognizing more than one epitope) as one of the antigenic determinant sites is already recognized by the coating antibody. A combination of monoclonal coating antibodies and polyclonal detection antibodies has previously been successful in developing sandwich ELISAs for apoAI by other groups (Atger V *et al*, 1995; Rothwell TC *et al*, 1995). However, a common problem associated with developing ELISA for apolipoproteins is related to the antigenic determinants of the particles being masked within the lipid phase of the protein, limiting the accessibility of antibodies used in the assay (Mao SJ *et al*, 1980; Schonfeld G *et al*, 1977). Consequently, it is advisable to use a suitable combination of polyclonal coating and

detection antibodies. Even though delipidated apoAI (antigen for setting up standard curves) was used in developing the ELISA described in *Chapter* 3, apoAI immunoreactivity might have been altered as a result of delipidation, handling and storage (Albers JJ *et al*, 1989).

Following the establishment of an ELISA for apoE quantification, and scanning densitometry for apoAI, CHO cells were transfected with an expression vector encoding full-length human apoAI cDNA, and stable clones were selected. Cells often acquire resistance to anti-proliferative agents such as MTX via amplification of the gene encoding the target enzyme DHFR. This enzyme catalyzes the reduction of dihydrofolate to tetrahydrofolate, which is converted to a variety of cofactors needed for *de novo* synthesis of thymidine, purines, and glycine (Singer MJ *et al*, 2000). In CHO cells, amplification of the *DHFR* gene is initiated through chromosomal breaks distal to the *DHFR* gene, and the subsequent fusion of sister chromatids (Ma C *et al*, 1993). Based on the data shown in *Chapter* 4, MTX addition to selected CHOAI clones did not improve apoAI secretion in the media. However, there have been reports of increased secretion of recombinant proteins after MTX amplification. Recombinant human prolactin production was improved after addition of MTX in the concentration range of 20-1000 nM (Soares CR *et al*, 2000). Dyring and colleagues showed a 25-fold elevation in hIGFBP-1 (human insulin-like growth factor binding protein-1) production by continuous cultivation over 8 months in medium supplemented with 100 nM MTX (Dyring C *et al*, 1997). In addition, our laboratory had a successful outcome with increasing expression of His6-LCAT through MTX (Vinogradov DV *et al*, 1998). However, these groups have spent a long time analyzing a large number of clones as well as using high concentrations of MTX in order to detect a fast growing clone with highest production. This was a time-consuming procedure that was not pursued in the selection analysis performed in this study.

Newly-secreted apoAI-containing particles from the generated CHOAI cell line were used as a positive control when studying the biological activities of newly-secreted apoE3-containing particles derived from CHOE3 cells (already present in our laboratory). Both apoAI and apoE3 particles were used without any purification steps such as delipidation or ultracentrifugation that might have affected their endogenous conformation. It has been documented that ultracentrifugation disturbs apoE association with lipoproteins and dissociates the protein from the particle surface or redistributes the

apoE to other lipoprotein classes (Murdoch SJ *et al*, 1994). Ladu and co-workers showed isoform-specific binding of apoE to Alzheimer's β-amyloid peptides (Ladu MJ *et al*, 1995). However, the affinity of binding was lowered and isoform specificity was abolished by delipidating apoE particles. Consequently, a more physiologically relevant mode of study of secreted apoE3 and apoAI particles was carried out by using conditioned medium from confluent cells without any subsequent purification steps.

Newly-synthesized apoE3 and apoAI particles were found to be biologically functional as they both sequestered cellular cholesterol from [^{3}H]-cholesterol labelled macrophages. Stimulation of particles with HDL-plasma (plasma depleted of the apoB-containing lipoproteins) significantly increased FC efflux ability of the particles compared to control medium. This was expected as HDL is an extracellular cholesterol acceptor that promotes FC efflux (Fielding CJ *et al*, 2001). THP-1 cells were selected as they simulate human monocyte-derived macrophages in various ways including secretion of apoE and lipoprotein lipase, accumulation of cholesteryl esters, and induction of scavenger receptors (Tajima S *et al*, 1985; Hassall DG *et al*, 1992; Hara H *et al*, 1987). Furthermore, accumulation of cellular cholesterol in THP-1 macrophages gives them a morphological appearance that resembles atherosclerotic foam cells (Golstein JL *et al*, 1979; Brown MS *et al*, 1983). Lipid-free apoE and apoAI have been shown to accept cholesterol from cholesterol-loaded macrophages (Hara H *et al*, 1991). Phospholipid association with the protein is required for apolipoprotein-mediated cholesterol removal from CHO cells, fibroblasts, and endothelial cells (Forte TM *et al*, 1993; Asztalos B *et al*, 1997; Savion N *et al*, 1993). Lipid-binding ability of apoE and apoAI was recently reported to occur in a two-step process. Initially, amphipathic α-helices in the carboxy-terminal domain facilitate binding to the lipid surface (Saito H *et al*, 2003). This is followed by opening of the helix bundle in the amino-terminal domain enabling interaction with phospholipids or cholesterol, thus modulating some of the biological functions of apoE or apoAI including cholesterol efflux (Saito H *et al*, 2003).

In the present study, the effect of newly-synthesised apoE3 and apoAI on sequestering cellular cholesterol was investigated in THP-1 macrophages. It is yet to be established whether CHOE3 cells that endogenously secrete apoE3 can promote cholesterol efflux when labelled with [^{3}H]-cholesterol. Lin *et al* have documented that endogenous apoE is even more efficient than exogenous apoE at cholesterol efflux (Lin CY *et al*, 1999). One mechanism for explaining such a difference might be that endogenous apoE could be

involved in efflux from a sub-cellular cholesterol pool that is separate from the one facilitated by exogenous apoE.

LCAT is responsible for esterification of cholesterol present in circulating plasma lipoproteins (Glomset JA, 1968). This enzyme mainly associates with HDL in plasma and generates cholesteryl esters, which are transferred to the core of HDL resulting in the formation of spherical HDL particles (Akanuma Y *et al*, 1968; Santamarina-Fojo S *et al*, 2000). LCAT assists in maintaining a concentration gradient for the efflux of cholesterol from peripheral cells to HDL and thus is essential for the RCT pathway. However, even in the absence of LCAT, HDL is capable of removing cellular cholesterol mainly accompanied by its interactions with apolipoproteins (Tsujita M *et al*, 1996). Berard *et al* demonstrated that LCAT-deficient plasma (from a patient with features of familial LCAT deficiency) was as efficient as control plasma in mediating cholesterol efflux from [^{3}H]-cholesterol loaded fibroblasts (Berard AM *et al*, 2001). In this project, both apoE3- and apoAI-containing particles activated LCAT with apoAI having significantly greater stimulation than that of apoE3 at 0.5 h or 1 h. This was expected as apoAI is the main co-factor of LCAT (*Section* 1.4.3.2). However, future stringent comparisons are required at shorter time points (< 0.5 h) when the esterification curve has true linearity to permit a conclusive comparison of the two particles' ability to activate LCAT.

A number of atheroprotective functions of apoE3 were previously demonstrated in our laboratory. For example, it was shown that apoE binding by apoER2 (Riddell DR *et al*, 1999), inhibits platelet aggregation and stimulates endothelial nitric oxide synthase (eNOS) to release NO (Riddell DR *et al*, 2001). This apoE-NO link was extended to endothelial cells, demonstrating suppression of vascular cell adhesion molecule-1 (VCAM-1) induction by cell-derived apoE (Stannard AK *et al*, 2001). It was also found that apoAI inhibits platelet aggregation, although the mechanism is NO-independent (Riddell AD *et al*, 1996). The apoAI secreted from my recombinant CHO cells and the recombinant apoE3 studied in this thesis provide a foundation for further experimental studies on biological functions of these proteins. For example, their effect in generating NO (Sacre SM *et al*, 2003) could be compared. Moreover, their anti-oxidant properties could be compared by studying inhibition of LDL oxidation by THP-1 macrophages (Graham A *et al*, 1997).

6.3 *In Vitro* Gene Targeting of *APOE3* with RDOs (Chimeraplasts) and SSOs

Successful conversion of *APOE3* to *APOE2* in a range of cell lines, including HepG2, THP-1, and recombinant CHO cells expressing human apoE3 (CHOE3) has been demonstrated in this thesis. As a consequence, *APOE3* can be targeted at the genomic (HepG2 and THP-1) as well as cDNA (CHOE3) level. Furthermore, HEK-293 cells, which do not express apoE, were targeted with the apoE3-to-apoE2 RDO1 molecule indicating that a single base can be exchanged in the apoE gene even when the gene is not transcribed. This is consistent with the report that another cell line, EBV-transformed lymphocytes derived from a patient homozygous for the *APOE2* gene, could be successfully targeted with an apoE2-to-apoE3 RDO even though apoE2 was not expressed (Tagalakis AD *et al*, 2001). In addition, it has been demonstrated in this project that the *APOE3* gene can be targeted at another locus (Cys112Arg) by converting *APOE3* to *APOE4* in HepG2 cells. These changes at the DNA level are promising results for the future of chimeraplasty-mediated gene repair.

In order to generate new liver and macrophage cell lines secreting apoE2/E2 or apoE4/E4 isoform, some of the successfully converted HepG2 and THP-1 cells were passaged several times followed by cryopreservation. After thawing, they were cloned by limiting dilution. However, upon analysis of approximately 50 clones of each cell type, it was established that no converted cells remained in what was believed to be a mixed population of converted and non-converted cells. This observation is compatible with the report of Olsen *et al*, which observed death of converted cells 4-6 days post-transfection (Olsen PA *et al*, 2003). This problem, which is widely attributed to a very low survival rate for converted cells, could be due to the toxicity of PEI or its modified versions as explained in *Chapter* 5. An alternative possibility is that the converted cells had been triggered to undergo apoptosis, which has been suggested by Nur-E-Kamal and colleagues following transfection with single-stranded DNA molecules as short as 5-mer (Nur-E-Kamal A *et al*, 2003). Future experiments should aim to systematically assess the transfection procedures explained in *Chapter* 5 and possibly determine the exact time of cell death. One way to achieve this is by using markers of apoptosis such as propidium iodide (PI) followed by FACS analysis in order to distinguish apoptotic cells (PI positive) from viable ones (Daniel V *et al*, 2004; Li K *et al*, 2003).

Chimeraplasty has been proven by some researchers to introduce permanent and clonal point mutations in plant and cultured mammalian cells (Beetham PR *et al*, 1999; Zhu T *et al*, 2000; Alexeev V *et al*, 2000; Tagalakis AD *et al*, 2001). However, in the reported publications, the cloning was performed without freezing the cells after transfection. Consequently, it was decided to repeat the transfection experiments (*Chapter* 5) and clone the cells without prior cryopreservation. This should avoid unnecessary stress upon the cells. Unfortunately at this stage, the original RDO1 molecule had all been used, and thus new RDO batches were ordered from different manufacturers (*Section* 2.5.1.3). These new RDO molecules failed to reproduce the positive data obtained with RDO1. This was possibly related to the quality of the new RDO molecules since the same cell lines, transfer reagents, and protocols were used as before. Due to their large size and self-associating nature, pure RDOs are hard to synthesize and a range of impurities including N-1 failure fragments could be generated (Gilar M, 2001; Agris PF *et al*, 2002). The purity of the RDOs was assessed by pre-cast TBE-Urea mini-gels (Williams DC, 1998). The functional RDO1 molecule had a more intense and compact band compared to other RDOs, although this oligonucleotide also showed the presence of an extra band. More sophisticated analytical procedures, such as reversed-phase high performance liquid chromatography (Gilar M, 2001), are essential for assessing the quality and purity of synthesized oligonucleotides, preferably by the manufacturer prior to their application in gene targeting experiments.

One of the goals of a successful gene therapy approach is attaining rapid and efficient delivery of desired genes. Important factors for improving efficiency of chimeraplasty-mediated gene targeting need to be considered as the field moves closer to clinical trials. These include optimizing the design of RDO molecules and the delivery system, and elucidating the exact mechanism of action of chimeraplasts. An optimal structure or sequence for designing an RDO molecule has not yet been determined. Consequently, there is a need for conducting further studies in this area. However, increasing the length of the homologous recombination sequence appears to improve the frequency of gene repair. When the RDO had 25 nucleotides in the homology region, it was about 40 times more efficient than an RDO with 15 nucleotides in the homology region. In addition, increasing the length of homology to 35 nucleotides, improved the functionality of the RDO by a factor of 10 (Kren BT *et al*, 1999b). Furthermore, based on studies in cell-free extract systems, if the all-DNA strand (*Section* 1.5.6.1) alone is mismatched with the target DNA, the efficiency of conversion is improved by 50% compared to a standard

RDO molecule, which has mismatches on both strands. Efficiency of conversion is reduced by ~90% if only the chimeric strand contains the mismatch. From these studies, it was suggested that the all-DNA strand enables gene correction to occur, while the modified RNA residues in the chimeric strand stabilize the structure (Gamper HB *et al*, 2000a; Gamper HB *et al*, 2000b). Despite these and other efforts, elucidating the exact mechanism of action of RDOs (*Section* 1.5.6.2) remains somewhat speculative and thus more work is required before chimeraplasty fulfils its enormous potential.

As discussed in *Section* 1.5.6.6, SSOs are an attractive alternative to RDOs due to their small size and lack of self-association, which makes their synthesis and purification easier. SSOs provide levels of gene repair comparable to chimeraplasts as demonstrated by Kmiec *et al* (Liu L *et al*, 2001; Parekh-Olmedo H *et al*, 2001), while Nickerson and colleagues demonstrated that SSOs give a significantly higher transfection rate in cultured cells compared to their RDO counterparts (Nickerson HD *et al*, 2003). Nevertheless, results from using SSOs in this project proved negative, even though the same genetic modification was shown in earlier experiments by RDO1. As a functional RDO was not available at the time when SSO experiments were performed, more work is essential before concluding that RDOs are more effective than SSOs for gene targeting of *APOE*.

From the available experimental data and the results discussed in *Chapter* 5, it is apparent that achieving successful gene conversions with chimeraplasty is more difficult in some cell lines than in others. Our apoE3-to-apoE4 was functional in HepG2, but not THP-1 cells, even though RDO1 (apoE3-to-apoE2) was active in both cell lines. One critical parameter in optimizing transfection efficiency is the ratio of the concentration of L-PEI and DNA in the polyplex (DNA-polycation complex) (Boussif O *et al*, 1996). In this project transfections were carried out using N:P ratios (molar ratio of nitrogen atoms in the delivery vehicle to phosphates in the oligonucleotide) above 4:1, the point at which net charge neutralization occurs. An excess of the polycation is required to achieve optimal transfection conditions. This is largely due to the net positive charge created by the polycation on the surface of the DNA-polycation complex, which increases the possibility of interaction with negatively charged moieties at the cell surface.

Correction of underlying mutations *in situ* via chimeraplasty has significant advantages over conventional and traditional gene therapy approaches including: a) the integrity of

the target gene is maintained within its native chromosomal context; b) the relationship of protein coding sequences and regulatory elements is retained; c) it is believed to have fewer random mutagenesis effects as it corrects the mutation in a site-specific way; d) the RDO molecule is synthetic like many approved drugs; e) it is expected to have a permanent effect; and f) as yet there have been no reports of immunogenecity, unlike viral-based strategies (Hacein-Bey-Abina S *et al*, 2003).

Despite numerous reports of chimeraplast-mediated gene repair in cultured mammalian and plant cells or in animal models (*Sections* 1.5.6.3, 1.5.6.5, & 1.5.6.4), this technique has its limitations and problems. By correcting the DNA of a cell, the modification can be passed on to the progeny and, thus, care must be taken to avoid unintentional alterations. However, this is an advantage over some of the other gene therapy strategies such as RNA interference (RNAi), which requires continual inactivation/silencing of the mutant RNA that results from the mutated DNA (Tuschl T, 2002). Rapid degradation of the therapeutic DNA may also take place before it reaches to the nucleus. Thus, chimeraplasty requires an efficient DNA delivery vector and conditions that are cell-specific. Other problems may be difficult to control, including effects due to the sequence of the target region or to the type of base conversion required. For example, my experience was that a C → T conversion (*APOE3* → *APOE2*) was easier, certainly in HepG2 cells, compared to a T → C conversion (*APOE3* → *APOE4*). However, T → C base exchanges have been successfully demonstrated in our laboratory (Tagalakis AD *et al*, 2001) and by another group studying the mdx mouse model (Chen Z *et al*, 2001). As a consequence a more detailed study of each cell line and base conversion is needed. Many single point mutations have been corrected by chimeraplasty (*Sections* 1.5.6.3-1.5.6.5), but it is not clear yet if this method can be extended to correction of multiple point mutations that have been reported for SSOs (Agarwal S *et al*, 2003).

The reliability of chimeraplasty-mediated gene repair was first criticized by Thomas *et al* and Zhang *et al* who claimed that RDO molecules might act as primers in PCR-based analyses, producing high conversion efficiencies as they contain the corrected sequences (Thomas KR *et al*, 1997; Zhang Z *et al*, 1998). However, this was ruled out after several investigations demonstrated conversions by non-PCR based techniques such as Southern blots of genomic DNA, in addition to confirming phenotypic conversion using protein analyses and functional biochemical assays (Tagalakis AD *et al*, 2001; Alexeev V *et al*, 2000; Alexeev V *et al*, 1998; Kren BT *et al*, 1998).

Some researchers are cautious about the potential of chimeraplasty despite large numbers of impressive and promising publications. Their concern is based on some reports of failure in gene repair with RDO molecules (Diaz-Font A *et al*, 2003; Manzano A *et al*, 2003). In fact, van der Steege *et al* and others have mentioned unpublished failures using this novel technology (van der Steege G *et al*, 2001; Albuquerque-Silva J *et al*, 2001; Baralle M *et al*, 2001). In addition, a recent commentary by Taubes questioned the validity and reproducibility of this technique as positive results of some groups failed to be regenerated by other researchers in different laboratories (Taubes G, 2002).

At a clinical level, the genotypic conversions in *APOE* described in this thesis could be useful for targeting the *APOE4* gene in the brain and converting it to *APOE3* (Zhang Y *et al*, 2002; Shi N *et al*, 2001). This could be a possible therapeutic tool for Alzheimer's disease and other neurodegenerative disorders, which should be initially explored in animal models considering the availability of transgenic mouse models of human disease (Schmitz C *et al*, 2004; Ho L *et al*, 2004). In addition, site-specific gene repair of the ε2 allele (*APOE2* → *APOE3*) could provide a cure for patients with type III hypercholesterolaemia specially since premature atherosclerosis has not been reported in individuals that are heterozygous for apoE2/apoE3 (Mahley RW *et al*, 2000). An animal model of hypercholesterolaemia has already been targeted by chimeraplasty (Tagalakis AD *et al*, 2001). This targeting could be extended further to other potential genes predisposing to atherosclerotic cardiovascular disease including *LDL-R* for patients with FH (Wilson DJ *et al*, 1998). Moreover, the aim of producing new liver and macrophage cell lines (HepG2 and THP-1) secreting apoE2/E2 or apoE4/E4 was important as these cells would have facilitated a comparative study of biological activities of liver- and macrophage-derived apoE particles and their isoform-dependency. However, the outcome of this project raises concerns and adds to the debate on reproducibility of chimeraplast-mediated gene repair and the quality of synthetic RDOs.

In conclusion, it is to be hoped that future systematic and critical analyses of the RDO molecules, identification of well-characterised transfection reagents, and an enhanced understanding of the molecular mechanisms of action will remove the anxieties and doubts concerning the consistency and reproducibility of chimeraplasty, and allow progress towards the final goal of attaining a viable treatment for disease causing point mutations.

BIBLIOGRAPHY

Achord DT, Brot FE, and Sly WS (1977) Inhibition of the rat clearance system for agalacto-orosomucoid by yeast mannans and by mannose. Biochem.Biophys.Res.Commun. 77:409-415.

Acsadi G, Dickson G, Love DR, Jani A, Walsh FS, Gurusinghe A, Wolff JA, and Davies KE (1991) Human dystrophin expression in mdx mice after intramuscular injection of DNA constructs. Nature 352:815-818.

Acton S, Osgood D, Donoghue M, Corella D, Pocovi M, Cenarro A, Mozas P, Keilty J, Squazzo S, Woolf EA, and Ordovas JM (1999) Association of polymorphisms at the SR-BI gene locus with plasma lipid levels and body mass index in a white population. Arterioscler.Thromb.Vasc.Biol. 19:1734-1743.

Agarwal S, Gamper HB, and Kmiec EB (2003) Nucleotide replacement at two sites can be directed by modified single-stranded oligonucleotides in vitro and in vivo. Biomol.Eng 20:7-20.

Aggerbeck LP, Wetterau JR, Weisgraber KH, Wu CS, and Lindgren FT (1988) Human apolipoprotein E3 in aqueous solution. II. Properties of the amino- and carboxyl-terminal domains. J.Biol.Chem. 263:6249-6258.

Aghi M, Hochberg F, and Breakefield XO (2000) Prodrug activation enzymes in cancer gene therapy. J.Gene Med. 2:148-164.

Agris PF, Smith S, Fu C, and Simkins SG (2002) QC in antisense oligo synthesis. Nat.Biotechnol. 20:871-872.

Albers JJ, Cabana VG, and Dee Barden SY (1976) Purification and characterization of human plasma lecithin:cholesterol acyltransferase. Biochemistry 15:1084-1087.

Albers JJ and Marcovina SM (1989) Standardization of apolipoprotein B and A-I measurements. Clin.Chem. 35:1357-1361.

Albuquerque-Silva J, Vassart G, Lavinha J, and Abramowicz MJ (2001) Chimeraplasty validation. Nat.Biotechnol. 19:1011.

Alexeev V and Yoon K (1998) Stable and inheritable changes in genotype and phenotype of albino melanocytes induced by an RNA-DNA oligonucleotide. Nat.Biotechnol. 16:1343-1346.

Alexeev V, Igoucheva O, Domashenko A, Cotsarelis G, and Yoon K (2000) Localized in vivo genotypic and phenotypic correction of the albino mutation in skin by RNA-DNA oligonucleotide. Nat.Biotechnol. 18:43-47.

Alton E and Kitson C (2000) Gene therapy for cystic fibrosis. Expert.Opin.Investig.Drugs 9:1523-1535.

Alton EW, Geddes DM, Gill DR, Higgins CF, Hyde SC, Innes JA, and Porteous DJ (1998) Towards gene therapy for cystic fibrosis: a clinical progress report. Gene Ther. 5:291-292.

Anderson WF (2000) Gene therapy. The best of times, the worst of times. Science 288:627-629.

Asztalos B, Zhang W, Roheim PS, and Wong L (1997) Role of free apolipoprotein A-I in cholesterol efflux. Formation of pre-alpha-migrating high-density lipoprotein particles. Arterioscler.Thromb.Vasc.Biol. 17:1630-1636.

Atger V, de la Llera MM, Bamberger M, Francone O, Cosgrove P, Tall A, Walsh A, Moatti N, and Rothblat G (1995) Cholesterol efflux potential of sera from mice expressing human cholesteryl ester transfer protein and/or human apolipoprotein AI . J.Clin.Invest 96:2613-2622.

Athanasopoulos T, Owen JS, Hassall D, Dunckley MG, Drew J, Goodman J, Tagalakis AD, Riddell DR, and Dickson G (2000) Intramuscular injection of a plasmid vector expressing human apolipoprotein E limits progression of xanthoma and aortic atheroma in apoE-deficient mice. Hum.Mol.Genet. 9:2545-2551.

Badimon JJ, Badimon L, and Fuster V (1990) Regression of atherosclerotic lesions by high density lipoprotein plasma fraction in the cholesterol-fed rabbit. J.Clin.Invest 85:1234-1241.

Baez JM, Barbour SE, and Cohen DE (2002) Phosphatidylcholine transfer protein promotes apolipoprotein A-I-mediated lipid efflux in Chinese hamster ovary cells. J.Biol.Chem. 277:6198-6206.

Ball RY, Stowers EC, Burton JH, Cary NR, Skepper JN, Mitchinson MJ (1995) Evidence that the death of macrophage foam cells contributes to the lipid core of atheroma. Atherosclerosis. 114:45-54.

Bandyopadhyay P, Kren BT, Ma X, and Steer CJ (1998) Enhanced gene transfer into HuH-7 cells and primary rat hepatocytes using targeted liposomes and polyethylenimine. Biotechniques 25:282-292.

Bandyopadhyay P, Ma X, Linehan-Stieers C, Kren BT, and Steer CJ (1999) Nucleotide exchange in genomic DNA of rat hepatocytes using RNA/DNA oligonucleotides. Targeted delivery of liposomes and polyethyleneimine to the asialoglycoprotein receptor. J.Biol.Chem. 274:10163-10172.

Baralle M and Baralle FE (2001) Genetics and molecular biology. Curr.Opin.Lipidol. 12:663-665.

Barra RM, Fenjves ES, and Taichman LB (1994) Secretion of apolipoprotein E by basal cells in cultures of epidermal keratinocytes. J.Invest Dermatol. 102:61-66.

Barre FX, Ait-Si-Ali S, Giovannangeli C, Luis R, Robin P, Pritchard LL, Helene C, and Harel-Bellan A (2000) Unambiguous demonstration of triple-helix-directed gene modification. Proc.Natl.Acad.Sci.U.S.A 97:3084-3088.

Bartlett RJ, Stockinger S, Denis MM, Bartlett WT, Inverardi L, Le TT, thi MN, Morris GE, Bogan DJ, Metcalf-Bogan J, and Kornegay JN (2000) In vivo targeted repair of a point mutation in the canine dystrophin gene by a chimeric RNA/DNA oligonucleotide. Nat.Biotechnol. 18:615-622.

Basu SK, Brown MS, Ho YK, Havel RJ, and Goldstein JL (1981) Mouse macrophages synthesize and secrete a protein resembling apolipoprotein E. Proc.Natl.Acad.Sci.U.S.A 78:7545-7549.

Basu SK, Ho YK, Brown MS, Bilheimer DW, Anderson RG, and Goldstein JL (1982) Biochemical and genetic studies of the apoprotein E secreted by mouse macrophages and human monocytes. J.Biol.Chem. 257:9788-9795.

Basu SK, Goldstein JL, and Brown MS (1983) Independent pathways for secretion of cholesterol and apolipoprotein E by macrophages. Science 219:871-873.

Beetham PR, Kipp PB, Sawycky XL, Arntzen CJ, and May GD (1999) A tool for functional plant genomics: chimeric RNA/DNA oligonucleotides cause in vivo gene-specific mutations. Proc.Natl.Acad.Sci.U.S.A 96:8774-8778.

Bekaert ED, Alaupovic P, Knight-Gibson CS, Franceschini G, and Sirtori CR (1993) Apolipoprotein A-I Milano: sex-related differences in the concentration and composition of apoA-I- and apoB-containing lipoprotein particles. J.Lipid Res. 34:111-123.

Bellosta S, Mahley RW, Sanan DA, Murata J, Newland DL, Taylor JM, and Pitas RE (1995) Macrophage-specific expression of human apolipoprotein E reduces atherosclerosis in hypercholesterolemic apolipoprotein E-null mice. J.Clin.Invest 96:2170-2179.

Benihoud K, Yeh P, and Perricaudet M (1999) Adenovirus vectors for gene delivery. Curr.Opin.Biotechnol. 10:440-447.

Benlian P, De Gennes JL, Foubert L, Zhang H, Gagne SE, and Hayden M (1996) Premature atherosclerosis in patients with familial chylomicronemia caused by mutations in the lipoprotein lipase gene. N.Engl.J.Med. 335:848-854.

Benoit P, Emmanuel F, Caillaud JM, Bassinet L, Castro G, Gallix P, Fruchart JC, Branellec D, Denefle P, and Duverger N (1999) Somatic gene transfer of human ApoA-I inhibits atherosclerosis progression in mouse models. Circulation 99:105-110.

Bensadoun A and Berryman DE (1996) Genetics and molecular biology of hepatic lipase. Curr.Opin.Lipidol. 7:77-81.

Berard AM, Clerc M, Brewer B, Jr., and Santamarina-Fojo S (2001) A normal rate of cellular cholesterol removal can be mediated by plasma from a patient with familial lecithin-cholesterol acyltransferase (LCAT) deficiency. Clin.Chim.Acta 314:131-139.

Bernal-Mendez E and Leumann CJ (2002) Stability and kinetics of nucleic acid triplexes with chimaeric DNA/RNA third strands. Biochemistry 41:12343-12349.

Bertoni C and Rando TA (2002) Dystrophin gene repair in mdx muscle precursor cells in vitro and in vivo mediated by RNA-DNA chimeric oligonucleotides. Hum.Gene Ther. 13:707-718.

Bielicki JK, McCall MR, Stoltzfus LJ, Ravandi A, Kuksis A, Rubin EM, and Forte TM (1997) Evidence that apolipoprotein A-IMilano has reduced capacity, compared with wild-type apolipoprotein A-I, to recruit membrane cholesterol. Arterioscler.Thromb.Vasc.Biol. 17:1637-1643.

Bieri S, Djordjevic JT, Daly NL, Smith R, and Kroon PA (1995) Disulfide bridges of a cysteine-rich repeat of the LDL receptor ligand-binding domain. Biochemistry 34:13059-13065.

Bijvoet SM, Wiebusch H, Ma Y, Reymer PW, Bruin T, Bakker HD, Funke H, Assmann G, Hayden MR, and Kastelein JJ (1996) Compound heterozygosity for a known and a novel defect in the lipoprotein lipase gene (Asp250-->Asn; Ser251-->Cys) resulting in lipoprotein lipase (LPL) deficiency. Neth.J.Med. 49:189-195.

Blaese RM, Culver KW, Miller AD, Carter CS, Fleisher T, Clerici M, Shearer G, Chang L, Chiang Y, Tolstoshev P, and . (1995) T lymphocyte-directed gene therapy for ADA- SCID: initial trial results after 4 years. Science 270:475-480.

Blanche PJ, Gong EL, Forte TM, and Nichols AV (1981) Characterization of human high-density lipoproteins by gradient gel electrophoresis. Biochim.Biophys.Acta 665:408-419.

Blue ML, Williams DL, Zucker S, Khan SA, and Blum CB (1983) Apolipoprotein E synthesis in human kidney, adrenal gland, and liver. Proc.Natl.Acad.Sci.U.S.A 80:283-287.

Blum CB, Aron L, and Sciacca R (1980) Radioimmunoassay studies of human apolipoprotein E. J.Clin.Invest 66:1240-1250.

Bodzioch M, Orso E, Klucken J, Langmann T, Bottcher A, Diederich W, Drobnik W, Barlage S, Buchler C, Porsch-Ozcurumez M, Kaminski WE, Hahmann HW, Oette K, Rothe G, Aslanidis C, Lackner KJ, and Schmitz G (1999) The gene encoding ATP-binding cassette transporter 1 is mutated in Tangier disease. Nat.Genet. 22:347-351.

Boisvert WA, Spangenberg J, and Curtiss LK (1995) Treatment of severe hypercholesterolemia in apolipoprotein E-deficient mice by bone marrow transplantation. J.Clin.Invest 96 :1118-1124.

Borchard G (2001) Chitosans for gene delivery. Adv.Drug Deliv.Rev. 52:145-150.

Boring L, Gosling J, Cleary M, Charo IF (2000) Decreased lesion formation in CCR2-/- mice reveals a role for chemokin the initiation of atherosclerosis. Nature. 394:894-7.

Boussif O, Lezoualc'h F, Zanta MA, Mergny MD, Scherman D, Demeneix B, and Behr JP (1995) A versatile vector for gene and oligonucleotide transfer into cells in culture and in vivo: polyethylenimine. Proc.Natl.Acad.Sci.U.S.A 92:7297-7301.

Boussif O, Zanta MA, and Behr JP (1996) Optimized galenics improve in vitro gene transfer with cationic molecules up to 1000-fold. Gene Ther. 3:1074-1080.

Boyles JK, Pitas RE, Wilson E, Mahley RW, and Taylor JM (1985) Apolipoprotein E associated with astrocytic glia of the central nervous system and with nonmyelinating glia of the peripheral nervous system. J.Clin.Invest 76:1501-1513.

Brachman EE and Kmiec EB (2002) The 'biased' evolution of targeted gene repair. Curr.Opin.Mol.Ther. 4:171-176.

Bradford MM (1976) A rapid and sensitive method for the quantitation of microgram quantities of protein utilizing the principle of protein-dye binding. Anal.Biochem. 72:248-254.

Bramson JL, Graham FL, and Gauldie J (1995) The use of adenoviral vectors for gene therapy and gene transfer in vivo. Curr.Opin.Biotechnol. 6:590-595.

Breslow JL, Ross D, McPherson J, Williams H, Kurnit D, Nussbaum AL, Karathanasis SK, and Zannis VI (1982) Isolation and characterization of cDNA clones for human apolipoprotein A-I. Proc.Natl.Acad.Sci.U.S.A 79:6861-6865.

Brewer HB, Jr., Fairwell T, LaRue A, Ronan R, Houser A, and Bronzert TJ (1978) The amino acid sequence of human APOA-I, an apolipoprotein isolated from high density lipoproteins. Biochem.Biophys.Res.Commun. 80:623-630.

Brissette L, Cahuzac-Bec N, Desforges M, Bec JL, Marcel YL, and Rassart E (1991) Expression of recombinant human apolipoprotein A-I in Chinese hamster ovary cells and Escherichia coli. Protein Expr.Purif. 2:296-303.

Brooks-Wilson A, Marcil M, Clee SM, Zhang LH, Roomp K, van Dam M, Yu L, Brewer C, Collins JA, Molhuizen HO, Loubser O, Ouelette BF, Fichter K, Ashbourne-Excoffon KJ, Sensen CW, Scherer S, Mott S, Denis M, Martindale D, Frohlich J, Morgan K, Koop B, Pimstone S, Kastelein JJ, Hayden MR, and . (1999) Mutations in ABC1 in Tangier disease and familial high-density lipoprotein deficiency. Nat.Genet. 22:336-345.

Brown MS and Goldstein JL (1983) Lipoprotein metabolism in the macrophage: implications for cholesterol deposition in atherosclerosis. Annu.Rev.Biochem. 52:223-261.

Brown MS and Goldstein JL (1986) A receptor-mediated pathway for cholesterol homeostasis. Science 232:34-47.

Brown MS, Herz J, and Goldstein JL (1997) LDL-receptor structure. Calcium cages, acid baths and recycling receptors. Nature 388:629-630.

Bukrinsky MI and Haffar OK (1999) HIV-1 nuclear import: in search of a leader. Front Biosci. 4:D772-D781.

Burgess JW, Frank PG, Franklin V, Liang P, McManus DC, Desforges M, Rassart E, and Marcel YL (1999) Deletion of the C-terminal domain of apolipoprotein A-I impairs cell surface binding and lipid efflux in macrophage. Biochemistry 38:14524-14533.

Bury J, Vercaemst R, Rosseneu M, and Belpaire F (1986) Apolipoprotein E quantified by enzyme-linked immunosorbent assay. Clin.Chem. 32:265-270.

Calabresi L, Canavesi M, Bernini F, and Franceschini G (1999) Cell cholesterol efflux to reconstituted high-density lipoproteins containing the apolipoprotein A-IMilano dimer. Biochemistry 38:16307-16314.

Campbell CR, Keown W, Lowe L, Kirschling D, and Kucherlapati R (1989) Homologous recombination involving small single-stranded oligonucleotides in human cells. New Biol. 1:223-227.

Cardin AD, Hirose N, Blankenship DT, Jackson RL, Harmony JA, Sparrow DA, and Sparrow JT (1986) Binding of a high reactive heparin to human apolipoprotein E: identification of two heparin-binding domains. Biochem.Biophys.Res.Commun. 134 :783-789.

Cardin AD, Bowlin TL, and Krstenansky JL (1988) Inhibition of lymphocyte proliferation by synthetic peptides homologous to human plasma apolipoproteins B and E. Biochem.Biophys.Res.Commun. 154:741-745.

Cavazzana-Calvo M, Hacein-Bey S, de Saint BG, Gross F, Yvon E, Nusbaum P, Selz F, Hue C, Certain S, Casanova JL, Bousso P, Deist FL, and Fischer A (2000) Gene therapy of human severe combined immunodeficiency (SCID)-X1 disease. Science 288:669-672.

Chaisomchit S, Tyrrell DL, and Chang LJ (1997) Development of replicative and nonreplicative hepatitis B virus vectors. Gene Ther. 4:1330-1340.

Chan PP, Lin M, Faruqi AF, Powell J, Seidman MM, and Glazer PM (1999) Targeted correction of an episomal gene in mammalian cells by a short DNA fragment tethered to a triplex-forming oligonucleotide. J.Biol.Chem. 274:11541-11548.

Chatelet F, Brianti E, Ronco P, Roland J, and Verroust P (1986) Ultrastructural localization by monoclonal antibodies of brush border antigens expressed by glomeruli. II. Extrarenal distribution. Am.J.Pathol. 122:512-519.

Chen Z, Felsheim R, Wong P, Augustin LB, Metz R, Kren BT, and Steer CJ (2001) Mitochondria isolated from liver contain the essential factors required for RNA/DNA oligonucleotide-targeted gene repair. Biochem.Biophys.Res.Commun. 285:188-194.

Chenchik A, Diachenko L, Moqadam F, Tarabykin V, Lukyanov S, and Siebert PD (1996) Full-length cDNA cloning and determination of mRNA 5' and 3' ends by amplification of adaptor-ligated cDNA. Biotechniques 21:526-534.

Cheung MC and Albers JJ (1984) Characterization of lipoprotein particles by immunoaffinity chromatography. Particles containing A-I and A-II and particles containing A-I but no A-II. J.Biol. Chem. 259:12201-12209.

Cheung MC, Brown BG, Wolf AC, and Albers JJ (1991) Altered particle size distribution of apolipoprotein A-I-containing lipoproteins in subjects with coronary artery disease. J.Lipid Res. 32:383-394.

Chiesa G, Monteggia E, Marchesi M, Lorenzon P, Laucello M, Lorusso V, Di Mario C, Karvouni E, Newton RS, Bisgaier CL, Franceschini G, and Sirtori CR (2002) Recombinant apolipoprotein A-I(Milano) infusion into rabbit carotid artery rapidly removes lipid from fatty streaks. Circ.Res. 90:974-980.

Chirmule N, Propert K, Magosin S, Qian Y, Qian R, and Wilson J (1999) Immune responses to adenovirus and adeno-associated virus in humans. Gene Ther. 6:1574-1583.

Choi SY, Komaromy MC, Chen J, Fong LG, and Cooper AD (1994) Acceleration of uptake of LDL but not chylomicrons or chylomicron remnants by cells that secrete apoE and hepatic lipase. J.Lipid Res. 35:848-859.

Christ M, Louis B, Stoeckel F, Dieterle A, Grave L, Dreyer D, Kintz J, Ali HD, Lusky M, and Mehtali M (2000) Modulation of the inflammatory properties and hepatotoxicity of recombinant adenovirus vectors by the viral E4 gene products. Hum.Gene Ther. 11:415-427.

Chung J, Abano DA, Fless GM, and Scanu AM (1979) Isolation, properties, and mechanism of in vitro action of lecithin: cholesterol acyltransferase from human plasma. J.Biol.Chem. 254:7456-7464.

Cianflone K, Vu H, Zhang Z, and Sniderman AD (1994) Effects of albumin on lipid synthesis, apo B-100 secretion, and LDL catabolism in HepG2 cells. Atherosclerosis 107:125-135.

Cioffi L, Sturtz FG, Wittmer S, Barut B, Smith-Gbur J, Moore V, Zupancic T , Gilligan B, Auerbach R, Gomez F, Chauvin F, Antczak M, Platika D, and Snodgrass HR (1999) A novel endothelial cell-based gene therapy platform for the in vivo delivery of apolipoprotein E. Gene Ther. 6:1153-1159.

Cole-Strauss A, Yoon K, Xiang Y, Byrne BC, Rice MC, Gryn J, Holloman WK , and Kmiec EB (1996) Correction of the mutation responsible for sickle cell anemia by an RNA-DNA oligonucleotide. Science 273:1386-1389.

Cole-Strauss A, Gamper H, Holloman WK, Munoz M, Cheng N, and Kmiec EB (1999) Targeted gene repair directed by the chimeric RNA/DNA oligonucleotide in a mammalian cell-free extract. Nucleic Acids Res. 27:1323-1330.

Collet X, Marcel YL, Tremblay N, Lazure C, Milne RW, Perret B, and Weech PK (1997) Evolution of mammalian apolipoprotein A-I and conservation of antigenicity: correlation with primary and secondary structure. J.Lipid Res. 38:634-644.

Collins RG, Velji R, Guevara NV, Hicks MJ, Chan L, Beaudet AL (2000) P-Selectin or intercellular adhesion molecule (ICAM)-1 deficiency substantially protects against atherosclerosis in apolipoprotein E-deficient mice. J.Exp.Med. 191:189-194.

Conrad CK, Allen SS, Afione SA, Reynolds TC, Beck SE, Fee-Maki M, Barrazza-Ortiz X, Adams R, Askin FB, Carter BJ, Guggino WB, and Flotte TR (1996) Safety of single-dose administration of an adeno-associated virus (AAV)-CFTR vector in the primate lung. Gene Ther. 3:658-668.

Consiglio A, Quattrini A, Martino S, Bensadoun JC, Dolcetta D, Trojani A, Benaglia G, Marchesini S, Cestari V, Oliverio A, Bordignon C, and Naldini L (2001) In vivo gene therapy of metachromatic leukodystrophy by lentiviral vectors: correction of neuropathology and protection against learning impairments in affected mice. Nat.Med. 7:310-316.

Corbo RM and Scacchi R (1999) Apolipoprotein E (APOE) allele distribution in the world. Is APOE*4 a 'thrifty' allele? Ann.Hum.Genet. 63 (Pt 4):301-310.

Corder EH, Robertson K, Lannfelt L, Bogdanovic N, Eggertsen G, Wilkins J, and Hall C (1998) HIV-infected subjects with the E4 allele for APOE have excess dementia and peripheral neuropathy. Nat.Med. 4:1182-1184.

Crowther JR (1995) ELISA theory and practice. In Methods in molecular biology. Walker JM Editor. Human Press, Totowa, New Jersey. p. 1-223.

Cullen P, Cignarella A, Brennhausen B, Mohr S, Assmann G, and von Eckardstein A (1998) Phenotype-dependent differences in apolipoprotein E metabolism and in cholesterol homeostasis in human monocyte-derived macrophages. J.Clin.Invest 101:1670-1677.

Cuthbert JA and Lipsky PE (1984) Modulation of human lymphocyte responses by low density lipoproteins (LDL): enhancement but not immunosuppression is mediated by LDL receptors. Proc.Natl.Acad.Sci.U.S.A 81:4539-4543.

Daniel V, Sadeghi M, Naujokat C, Weimer R, Huth-Kuhne A, Zimmermann R, and Opelz G (2004) Evidence for autoantibody-induced CD4 depletion mediated by apoptotic and non-apoptotic mechanisms in HIV-positive long-term surviving haemophilia patients. Clin.Exp.Immunol. 135:94-104.

Das HK, McPherson J, Bruns GA, Karathanasis SK, and Breslow JL (1985) Isolation, characterization, and mapping to chromosome 19 of the human apolipoprotein E gene. J.Biol.Chem. 260:6240-6247.

Davis BR, Yannariello-Brown J, Prokopishyn NL, Luo Z, Smith MR, Wang J, Carsrud ND, and Brown DB (2000) Glass needle-mediated microinjection of macromolecules and transgenes into primary human blood stem/progenitor cells. Blood 95:437-444.

Davis CG, Goldstein JL, Sudhof TC, Anderson RG, Russell DW, and Brown MS (1987) Acid-dependent ligand dissociation and recycling of LDL receptor mediated by growth factor homology region. Nature 326:760-765.

de Bont N, Netea MG, Demacker PN, Verschueren I, Kullberg BJ, van Dijk KW, van der Meer JW, and Stalenhoef AF (1999) Apolipoprotein E knock-out mice are highly susceptible to endotoxemia and Klebsiella pneumoniae infection. J.Lipid Res. 40:680-685.

De Geest B, Zhao Z, Collen D, and Holvoet P (1997) Effects of adenovirus-mediated human apo A-I gene transfer on neointima formation after endothelial denudation in apo E-deficient mice. Circulation 96:4349-4356.

de Knijff P, van den Maagdenberg AM, Frants RR, and Havekes LM (1994) Genetic heterogeneity of apolipoprotein E and its influence on plasma lipid and lipoprotein levels. Hum.Mutat. 4:178-194.

Dean B, Laws SM, Hone E, Taddei K, Scarr E , Thomas EA, Harper C, McClean C, Masters C, Lautenschlager N, Gandy SE, and Martins RN (2003) Increased levels of apolipoprotein E in the frontal cortex of subjects with schizophrenia. Biol.Psychiatry 54:616-622.

Dempsey CE (1990) The actions of melittin on membranes. Biochim.Biophys.Acta 1031:143-161.

Desurmont C, Caillaud JM, Emmanuel F, Benoit P, Fruchart JC, Castro G, Branellec D, Heard JM, and Duverger N (2000) Complete atherosclerosis regression after human ApoE gene transfer in ApoE-deficient/nude mice. Arterioscler.Thromb.Vasc.Biol. 20:435-442.

Dhabhar FS (2003) Stress, leukocyte trafficking, and the augmentation of skin immune function. Ann.N.Y.Acad.Sci. 992:205-217.

Dhoest A, Zhao Z, De Geest B, Deridder E, Sillen A, Engelborghs Y, Collen D, and Holvoet P (1997) Role of the Arg123-Tyr166 paired helix of apolipoprotein A-I in lecithin:cholesterol acyltransferase activation. J.Biol.Chem. 272:15967-15972.

Diaz-Font A, Cormand B, Chabas A, Vilageliu L, and Grinberg D (2003) Unsuccessful chimeraplast strategy for the correction of a mutation causing Gaucher disease. Blood Cells Mol.Dis. 31:183-186.

Dobson CB and Itzhaki RF (1999) Herpes simplex virus type 1 and Alzheimer's disease. Neurobiol.Aging 20:457-465.

Dong LM, Parkin S, Trakhanov SD, Rupp B, Simmons T, Arnold KS, Newhouse YM, Innerarity TL, and Weisgraber KH (1996) Novel mechanism for defective receptor binding of apolipoprotein E2 in type III hyperlipoproteinemia. Nat.Struct.Biol. 3:718-722.

Driscoll DM, Schreiber JR, Schmit VM, and Getz GS (1985) Regulation of apolipoprotein E synthesis in rat ovarian granulosa cells. J.Biol.Chem. 260:9031-9038.

Duan H, Li Z, and Mazzone T (1995) Tumor necrosis factor-alpha modulates monocyte/macrophage apoprotein E gene expression. J.Clin.Invest 96:915-922.

Durany N, Riederer P, and Cruz-Sanchez FF (2000) Apolipoprotein E genotype in Spanish schizophrenic patients. Psychiatr.Genet. 10:73-77.

Duverger N, Kruth H, Emmanuel F, Caillaud JM, Viglietta C, Castro G, Tailleux A, Fievet C, Fruchart JC, Houdebine LM, and Denefle P (1996) Inhibition of atherosclerosis development in cholesterol-fed human apolipoprotein A-I-transgenic rabbits. Circulation 94:713-717.

Dyring C and Mellstrom K (1997) Stable, recombinant expression of human insulin-like factor binding protein-1 (hIGFBP) in Chinese hamster ovary (CHO) cells. Cytotechnology 24(3): 193-200.

Dzau VJ (2003) Predicting the future of human gene therapy for cardiovascular diseases: what will the management of coronary artery disease be like in 2005 and 2010? Am.J.Cardiol. 92:32N-35N.

Ehrlich M, Sarafyan LP, and Myers DJ (1976) Interaction of microbial DNA with cultured mammalian cells. Binding of the donor DNA to the cell surface. Biochim.Biophys.Acta 454:397-409.

Erbacher P, Bousser MT, Raimond J, Monsigny M, Midoux P, and Roche AC (1996) Gene transfer by DNA/glycosylated polylysine complexes into human blood monocyte-derived macrophages. Hum.Gene Ther. 7:721-729.

Esser D, Amanuma H, Yoshiki A, Kusakabe M, Rudolph R, and Bohm G (2000) A hyperthermostable bacterial histone-like protein as an efficient mediator for transfection of eukaryotic cells. Nat.Biotechnol. 18:1211-1213.

Faggiotto A and Ross R (1984) Studies of hypercholesterolemia in the nonhuman primate. II. Fatty streak conversion to fibrous plaque. Arteriosclerosis 4:341-356.

Fass D, Blacklow S, Kim PS, and Berger JM (1997) Molecular basis of familial hypercholesterolaemia from structure of LDL receptor module. Nature 388:691-693.

Fazio S, Babaev VR, Murray AB, Hasty AH, Carter KJ, Gleaves LA, Atkinson JB, and Linton MF (1997) Increased atherosclerosis in mice reconstituted with apolipoprotein E null macrophages. Proc.Natl.Acad.Sci.U.S.A 94:4647-4652.

Fazio S, Linton MF, Hasty AH, and Swift LL (1999) Recycling of apolipoprotein E in mouse liver. J.Biol.Chem. 274:8247-8253.

Fazio VM, Fazio S, Rinaldi M, Catani MV, Zotti S, Ciafre SA, Seripa D, Ricci G, and Farace MG (1994) Accumulation of human apolipoprotein-E in rat plasma after in vivo intramuscular injection of naked DNA. Biochem.Biophys.Res.Commun. 200:298-305.

Febbraio M, Podrez EA, Smith JD, Hajjar DP, Hazen SL, Hoff HF, Sharma K, Silverstein RL (2000) Targeted disruption of the class B scavenger receptor CD36 protects against atherosclerotic lesion development in mice. J.Clin..Invest. 105:1049-1056.

Feng M, Morales AB, Poot A, Beugeling T, and Bantjes A (1995) Effects of Tween 20 on the desorption of proteins from polymer surfaces. J.Biomater.Sci.Polym.Ed 7:415-424.

Ferrero RL and Labigne A (1993) Cloning, expression and sequencing of Helicobacter felis urease genes. Mol.Microbiol. 9:323-333.

Fielding CJ and Fielding PE (1995) Molecular physiology of reverse cholesterol transport. J.Lipid Res. 36:211-228.

Fielding CJ and Fielding PE (1997) Intracellular cholesterol transport. J.Lipid Res. 38:1503-1521.

Fielding CJ and Fielding PE (2001) Cellular cholesterol efflux. Biochim.Biophys.Acta 1533:175-189.

Forte TM, Goth-Goldstein R, Nordhausen RW, and McCall MR (1993) Apolipoprotein A-I-cell membrane interaction: extracellular assembly of heterogeneous nascent HDL particles. J.Lipid Res. 34:317-324.

Fox JL (1999) Gene therapy safety issues come to fore. Nat.Biotechnol. 17:1153.

Franceschini G, Sirtori CR, Capurso A, Weisgraber KH, and Mahley RW (1980) A-IMilano apoprotein. Decreased high density lipoprotein cholesterol levels with significant lipoprotein modifications and without clinical atherosclerosis in an Italian family. J.Clin.Invest 66:892-900.

Franceschini G, Sirtori CR, Bosisio E, Gualandri V, Orsini GB, Mogavero AM, and Capurso A (1985) Relationship of the phenotypic expression of the A-IMilano apoprotein with plasma lipid and lipoprotein patterns. Atherosclerosis 58:159-174.

Franceschini G, Calabresi L, Chiesa G, Parolini C, Sirtori CR, Canavesi M, and Bernini F (1999) Increased cholesterol efflux potential of sera from ApoA-IMilano carriers and transgenic mice. Arterioscler.Thromb.Vasc.Biol. 19:1257-1262.

Francke U, Brown MS, and Goldstein JL (1984) Assignment of the human gene for the low density lipoprotein receptor to chromosome 19: synteny of a receptor, a ligand, and a genetic disease. Proc.Natl.Acad.Sci.U.S.A 81:2826-2830.

Francone OL, Haghpassand M, Bennett JA, Royer L, and McNeish J (1997) Expression of human lecithin:cholesterol acyltransferase in transgenic mice: effects on cholesterol efflux, esterification, and transport. J.Lipid Res. 38:813-822.

Frank PG, N'Guyen D, Franklin V, Neville T, Desforges M, Rassart E, Sparks DL, and Marcel YL (1998) Importance of central alpha-helices of human apolipoprotein A-I in the maturation of high-density lipoproteins. Biochemistry 37:13902-13909.

Fyfe AI, Qiao JH, and Lusis AJ (1994) Immune-deficient mice develop typical atherosclerotic fatty streaks when fed an atherogenic diet. J.Clin.Invest 94:2516-2520.

Gafvels ME, Paavola LG, Boyd CO, Nolan PM, Wittmaack F, Chawla A, Lazar MA, Bucan M, Angelin BO, and Strauss JF, III (1994) Cloning of a complementary deoxyribonucleic acid encoding the murine homolog of the very low density lipoprotein/apolipoprotein-E receptor: expression pattern and assignment of the gene to mouse chromosome 19. Endocrinology 135:387-394.

Gamper HB, Parekh H, Rice MC, Bruner M, Youkey H, and Kmiec EB (2000a) The DNA strand of chimeric RNA/DNA oligonucleotides can direct gene repair/conversion activity in mammalian and plant cell-free extracts. Nucleic Acids Res. 28:4332-4339.

Gamper HB, Jr., Cole-Strauss A, Metz R, Parekh H, Kumar R, and Kmiec EB (2000b) A plausible mechanism for gene correction by chimeric oligonucleotides. Biochemistry 39:5808-5816.

Garcia CK, Wilund K, Arca M, Zuliani G, Fellin R, Maioli M, Calandra S, Bertolini S, Cossu F, Grishin N, Barnes R, Cohen JC, and Hobbs HH (2001) Autosomal recessive hypercholesterolemia caused by mutations in a putative LDL receptor adaptor protein. Science 292:1394-1398.

Gebhart CL and Kabanov AV (2001) Evaluation of polyplexes as gene transfer agents. J.Control Release 73:401-416.

Gerrity RG (1981) The role of the monocyte in atherogenesis: I. Transition of blood-borne monocytes into foam cells in fatty lesions. Am.J.Pathol. 103:181-190.

Ghosh P, Hale EA, Mayur K, Seddon J, and Lakshman MR (2000) Effects of chronic alcohol treatment on the synthesis, sialylation, and disposition of nascent apolipoprotein E by peritoneal macrophages of rats. Am.J.Clin.Nutr. 72:190-198.

Gilar M (2001) Analysis and purification of synthetic oligonucleotides by reversed-phase high-performance liquid chromatography with photodiode array and mass spectrometry detection. Anal.Biochem. 298:196-206.

Gillett MPT and Owen JS (1992). Cholesterol esterifying enzymes-lecithin:cholesterol acyltransferase (LCAT) and acylcoenzyme A:cholesterol acyltransferase (ACAT). In: Lipoprotein Analysis: A Practical Approach. Converse CA and Skinner, Editors. Oxford Unversity Press, New York. p. 187-201.

Glass C, Pittman RC, Weinstein DB, and Steinberg D (1983) Dissociation of tissue uptake of cholesterol ester from that of apoprotein A-I of rat plasma high density lipoprotein: selective delivery of cholesterol ester to liver, adrenal, and gonad. Proc.Natl.Acad.Sci.U.S.A 80:5435-5439.
Glomset JA (1968) The plasma lecithins:cholesterol acyltransferase reaction. J.Lipid Res. 9:155-167.

Godbey WT, Wu KK, and Mikos AG (1999) Poly(ethylenimine) and its role in gene delivery. J.Control Release 60:149-160.

Goldberg IJ (1996) Lipoprotein lipase and lipolysis: central roles in lipoprotein metabolism and atherogenesis. J.Lipid Res. 37:693-707.

Goldstein JL and Brown MS (1974) Binding and degradation of low density lipoproteins by cultured human fibroblasts. Comparison of cells from a normal subject and from a patient with homozygous familial hypercholesterolemia. J.Biol.Chem. 249:5153-5162.

Gollins H, McMahon J, Wells KE, and Wells DJ (2003) High-efficiency plasmid gene transfer into dystrophic muscle. Gene Ther. 10:504-512.

Goncz KK, Prokopishyn NL, Chow BL, Davis BR, and Gruenert DC (2002) Application of SFHR to gene therapy of monogenic disorders. Gene Ther. 9:691-694.

Goula D, Benoist C, Mantero S, Merlo G, Levi G, and Demeneix BA (1998) Polyethylenimine-based intravenous delivery of transgenes to mouse lung. Gene Ther. 5:1291-1295.

Grabenhorst E, Schlenke P, Pohl S, Nimtz M, and Conradt HS (1999) Genetic engineering of recombinant glycoproteins and the glycosylation pathway in mammalian host cells. Glycoconj.J. 16:81-97.

Gracia V, Fiol C, Hurtado I, Pinto X, Argimon JM, and Castineiras MJ (1994) An enzyme-linked immunosorbent assay method to measure human apolipoprotein E levels using commercially available reagents: effect of apolipoprotein E polymorphism on serum apolipoprotein E concentration. Anal.Biochem. 223:212-217.

Graham A, Hassall DG, Rafique S, and Owen JS (1997) Evidence for a paraoxonase-independent inhibition of low-density lipoprotein oxidation by high-density lipoprotein. Atherosclerosis 135:193-204.

Groot PH, van Vlijmen BJ, Benson GM, Hofker MH, Schiffelers R, Vidgeon-Hart M, and Havekes LM (1996) Quantitative assessment of aortic atherosclerosis in APOE*3 Leiden transgenic mice and its relationship to serum cholesterol exposure. Arterioscler.Thromb.Vasc.Biol. 16:926-933.

Grossman M, Raper SE, Kozarsky K, Stein EA, Engelhardt JF, Muller D, Lupien PJ, and Wilson JM (1994) Successful ex vivo gene therapy directed to liver in a patient with familial hypercholesterolaemia. Nat.Genet. 6 :335-341.

Grundy SM, Pasternak R, Greenland P, Smith S, Jr., and Fuster V (1999) Assessment of cardiovascular risk by use of multiple-risk-factor assessment equations: a statement for healthcare professionals from the American Heart Association and the American College of Cardiology. Circulation 100:1481-1492.

Gu X, Lawrence R, and Krieger M (2000) Dissociation of the high density lipoprotein and low density lipoprotein binding activities of murine scavenger receptor class B type I (mSR-BI) using retrovirus library-based activity dissection. J.Biol.Chem. 275:9120-9130.

Hacein-Bey-Abina S, Fischer A, and Cavazzana-Calvo M (2002) Gene therapy of X-linked severe combined immunodeficiency. Int.J.Hematol. 76:295-298.

Hacein-Bey-Abina S, von Kalle C, Schmidt M, McCormack MP, Wulffraat N, Leboulch P, Lim A, Osborne CS, Pawliuk R, Morillon E, Sorensen R, Forster A, Fraser P, Cohen JI, de Saint BG, Alexander I, Wintergerst U, Frebourg T, Aurias A, Stoppa-Lyonnet D, Romana S, Radford-Weiss I, Gross F, Valensi F, Delabesse E, Macintyre E, Sigaux F, Soulier J, Leiva LE, Wissler M, Prinz C, Rabbitts TH, Le Deist F, Fischer A, and Cavazzana-Calvo M (2003) LMO2-associated clonal T cell proliferation in two patients after gene therapy for SCID-X1. Science 302:415-419.

Haghpassand M and Moberly JB (1995) 9-cis-retinoic acid increases apolipoprotein AI secretion and mRNA expression in HepG2 cells. Atherosclerosis 117:199-207.

Hames BD (1983) An introduction to polyacrylamide gel electrophoresis. In Gel Electrophoresis of Proteins: A Practical Approach. BD Hames and D Rickwood, Editors. IRL Press Ltd, Oxford. p. 1-92.

Hamilton RL, Williams MC, Fielding CJ, and Havel RJ (1976) Discoidal bilayer structure of nascent high density lipoproteins from perfused rat liver. J.Clin.Invest 58:667-680.

Hammad SM, Stefansson S, Twal WO, Drake CJ, Fleming P, Remaley A, Brewer HB, Jr., and Argraves WS (1999) Cubilin, the endocytic receptor for intrinsic factor-vitamin B(12) complex, mediates high-density lipoprotein holoparticle endocytosis. Proc.Natl.Acad.Sci.U.S.A 96:10158-10163.

Han H, Sasaki J, Matsunaga A, Hakamata H, Huang W, Ageta M, Taguchi T, Koga T, Kugi M, Horiuchi S, and Arakawa K (1999) A novel mutant, ApoA-I nichinan (Glu235-->0), is associated with low HDL cholesterol levels and decreased cholesterol efflux from cells. Arterioscler.Thromb.Vasc.Biol. 19:1447-1455.

Hanahan D (1983) Studies on transformation of Escherichia coli with plasmids. J.Mol.Biol. 166:557-580.

Hannon GJ (2002) RNA interference. Nature 418:244-251.

Hara H, Tanishita H, Yokoyama S, Tajima S, and Yamamoto A (1987) Induction of acetylated low density lipoprotein receptor and suppression of low density lipoprotein receptor on the cells of human monocytic leukemia cell line (THP-1 cell). Biochem.Biophys.Res.Commun. 146:802-808.

Hara H and Yokoyama S (1991) Interaction of free apolipoproteins with macrophages. Formation of high density lipoprotein-like lipoproteins and reduction of cellular cholesterol. J.Biol.Chem. 266:3080-3086.

Harrington CR, Roth M, Xuereb JH, McKenna PJ, and Wischik CM (1995) Apolipoprotein E type epsilon 4 allele frequency is increased in patients with schizophrenia. Neurosci.Lett. 202:101-104.

Harris JD, Graham IR, Schepelmann S, Stannard AK, Roberts ML, Hodges BL, Hill V, Amalfitano A, Hassall DG, Owen JS, and Dickson G (2002a) Acute regression of advanced and retardation of early aortic atheroma in immunocompetent apolipoprotein-E (apoE) deficient mice by administration of a second generation [E1(-), E3(-), polymerase(-)] adenovirus vector expressing human apoE. Hum.Mol.Genet. 11:43-58.

Harris JD, Schepelmann S, Athanasopoulos T, Graham IR, Stannard AK, Mohri Z, Hill V, Hassall DG, Owen JS, and Dickson G (2002b) Inhibition of atherosclerosis in apolipoprotein-E-deficient mice following muscle transduction with adeno-associated virus vectors encoding human apolipoprotein-E. Gene Ther. 9:21-29.

Hassall DG (1992) Three probe flow cytometry of a human foam-cell forming macrophage. Cytometry 13:381-388.

Hauser H, Dyer JH, Nandy A, Vega MA, Werder M, Bieliauskaite E, Weber FE , Compassi S, Gemperli A, Boffelli D, Wehrli E, Schulthess G, and Phillips MC (1998) Identification of a receptor mediating absorption of dietary cholesterol in the intestine. Biochemistry 37:17843-17850.

Havel RJ, Kane JP (1995) Introduction: structure and metabolism of plasma lipoproteins. In: The metabolic and molecular bases of inherited disease. Scriver CR, Beaudet AL, Sly SW, and Valle D, Editors. 7th edition. New York, NY: McGraw-Hill, Inc, p. 1841-51.

Heeren J, Grewal T, Jackle S, and Beisiegel U (2001) Recycling of apolipoprotein E and lipoprotein lipase through endosomal compartments in vivo. J.Biol.Chem. 276:42333-42338.

Heeren J, Grewal T, Laatsch A, Rottke D, Rinninger F, Enrich C, and Beisiegel U (2003) Recycling of apoprotein E is associated with cholesterol efflux and high density lipoprotein internalization. J.Biol.Chem. 278:14370-14378.

Hengge UR, Chan EF, Foster RA, Walker PS, and Vogel JC (1995) Cytokine gene expression in epidermis with biological effects following injection of naked DNA. Nat.Genet. 10:161-166.

Herz J, Hamann U, Rogne S, Myklebost O, Gausepohl H, and Stanley KK (1988) Surface location and high affinity for calcium of a 500-kd liver membrane protein closely related to the LDL-receptor suggest a physiological role as lipoprotein receptor. EMBO J. 7:4119-4127.

High KA (2003) Theodore E. Woodward Award. AAV-mediated gene transfer for hemophilia. Trans.Am.Clin.Climatol.Assoc. 114:337-351.

Hixson JE and Vernier DT (1990) Restriction isotyping of human apolipoprotein E by gene amplification and cleavage with HhaI. J.Lipid Res. 31:545-548.

Ho L, Qin W, Pompl PN, Xiang Z, Wang J, Zhao Z, Peng Y, Cambareri G, Rocher A, Mobbs CV, Hof PR, and Pasinetti GM (2004) Diet-induced insulin resistance promotes amyloidosis in a transgenic mouse model of Alzheimer's disease. FASEB J.

Hoang BH, Kubo T, Healey JH, Sowers R, Mazza B, Yang R, Huvos AG, Meyers PA, and Gorlick R (2004) Expression of LDL receptor-related protein 5 (LRP5) as a novel marker for disease progression in high-grade osteosarcoma. Int.J.Cancer 109:106-111.

Hoeg JM, Santamarina-Fojo S, Berard AM, Cornhill JF, Herderick EE, Feldman SH, Haudenschild CC, Vaisman BL, Hoyt RF, Jr., Demosky SJ, Jr., Kauffman RD, Hazel CM, Marcovina SM, and Brewer HB, Jr. (1996) Overexpression of lecithin:cholesterol acyltransferase in transgenic rabbits prevents diet-induced atherosclerosis. Proc.Natl.Acad.Sci.U.S.A 93:11448-11453.

Hokanson JE and Austin MA (1996) Plasma triglyceride level is a risk factor for cardiovascular disease independent of high-density lipoprotein cholesterol level: a meta-analysis of population-based prospective studies. J.Cardiovasc.Risk 3:213-219.

Holmquist L (1980) Quantitation of human serum very low density apolipoproteins C-I, C-II, C-III and E by enzyme immunoassay. J.Immunol.Methods 34:243-251.

Hong CJ, Yu YW, Lin CH, Song HL, Lai HC, Yang KH, and Tsai SJ (2000) Association study of apolipoprotein E epsilon4 with clinical phenotype and clozapine response in schizophrenia. Neuropsychobiology 42:172-174.

Huang Y, von Eckardstein A, Wu S, Maeda N, and Assmann G (1994) A plasma lipoprotein containing only apolipoprotein E and with gamma mobility on electrophoresis releases cholesterol from cells. Proc.Natl.Acad.Sci.U.S.A 91:1834-1838.

Huang Y, Liu XQ, Rall SC, Jr., Taylor JM, von Eckardstein A, Assmann G, and Mahley RW (1998) Overexpression and accumulation of apolipoprotein E as a cause of hypertriglyceridemia. J.Biol.Chem. 273:26388-26393.

Huang Y, Ji ZS, Brecht WJ, Rall SC, Jr., Taylor JM, and Mahley RW (1999) Overexpression of apolipoprotein E3 in transgenic rabbits causes combined hyperlipidemia by stimulating hepatic VLDL production and impairing VLDL lipolysis. Arterioscler.Thromb.Vasc.Biol. 19:2952-2959.

Hui DY, Harmony JA, Innerarity TL, and Mahley RW (1980a) Immunoregulatory plasma lipoproteins. Role of apoprotein E and apoprotein B. J.Biol.Chem. 255:11775-11781.

Hui DY and Harmony JA (1980b) Inhibition of Ca2+ accumulation in mitogen-activated lymphocytes: role of membrane-bound plasma lipoproteins. Proc.Natl.Acad.Sci.U.S.A 77:4764-4768.

Hui SW, Langner M, Zhao YL, Ross P, Hurley E, and Chan K (1996) The role of helper lipids in cationic liposome-mediated gene transfer. Biophys.J. 71:590-599.

Humphries SE, Berg K, Gill L, Cumming AM, Robertson FW, Stalenhoef AF, Williamson R, and Borresen AL (1984) The gene for apolipoprotein C-II is closely linked to the gene for apolipoprotein E on chromosome 19. Clin.Genet. 26:389-396.

Hussain MM, Strickland DK, and Bakillah A (1999) The mammalian low-density lipoprotein receptor family. Annu.Rev.Nutr. 19:141-172.

Igoucheva O, Alexeev V, and Yoon K (2001) Targeted gene correction by small single-stranded oligonucleotides in mammalian cells. Gene Ther. 8:391-399.

Innerarity TL and Mahley RW (1978) Enhanced binding by cultured human fibroblasts of apo-E-containing lipoproteins as compared with low density lipoproteins. Biochemistry 17:1440-1447.

Innerarity TL, Friedlander EJ, Rall SC, Jr., Weisgraber KH, and Mahley RW (1983) The receptor-binding domain of human apolipoprotein E. Binding of apolipoprotein E fragments. J.Biol.Chem. 258:12341-12347.

Inoue H, Hayase Y, Iwai S, and Ohtsuka E (1987) Sequence-dependent hydrolysis of RNA using modified oligonucleotide splints and RNase H. FEBS Lett. 215:327-330.

Ishibashi S, Goldstein JL, Brown MS, Herz J, and Burns DK (1994) Massive xanthomatosis and atherosclerosis in cholesterol-fed low density lipoprotein receptor-negative mice. J.Clin.Invest 93:1885-1893.

Ishiguro H, Yoshida H, Major AS, Zhu T, Babaev VR, Linton MF, and Fazio S (2001) Retrovirus-mediated expression of apolipoprotein A-I in the macrophage protects against atherosclerosis in vivo. J.Biol.Chem. 276:36742-36748.

Jarad G, Simske JS, Sedor JR, and Schelling JR (2003) Nucleic acid-based techniques for post-transcriptional regulation of molecular targets. Curr.Opin.Nephrol.Hypertens. 12:415-421.

Jayasena VK and Johnston BH (1993) Complement-stabilized D-loop. RecA-catalyzed stable pairing of linear DNA molecules at internal sites. J.Mol.Biol. 230:1015-1024.

Jaye M, Lynch KJ, Krawiec J, Marchadier D, Maugeais C, Doan K, South V, Amin D, Perrone M, and Rader DJ (1999) A novel endothelial-derived lipase that modulates HDL metabolism. Nat.Genet. 21:424-428.

Jenkins N and Curling EM (1994) Glycosylation of recombinant proteins: problems and prospects. Enzyme Microb.Technol. 16:354-364.

Ji ZS, Fazio S, Lee YL, and Mahley RW (1994) Secretion-capture role for apolipoprotein E in remnant lipoprotein metabolism involving cell surface heparan sulfate proteoglycans. J.Biol.Chem. 269:2764-2772.

Ji ZS, Dichek HL, Miranda RD, and Mahley RW (1997) Heparan sulfate proteoglycans participate in hepatic lipaseand apolipoprotein E-mediated binding and uptake of plasma lipoproteins, including high density lipoproteins. J.Biol.Chem. 272:31285-31292.

Johnson WJ, Mahlberg FH, Rothblat GH, and Phillips MC (1991) Cholesterol transport between cells and high-density lipoproteins. Biochim.Biophys.Acta 1085:273-298.

Jokinen EV, Landschulz KT, Wyne KL, Ho YK, Frykman PK, and Hobbs HH (1994) Regulation of the very low density lipoprotein receptor by thyroid hormone in rat skeletal muscle. J.Biol.Chem. 269:26411-26418.

Jonas A (1986) Reconstitution of high-density lipoproteins. Methods Enzymol. 128:553-582.

Jonas A (1998) Regulation of lecithin cholesterol acyltransferase activity. Prog.Lipid Res. 37:209-234.

Karathanasis SK, Zannis VI, and Breslow JL (1983) Isolation and characterization of the human apolipoprotein A-I gene. Proc.Natl.Acad.Sci.U.S.A 80:6147-6151.

Kashyap VS, Santamarina-Fojo S, Brown DR, Parrott CL, Applebaum-Bowden D, Meyn S, Talley G, Paigen B, Maeda N, and Brewer HB, Jr. (1995) Apolipoprotein E deficiency in mice: gene replacement and prevention of atherosclerosis using adenovirus vectors. J.Clin.Invest 96:1612-1620.

Kay MA, Manno CS, Ragni MV, Larson PJ, Couto LB, McClelland A, Glader B, Chew AJ, Tai SJ, Herzog RW, Arruda V, Johnson F, Scallan C, Skarsgard E, Flake AW, and High KA (2000) Evidence for gene transfer and expression of factor IX in haemophilia B patients treated with an AAV vector. Nat.Genet. 24:257-261.

Kay MA, Glorioso JC, and Naldini L (2001) Viral vectors for gene therapy: the art of turning infectious agents into vehicles of therapeutics. Nat.Med. 7:33-40.

Kemeny DM (1991) A practical guide to ELISA. Pergamon Press, Oxford, UK. p. 1-97.

Khachadurian AK and Uthman SM (1973) Experiences with the homozygous cases of familial hypercholesterolemia. A report of 52 patients. Nutr.Metab 15:132-140.

Kim DH, Iijima H, Goto K, Sakai J, Ishii H , Kim HJ, Suzuki H, Kondo H, Saeki S, and Yamamoto T (1996) Human apolipoprotein E receptor 2. A novel lipoprotein receptor of the low density lipoprotein receptor family predominantly expressed in brain. J.Biol.Chem. 271:8373-8380.

Kim EJ, Kim NS, and Lee GM (1998) Development of a serum-free medium for the production of humanized antibody from Chinese hamster ovary cells using a statistical design. In Vitro Cell Dev.Biol.Anim 34:757-761.

Kimura N, Tanemura K, Nakamura S, Takashima A, Ono F, Sakakibara I, Ishii Y, Kyuwa S, and Yoshikawa Y (2003) Age-related changes of Alzheimer's disease-associated proteins in cynomolgus monkey brains. Biochem.Biophys.Res.Commun. 310:303-311.

Kmiec EB (1999) Targeted gene repair. Gene Ther. 6:1-3.

Knowles JW and Maeda N (2000) Genetic modifiers of atherosclerosis in mice. Arterioscler.Thromb.Vasc.Biol. 20:2336-2345.

Kordower JH, Emborg ME, Bloch J, Ma SY, Chu Y, Leventhal L, McBride J, Chen EY, Palfi S, Roitberg BZ, Brown WD, Holden JE, Pyzalski R, Taylor MD, Carvey P, Ling Z, Trono D, Hantraye P, Deglon N, and Aebischer P (2000) Neurodegeneration prevented by lentiviral vector delivery of GDNF in primate models of Parkinson's disease. Science 290:767-773.

Kotani H, Germann MW, Andrus A, Vinayak R, Mullah B, and Kmiec EB (1996) RNA facilitates RecA-mediated DNA pairing and strand transfer between molecules bearing limited regions of homology. Mol.Gen.Genet. 250:626-634.

Kozyraki R, Fyfe J, Kristiansen M, Gerdes C, Jacobsen C, Cui S, Christensen EI, Aminoff M, de la CA, Krahe R, Verroust PJ, and Moestrup SK (1999) The intrinsic factor-vitamin B12 receptor, cubilin, is a high-affinity apolipoprotein A-I receptor facilitating endocytosis of high-density lipoprotein. Nat.Med. 5:656-661.

Kren BT, Cole-Strauss A, Kmiec EB, and Steer CJ (1997) Targeted nucleotide exchange in the alkaline phosphatase gene of HuH-7 cells mediated by a chimeric RNA/DNA oligonucleotide. Hepatology 25:1462-1468.

Kren BT, Bandyopadhyay P, and Steer CJ (1998) In vivo site-directed mutagenesis of the factor IX gene by chimeric RNA/DNA oligonucleotides. Nat.Med. 4:285-290.

Kren BT, Parashar B, Bandyopadhyay P, Chowdhury NR, Chowdhury JR, and Steer CJ (1999a) Correction of the UDP-glucuronosyltransferase gene defect in the gunn rat model of crigler-najjar syndrome type I with a chimeric oligonucleotide. Proc.Natl.Acad.Sci.U.S.A 96:10349-10354.

Kren BT, Metz R, Kumar R, and Steer CJ (1999b) Gene repair using chimeric RNA/DNA oligonucleotides. Semin.Liver Dis. 19:93-104.

Krieg AM and Davis HL (2001) Enhancing vaccines with immune stimulatory CpG DNA. Curr.Opin.Mol.Ther. 3:15-24.

Kritharides L, Jessup W, Mander EL, and Dean RT (1995) Apolipoprotein A-I-mediated efflux of sterols from oxidized LDL-loaded macrophages. Arterioscler.Thromb.Vasc.Biol. 15:276-289.

Kritharides L, Christian A, Stoudt G, Morel D, and Rothblat GH (1998) Cholesterol metabolism and efflux in human THP-1 macrophages. Arterioscler.Thromb.Vasc.Biol. 18:1589-1599.

Kuivenhoven JA, Pritchard H, Hill J, Frohlich J, Assmann G, and Kastelein J (1997) The molecular pathology of lecithin:cholesterol acyltransferase (LCAT) deficiency syndromes. J.Lipid Res. 38:191-205.

Kushwaha RS, Hazzard WR, Wahl PW, and Hoover JJ (1977) Type III hyperlipoproteinemia: diagnosis in whole plasma by apolipoprotein-E immunoassay. Ann.Intern.Med. 87:509-516.

Kusumawati A, Commes T, Liautard JP, and Widada JS (1999) Transfection of myelomonocytic cell lines: cellular response to a lipid-based reagent and electroporation. Anal.Biochem. 269:219-221.

LaDu MJ, Pederson TM, Frail DE, Reardon CA, Getz GS, and Falduto MT (1995) Purification of apolipoprotein E attenuates isoform-specific binding to beta-amyloid. J.Biol.Chem. 270:9039-9042.

Laffitte BA, Repa JJ, Joseph SB, Wilpitz DC, Kast HR, Mangelsdorf DJ, and Tontonoz P (2001) LXRs control lipid-inducible expression of the apolipoprotein E gene in macrophages and adipocytes. Proc.Natl.Acad.Sci.U.S.A 98:507-512.

Lagrost L, Desrumaux C, Masson D, Deckert V, and Gambert P (1998) Structure and function of the plasma phospholipid transfer protein. Curr.Opin.Lipidol. 9:203-209.

Lahoz C, Osgood D, Wilson PW, Schaefer EJ, and Ordovas JM (1996) Frequency of phenotype-genotype discrepancies at the apolipoprotein E locus in a large population study. Clin.Chem. 42:1817-1823.

Lai LW, O'Connor HM, and Lien YH (1998) In: Conference Proceedings: 1st Annual Meeting of the American Society of Gene Therapy. American Society of Gene Therapy, Seattle, WA, p. 183a.

Lai LW and Lien YH (1999) Homologous recombination based gene therapy. Exp.Nephrol. 7:11-14.

Laitinen S, Lehto M, Lehtonen S, Hyvarinen K, Heino S, Lehtonen E, Ehnholm C, Ikonen E, and Olkkonen VM (2002) ORP2, a homolog of oxysterol binding protein, regulates cellular cholesterol metabolism. J.Lipid Res. 43:245-255.

Lee NS, Dohjima T, Bauer G, Li H, Li MJ, Ehsani A, Salvaterra P, and Rossi J (2002) Expression of small interfering RNAs targeted against HIV-1 rev transcripts in human cells. Nat.Biotechnol. 20:500-505.

Legendre JY, Trzeciak A, Bohrmann B, Deuschle U, Kitas E, and Supersaxo A (1997) Dioleoylmelittin as a novel serum-insensitive reagent for efficient transfection of mammalian cells. Bioconjug.Chem. 8:57-63.

Lennartz MR, Wileman TE, and Stahl PD (1987) Isolation and characterization of a mannose-specific endocytosis receptor from rabbit alveolar macrophages. Biochem.J. 245:705-711.

Leroy A, Vu-dac N, Koffigan M, Clavey V, and Fruchart JC (1988) Characterization of a monoclonal antibody that binds to apolipoprotein E and to lipoprotein of human plasma containing apo E. Applications to ELISA quantification of plasma apo E. J.Immunoassay 9:309-334.

Levinson AD (1990) Expression of heterologous genes in mammalian cells. Methods Enzymol. 185:485-487.

Li H, Reddick RL, and Maeda N (1993) Lack of apoA-I is not associated with increased susceptibility to atherosclerosis in mice. Arterioscler.Thromb. 13:1814-1821.

Li K, Yang M, Yuen PM, Chik KW, Li CK, Shing MM, Lam HK, and Fok TF (2003) Thrombospondin-1 induces apoptosis in primary leukemia and cell lines mediated by CD36 and Caspase-3. Int.J.Mol.Med. 12:995-1001.

Li ZH, Liu DP, Yin WX, Guo ZC, and Liang CC (2001) Targeted correction of the point mutations of beta-thalassemia and targeted mutagenesis of the nucleotide associated with HPFH by RNA/DNA oligonucleotides: potential for beta-thalassemia gene therapy. Blood Cells Mol.Dis. 27:530-538.

Liang Y, Lin S, Beyer TP, Zhang Y, Wu X, Bales KR, DeMattos RB, May PC, Li SD, Jiang XC, Eacho PI, Cao G, and Paul SM (2004) A liver X receptor and retinoid X receptor heterodimer mediates apolipoprotein E expression, secretion and cholesterol homeostasis in astrocytes. J.Neurochem. 88:623-634.

Lieber A, Steinwaerder DS, Carlson CA, and Kay MA (1999) Integrating adenovirus-adeno-associated virus hybrid vectors devoid of all viral genes. J.Virol. 73:9314-9324.

Lieber A, Kay MA, and Li ZY (2000) Nuclear import of moloney murine leukemia virus DNA mediated by adenovirus preterminal protein is not sufficient for efficient retroviral transduction in nondividing cells. J.Virol. 74:721-734.

Lin CY, Lucas M, and Mazzone T (1998) Endogenous apoE expression modulates HDL3 binding to macrophages. J.Lipid Res. 39:293-301.

Lin CY, Duan H, and Mazzone T (1999) Apolipoprotein E-dependent cholesterol efflux from macrophages: kinetic study and divergent mechanisms for endogenous versus exogenous apolipoprotein E. J.Lipid Res. 40:1618-1627.

Linden RM and Woo SL (1999) AAVant-garde gene therapy. Nat.Med. 5:21-22.

Lindholm EM, Bielicki JK, Curtiss LK, Rubin EM, and Forte TM (1998) Deletion of amino acids Glu146-->Arg160 in human apolipoprotein A-I (ApoA-ISeattle) alters lecithin:cholesterol acyltransferase activity and recruitment of cell phospholipid. Biochemistry 37:4863-4868.

Linton MF, Farese RV, Jr., Chiesa G, Grass DS, Chin P, Hammer RE, Hobbs HH , and Young SG (1993) Transgenic mice expressing high plasma concentrations of human apolipoprotein B100 and lipoprotein(a). J.Clin.Invest 92:3029-3037.

Linton MF, Atkinson JB, and Fazio S (1995) Prevention of atherosclerosis in apolipoprotein E-deficient mice by bone marrow transplantation. Science 267:1034-1037.

Linton MF, Hasty AH, Babaev VR, and Fazio S (1998) Hepatic apo E expression is required for remnant lipoprotein clearance in the absence of the low density lipoprotein receptor. J.Clin.Invest 101:1726-1736.

Liu L, Rice MC, and Kmiec EB (2001) In vivo gene repair of point and frameshift mutations directed by chimeric RNA/DNA oligonucleotides and modified single-stranded oligonucleotides. Nucleic Acids Res. 29:4238-4250.

Liu L, Cheng S, van Brabant AJ, and Kmiec EB (2002a) Rad51p and Rad54p, but not Rad52p, elevate gene repair in Saccharomyces cerevisiae directed by modified single-stranded oligonucleotide vectors. Nucleic Acids Res. 30:2742-2750.

Liu L, Rice MC, Drury M, Cheng S, Gamper H , and Kmiec EB (2002b) Strand bias in targeted gene repair is influenced by transcriptional activity. Mol.Cell Biol. 22:3852-3863.

Loser P, Jennings GS, Strauss M, and Sandig V (1998) Reactivation of the previously silenced cytomegalovirus major immediate-early promoter in the mouse liver: involvement of NFkappaB. J.Virol. 72:180-190.

Luciani MF, Denizot F, Savary S, Mattei MG, and Chimini G (1994) Cloning of two novel ABC transporters mapping on human chromosome 9. Genomics 21:150-159.

Luo CC, Li WH, Moore MN, and Chan L (1986) Structure and evolution of the apolipoprotein multigene family. J.Mol.Biol. 187:325-340.

Lusis AJ (2000) Atherosclerosis. Nature 407:233-241.

Ma C, Martin S, Trask B, and Hamlin JL (1993) Sister chromatid fusion initiates amplification of the dihydrofolate reductase gene in Chinese hamster cells. Genes Dev. 7:605-620.

Mabile L, Lefebvre C, Lavigne J, Boulet L, Davignon J, Lussier-Cacan S, and Bernier L (2003) Secreted apolipoprotein E reduces macrophage-mediated LDL oxidation in an isoform-dependent way. J.Cell Biochem. 90:766-776.

Mahley RW, Innerarity TL, Pitas RE, Weisgraber KH, Brown JH, and Gross E (1977) Inhibition of lipoprotein binding to cell surface receptors of fibroblasts following selective modification of arginyl residues in arginine-rich and B apoproteins. J.Biol.Chem. 252:7279-7287.

Mahley RW (1985) Atherogenic lipoproteins and coronary artery disease: concepts derived from recent advances in cellular and molecular biology. Circulation 72:943-948.

Mahley RW, Hui DY, Innerarity TL, and Beisiegel U (1989) Chylomicron remnant metabolism. Role of hepatic lipoprotein receptors in mediating uptake. Arteriosclerosis 9:I14-I18.

Mahley RW, Weisgraber KH, and Farese RV (1998) Disorders of lipid metabolism. In: Wiliams Textbook of Endocrinology. Wilson JD, Foster DW, Kronenberg HM, and Larsen PR, Editors. 9th edition. WB Saunders, Philadelphia. p. 1099-1153.

Mahley RW and Ji ZS (1999) Remnant lipoprotein metabolism: key pathways involving cell-surface heparan sulfate proteoglycans and apolipoprotein E. J.Lipid Res. 40:1-16.
Mahley RW and Rall SC, Jr. (2000) Apolipoprotein E: far more than a lipid transport protein. Annu.Rev.Genomics Hum.Genet. 1:507-537.

Makrides SC, Ruiz-Opazo N, Hayden M, Nussbaum AL, Breslow JL, and Zannis VI (1988) Sequence and expression of Tangier apoA-I gene. Eur.J.Biochem. 173:465-471.

Mamotte CD, Sturm M, Foo JI, van Bockxmeer FM, and Taylor RR (1999) Comparison of the LDL-receptor binding of VLDL and LDL from apoE4 and apoE3 homozygotes. Am.J.Physiol 276:E553-E557.

Manzano A, Mohri Z, Sperber G, Ogris M, Graham I, Dickson G, and Owen JS (2003) Failure to generate atheroprotective apolipoprotein AI phenotypes using synthetic RNA/DNA oligonucleotides (chimeraplasts). J.Gene Med. 5:795-802.

Mao SJ and Kottke BA (1980) Tween-20 increases the immunoreactivity of apolipoprotein A-I in plasma. Biochim.Biophys.Acta 620:447-453.

Marcil M, Brooks-Wilson A, Clee SM, Roomp K, Zhang LH, Yu L, Collins JA, van Dam M, Molhuizen HO, Loubster O, Ouellette BF, Sensen CW, Fichter K, Mott S, Denis M, Boucher B,

Pimstone S, Genest J, Jr., Kastelein JJ, and Hayden MR (1999) Mutations in the ABC1 gene in familial HDL deficiency with defective cholesterol efflux. Lancet 354:1341-1346.

Marcovina S, Di Cola G, and Catapano AL (1986) Radial-immunodiffusion assay of human apolipoprotein A-I with use of two monoclonal antibodies combined. Clin.Chem. 32:2155-2159.

Margolis J and Kenrick KC (1967) Polyacrylamide gel-electrophoresis across a molecular sieve gradient. Nature 214:1334-1336.

Marshall P, Rohlmann A, Nussenzweig V, Herz J, and Sinnis P (2000) Plasmodium sporozoites invade cells with targeted deletions in the LDL receptor related protein. Mol.Biochem.Parasitol. 106:293-298.

Martino G, Poliani PL, Marconi PC, Comi G, and Furlan R (2000) Cytokine gene therapy of autoimmune demyelination revisited using herpes simplex virus type-1-derived vectors. Gene Ther. 7:1087-1093.

Mathei C, Van Damme P, and Meheus A (1997) Hepatitis B vaccine administration: comparison between jet-gun and syringe and needle. Vaccine 15:402-404.

Mazzone T and Reardon C (1994) Expression of heterologous human apolipoprotein E by J774 macrophages enhances cholesterol efflux to HDL3. J.Lipid Res. 35:1345-1353.

McDowell IF, Wisdom GB, and Trimble ER (1989) Apolipoprotein E phenotype determined by agarose gel electrofocusing and immunoblotting. Clin.Chem. 35:2070-2073.

McLachlan AD (1977) Repeated helical pattern in apolipoprotein-A-I. Nature 267:465-466.

McLean J, Fielding C, Drayna D, Dieplinger H, Baer B, Kohr W, Henzel W, and Lawn R (1986) Cloning and expression of human lecithin-cholesterol acyltransferase cDNA. Proc.Natl.Acad.Sci.U.S.A 83:2335-2339.

McLean JW, Fukazawa C, and Taylor JM (1983) Rat apolipoprotein E mRNA. Cloning and sequencing of double-stranded cDNA. J.Biol.Chem. 258:8993-9000.

McNeish J, Aiello RJ, Guyot D, Turi T, Gabel C, Aldinger C, Hoppe KL, Roach ML, Royer LJ, de Wet J, Broccardo C, Chimini G, and Francone OL (2000) High density lipoprotein deficiency and foam cell accumulation in mice with targeted disruption of ATP-binding cassette transporter-1. Proc.Natl.Acad.Sci.U.S.A 97:4245-4250.

Meade TW, Mellows S, Brozovic M, Miller GJ, Chakrabarti RR, North WR, Haines AP, Stirling Y, Imeson JD, and Thompson SG (1986) Haemostatic function and ischaemic heart disease: principal results of the Northwick Park Heart Study. Lancet 2:533-537.

Miao CH, Snyder RO, Schowalter DB, Patijn GA, Donahue B, Winther B, and Kay MA (1998) The kinetics of rAAV integration in the liver. Nat.Genet. 19:13-15.

Miller DG, Adam MA, and Miller AD (1990) Gene transfer by retrovirus vectors occurs only in cells that are actively replicating at the time of infection. Mol.Cell Biol. 10 :4239-4242.

Mir LM, Bureau MF, Gehl J, Rangara R, Rouy D, Caillaud JM, Delaere P, Branellec D, Schwartz B, and Scherman D (1999) High-efficiency gene transfer into skeletal muscle mediated by electric pulses. Proc.Natl.Acad.Sci.U.S.A 96:4262-4267.

Mitrophanous K, Yoon S, Rohll J, Patil D, Wilkes F, Kim V, Kingsman S, Kingsman A, and Mazarakis N (1999) Stable gene transfer to the nervous system using a non-primate lentiviral vector. Gene Ther. 6:1808-1818.

Miyata M and Smith JD (1996) Apolipoprotein E allele-specific antioxidant activity and effects on cytotoxicity by oxidative insults and beta-amyloid peptides. Nat.Genet. 14:55-61.

Miyazaki A, Sakai M, Suginohara Y, Hakamata H, Sakamoto Y, Morikawa W, and Horiuchi S (1994) Acetylated low density lipoprotein reduces its ligand activity for the scavenger receptor after interaction with reconstituted high density lipoprotein. J.Biol.Chem. 269:5264-5269.

Miyazaki A, Sakuma S, Morikawa W, Takiue T, Miake F, Terano T, Sakai M, Hakamata H, Sakamoto Y, Natio M, and . (1995) Intravenous injection of rabbit apolipoprotein A-I inhibits the progression of atherosclerosis in cholesterol-fed rabbits. Arterioscler.Thromb.Vasc.Biol. 15:1882-1888.

Moerschell RP, Tsunasawa S, and Sherman F (1988) Transformation of yeast with synthetic oligonucleotides. Proc.Natl.Acad.Sci.U.S.A 85:524-528.

Monahan PE and Samulski RJ (2000) AAV vectors: is clinical success on the horizon? Gene Ther. 7:24-30.

Morrissey DV, Lee PA, Johnson DA, Overly SL, McSwiggen JA, Beigelman L, Mokler VR, Maloney L, Vargeese C , Bowman K, O'Brien JT, Shaffer CS, Conrad A, Schmid P, Morrey JD, Macejak DG, Pavco PA, and Blatt LM (2002) Characterization of nuclease-resistant ribozymes directed against hepatitis B virus RNA. J.Viral Hepat. 9:411-418.

Mountain A (2000) Gene therapy: the first decade. Trends Biotechnol. 18:119-128.

Mumper RJ and Ledebur HC, Jr. (2001) Dendritic cell delivery of plasmid DNA. Applications for controlled genetic immunization. Mol.Biotechnol. 19:79-95.

Murdoch SJ and Breckenridge WC (1994) Development of a density gradient ultracentrifugation technique for the resolution of plasma lipoproteins which avoids apo E dissociation. Anal.Biochem. 222:427-434.

Narayanaswami V and Ryan RO (2000) Molecular basis of exchangeable apolipoprotein function . Biochim.Biophys.Acta 1483:15-36.

Nathan BP, Bellosta S, Sanan DA, Weisgraber KH, Mahley RW, and Pitas RE (1994) Differential effects of apolipoproteins E3 and E4 on neuronal growth in vitro. Science 264:850-852.

Nickerson HD and Colledge WH (2003) A comparison of gene repair strategies in cell culture using a lacZ reporter system. Gene Ther. 10:1584-1591.

Niidome T and Huang L (2002) Gene therapy progress and prospects: nonviral vectors. Gene Ther. 9:1647-1652.

Nur EK, Li TK, Zhang A, Qi H, Hars ES, and Liu LF (2003) Single-stranded DNA induces ataxia telangiectasia mutant (ATM)/p53-dependent DNA damage and apoptotic signals. J.Biol.Chem. 278:12475-12481.

O'Brien KD, Deeb SS, Ferguson M, McDonald TO, Allen MD, Alpers CE, and Chait A (1994) Apolipoprotein E localization in human coronary atherosclerotic plaques by in situ hybridization and immunohistochemistry and comparison with lipoprotein lipase. Am.J.Pathol. 144:538-548.

Ogris M, Steinlein P, Kursa M, Mechtler K, Kircheis R, and Wagner E (1998) The size of DNA/transferrin-PEI complexes is an important factor for gene expression in cultured cells. Gene Ther. 5:1425-1433.

Ogris M, Carlisle RC, Bettinger T, and Seymour LW (2001) Melittin enables efficient vesicular escape and enhanced nuclear access of nonviral gene delivery vectors. J.Biol.Chem. 276:47550-47555.

Ohashi K, Marion PL, Nakai H, Meuse L, Cullen JM, Bordier BB, Schwall R , Greenberg HB, Glenn JS, and Kay MA (2000) Sustained survival of human hepatocytes in mice: A model for in vivo infection with human hepatitis B and hepatitis delta viruses. Nat.Med. 6:327-331.

Olsen PA, McKeen C, and Krauss S (2003) Branched oligonucleotides induce in vivo gene conversion of a mutated EGFP reporter. Gene Ther. 10:1830-1840.

Oram JF and Yokoyama S (1996) Apolipoprotein-mediated removal of cellular cholesterol and phospholipids. J.Lipid Res. 37:2473-2491.

Owen JS (1999) Role of ABC1 gene in cholesterol efflux and atheroprotection. Lancet 354:1402-1403.

Page NM, Butlin DJ, Lomthaisong K, and Lowry PJ (2001) The human apolipoprotein L gene cluster: identification, classification, and sites of distribution. Genomics 74:71-78.

Paigen B, Morrow A, Brandon C, Mitchell D, and Holmes P (1985) Variation in susceptibility to atherosclerosis among inbred strains of mice. Atherosclerosis 57:65-73.

Paigen B, Holmes PA, Mitchell D, and Albee D (1987) Comparison of atherosclerotic lesions and HDL-lipid levels in male, female, and testosterone-treated female mice from strains C57BL/6, BALB/c, and C3H . Atherosclerosis 64:215-221.

Paik YK, Chang DJ, Reardon CA, Davies GE, Mahley RW, and Taylor JM (1985) Nucleotide sequence and structure of the human apolipoprotein E gene. Proc.Natl.Acad.Sci.U.S.A 82:3445-3449.

Paka L, Kako Y, Obunike JC, and Pillarisetti S (1999) Apolipoprotein E containing high density lipoprotein stimulates endothelial production of heparan sulfate rich in biologically active heparin-like domains. A potential mechanism for the anti-atherogenic actions of vascular apolipoprotein e. J.Biol.Chem. 274:4816-4823.

Palese P, Zheng H, Engelhardt OG, Pleschka S, and Garcia-Sastre A (1996) Negative-strand RNA viruses: genetic engineering and applications. Proc.Natl.Acad.Sci.U.S.A 93:11354-11358.

Paludan SR (2001) Requirements for the induction of interleukin-6 by herpes simplex virus-infected leukocytes. J.Virol. 75:8008-8015.

Parekh-Olmedo H, Czymmek K, and Kmiec EB (2001) Targeted gene repair in mammalian cells using chimeric RNA/DNA oligonucleotides and modified single-stranded vectors. Sci.STKE. 2001:L1.

Park F, Ohashi K, Chiu W, Naldini L, and Kay MA (2000) Efficient lentiviral transduction of liver requires cell cycling in vivo. Nat.Genet. 24:49-52.

Parthasarathy S, Barnett J, and Fong LG (1990) High-density lipoprotein inhibits the oxidative modification of low-density lipoprotein. Biochim.Biophys.Acta 1044:275-283.

Paszty C, Maeda N, Verstuyft J, and Rubin EM (1994) Apolipoprotein AI transgene corrects apolipoprotein E deficiency-induced atherosclerosis in mice. J.Clin.Invest 94:899-903.

Paul S, Bizouarne N, Dott K, Ruet L, Dufour P, Acres RB, and Kieny MP (2000) Redirected cellular cytotoxicity by infection of effector cells with a recombinant vaccinia virus encoding a tumor-specific monoclonal antibody. Cancer Gene Ther. 7:615-623.

Phillips MC, Gillotte KL, Haynes MP, Johnson WJ, Lund-Katz S, and Rothblat GH (1998) Mechanisms of high density lipoprotein-mediated efflux of cholesterol from cell plasma membranes. Atherosclerosis 137 Suppl:S13-S17.

Pitas RE, Boyles JK, Lee SH, Hui D, and Weisgraber KH (1987) Lipoproteins and their receptors in the central nervous system. Characterization of the lipoproteins in cerebrospinal fluid and identification of apolipoprotein B,E(LDL) receptors in the brain. J.Biol.Chem. 262:14352-14360.

Plump AS, Scott CJ, and Breslow JL (1994) Human apolipoprotein A-I gene expression increases high density lipoprotein and suppresses atherosclerosis in the apolipoprotein E-deficient mouse. Proc.Natl.Acad.Sci.U.S.A 91:9607-9611.

Pomp D and Medrano JF (1991) Organic solvents as facilitators of polymerase chain reaction. Biotechniques 10:58-59.

Pruvot I, Fievet C, Fruchart JC, Beucler I, Salmon S, Goldstein S, Ayrault-Jarrier M, and Girault A (1987) Electroimmunoassay for determination of ApoB in human sera by using a mixture of monoclonal antibodies. Clin.Chem. 33:1070.

Purcell-Huynh DA, Farese RV, Jr., Johnson DF, Flynn LM, Pierotti V, Newland DL, Linton MF, Sanan DA, and Young SG (1995) Transgenic mice expressing high levels of human apolipoprotein B develop severe atherosclerotic lesions in response to a high-fat diet. J.Clin.Invest 95:2246-2257.

Rabes JP, Varret M, Devillers M, Aegerter P, Villeger L, Krempf M, Junien C, and Boileau C (2000) R3531C mutation in the apolipoprotein B gene is not sufficient to cause hypercholesterolemia. Arterioscler.Thromb.Vasc.Biol. 20:E76-E82.

Rader DJ, Ikewaki K, Duverger N, Schmidt H, Pritchard H, Frohlich J, Clerc M, Dumon MF, Fairwell T, Zech L, and . (1994) Markedly accelerated catabolism of apolipoprotein A-II (ApoA-II) and high density lipoproteins containing ApoA-II in classic lecithin: cholesterol acyltransferase deficiency and fish-eye disease. J.Clin.Invest 93:321-330.

Rall SC, Jr. and Mahley RW (1992) The role of apolipoprotein E genetic variants in lipoprotein disorders. J.Intern.Med. 231:653-659.

Rando TA, Disatnik MH, and Zhou LZ (2000) Rescue of dystrophin expression in mdx mouse muscle by RNA/DNA oligonucleotides. Proc.Natl.Acad.Sci.U.S.A 97:5363-5368.

Recchia A, Parks RJ, Lamartina S, Toniatti C, Pieroni L, Palombo F, Ciliberto G, Graham FL, Cortese R, La Monica N, and Colloca S (1999) Site-specific integration mediated by a hybrid adenovirus/adeno-associated virus vector. Proc.Natl.Acad.Sci.U.S.A 96:2615-2620.

Rees A, Shoulders CC, Stocks J, Galton DJ, and Baralle FE (1983) DNA polymorphism adjacent to human apoprotein A-1 gene: relation to hypertriglyceridaemia. Lancet 1:444-446.

Rice MC, May GD, Kipp PB, Parekh H, and Kmiec EB (2000) Genetic repair of mutations in plant cell-free extracts directed by specific chimeric oligonucleotides. Plant Physiol 123:427-438.

Rice MC, Bruner M, Czymmek K, and Kmiec EB (2001a) In vitro and in vivo nucleotide exchange directed by chimeric RNA/DNA oligonucleotides in Saccharomyces cerevisae. Mol.Microbiol. 40:857-868.

Rice MC, Czymmek K, and Kmiec EB (2001b) The potential of nucleic acid repair in functional genomics. Nat.Biotechnol. 19:321-326.

Richter S, Shih DQ, Pearson ER, Wolfrum C, Fajans SS, Hattersley AT, and Stoffel M (2003) Regulation of apolipoprotein M gene expression by MODY3 gene hepatocyte nuclear factor-1alpha: haploinsufficiency is associated with reduced serum apolipoprotein M levels. Diabetes 52:2989-2995.

Riddell DR, Graham A, and Owen JS (1997) Apolipoprotein E inhibits platelet aggregation through the L-arginine:nitric oxide pathway. Implications for vascular disease. J.Biol.Chem. 272:89-95.

Riddell DR, Vinogradov DV, Stannard AK, Chadwick N, and Owen JS (1999) Identification and characterization of LRP8 (apoER2) in human blood platelets. J.Lipid Res. 40:1925-1930.

Riddell DR, Sun XM, Stannard AK, Soutar AK, and Owen JS (2001) Localization of apolipoprotein E receptor 2 to caveolae in the plasma membrane. J.Lipid Res. 42:998-1002.

Rigotti A, Trigatti BL, Penman M, Rayburn H, Herz J, and Krieger M (1997) A targeted mutation in the murine gene encoding the high density lipoprotein (HDL) receptor scavenger receptor class B type I reveals its key role in HDL metabolism. Proc.Natl.Acad.Sci.U.S.A 94:12610-12615.

Rinaldi M, Catapano AL, Parrella P, Ciafre SA, Signori E, Seripa D, Uboldi P, Antonini R, Ricci G, Farace MG, and Fazio VM (2000) Treatment of severe hypercholesterolemia in apolipoprotein E-deficient mice by intramuscular injection of plasmid DNA. Gene Ther. 7:1795-1801.

Rivera-Marrero CA, Schuyler W, Roser S, Ritzenthaler JD, Newburn SA, and Roman J (2002) M. tuberculosis induction of matrix metalloproteinase-9: the role of mannose and receptor-mediated mechanisms. Am.J.Physiol Lung Cell Mol.Physiol 282:L546-L555.

Rizzuto G, Cappelletti M, Maione D, Savino R, Lazzaro D, Costa P, Mathiesen I, Cortese R, Ciliberto G, Laufer R, La Monica N, and Fattori E (1999) Efficient and regulated erythropoietin production by naked DNA injection and muscle electroporation. Proc.Natl.Acad.Sci.U.S.A 96:6417-6422.

Roberts ML, Wells DJ, Graham IR, Fabb SA, Hill VJ, Duisit G, Yuasa K, Takeda S, Cosset FL, and Dickson G (2002) Stable micro-dystrophin gene transfer using an integrating adeno-retroviral hybrid vector ameliorates the dystrophic pathology in mdx mouse muscle. Hum.Mol.Genet. 11:1719-1730.

Roe T, Reynolds TC, Yu G, and Brown PO (1993) Integration of murine leukemia virus DNA depends on mitosis. EMBO J. 12:2099-2108.

Rohlmann A, Gotthardt M, Hammer RE, and Herz J (1998) Inducible inactivation of hepatic LRP gene by cre-mediated recombination confirms role of LRP in clearance of chylomicron remnants. J.Clin.Invest 101:689-695.

Roselaar SE and Daugherty A (1998) Apolipoprotein E-deficient mice have impaired innate immune responses to Listeria monocytogenes in vivo. J.Lipid Res. 39:1740-1743.

Rosenberg SA, Aebersold P, Cornetta K, Kasid A, Morgan RA, Moen R, Karson EM, Lotze MT, Yang JC, Topalian SL, and . (1990) Gene transfer into humans--immunotherapy of patients with advanced melanoma, using tumor-infiltrating lymphocytes modified by retroviral gene transduction. N.Engl.J.Med. 323:570-578.

Rosenfeld ME, Tsukada T, Chait A, Bierman EL, Gown AM, and Ross R (1987) Fatty streak expansion and maturation in Watanabe Heritable Hyperlipemic and comparably hypercholesterolemic fat-fed rabbits. Arteriosclerosis 7:24-34.

Rosengart TK, Lee LY, Patel SR, Sanborn TA, Parikh M, Bergman GW, Hachamovitch R, Szulc M, Kligfield PD , Okin PM, Hahn RT, Devereux RB, Post MR, Hackett NR, Foster T, Grasso TM, Lesser ML, Isom OW, and Crystal RG (1999) Angiogenesis gene therapy: phase I assessment of direct intramyocardial administration of an adenovirus vector expressing VEGF121 cDNA to individuals with clinically significant severe coronary artery disease. Circulation 100:468-474.

Ross R (1999) Atherosclerosis is an inflammatory disease. N. Engl. J. Med. 340:115-126.

Roth JA and Cristiano RJ (1997) Gene therapy for cancer: what have we done and where are we going? J.Natl.Cancer Inst. 89:21-39.

Rothblat GH, Mahlberg FH, Johnson WJ, and Phillips MC (1992) Apolipoproteins, membrane cholesterol domains, and the regulation of cholesterol efflux. J.Lipid Res. 33:1091-1097.

Rothblat GH, Llera-Moya M, Atger V, Kellner-Weibel G, Williams DL, and Phillips MC (1999) Cell cholesterol efflux: integration of old and new observations provides new insights. J.Lipid Res. 40:781-796.

Rothwell TC, Kamanna VS, Jin FY, Koren E, Foley T, and Kashyap ML (1995) Characterization of a monoclonal antibody (HB-22) and development of an ELISA for human apolipoprotein A-I. Clin.Chem. 41:1150-1158.

Rubin EM, Krauss RM, Spangler EA, Verstuyft JG, and Clift SM (1991) Inhibition of early atherogenesis in transgenic mice by human apolipoprotein AI. Nature 353:265-267.

Rumsey SC, Obunike JC, Arad Y, Deckelbaum RJ, Goldberg IJ (1992) Lipoprotein lipase-mediated uptake and degradation of low density lipoproteins by fibroblasts and macrophages. J. Clin. Invest. 90:1504-1512.

Rust S, Rosier M, Funke H, Real J, Amoura Z, Piette JC, Deleuze JF, Brewer HB, Duverger N, Denefle P, and Assmann G (1999) Tangier disease is caused by mutations in the gene encoding ATP-binding cassette transporter 1. Nat.Genet. 22:352-355.

Rye KA, Clay MA, and Barter PJ (1999) Remodelling of high density lipoproteins by plasma factors. Atherosclerosis 145:227-238.

Sacre SM, Stannard AK, and Owen JS (2003) Apolipoprotein E (apoE) isoforms differentially induce nitric oxide production in endothelial cells. FEBS Lett. 540:181-187.

Saito H, Dhanasekaran P, Nguyen D, Holvoet P, Lund-Katz S, and Phillips MC (2003) Domain structure and lipid interaction in human apolipoproteins A-I and E, a general model. J.Biol.Chem. 278:23227-23232.

Sakai J, Hoshino A, Takahashi S, Miura Y, Ishii H, Suzuki H, Kawarabayasi Y, and Yamamoto T (1994) Structure, chromosome location, and expression of the human very low density lipoprotein receptor gene. J.Biol.Chem. 269:2173-2182.

Sambrook J, Fritsch EF, and Maniatis T (1989a) Enzymes used in molecular cloning. Molecular Cloning: A Laboratory Manual. Cold Spring Harbor Publications, New York, p. 5.3-5.32.

Sambrook J, Fritsch EF, and Maniatis T (1989b) Gel electrophoresis of DNA. Molecular Cloning: A Laboratory Manual. Cold Spring Harbor Publications, New York, p. 6.1-6.62.

Sambrook J, Fritsch EF, and Maniatis T (1989c) In vitro amplification of DNA by the polymerase chain reaction. Molecular Cloning: A Laboratory Manual. Cold Spring Harbor Publications, New York, p. 14.1-14.22.

Sanan DA, Newland DL, Tao R, Marcovina S, Wang J, Mooser V, Hammer RE, and Hobbs HH (1998) Low density lipoprotein receptor-negative mice expressing human apolipoprotein B-100 develop complex atherosclerotic lesions on a chow diet: no accentuation by apolipoprotein(a). Proc.Natl.Acad.Sci.U.S.A 95:4544-4549.

Sangiuolo F, Bruscia E, Serafino A, Nardone AM, Bonifazi E, Lais M, Gruenert DC, and Novelli G (2002) In vitro correction of cystic fibrosis epithelial cell lines by small fragment homologous replacement (SFHR) technique. BMC.Med.Genet. 3:8.

Santamarina-Fojo S, Lambert G, Hoeg JM, and Brewer HB, Jr. (2000) Lecithin-cholesterol acyltransferase: role in lipoprotein metabolism, reverse cholesterol transport and atherosclerosis. Curr.Opin.Lipidol. 11:267-275.

Savion N and Kotev-Emeth S (1993) Role of apolipoproteins A-I, A-II and C-I in cholesterol efflux from endothelial and smooth muscle cells. Eur.Heart J. 14:930-935.

Schiedner G, Morral N, Parks RJ, Wu Y, Koopmans SC, Langston C, Graham FL, Beaudet AL, and Kochanek S (1998) Genomic DNA transfer with a high-capacity adenovirus vector results in improved in vivo gene expression and decreased toxicity. Nat.Genet. 18:180-183.

Schmidt HH, Genschel J, Haas R, Buttner C, and Manns MP (1997) Expression and purification of recombinant human apolipoprotein A-I in Chinese hamster ovary cells. Protein Expr.Purif. 10:226-236.

Schmitz C, Rutten BP, Pielen A, Schafer S, Wirths O, Tremp G, Czech C, Blanchard V, Multhaup G, Rezaie P, Korr H, Steinbusch HW, Pradier L, and Bayer TA (2004) Hippocampal neuron loss exceeds amyloid plaque load in a transgenic mouse model of Alzheimer's disease. Am.J.Pathol. 164:1495-1502.

Schonbeck U, Sukhova GK, ShimizuK, Mach F, Libby P (2000) Inhibition of CD40 signalling limits evolution of established atherosclerosis in mice. Proc.Natl.Acad.Sci.USA. 97:7458-7463.

Schonfeld G, Chen JS, and Roy RG (1977) Antigenic properties of apoproteins A-I and A-II in intact high density lipoprotein. J.Biol.Chem. 252:6651-6654.

Schreyer SA, Peschon JJ, and LeBoeuf RC (1996) Accelerated atherosclerosis in mice lacking tumor necrosis factor receptor p55. J.Biol.Chem. 271:26174-26178.

Schroers R, Sinha I, Segall H, Schmidt-Wolf IG, Rooney CM, Brenner MK, Sutton RE, and Chen SY (2000) Transduction of human PBMC-derived dendritic cells and macrophages by an HIV-1-based lentiviral vector system. Mol.Ther. 1:171-179.

Schroth GP and Ho PS (1995) Occurrence of potential cruciform and H-DNA forming sequences in genomic DNA. Nucleic Acids Res. 23:1977-1983.

Schwiegelshohn B, Presley JF, Gorecki M, Vogel T, Carpentier YA, Maxfield FR, and Deckelbaum RJ (1995) Effects of apoprotein E on intracellular metabolism of model triglyceride-rich particles are distinct from effects on cell particle uptake. J.Biol.Chem. 270:1761-1769.

Segrest JP, Jackson RL, Morrisett JD, and Gotto AM, Jr. (1974) A molecular theory of lipid-protein interactions in the plasma lipoproteins. FEBS Lett. 38:247-258.

Shah PK, Nilsson J, Kaul S, Fishbein MC, Ageland H, Hamsten A, Johansson J, Karpe F, and Cercek B (1998) Effects of recombinant apolipoprotein A-I(Milano) on aortic atherosclerosis in apolipoprotein E-deficient mice. Circulation 97:780-785.

Shah PK, Yano J, Reyes O, Chyu KY, Kaul S, Bisgaier CL, Drake S, and Cercek B (2001) High-dose recombinant apolipoprotein A-I(milano) mobilizes tissue cholesterol and rapidly reduces plaque lipid and macrophage content in apolipoprotein e-deficient mice. Potential implications for acute plaque stabilization. Circulation 103:3047-3050.

Shi N, Zhang Y, Zhu C, Boado RJ, and Pardridge WM (2001) Brain-specific expression of an exogenous gene after i.v. administration. Proc.Natl.Acad.Sci.U.S.A 98:12754-12759.

Shi W, Wang NJ, Shih DM, Sun VZ, Wang X, and Lusis AJ (2000a) Determinants of atherosclerosis susceptibility in the C3H and C57BL/6 mouse model: evidence for involvement of endothelial cells but not blood cells or cholesterol metabolism. Circ.Res. 86:1078-1084.

Shi W, Wang X, Wang NJ, McBride WH, and Lusis AJ (2000b) Effect of macrophage-derived apolipoprotein E on established atherosclerosis in apolipoprotein E-deficient mice. Arterioscler.Thromb.Vasc.Biol. 20:2261-2266.

Shih SJ, Allan C, Grehan S, Tse E, Moran C , and Taylor JM (2000) Duplicated downstream enhancers control expression of the human apolipoprotein E gene in macrophages and adipose tissue. J.Biol.Chem. 275:31567-31572.

Shinohara A, Ogawa H, Matsuda Y, Ushio N, Ikeo K, and Ogawa T (1993) Cloning of human, mouse and fission yeast recombination genes homologous to RAD51 and recA. Nat.Genet. 4:239-243.

Shore VG and Shore B (1973) Heterogeneity of human plasma very low density lipoproteins. Separation of species differing in protein components. Biochemistry 12:502-507.

Siest G, Pillot T, Regis-Bailly A, Leininger-Muller B, Steinmetz J, Galteau MM, and Visvikis S (1995) Apolipoprotein E: an important gene and protein to follow in laboratory medicine. Clin.Chem. 41:1068-1086.

Singer MJ, Mesner LD, Friedman CL, Trask BJ, and Hamlin JL (2000) Amplification of the human dihydrofolate reductase gene via double minutes is initiated by chromosome breaks. Proc.Natl.Acad.Sci.U.S.A 97:7921-7926.

Slooter AJ, Tang MX, van Duijn CM, Stern Y, Ott A, Bell K, Breteler MM, Van Broeckhoven C, Tatemichi TK, Tycko B, Hofman A, and Mayeux R (1997) Apolipoprotein E epsilon4 and the risk of dementia with stroke. A population-based investigation. JAMA 277:818-821.

Smith PK, Krohn RI, Hermanson GT, Mallia AK, Gartner FH, Provenzano MD, Fujimoto EK, Goeke NM, Olson BJ, and Klenk DC (1985) Measurement of protein using bicinchoninic acid. Anal.Biochem. 150:76-85.

Smith SC, Jr., Blair SN, Criqui MH, Fletcher GF, Fuster V, Gersh BJ, Gotto AM, Gould KL, Greenland P, Grundy SM, and . (1995) Preventing heart attack and death in patients with coronary disease. Circulation 92:2-4.

Soares CR, Morganti L, Miloux B, Lupker JH, Ferrara P, and Bartolini P (2000) High-level synthesis of human prolactin in Chinese-Hamster ovary cells. Biotechnol.Appl.Biochem. 32 (Pt 2):127-135.

Soma MR, Donetti E, Parolini C, Sirtori CR, Fumagalli R, and Franceschini G (1995) Recombinant apolipoprotein A-IMilano dimer inhibits carotid intimal thickening induced by perivascular manipulation in rabbits. Circ.Res. 76:405-411.

Somia N and Verma IM (2000) Gene therapy: trials and tribulations. Nat.Rev.Genet. 1:91-99.

Sparks DL, Frank PG, and Neville TA (1998) Effect of the surface lipid composition of reconstituted LPA-I on apolipoprotein A-I structure and lecithin: cholesterol acyltransferase activity. Biochim.Biophys.Acta 1390:160-172.

Spector T (1978) Refinement of the coomassie blue method of protein quantitation. A simple and linear spectrophotometric assay for less than or equal to 0.5 to 50 microgram of protein. Anal.Biochem. 86:142-146.

Stannard AK, Riddell DR, Sacre SM, Tagalakis AD, Langer C, von Eckardstein A, Cullen P, Athanasopoulos T, Dickson G, and Owen JS (2001) Cell-derived apolipoprotein E (ApoE) particles inhibit vascular cell adhesion molecule-1 (VCAM-1) expression in human endothelial cells. J.Biol.Chem. 276:46011-46016.

Starck M, Bertrand P, Pepin S, Schiele F, Siest G, and Galteau MM (2000) Effects of pro-inflammatory cytokines on apolipoprotein E secretion by a human astrocytoma cell line (CCF-STTG1). Cell Biochem.Funct. 18:9-16.

Steinberg D, Parthasarathy S, Carew TE, Khoo JC, and Witztum JL (1989) Beyond cholesterol. Modifications of low-density lipoprotein that increase its atherogenicity. N.Engl.J.Med. 320:915-924.

Steinmetz A and Utermann G (1985) Activation of lecithin: cholesterol acyltransferase by human apolipoprotein A-IV. J.Biol.Chem. 260:2258-2264.

Stern M, Ulrich K, Geddes DM, and Alton EW (2003) Poly (D, L-lactide-co-glycolide)/DNA microspheres to facilitate prolonged transgene expression in airway epithelium in vitro, ex vivo and in vivo. Gene Ther. 10:1282-1288.

Stevenson SC, Marshall-Neff J, Teng B, Lee CB, Roy S, and McClelland A (1995) Phenotypic correction of hypercholesterolemia in apoE-deficient mice by adenovirus-mediated in vivo gene transfer. Arterioscler.Thromb.Vasc.Biol. 15:479-484.

Subramanian VS, Goyal J, Miwa M, Sugatami J, Akiyama M, Liu M, and Subbaiah PV (1999) Role of lecithin-cholesterol acyltransferase in the metabolism of oxidized phospholipids in plasma: studies with platelet-activating factor-acetyl hydrolase-deficient plasma. Biochim.Biophys.Acta 1439:95-109.

Suc I, Escargueil-Blanc I, Troly M, Salvayre R, and Negre-Salvayre A (1997) HDL and ApoA prevent cell death of endothelial cells induced by oxidized LDL. Arterioscler.Thromb.Vasc.Biol. 17:2158-2166.

Sullivan PM, Mezdour H, Quarfordt SH, and Maeda N (1998) Type III hyperlipoproteinemia and spontaneous atherosclerosis in mice resulting from gene replacement of mouse Apoe with human Apoe*2. J.Clin.Invest 102:130-135.

Szymanski PT, Szymanska G, and Goyal RK (2002) Differences in calmodulin and calmodulin-binding proteins in phasic and tonic smooth muscles. Am.J.Physiol Cell Physiol 282:C94-C104.

Tabas I (2000) Cholesterol and phospholipids metabolism in macrophages. Nature. 1529:164-174.

Tada H (2001) The E4 allele of apolipoprotein E is associated with increased restenosis after coronary angioplasty . Tokai J.Exp.Clin.Med. 26:81-92.

Tagalakis AD, Graham IR, Riddell DR, Dickson JG, and Owen JS (2001) Gene correction of the apolipoprotein (Apo) E2 phenotype to wild-type ApoE3 by in situ chimeraplasty. J.Biol.Chem. 276:13226-13230.

Tajima S, Hayashi R, Tsuchiya S, Miyake Y, and Yamamoto A (1985) Cells of a human monocytic leukemia cell line (THP-1) synthesize and secrete apolipoprotein E and lipoprotein lipase. Biochem.Biophys.Res.Commun. 126:526-531.

Takada D, Ezura Y, Ono S, Iino Y, Katayama Y, Xin Y, Wu LL, Larringa-Shum S, Stephenson SH, Hunt SC, Hopkins PN, and Emi M (2003) Apolipoprotein H variant modifies plasma triglyceride phenotype in familial hypercholesterolemia: a molecular study in an eight-generation hyperlipidemic family. J.Atheroscler.Thromb. 10:79-84.

Tall AR, Small DM, Deckelbaum RJ, and Shipley GG (1977) Structure and thermodynamic properties of high density lipoprotein recombinants. J.Biol.Chem. 252:4701-4711.

Tall AR (1995) Plasma cholesteryl ester transfer protein and high-density lipoproteins: new insights from molecular genetic studies. J.Intern.Med. 237:5-12.

Tangirala RK, Pratico D, FitzGerald GA, Chun S, Tsukamoto K, Maugeais C, Usher DC, Pure E, and Rader DJ (2001) Reduction of isoprostanes and regression of advanced atherosclerosis by apolipoprotein E. J.Biol.Chem. 276:261-266.

Taniyama Y, Tachibana K, Hiraoka K, Aoki M, Yamamoto S, Matsumoto K, Nakamura T, Ogihara T, Kaneda Y, and Morishita R (2002) Development of safe and efficient novel nonviral gene transfer using ultrasound: enhancement of transfection efficiency of naked plasmid DNA in skeletal muscle. Gene Ther. 9:372-380.

Taubes G (2002) Gene therapy. The strange case of chimeraplasty. Science 298:2116-2120.

Thomas KR, Folger KR, and Capecchi MR (1986) High frequency targeting of genes to specific sites in the mammalian genome. Cell 44:419-428.

Thomas KR and Capecchi MR (1997) Recombinant DNA technique and sickle cell anemia research . Science 275:1404-1405.

Thomas MJ (2000) Physiological aspects of low-density lipoprotein oxidation. Curr.Opin.Lipidol. 11:297-301.

Thorpe PH, Stevenson BJ, and Porteous DJ (2002) Functional correction of episomal mutations with short DNA fragments and RNA-DNA oligonucleotides. J.Gene Med. 4:195-204.

Tozuka M, Yoshida Y, Tanigami J, Miyachi M, Katsuyama T, and Kanai M (1991) Development of an enzyme-linked immunosorbent assay of apolipoprotein E-AII complex in plasma. Clin.Chem. 37:1645-1648.

Tripathy SK, Black HB, Goldwasser E, and Leiden JM (1996) Immune responses to transgene-encoded proteins limit the stability of gene expression after injection of replication-defective adenovirus vectors. Nat.Med. 2:545-550.

Trougakos IP and Gonos ES (2002) Clusterin/apolipoprotein J in human aging and cancer. Int.J.Biochem.Cell Biol. 34:1430-1448.

Tsai MY, Suess P, Schwichtenberg K, Eckfeldt JH, Yuan J, Tuchman M, and Hunninghake D (1993) Determination of apolipoprotein E genotypes by single-strand conformational polymorphism. Clin.Chem. 39:2121-2124.

Tsuchiya S, Kobayashi Y, Goto Y, Okumura H, Nakae S, Konno T, and Tada K (1982) Induction of maturation in cultured human monocytic leukemia cells by a phorbol diester. Cancer Res. 42:1530-1536.

Tsujita M and Yokoyama S (1996) Selective inhibition of free apolipoprotein-mediated cellular lipid efflux by probucol. Biochemistry 35:13011-13020.

Tsukamoto K, Smith P, Glick JM, and Rader DJ (1997a) Liver-directed gene transfer and prolonged expression of three major human ApoE isoforms in ApoE-deficient mice. J.Clin.Invest 100:107-114.

Tsukamoto K, Hiester KG, Smith P, Usher DC, Glick JM, and Rader DJ (1997b) Comparison of human apoA-I expression in mouse models of atherosclerosis after gene transfer using a second generation adenovirus. J.Lipid Res. 38:1869-1876.

Tsukamoto K, Tangirala R, Chun SH, Pure E, and Rader DJ (1999) Rapid regression of atherosclerosis induced by liver-directed gene transfer of ApoE in ApoE-deficient mice. Arterioscler.Thromb.Vasc.Biol. 19:2162-2170.

Tuschl T (2002) Expanding small RNA interference. Nat.Biotechnol. 20:446-448.

Underwood PA and Steele JG (1991) Practical limitations of estimation of protein adsorption to polymer surfaces. J.Immunol.Methods 142:83-94.

Urlaub G and Chasin LA (1980) Isolation of Chinese hamster cell mutants deficient in dihydrofolate reductase activity. Proc.Natl.Acad.Sci.U.S.A 77:4216-4220.

Utermann G (1975) Isolation and partial characterization of an arginine-rich apolipoprotein from human plasma very-low-density lipoproteins: apolipoprotein E. Hoppe Seylers.Z.Physiol Chem. 356:1113-1121.

Utermann G, Pruin N, and Steinmetz A (1979) Polymorphism of apolipoprotein E. III. Effect of a single polymorphic gene locus on plasma lipid levels in man. Clin.Genet. 15:63-72.

Utsumi J, Mizuno Y, Hosoi K, Okano K, Sawada R, Kajitani M, Sakai I, Naruto M, and Shimizu H (1989) Characterization of four different mammalian-cell-derived recombinant human interferon-beta 1s. Identical polypeptides and non-identical carbohydrate moieties compared to natural ones. Eur.J.Biochem. 181:545-553.

van der SG, Schuilenga-Hut PH, Buys CH, Scheffer H, Pas HH, and Jonkman MF (2001) Persistent failures in gene repair. Nat.Biotechnol. 19:305-306.

Van Eck M, Herijgers N, Yates J, Pearce NJ, Hoogerbrugge PM, Groot PH, and van Berkel TJ (1997) Bone marrow transplantation in apolipoprotein E-deficient mice. Effect of ApoE gene dosage on serum lipid concentrations, (beta)VLDL catabolism, and atherosclerosis. Arterioscler.Thromb.Vasc.Biol. 17:3117-3126.

van Ree JH, van den Broek WJ, Dahlmans VE, Groot PH, Vidgeon-Hart M, Frants RR, Wieringa B, Havekes LM, and Hofker MH (1994) Diet-induced hypercholesterolemia and atherosclerosis in heterozygous apolipoprotein E-deficient mice. Atherosclerosis 111:25-37.

Van Tendeloo VF, Van Broeckhoven C , and Berneman ZN (2001) Gene-based cancer vaccines: an ex vivo approach. Leukemia 15:545-558.

Vasquez KM, Marburger K, Intody Z, and Wilson JH (2001) Manipulating the mammalian genome by homologous recombination. Proc.Natl.Acad.Sci.U.S.A 98:8403-8410.

Vicat JM, Boisseau S, Jourdes P, Laine M, Wion D, Bouali-Benazzouz R, Benabid AL, and Berger F (2000) Muscle transfection by electroporation with high-voltage and short-pulse currents provides high-level and long-lasting gene expression. Hum.Gene Ther. 11:909-916.

Vinals M, Martinez-Gonzalez J, Badimon JJ, and Badimon L (1997) HDL-induced prostacyclin release in smooth muscle cells is dependent on cyclooxygenase-2 (Cox-2). Arterioscler.Thromb.Vasc.Biol. 17:3481-3488.

Vinogradov DV, Hongqun L, and Owen JS (1998) C-terminal His6-tagged lecithin-cholesterol acyltransferase (LCAT) is catalytically active. Biochem.Soc.Trans. 26:S146.

Voyiaziakis E, Goldberg IJ, Plump AS, Rubin EM, Breslow JL, and Huang LS (1998) ApoA-I deficiency causes both hypertriglyceridemia and increased atherosclerosis in human apoB transgenic mice. J.Lipid Res. 39:313-321.

Wadman M (1995) Hyping results 'could damage' gene therapy. Nature 378:655.

Wadman M (1998) Germline gene therapy 'must be spared excessive regulation'. Nature 392:317.

Wagner JA, Reynolds T, Moran ML, Moss RB, Wine JJ, Flotte TR, and Gardner P (1998) Efficient and persistent gene transfer of AAV-CFTR in maxillary sinus. Lancet 351:1702-1703.

Wahlfors JJ, Zullo SA, Loimas S, Nelson DM, and Morgan RA (2000) Evaluation of recombinant alphaviruses as vectors in gene therapy. Gene Ther. 7:472-480.

Wang G, Seidman MM, and Glazer PM (1996) Mutagenesis in mammalian cells induced by triple helix formation and transcription-coupled repair. Science 271:802-805.

Wang N, Arai T, Ji Y, Rinninger F, and Tall AR (1998) Liver-specific overexpression of scavenger receptor BI decreases levels of very low density lipoprotein ApoB, low density lipoprotein ApoB, and high density lipoprotein in transgenic mice. J.Biol.Chem. 273:32920-32926.

Wang N, Silver DL, Thiele C, and Tall AR (2001) ATP-binding cassette transporter A1 (ABCA1) functions as a cholesterol efflux regulatory protein. J.Biol.Chem. 276:23742-23747.

Wang R, Doolan DL, Le TP, Hedstrom RC, Coonan KM, Charoenvit Y, Jones TR, Hobart P, Margalith M, Ng J, Weiss WR, Sedegah M, de Taisne C, Norman JA, and Hoffman SL (1998) Induction of antigen-specific cytotoxic T lymphocytes in humans by a malaria DNA vaccine. Science 282:476-480.

Weikert S, Papac D, Briggs J, Cowfer D, Tom S, Gawlitzek M, Lofgren J, Mehta S, Chisholm V, Modi N, Eppler S, Carroll K, Chamow S, Peers D, Berman P, and Krummen L (1999) Engineering Chinese hamster ovary cells to maximize sialic acid content of recombinant glycoproteins. Nat.Biotechnol. 17:1116-1121.

Weisgraber KH, Bersot TP, Mahley RW, Franceschini G, and Sirtori CR (1980) A-Imilano apoprotein. Isolation and characterization of a cysteine-containing variant of the A-I apoprotein from human high density lipoproteins. J.Clin.Invest 66:901-907.

Weisgraber KH, Newhouse YM, and Mahley RW (1988) Apolipoprotein E genotyping using the polymerase chain reaction and allele-specific oligonucleotide probes. Biochem.Biophys.Res.Commun. 157:1212-1217.

Weisgraber KH (1990) Apolipoprotein E distribution among human plasma lipoproteins: role of the cysteine-arginine interchange at residue 112. J.Lipid Res. 31:1503-1511.

Weisgraber KH, Roses AD, and Strittmatter WJ (1994a) The role of apolipoprotein E in the nervous system. Curr.Opin.Lipidol. 5:110-116.

Weisgraber KH (1994b) Apolipoprotein E: structure-function relationships. Adv.Protein Chem. 45:249-302.

Weisgraber KH and Mahley RW (1996) Human apolipoprotein E: the Alzheimer's disease connection. FASEB J. 10:1485-1494.

Weiss B, Jacquemin-Sablon A, Live TR, Fareed GC, and Richardson CC (1968) Enzymatic breakage and joining of deoxyribonucleic acid. VI. Further purification and properties of polynucleotide ligase from Escherichia coli infected with bacteriophage T4. J.Biol.Chem. 243:4543-4555.

Weisweiler P and Schwandt P (1983) Immunonephelometric quantitation of apolipoprotein E in human serum. J.Clin.Chem.Clin.Biochem. 21:227-230.

Wenham PR, Newton CR, and Price WH (1991) Analysis of apolipoprotein E genotypes by the Amplification Refractory Mutation System. Clin.Chem. 37:241-244.

Wernette-Hammond ME, Lauer SJ, Corsini A, Walker D, Taylor JM, and Rall SC, Jr. (1989) Glycosylation of human apolipoprotein E. The carbohydrate attachment site is threonine 194. J.Biol.Chem. 264:9094-9101.

Westerlund JA and Weisgraber KH (1993) Discrete carboxyl-terminal segments of apolipoprotein E mediate lipoprotein association and protein oligomerization. J.Biol.Chem. 268:15745-15750.

Whitehead TP, Kricka LJ, Carter TJ, and Thorpe GH (1979) Analytical luminescence: its potential in the clinical laboratory. Clin.Chem. 25:1531-1546.

Wightman L, Kircheis R, Rossler V, Carotta S, Ruzicka R, Kursa M, and Wagner E (2001) Different behavior of branched and linear polyethylenimine for gene delivery in vitro and in vivo. J.Gene Med. 3:362-372.

Williams DC (1998) A method for assessing the quality of synthetic oligonucleotides using pre-cast polyacrylamide minigels. (www. abrf.org/ABRFNews/1998/June98/jun98/Minigels.html).

Willnow TE and Herz J (1995) Animal models for disorders of hepatic lipoprotein metabolism. J.Mol.Med. 73:213-220.

Wilson C, Mau T, Weisgraber KH, Wardell MR, Mahley RW, and Agard DA (1994) Salt bridge relay triggers defective LDL receptor binding by a mutant apolipoprotein. Structure. 2:713-718.

Wilson DJ, Gahan M, Haddad L, Heath K, Whittall RA, Williams RR, Humphries SE, and Day IN (1998) A World Wide Web site for low-density lipoprotein receptor gene mutations in familial hypercholesterolemia: sequence-based, tabular, and direct submission data handling. Am.J.Cardiol. 81:1509-1511.

Wilson PW, Myers RH, Larson MG, Ordovas JM, Wolf PA, and Schaefer EJ (1994) Apolipoprotein E alleles, dyslipidemia, and coronary heart disease. The Framingham Offspring Study. JAMA 272:1666-1671.

Wolff JA, Ludtke JJ, Acsadi G, Williams P, and Jani A (1992) Long-term persistence of plasmid DNA and foreign gene expression in mouse muscle. Hum.Mol.Genet. 1:363-369.

Woodle MC, Scaria P, Ganesh S, Subramanian K, Titmas R, Cheng C, Yang J, Pan Y, Weng K, Gu C, and Torkelson S (2001) Sterically stabilized polyplex: ligand-mediated activity. J.Control Release 74:309-311.

Wozniak MA, Itzhaki RF, Faragher EB, James MW, Ryder SD, and Irving WL (2002) Apolipoprotein E-epsilon 4 protects against severe liver disease caused by hepatitis C virus. Hepatology 36:456-463.

Wozniak MA, Faragher EB, Todd JA, Koram KA, Riley EM, and Itzhaki RF (2003) Does apolipoprotein E polymorphism influence susceptibility to malaria? J.Med.Genet. 40:348-351.

Wu X, Wakefield JK, Liu H, Xiao H, Kralovics R, Prchal JT, and Kappes JC (2000) Development of a novel trans-lentiviral vector that affords predictable safety. Mol.Ther. 2:47-55.

Xiang Y, Cole-Strauss A, Yoon K, Gryn J, and Kmiec EB (1997) Targeted gene conversion in a mammalian CD34+-enriched cell population using a chimeric RNA/DNA oligonucleotide. J.Mol.Med. 75:829-835.

Xing X, Zhang S, Chang JY, Tucker SD, Chen H, Huang L, and Hung MC (1998) Safety study and characterization of E1A-liposome complex gene-delivery protocol in an ovarian cancer model. Gene Ther. 5:1538-1544.

Yamamoto T, Moerschell RP, Wakem LP, Komar-Panicucci S, and Sherman F (1992) Strand-specificity in the transformation of yeast with synthetic oligonucleotides. Genetics 131:811-819.

Yamamoto T and Bujo H (1996) Close encounters with apolipoprotein E receptors. Curr.Opin.Lipidol. 7:298-302.

Yamashita S, Sakai N, Hirano K, Ishigami M, Maruyama T, Nakajima N, and Matsuzawa Y (2001) Roles of plasma lipid transfer proteins in reverse cholesterol transport. Front Biosci. 6:D366-D387.

Yang DS, Smith JD, Zhou Z, Gandy SE, and Martins RN (1997) Characterization of the binding of amyloid-beta peptide to cell culture-derived native apolipoprotein E2, E3, and E4 isoforms and to isoforms from human plasma. J.Neurochem. 68:721-725.

Yant SR, Meuse L, Chiu W, Ivics Z, Izsvak Z, and Kay MA (2000) Somatic integration and long-term transgene expression in normal and haemophilic mice using a DNA transposon system. Nat.Genet. 25:35-41.

Ye SQ, Reardon CA, and Getz GS (1993) Inhibition of apolipoprotein E degradation in a post-Golgi compartment by a cysteine protease inhibitor. J.Biol.Chem. 268:8497-8502.

Yoon K, Cole-Strauss A, and Kmiec EB (1996) Targeted gene correction of episomal DNA in mammalian cells mediated by a chimeric RNA.DNA oligonucleotide. Proc.Natl.Acad.Sci.U.S.A 93:2071-2076.

Yoshida H, Hasty AH, Major AS, Ishiguro H, Su YR, Gleaves LA, Babaev VR , Linton MF, and Fazio S (2001) Isoform-specific effects of apolipoprotein E on atherogenesis: gene transduction studies in mice. Circulation 104:2820-2825.

Yotnda P, Chen DH, Chiu W, Piedra PA, Davis A, Templeton NS, and Brenner MK (2002) Bilamellar cationic liposomes protect adenovectors from preexisting humoral immune responses. Mol.Ther. 5:233-241.

Zanni EE, Kouvatsi A, Hadzopoulou-Cladaras M, Krieger M, and Zannis VI (1989) Expression of ApoE gene in Chinese hamster cells with a reversible defect in O-glycosylation. Glycosylation is not required for apoE secretion. J.Biol.Chem. 264:9137-9140.

Zannis VI and Breslow JL (1981) Human very low density lipoprotein apolipoprotein E isoprotein polymorphism is explained by genetic variation and posttranslational modification. Biochemistry 20:1033-1041.

Zanta MA, Boussif O, Adib A, and Behr JP (1997) In vitro gene delivery to hepatocytes with galactosylated polyethylenimine . Bioconjug.Chem. 8:839-844.

Zhang WY, Gaynor PM, and Kruth HS (1996) Apolipoprotein E produced by human monocyte-derived macrophages mediates cholesterol efflux that occurs in the absence of added cholesterol acceptors. J.Biol.Chem. 271:28641-28646.

Zhang Y, Jeong LH, Boado RJ, and Pardridge WM (2002) Receptor-mediated delivery of an antisense gene to human brain cancer cells. J.Gene Med. 4:183-194.

Zhang Z, Eriksson M, Falk G, Graff C, Presnell SC, Read MS, Nichols TC, Blomback M, and Anvret M (1998) Failure to achieve gene conversion with chimeric circular oligonucleotides: potentially misleading PCR artifacts observed. Antisense Nucleic Acid Drug Dev. 8:531-536.

Zheng C, Baum BJ, Iadarola MJ, and O'Connell BC (2000) Genomic integration and gene expression by a modified adenoviral vector. Nat.Biotechnol. 18:176-180.

Zhu T, Peterson DJ, Tagliani L, St Clair G, Baszczynski CL, and Bowen B (1999) Targeted manipulation of maize genes in vivo using chimeric RNA/DNA oligonucleotides. Proc.Natl.Acad.Sci.U.S.A 96:8768-8773.

Zhu T, Mettenburg K, Peterson DJ, Tagliani L, and Baszczynski CL (2000) Engineering herbicide-resistant maize using chimeric RNA/DNA oligonucleotides. Nat.Biotechnol. 18:555-558.

Zhu Y, Bellosta S, Langer C, Bernini F, Pitas RE, Mahley RW, Assmann G, and von Eckardstein A (1998) Low-dose expression of a human apolipoprotein E transgene in macrophages restores cholesterol efflux capacity of apolipoprotein E-deficient mouse plasma. Proc.Natl.Acad.Sci.U.S.A 95:7585-7590.

PUBLICATIONS

Original Articles

Mohri Z, Manzano A, Mulcahy J, Dickson JG, Owen JS. ApoAI natural mutations (Milano and Paris): understanding their characteristics. *Manuscript in preparation*

Manzano A, **Mohri Z**, Sperber G, Ogris M, Graham IR, Dickson JG, Owen JS (2003). Failure to generate apolipoprotein AI phenotypes using synthetic RNA/DNA oligonucleotides (chimeraplasts). *J Gene Medicine* 5(9):795-802

Harris JD, Schepelmann S, Athanasopoulos T, Graham IR, Stannard AK, **Mohri Z**, Hassall DG, Hill V, Owen JS, Dickson JG (2002). Inhibition of atherosclerosis in apolipoprotein-E deficient mice following muscle transduction with adeno-associated virus vectors encoding human apolipoprotein E. *Gene Therapy* 9:21-29

Letter to the Editor

Graham I, Manzano A, Tagalakis A, **Mohri Z**, Sperber G, Hill V, Beattie S, Schepelmann S, Dickson JG, Owen JS (2001). Gene repair validation. *Nature Biotechnology* 19:507

Invited Oral Presentations

Mohri Z, Tagalakis A, Graham IR, Dickson JG, Owen JS. Gene correction of apolipoprotein (apo) E2 and apoE4 phenotypes to wild-type apoE3 by in situ chimeraplasty. **7th Annual Scandinavian Atherosclerosis Conference**, Copenhagen, Denmark – May 2001. *Winner of first prize (Young investigator award)*

Mohri Z, Tagalakis A, Graham IR, Dickson JG, Owen JS. ApoE, apoAI, and atheroprotection. **Postgraduate Symphosium**, Royal Holloway University of London, London, UK – May 2001

Poster Presentation

Mohri Z, Tagalakis A, Dickson JG, Owen JS. Generation of apoE2- & apoE4-secreting cell lines by targeting of wild-type apoE3 cells using *in situ* chimeraplasty. **73rd European Atherosclerosis Society Congress**, Salzburg, Austria – July 2002

Mohri Z, Dickson JG, Owen JS. ApoE, apoAI, and atheroprotection. **Royal Free Poster Competition**, Royal Free Hospital, London, UK – April 2002, *Winner of the third prize*
Manzano A, **Mohri Z**, Mulcahy J, Graham IR, Dickson JG, Owen JS. Taking advantage of apoAI natural mutations: cell models and gain-of-function chimeraplasty. **9th Annual Conference of the European Society of Gene Therapy**, Antalya, Turkey – Nov 2001. *Winner of third prize*

Sperber G, Ogris M, Bettinger T, **Mohri Z**, Dickson JG, Owen JS. Improving chimeraplast uptake and gene conversion using chemically-modified polyehtylenimine (PEI). **9th Annual Conference of the European Society of Gene Therapy**, Antalya, Turkey – Nov 2001

Dickson JG, Tagalakis A, Graham IR, Owen JS, **Mohri Z.** Gene repair for hyperlipidaemia by in situ chimeraplasty. **4th Annual Conference of the American Society of Gene Therapy**, Seattle, USA - 2001